

ORIGIN AND CHARACTERISTICS OF DEVONIAN-
MISSISSIPPIAN NOVACULITIC CHERT IN
OKLAHOMA

By

KYRSTI A. CECIL

Bachelor of Science in Geology

Oklahoma State University

Stillwater, OK

2011

Submitted to the Faculty of the
Graduate College of the
Oklahoma State University
in partial fulfillment of
the requirements for
the Degree of
MASTER OF SCIENCE
July, 2016

ORIGIN AND CHARACTERISTICS OF DEVONIAN-MISSISSIPPIAN
NOVACULITIC CHERT IN OKLAHOMA

Thesis Approved:

Dr. Jack C. Pashin

Thesis Adviser

Dr. Mohamed Abdelsalam

Dr. James O. Puckette

ACKNOWLEDGEMENTS

I would like to express my deep gratitude to my thesis advisor, Dr. Jack Pashin. This project would not have been possible without the direction and support he provided during the past two years. Dr. Pashin willingly and happily participated in all steps of my thesis research, from numerous trips to the field across the state on hot Oklahoma days, to the countless hours he spent discussing ideas and helping me complete my final thesis. This project would not have been possible without his expert guidance and selfless support. I would also like to thank my committee members Dr. James Puckette and Dr. Mohamed Abdelsalam for their help and advice throughout this process. Additionally, Dr. Jeffrey Byrnes provided much support and guidance during the past two years. Thank you to the Boone Pickens School of Geology for the financial support in the form of a graduate fellowship. Special thanks to the other students in the geology department who helped me in various ways along this process: Jenny Meng, Sahar Mohammadi, Bradley Jackson, Beth Vanden Berg, and Danielle Martin. My dear friends and fellow geologists Michael Parks and Brandy Michael provided support throughout the years through advice and personal support. I would especially like to thank my friends, loved ones and family for their constant moral and emotional support they have provided throughout the years. I could not have completed this journey without you.

Acknowledgments reflect the views of the author and are not endorsed by committee members of Oklahoma State University.

Name: KYRSTI A. CECIL

Date of Degree: July, 2016

Title of Study: ORIGIN AND CHARACTERISTICS OF DEVONIAN-MISSISSIPPIAN
NOVACULITIC CHERT IN OKLAHOMA

Major Field: GEOLOGY

Abstract: Limited research has been performed since 1980 on the origin of novaculitic chert in the Arkansas Novaculite in the Ouachita Orogen of southeastern Oklahoma and in the Woodford Shale in the Oklahoma Shelf. Further research needs to be performed that applies emerging analytical technology and geologic concepts in order to formulate a more modern set of paleoenvironmental interpretations and to identify characteristics unique to each depositional setting. This study employed outcrop, core, thin section and SEM/EDS analysis to characterize and interpret the chert from megascopic to nanoscopic scales. Based on the high abundance of siliceous microfossils and the phosphatic nature of the chert, it is proposed that it formed from a biogenic silica source in a region influenced by marine upwelling and high organic productivity, which led to the development of an oxygen minimum zone. There is great similarity between the structures, sedimentation, and fabric on all scales in Woodford chert and the Arkansas Novaculite. The chert was deposited in a broad range of shelf, slope and basinal environments. On the Oklahoma Shelf, for example, the novaculitic chert was deposited atop a major Cambrian-Devonian carbonate bank. In the Ouachita Embayment, by contrast, similar chert was deposited in an oceanic setting above a succession including Cambrian-Silurian turbidite fan deposits that were probably deposited on the continental rise. Thicker bedding, a lower proportion of terrigenous sediment, and an absence of phosphate suggests that novaculite in the Broken Bow uplift was deposited in a distal setting where upwelling was less intense. Novaculitic chert within the Woodford Shale is an important component of unconventional reservoirs in the southern Midcontinent, from not only the standpoint of brittleness, but also in terms of organic content and hydrocarbon storage potential. Similarity between Woodford chert and the Arkansas Novaculite suggests that the hydrocarbon potential of novaculitic chert in the southern Midcontinent is underexplored.

TABLE OF CONTENTS

Chapter	Page
I. INTRODUCTION	1
II. GEOLOGICAL SETTING AND PREVIOUS WORK	8
II.1 Tectonic Setting.....	8
II.2 Arkansas Novaculite	10
II.3 Woodford Shale.....	13
II.4 Competing and Evolving Schools of Thought	17
III. METHODOLOGY	26
IV. RESULTS	29
IV.1 Outcrop and Core Description: Overview	29
IV.1.A I-35 Outcrop: Novaculitic Chert.....	29
IV.1.B Poe #1-29 Core: Novaculitic Chert.....	35
IV.1.C Hall 2B Core: Novaculitic Chert.....	41
IV.1.D Atoka Chert Pit Outcrop at Scratch Hill: Arkansas Novaculite.....	46
IV.1.E Beavers Bend/Broken Bow Outcrop: Arkansas Novaculite	54
IV.2 Thin Section Analysis: Overview	62
IV.2.A Chert-Organic Matrix	64
IV.2.B Biogenic Structures	73
IV.2.C Diagenetic Features.....	85
IV.2.D Phosphate Nodules.....	94
IV.2.E Veining	103
IV.3 SEM-Image Analysis: Overview	109
IV.3.A Chert-Organic Matrix	110
IV.3.B Biogenic Structures	113
IV.3.C Diagenetic Features.....	118
IV.3.D Porosity	122

Chapter	Page
V. DISCUSSION	132
VI. CONCLUSION.....	145
REFERENCES	147

LIST OF TABLES

Table	Page
1. Outcrop and core locations	6
2. Arkansas Novaculite hypothesis comparison chart	19
3. Chart labeling system of thin section samples	62
4. Chart labeling system of SEM-samples	110

LIST OF FIGURES

Figure	Page
1. Geologic map of Oklahoma showing locations of outcrops, cores, thin sections and SEM samples	5
2. Index map of the Ouachita orogenic belt	10
3. Stratigraphic column of the Anadarko Basin, Arbuckle Mountains, Arkoma Basin and Ouachita Mountains	12
4. Wheeler diagram showing formations and unconformities bounding the Woodford Shale.....	15
5. Photos comparing novaculitic chert radiolaria to shale <i>Tasmanites</i>	17
6. Comparison of interbedded shale and chert from the Arbuckle and Ouachita Mountains	24
7. I-35 Woodford Shale outcrop locations	31
8. Woodford/Sycamore contact in the I-35 outcrop.....	32
9. Location of sample eight from the I-35 outcrop	32
10. I-35 outcrop measured section	33
11. Alternating layers of fissile Woodford Shale and blocky novaculitic chert in the I-35 outcrop	34
12. Abundant phosphate nodules in I-35 outcrop	35
13. Measured section of the Poe #1-29 core	37
14. Chert layers containing strata-bound shear veins, Poe #1-29 core	38
15. Strata-bound fractures in novaculitic chert, Poe #1-29 core.....	39
16. Recumbent fold in bedded chert near the top of the Woodford Shale in the Poe #1-29 core.....	40
17. Measured section of the Hall-2B core	42
18. Image of normally faulted chert overlain by undeformed chert layers in Hall 2B core.....	43
19. Reverse fault and strata-bound filled fractures within Hall 2B core	44
20. Shale laminae and thin chert beds in Woodford Shale, Hall 2B core.....	45
21. Subcircular phosphate nodule in bedded chert, Woodford Shale, Hall 2B core.....	46
22. Map showing location of the Atoka Chert Pit	48
23. Steeply dipping and folded strata of the Arkansas Novaculite, Atoka Chert Pit.....	49
24. Reddish and greenish shale in the upper part of the Atoka Chert Pit	50
25. Mottled texture on fresh broken surface sample #2 from the Atoka Chert Pit	51
26. Hummocky bedding surface in steeply dipping novaculite layer in the Atoka Chert Pit	52
27. Abundant phosphate nodules in the Atoka Chert Pit	53
28. Exposed marcasite nodule in chert at the Atoka Chert Pit.....	54

29. Map showing outcrop locations in the Broken Bow Uplift in and around Beavers Bend State Park. Yellow stars represent outcrop locations.	56
30. Outcrop containing contact between Blaylock Sandstone and Arkansas Novaculite at Beavers Bend State Park.	57
31. Photo comparing Blaylock Sandstone quartz vein and cryptocrystalline Arkansas Novaculite	58
32. Beavers Bend/Broken Bow outcrop exposing the Missouri Mountain Shale, Arkansas Novaculite, and Stanley Shale next to the hydroelectric power station.	59
33. Beavers Bend/Broken Bow outcrop exposing the Arkansas Novaculite below the water tower.....	60
34. Outcrop north of Beavers Bend State Park exposing the Arkansas Novaculite .	61
35. Photo comparing sample 9 from Broken Bow/Beavers Bend to a weathered sample from the I-35 outcrop.	61
36. Thin section photomicrograph of radiolarian-rich novaculitic chert from the I-35 outcrop.	65
37. Dark novaculite specimen with abundant silica spherules and white silica veins from the power plant at the Broken Bow/Beavers Bend outcrop.	66
38. Dark spicular chert with silica veins from the power plant at the Broken Bow/Beavers Bend outcrop	67
39. Photomicrograph of chert and vein quartz from the Arkansas Novaculite near the Blaylock Sandstone contact, Broken Bow/Beavers Bend outcrop	68
40. Novaculitic chert with a grainstone-packstone texture from the Poe #1-29 core	70
41. Novaculitic chert with twinning from the Poe #1-29 core.....	71
42. Cross-polarized novaculitic chert photomicrography with a packstone-like texture along with possible twinning from the Poe #1-29 core	72
43. Novaculitic chert with various silica crystal sizes (cryptocrystalline-microcrystalline) from the Poe #1-29 core	73
44. Novaculitic chert thin section with abundant silica spherules in organic-rich amorphous to cryptocrystalline silica matrix Hall 2B core	75
45. Thin section photomicrograph of organic film coating a botryoidal silica spherule from the Hall 2B core	76
46. Thin section photomicrograph of novaculitic chert with spherules containing faint ghosts of radiolaria tests from the I-35 outcrop.....	77
47. Novaculitic chert thin section with a botryoidal silica spherule inside of possible Spumellaria radiolarian test from I-35.....	78
48. Novaculitic chert thin section showing a silica spherule in a possible acritarch from the Hall 2B core	79
49. Thin section photomicrograph of novaculitic chert with organic-walled <i>Tasmanites</i> specimen from the I-35 outcrop.....	80
50. Thin section photomicrograph of novaculitic chert showing a close up of organic-walled <i>Tasmanites</i> specimen from the I-35 outcrop.....	81
51. Thin section photomicrograph of a phosphate nodule showing diversity of Spumellaria in the Woodford Shale, Hall 2B core	82
52. Thin section photomicrograph showing abundant sponge spicules and Radiolaria, Hall 2B core	83
53. Spumellarian radiolarian with preserved spines, Hall 2B core.....	84

54. Thin section photomicrograph showing well-preserved Spumellaria and Nassellaria, Hall 2B core	85
55. Photomicrograph a phosphate nodule from the Atoka outcrop	86
56. Photomicrograph of dark Arkansas Novaculite with cubic pyrite from the power plant at Broken Bow/Beavers Bend.....	87
57. Arkansas Novaculite sample exhibiting acicular crystals from the power plant at Broken Bow/Beavers Bend.....	88
58. Photomicrograph of dark Arkansas Novaculite with acicular crystals and veining from the power plant at Broken Bow/Beavers Bend	89
59. Novaculitic chert thin section with medium-brown chert matrix, veined and brecciated, in the Hall 2B core from the Hall 2B core.....	90
60. Sample showing the complexity of veining in a sample from the power plant at Broken Bow/Beavers Bend.....	91
61. Arkansas Novaculite sample containing isolated rhombohedra of ferroan dolomite from Highway 259 from Broken Bow/Beavers Bend.....	92
62. Arkansas Novaculite sample showing microcrystalline vein fill as well as cryptocrystalline matrix from Highway 259 in Broken Bow/Beavers Bend.....	93
63. Cross-polarized photomicrograph displays veins lined and bridged by microcrystalline silica and filled with ferroan dolomite in dark Arkansas Novaculite from the power plant at Broken Bow/Beavers Bend	94
64. Phosphate nodule containing botryoidal phosphate with chalcedony from the Atoka Chert Pit	96
65. Photomicrograph of a phosphate nodule from the Atoka Chert Pit.....	97
66. Thin section photomicrograph of phosphate nodule with a clotted, peloidal texture from I-35 outcrop.....	98
67. Thin section photomicrograph of phosphate nodule containing spherulites of prismatic apatite crystals within a groundmass of chalcedony from the I-35 outcrop	99
68. Thin section of photomicrograph phosphate nodule showing spherulites of prismatic apatite in a linear array in a chalcedony groundmass from the I-35 outcrop....	100
69. Thin section of photomicrograph phosphate nodule with botryoidal apatite crystals outlining the shape of Radiolaria from the Hall 2B core	101
70. Photomicrograph of phosphate nodule pore filled mostly with bitumen from the Atoka Chert Pit	102
71. Photomicrograph of phosphate nodule shows two generations of phosphate and a large pore lined with dolomite and filled with bitumen from the Atoka Chert Pit outcrop	103
72. Quartz veining in black Arkansas Novaculite from the power plant Broken Bow/Beavers Bend.....	105
73. Thin section photomicrograph of Arkansas Novaculite with planar veins with silica lining and pyrite fill from the Atoka Chert Pit.....	106
74. Thin section photomicrograph of a pyrite-filled vein and bitumen in the I-35 outcrop	107
75. Arkansas Novaculite sample showing bitumen, pyrite veins and quartz veining from near the Arkansas Novaculite and Blaylock Sandstone contact in Broken Bow/Beavers Bend.....	108

76. Backscattered electron micrograph showing peloidal chert matrix with interstitial amorphous organic matter from the I-35 outcrop	111
77. SEM image showing homogeneous chert matrix with curled organic films in Arkansas Novaculite from the Atoka Chert Pit	112
78. SEM image showing abundant organic matter, peloidal chert matrix, and angular to subround chert clasts in the Woodford Shale from the Hall 2B core	113
79. SEM image showing organic films coating and within silica spherules, I-35..	114
80. SEM image showing complex spiral forms in organic film, Atoka Chert Pit ..	115
81. SEM image showing irregular spiral film in novaculitic chert that is curled at both ends from novaculitic chert at the I-35 outcrop	116
82. SEM image showing irregular organic film in novaculitic chert from the Poe #1-29 core.....	117
83. SEM image showing framboidal and dispersed euhedral pyrite within Arkansas Novaculite, Atoka Chert Pit.....	119
84. SEM image showing pyrite framboid, Arkansas Novaculite, Atoka Chert Pit..	120
85. SEM image showing cubic crystal and nanometer-scale porosity within an argon ion milled sample of novaculitic chert from the Poe #1-29 core	121
86. SEM image showing iron cross pyrite twin in circular mass of organic matter within Arkansas Novaculite, Atoka Chert Pit	122
87. Backscattered SEM image showing isolated pores in novaculitic chert, I-35 ..	124
88. Close up SEM image showing pore containing euhedral crystals in novaculitic chert, I-35 outcrop.....	125
89. SEM image showing fissure porosity associated with natural fractures in Woodford chert, Poe #1-29 core	126
90. SEM image showing abundant fissure porosity in a platy clay particle, Woodford Shale, Poe #1-29 core	127
91. SEM image showing fissure porosity and irregularly shaped pores in the Broken Bow/Beavers Bend outcrop	128
92. SEM image showing intercrystalline porosity within a pyrite framboid, Atoka Chert Pit	129
93. SEM image showing hexagonal porosity within an argon ion milled sample of Arkansas Novaculite Atoka Chert Pit	130
94. SEM image showing nanometer-scale fissure porosity within organic matter, I-35 outcrop	131
95. Depositional model of the Woodford Shale and Arkansas Novaculite	137
96. Paragenetic sequence for the Arkansas Novaculite and novaculitic chert in Oklahoma.....	139
97. Present day cross-section through the Ouachita Mountains fold and thrust belt in Oklahoma.....	140

CHAPTER I

INTRODUCTION

Limited research has been performed in recent years on the origin of novaculitic chert and the Arkansas Novaculite in the Ouachita Orogen of southeastern Oklahoma and in the Woodford Shale in the Oklahoma Shelf, which spans the modern-day Arkoma, Anadarko, and Ardmore Basins. Most literature on this subject was published prior to 1980 (e.g., Goldstein and Hendricks, 1953; McBride and Thomson, 1970; Jones and Knauth, 1979). Many hypotheses exist to explain the origin and depositional environment of the chert, but further research needs to be performed that applies emerging analytical technology and geologic concepts in order to formulate a more modern set of paleoenvironmental interpretations.

The term, Arkansas Novaculite, was first used by Griswold in 1892. In 1909, Purdue constrained the name to siliceous rocks between the Missouri Mountain Shale and the Stanley Shale in the Ouachita Mountains. Twenty-five years later, Miser (1917) was the first to subdivide the Arkansas Novaculite into three distinct members. The lower and upper members consists of white, massive, fine-grained chert, whereas the middle member consists of rhythmically interbedded brownish-gray chert and black shale (Neilsen, 1988; Lowe, 1989). The three

members are most easily recognized in Arkansas, while in Oklahoma the chert is contained principally in rhythmic successions that are characteristic of the middle member. Although the novaculite is predominantly a sedimentary rock, some of the formation has been weakly metamorphosed within the interior of the Ouachita Orogen in southeastern Oklahoma and southwestern Arkansas. Chert exhibiting a polygonal triple-point texture characteristic of this metamorphism is in Magnet Cove, Little Rock, and Potash Sulfur Springs, Arkansas, and near Broken Bow, Oklahoma (Keller et. al., 1985).

The Arkansas Novaculite is of Silurian-Mississippian age in the Ouachita orogenic belt; it has been interpreted as a petroleum source rock and has been productive locally as a reservoir (Godo, et. al., 2011). Similar deposits occur in the Devonian-Mississippian strata of the Woodford Shale in the Arkoma, Anadarko and Ardmore Basins, and the significance of the chert for reservoir development in these basins is incompletely understood, particularly the degree that the chert contributed to oil generation and the potential of the chert to transmit hydrocarbons in commercial reservoirs. Further research concerning the depositional, diagenetic and tectonic setting of the Arkansas Novaculite will lead to an expanded knowledge of the depositional setting of the novaculitic chert and the paleoceanography of the southern Midcontinent, as well as the significance of the chert as a petroleum source rock and reservoir rock.

Taff (1902) was among the first geologists to map Woodford strata on the southern side of the Arbuckle Mountains in Oklahoma. Interestingly, he applied the term, Woodford Chert to the strata that are today mapped as Woodford Shale. After nearly a century of research on the Woodford Shale, a regional picture of the Woodford deposition has emerged (Comer, 1992, 2008). According to Comer (2008), preservation of organic matter and generation of the novaculitic chert within the Woodford Shale were influenced by development of an oxygen-deficient water column and marine upwelling. He suggested that the upwelling was primarily a coastal process resulting from Ekman circulation driven by trade winds. He further suggested that

hypersaline brines (i.e., a halocline) contributed to density stratification, oxygen deficiency, and organic matter preservation. Alternatively, Kvale and Bynum (2014) suggest that upwelling during Late Devonian and Early Mississippian time was more likely related to oceanic circulation at the subtropical margin of the southern tradewind belt, rather than coastal upwelling driven by aridity and high evaporation rates.

Modern oceanic upwelling systems are best developed in the tropics and subtropics on the leeward sides of continents, although they are present in high latitudes as well. The ocean floors and outer continental shelves beneath these systems are typically covered with sediment rich in opaline silica and have elevated concentrations of phosphate (Witzke, 1987; Kvale and Bynum, 2014). Indeed, it is widely known that novaculitic chert contains an abundance of siliceous microfossils and phosphate nodules (Kvale and Bynum, 2014). The Arkansas Novaculite and the novaculitic chert in the Woodford Shale are similar in appearance and are thought to be parts of the same depositional system (Sholes and McBride, 1975). It has been suggested that the chert formed only in oceanic settings (Sholes and McBride, 1975). However, the novaculitic chert in the Woodford Shale clearly extended onto the continental shelf (Rich, 1951; Comer, 1992; Piper and Calvert, 2009; Schieber and Riciputi, 2004). Modern analysis of Devonian shale and chert, which reveals evidence of erosion, current reworking, and slope instability, supports a wider range of depositional processes settings along the Ouachita embayment (Byers, 1973; Pashin and Ettensohn, 1992, 1995; Schieber, 1994; Pashin et. al., 2011; Callner, 2014).

Due to the chert's high silica content, the formation is naturally brittle and contains abundant natural fractures. This brittleness helps facilitate hydraulic fracturing during Woodford Shale drilling (Morrison, 1984; Foltz et. al., 2016). Because of abundant natural fractures characteristics, the chert also may transmit significant amounts of fluid. However, little is known

about matrix porosity in the novaculitic chert, and the ability of the matrix to store and transmit hydrocarbons.

The overarching goal of the proposed research is to conduct an integrated sedimentologic and petrologic investigation of novaculitic chert in the Ouachita foreland, which includes the Ouachita Orogen, the Arkoma Basin, the Anadarko Basin and the Ardmore Basin, as well as the flanks of the major intervening basement uplifts, including the Arbuckle and Wichita uplifts. Study locations for this research include Caddo, Carter, Hughes, Atoka, and McCurtain Counties (Fig. 1, Table 1).

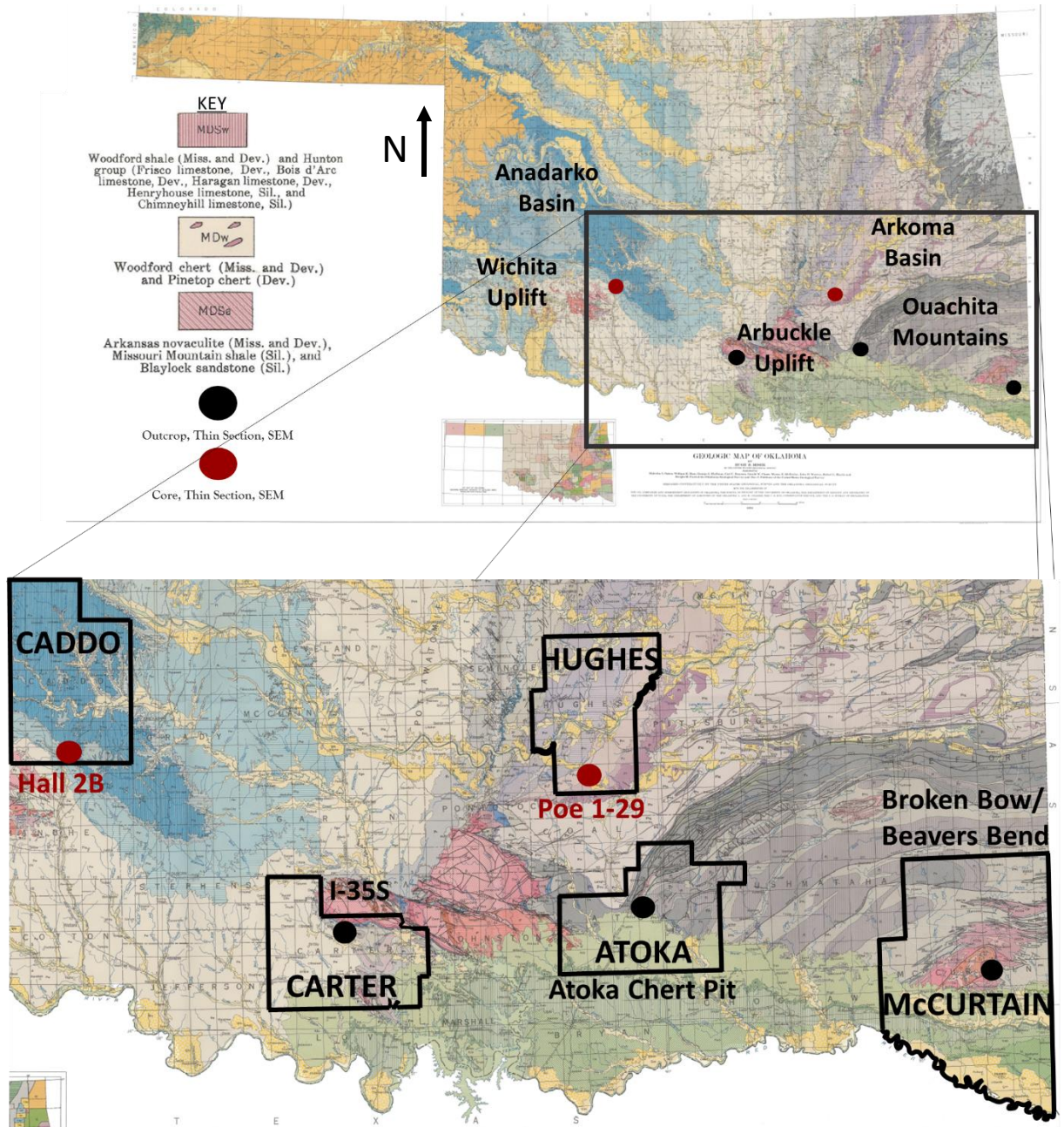


Figure 1. Geologic map of Oklahoma showing locations of outcrops and cores used in this study (map after Miser, 1954).

Table 1. Locality register of outcrops and cores used in this study.

Location	Type	Description	County	Latitude and Longitude
I-35S	Outcrop 1	Southern Outcrop	Carter	34.351945 N, -97.14884 W
I-35S	Outcrop 2	Northern Outcrop	Carter	34.353000 N, -97.149025 W
Atoka	Outcrop 1	Chert Pit Outcrop	Atoka	34.375125 N, -96.109858 W
Broken Bow	Outcrop 1	Outcrop at U.S. Rte 259A	McCurtain	34.129142 N, -94.686043 W
Broken Bow	Outcrop 2	Float at Powerplant	McCurtain	34.139030 N, -94.686440 W
Broken Bow	Outcrop 3	Outcrop at U.S. Rte 259	McCurtain	34.251694 N, -94.784493 W
Poe 1-29	Core	Core from Hughes County	Hughes	34.793961 N, -96.248350 W
Hall 2B	Core	Core from Caddo County	Caddo	34.897133 N, -98.325991 W

Outcrops and cores formed the basis this study and were examined using a variety of analytical techniques to help characterize and determine the origin of the chert. To achieve this goal, basic features such as rock type, physical and biogenic sedimentary structures, petrology, and diagenesis were characterized and analyzed in outcrop, hand sample, thin section, and SEM images. The following four hypotheses were developed that constitute the basis of this research:

- i. Novaculite formed from a biogenic silica source in a region influenced by marine upwelling.
- ii. The Arkansas Novaculite and Woodford novaculitic chert formed by similar depositional processes.
- iii. The chert has a depositional setting spanning continental shelf, continental slope and basinal environments.

- iv. Novaculitic chert is an important component of unconventional reservoirs in the southern Midcontinent, not only from the standpoints of brittleness and organic content, but also in terms of hydrocarbon storage potential.

To test each hypothesis, a series of analytical methods was utilized to produce data and inform interpretations of origin and hydrocarbon potential. To determine the origin of the novaculitic chert, outcrop analysis, core analysis, thin section analysis, and SEM analysis enabled observation from meter- to nanometer-scale, thereby enabling the examination of a broad range of depositional characteristics. Thin section and SEM analysis provided critical information on reservoir characteristics, including pore habit and geometry, natural fractures, and the habit and distribution of organic matter. The next section focuses on geologic setting and previous work, and a methods section follows that provides a detailed description of the analytical methods used in this study.

CHAPTER II

GEOLOGICAL SETTING AND PREVIOUS WORK

II.1 Tectonic Setting

The Ouachita Mountains are a complex, sinuous, and primarily east-west trending orogenic belt that is exposed at the surface in southwest Arkansas, southeast Oklahoma, central and southwest Texas and a small portion of Mexico (Fig. 2) (Miser, 1929; Keller and Cebull, 1973; Arbenz, 1989; Suneson, 2008). Part of the frontal orogen is exposed in southeastern Oklahoma as a series of arcuate folds and thrust faults with traces that curve from west at the Arkansas-Oklahoma state line to south where the orogen is overlapped by the Gulf of Mexico coastal plain. Formation of the Ouachita Orogen can be broken down into three major tectonic events: (1) Iapetan rifting and formation of the Southern Oklahoma Aulacogen and the Ouachita Embayment, (2) mid-Paleozoic initiation of subduction and late-Paleozoic growth of the Ouachita orogenic belt, and (3) late-Paleozoic subsidence of the associated foreland basins (Lowe, 1985; Thomas, 2006). Opening of the Ouachita Embayment began around 530 Ma (Early Cambrian) during the breakup of the supercontinent, Rodinia. During this time, a triple-junction rifting event occurred—two of the rift arms formed the spreading and transform zones bounding the an embayment of the Rheic Ocean called the Ouachita Embayment; the third rift-arm failed, thereby forming the continental rift arm that is known as the Southern Oklahoma Aulacogen (Thomas,

2006). While the ocean floor was spreading and subsidence was occurring during Iapetan rifting, shale, sandstone and chert slowly accumulated along the margin of the Ouachita Embayment (Viele, 1979).

The overall outline of the Ouachita Embayment is expressed today in the general outline of the current thrust belt (Fig. 2). During closure of the Rheic Ocean, an Ouachita accretionary complex formed in eastern Texas, southeast Oklahoma, southern Arkansas, northern Louisiana and central Mississippi. As collision began, the accretionary wedge was obducted onto the Laurussian craton, thereby forming the Ouachita Orogen. Closure of the Iapetus and Rheic Oceans and the collision of Laurussia and Gondwana culminated in the formation of Pangea (Wickham, 1976; Viele, 1979; Arbenz, 1989; Thomas, 2006).

The Broken Bow Uplift, which forms the core of the orogen in southeastern Oklahoma, is oriented northeast to southwest and is structurally higher than the rest of the surrounding area. The cause of this change in orientation and structural elevation is still debated (Suneson, 1995). Subsequent breakup of Pangea resulted in the opening of the Atlantic and Gulf of Mexico basins and subsequent onlap of the Gulf of Mexico coastal plain onto the southern part of the Ouachita Orogen in Oklahoma. Today, the Ouachita Orogen is an extensive, intricate tectonic belt containing innumerable large-scale folds and thrust faults (Goldstein, 1952; Arbenz, 1989, 2008). The Ouachita fold belt stretches from Mississippi to Mexico and exposes Paleozoic sedimentary and low grade metamorphic rocks (Goldstein, 1952; Goldstein and Hendricks, 1953; Arbenz, 2008). The exposed rock generally weathered and has been deeply eroded. Rock types contained within the Ouachita Orogen include sandstone, shale, chert, novaculite, limestone, and tuff (Fig. 3) (Miser, 1929; Neilsen, 1988; Suneson, 1995; Cardott, 2013).

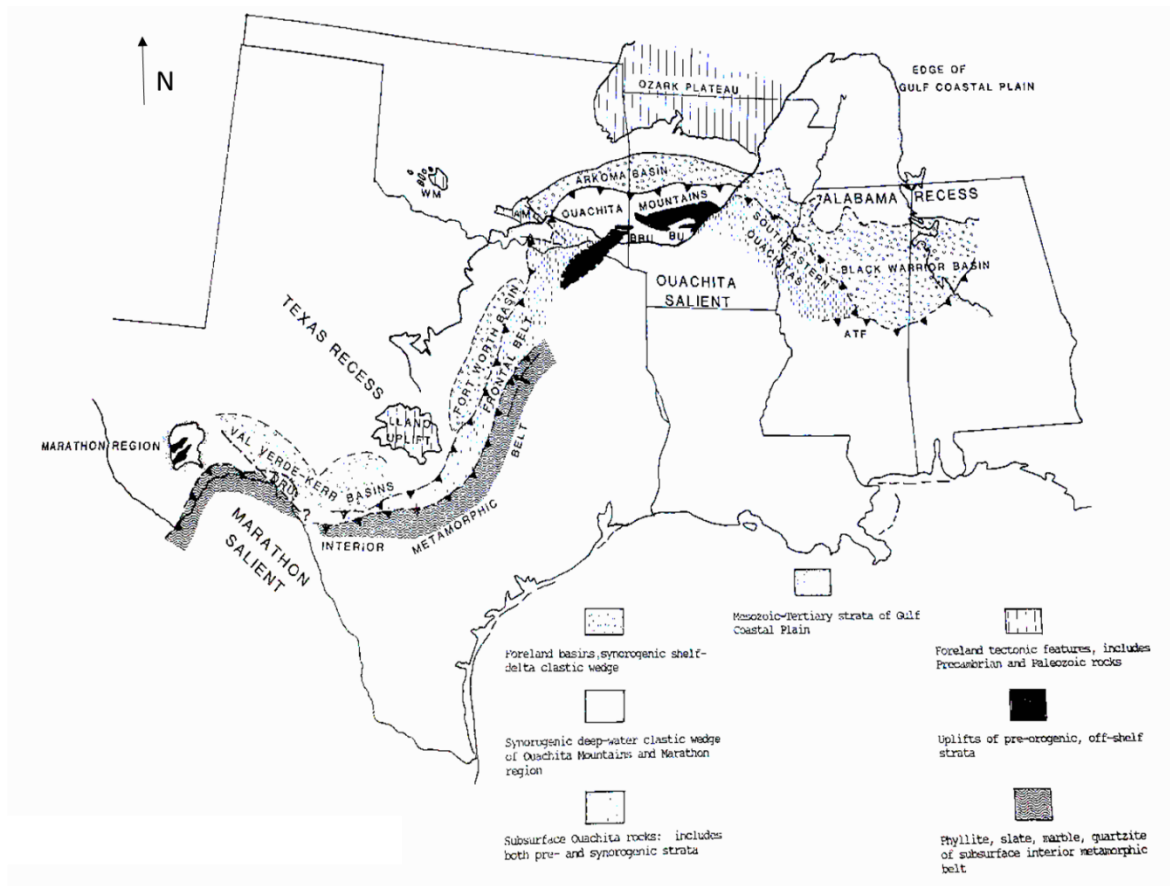


Figure 2. Index map of Ouachita orogenic belt (after Viele, 1989).

II.2 Arkansas Novaculite

The Arkansas Novaculite is Middle Silurian-Early Mississippian in age and is composed principally of cryptocrystalline to microcrystalline silica with abundant natural fractures (Fig. 3) (Miser and Purdue, 1929; Goldstein, 1952; Morris, 1974). The formation ranges in thickness from 250-950 feet (Miser and Purdue, 1929; Goldstein and Hendricks 1953; Morris 1974; Jones and Knauth, 1979). Although the formation is relatively thin, it was deposited over a timespan of ~55 million years (Suneson, 1995). The Arkansas Novaculite is composed of three informal members: a lower, middle, and upper member (Honess, 1923; Miser and Purdue, 1929; Neilsen, 1988). The lower member of the Arkansas Novaculite is white-light gray in color, massive, fine-grained, and

commonly spiculitic and calcareous (Goldstein and Hendricks, 1953; Morris, 1974; Lowe, 1989; Cecil 2004). The lower member's age is loosely constrained as Silurian and/or Devonian due to a lack of fossils (Lowe, 1989). Next, the middle member (Devonian – Mississippian) contains black shale that is interbedded with massive to laminated chert beds having sharp to gradational contacts and abundant radiolaria. Finally, the upper member (Mississippian) is white-light gray, laminated, granular, and contains breccias of black chert and phosphate. Although a large portion of the formation is white, many areas vary in color and shade (green, brown, red, black and yellow) due to the influence of carbonaceous matter and iron and manganese oxides (Purdue and Miser, 1923). In addition to this, numerous phosphate nodules occur in the formation (Puckette, 2013).

The Arkansas Novaculite is, in large part, laterally equivalent to the Woodford Shale in Oklahoma and the Caballos Novaculite of the Marathon Uplift in the Ouachita Orogen in west Texas (Miser and Purdue, 1923; Goldstein and Hendricks, 1953; Morris, 1974; Arbenz, 1989) (Fig. 3). The Novaculite has been subjected to low-grade metamorphism in the area of the Broken Bow Uplift, as exhibited by polygonal, triple-point texture, particularly in western Arkansas and McCurtain County, OK (Keller et. al. 1985; Suneson, 1995). The Arkansas Novaculite is primarily a bedded chert deposit that contains abundant radiolaria. However, it also includes spicular chert, sapropelic chert, calcareous chert, siliceous shale, argillite, and highly fissile, sapropelic shale (Goldstein and Hendricks, 1953; Suneson, 1995). All of these rock types in places grade into one another and can be difficult to distinguish (Suneson, 1995). Many geologists have differing opinions as to the origin of the Arkansas Novaculite, but many agree that a large portion of it was deposited under relatively deep and quiet marine conditions (Sholes and McBride, 1975). However, disagreement exists concerning the deposition of the various rock types within the formation. Ideas range from subaerial to deep marine (Neilsen, 1988; Suneson, 1995).

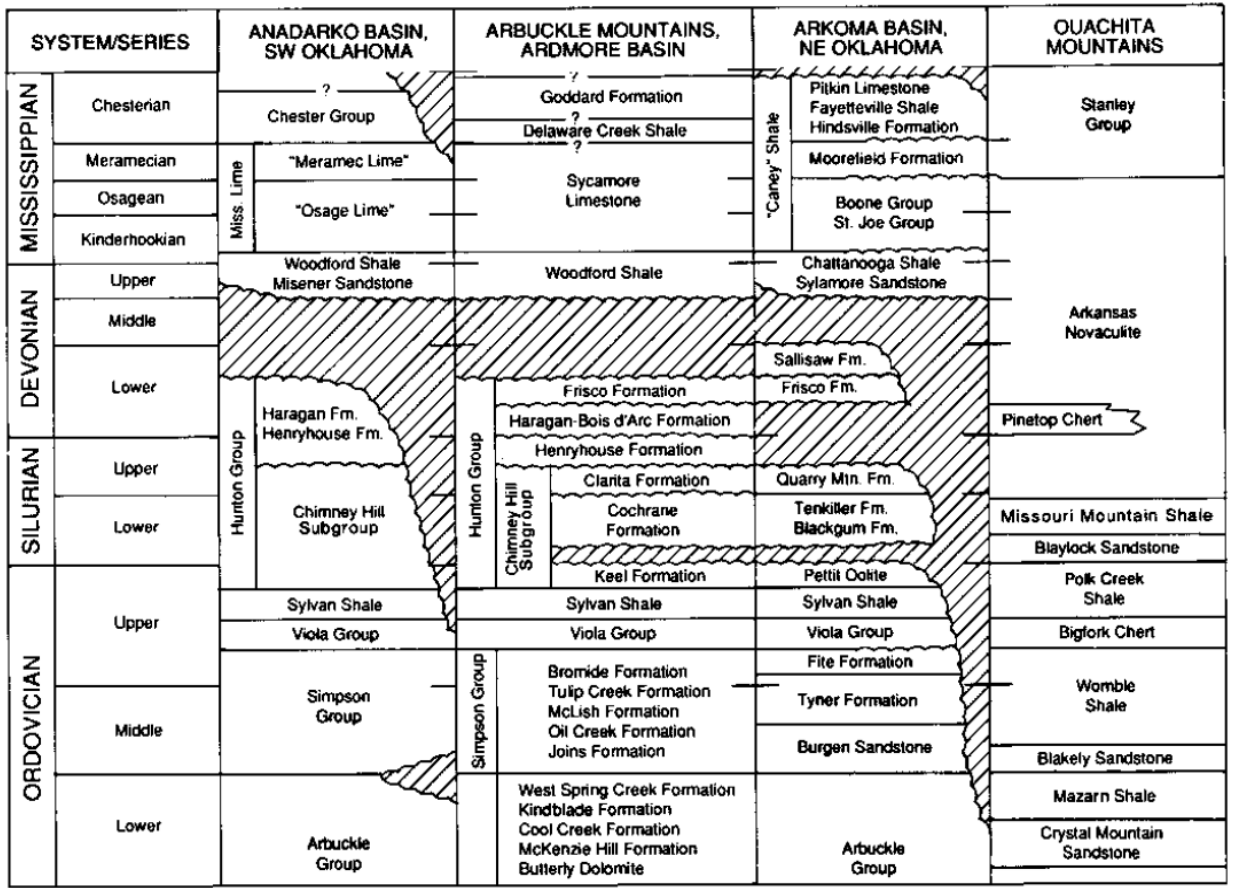


Figure 3. Stratigraphic column of the Anadarko Basin, Arbuckle Mountains, Arkoma Basin and Ouachita Mountains (modified from Johnson and Cardott, 1992).

There is confusion about the definition of the term, novaculite, and the differences between novaculitic chert and common chert. Many scholars use the two terms interchangeably, while others make clear distinctions between the two types of rocks. Novaculite is a word derived from the Latin word for razor (novacula) and has been used for centuries to make tools, whetstones and razors (Goldstein, 1959). The term "novaculite" was first used in the Ouachita Mountains by Schoolcraft in 1819, who referred to a mineral called novaculite at Hot Springs, Arkansas (Sholes and McBride, 1975). According to Folk and Weaver (1952), Arkansas Novaculite is a type of chert that is homogeneous. They also stated in reference to chert deposits that "sedimentary silica exists in at least three major modifications, those of normal quartz,

chalcedony, and opal. The sequence from quartz through chalcedony to opal is marked by decreasing grain size, increasing water content, and decreasing refractive index and density” (p. 498). According to Sholes and McBride (1975), novaculite is a variety of chert that breaks with a subconchoidal fracture and has a slightly gritty texture and dull lustre on fresh fracture surfaces. In addition, they also proposed that fracture surfaces in common chert are smooth and lustrous when freshly broken the chert has much less uniform particle size than novaculite, and contains many grains smaller than one micron in diameter. Morris (1975) defined novaculite as a “light colored, extremely fine-grained, homogeneous, highly fractured siliceous rock similar to chert but characterized by a dominance of quartz rather than chalcedony” (p.128). In 1976, Keller et. al. concluded that the term “novaculite” is a petrologic name for a thermally metamorphosed chert which shows polygonal, triple-point texture. Hesse (1988) proposed that novaculite is light colored and a very dense, quartz chert that has undergone diagenesis and low-intermediate-grade metamorphism and is from the Ouachita Mountains in Arkansas and Oklahoma. According to Suneson (1995), chert is an extremely fine-grained rock that is 100% silica, shatters when hit with a hammer, and has a smooth texture on fracture surfaces, while novaculite is a variety of chert that is characterized by fracture surfaces that are gritty in texture. Based on literature and sample analysis, novaculite, according to this paper, is defined by a dull, chalky luster, is well bedded and contains abundant orthogonal fractures. Novaculitic chert is truly cryptocrystalline because the individual quartz crystals are extremely difficult to discern under plane-polarized and cross-polarized light. This type of chert also appears blueish on fresh surfaces, which is thought to be related to opaline silica preservation. Chert on the other hand has a vitreous luster on fresh surfaces, is poorly bedded and exhibits concoidal fractures.

II.3 Woodford Shale

The Woodford Shale is an extremely important hydrocarbon source rock in Oklahoma and the Midcontinent (Cardott, 2012). Since 2008, more than 500 directional wells have been completed in the Woodford Shale in the Anadarko Basin alone (Callner, 2014). The chert, which aids the hydraulic fracturing process due to its brittle nature but can cause excessive bit wear during drilling, is interbedded with radioactive sapropelic shale in much of the Woodford Shale in Oklahoma, and where present tends to increase in abundance in the upper part of the Devonian section (Sullivan, 1985; Cardott, 2012; Puckette et al., 2013; Foltz et. al., 2016) (Fig. 4). The Woodford Shale is Middle Devonian to Early Mississippian in age. The Woodford disconformably overlies the Hunton Group (Late Ordovician-Early Devonian), and is disconformably overlain by the Sycamore Limestone, Mississippi lime, and Caney Formation which contain strata ranging from Early to Late Mississippian in age (Tournasian-Serpukhovian) (Sullivan, 1985). The novaculitic chert within the Woodford Shale is largely Upper-Devonian-Mississippian, with the Devonian portion containing more chert than the Mississippian. The shale is light gray to black in color, marine in origin, contains abundant *Tasmanites* algal cysts and is carbonaceous to siliceous. It is also fissile to blocky, and contains subordinate amounts of greenish-gray shale, phosphate nodules and pyrite (Krystyniak, 2003; Cardott, 2012).

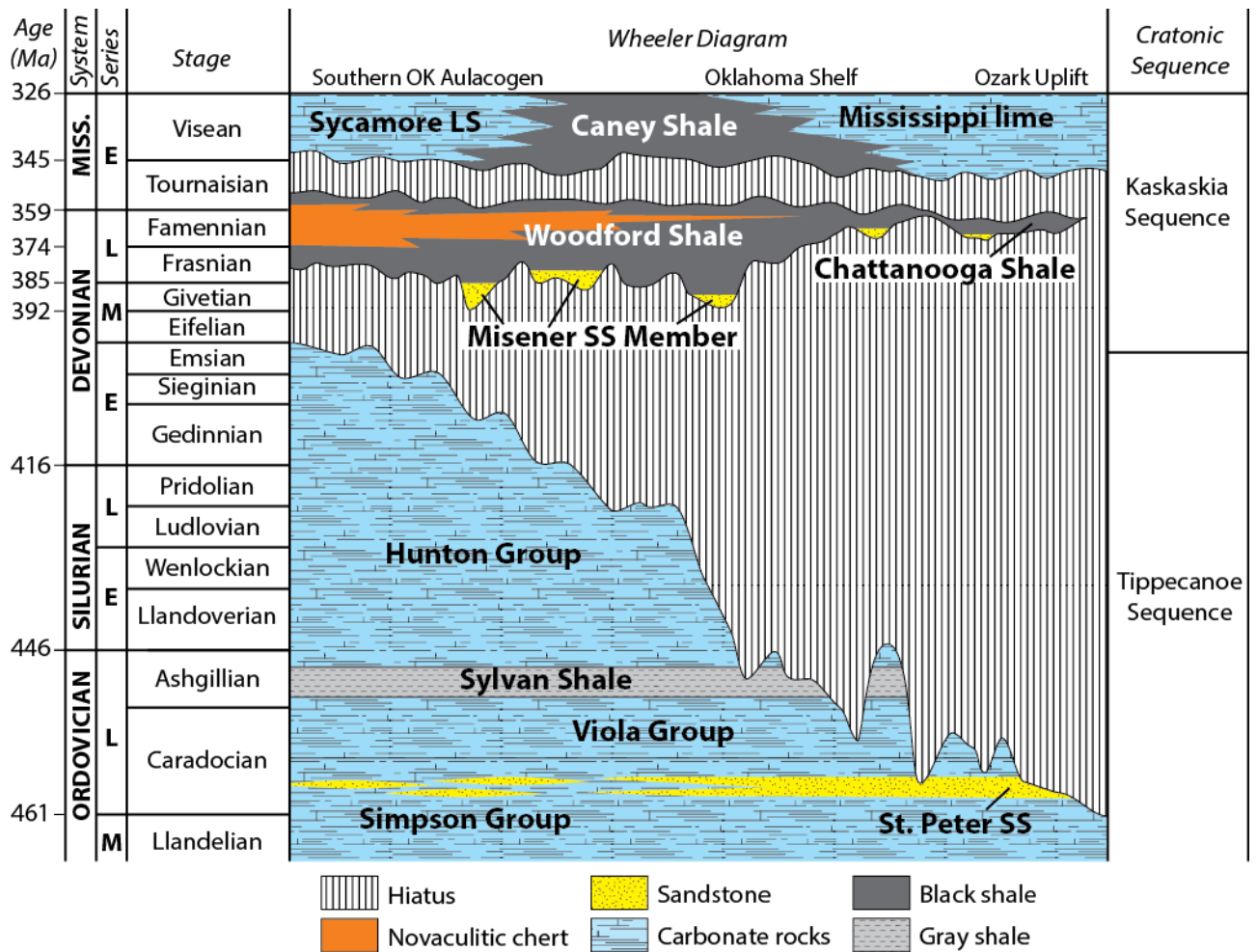


Figure 4. Wheeler diagram showing formations and unconformities bounding the Woodford Shale. Note the novaculitic chert and the Misener Sandstone Member within the Woodford Shale.

The Woodford Shale was deposited contemporaneously with other organic-rich, dark shale formations of Middle Devonian-Early Carboniferous age, which include Ohio Shale, the Chattanooga Shale, and the New Albany Shale. These units cover a substantial part of North America and are generally thought to have been deposited in oxygen deficient basins (Ettensohn, 1985; Over, 1990). Sedimentologic, paleontologic, and geochemical evidence indicates that Woodford Shale depositional environments varied from oxic to anoxic and was at times euxinic (Callner, 2014). Thickness of the formation ranges from near zero to 125 feet in much of the

Oklahoma shelf, with thickness locally exceeding 400 feet in the Anadarko Basin (Schmoker and Hester, 1990).

The Woodford Shale is typically divided into three informal members: a lower, middle and upper member. These divisions are based on composition, palynomorphs, geochemistry and log signatures (Slatt et. al., 2012; Cardott, 2005; Cardott, 2013). However, these members appear to be highly time transgressive and thus do not appear to be marker-bound stratigraphic units (Callner, 2014). In 2011, Caldwell subdivided the Woodford Shale into seven lithofacies and fifteen stratigraphic units based upon mineralogy and total organic carbon (TOC) content, and this type of finer subdivision appears to more accurately represent the internal stratigraphy of the formation (e.g., Slatt, 2012).

The shale and chert layers in the Woodford can be differentiated visually at macroscopic and microscopic level. According to Fishman et. al. (2010), the siliceous mudrocks are composed primarily of microfossils like *Tasmanites* and terrigenous detrital material. The chert appears to be composed primarily of recrystallized radiolaria and other siliceous microfossils and contains little terrigenous material (Fig. 5). The sapropelic shale has an average of 13.3% TOC, while the chert has an average of 4.5% TOC (Fishman et. al., 2010). This could possibly be due to the high *Tasmanites* and amorphous kerogen content of the siliceous mudstone. Vigran et al. (2008) suggested that *Tasmanites* can be a major source for hydrocarbons in organic-rich formations.

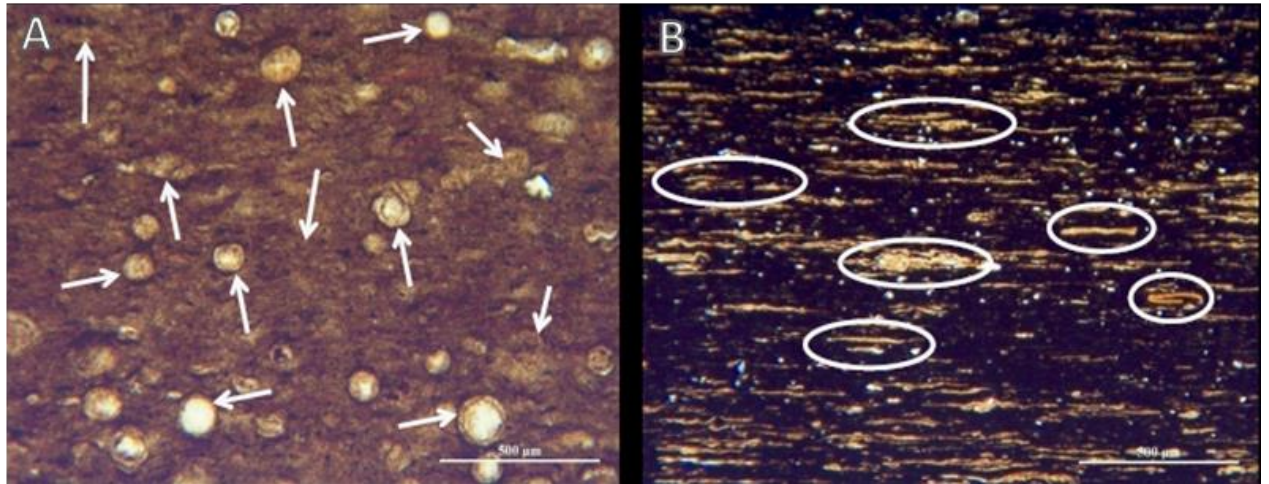


Figure 5. (A) Novaculitic chert containing silica spherules thought to have replaced Radiolaria (white arrows). (B) Siliceous mudstone containing flattened Tasmanites (white circles) (Fishman et. al., 2010).

II.4 Competing and Evolving Schools of Thought

There is no formal agreement about the origin of the Arkansas Novaculite, and many of the explanations are from the 1970s and earlier. There are multiple competing schools of thought about the origin of the chert and the environments in which the chert was deposited (Jones and Knauth, 1979; Hesse, 1988; Viele, 1989; Suneson, 1995). As stated by Goldstein and Hendricks (1953, p. 428) the Arkansas Novaculite is “the best known yet, most controversial of the siliceous sediments of the Ouachita facies”. The hypotheses range from subaerial to abyssal in deposition locale, with sources of the silica ranging from detrital grains, biota and volcanic ash (Folk and McBride, 1976). The oldest known interpretation of origin dates back to 1860 when David Dale Owen suggested that metamorphism of sandstone contributed to the formation of the novaculite (Owen, 1860). Overall, there are five broad categories in which interpretations can be categorized (McBride and Thomson, 1970) (Table 2):

Table 2. Comparison of hypotheses for the origin of the Arkansas Novaculite in the Ouachita Mountains (Griswold, 1890; Beecher et. al, 1895; Goldstein and Hendricks, 1953; McBride and Thomson, 1970; Jones and Knauth, 1979).

Author(s)	Year	Hypothesis
Owen	1860	Hydrothermal alteration of sandstone
Branner	1888	Metamorphosed chert
Comstock	1888	Hydrothermal deposits and alteration of older silica
Griswold	1892	Deposition of a very fine-grained detrital quartz
Hinde	1894	Accumulation of biogenic silica
Rutley	1894	Silicification of dolomite or dolomitic limestone
Derby	1898	Silicification of limestone
Weed	1902	Chemical precipitate in deep sea
Van Hise	1904	Recrystallized biogenic silica
Baker	1918	Metamorphosed chert
Honess	1923	Part silicified and devitrified volcanic ash (abiotic precipitation) But mostly abiotic precipitation
Honess	1923	Altered of volcanic ash
Miser and Purdue	1923	Chemical precipitation of silica and scarce amounts of calcareous material
Miser and Purdue	1929	Chemical precipitation of silica and scarce amounts of calcareous material
Henbest	1936	Chemical precipitation
Hendricks et al	1937	Accumulation of biogenic silica
Goldstein and Hendricks	1953	Diagenetic alteration of volcanic ash; minor contribution from siliceous biota
Harlton	1953	Replacement of limestone driven by syntectonic fracturing
Goldstein	1959	Alteration of volcanic ash
Park	1961	Recrystallized biogenic silica
Park and Croneis	1969	Recrystallized biogenic silica
McBride and Thomson	1970	Diagenetic alteration of biogenic silica
Folk	1973	Accumulation of biogenic silica
Keller and Cebull	1973	Volcanic source of silica
Morris	1974	Recrystallized biogenic silica
Lowe	1975	Accumulation of biogenic silica
Folk and McBride	1976	Diagenetic alteration of biogenic silica accumulations
Folk and McBride	1977	Diagenetic alteration of biogenic silica accumulations
Jones and Knauth	1979	Accumulation of biogenic silica
Cecil	2004	Eolian dust as source of silica

Alteration of volcanic ash
Chemical precipitation
Metamorphism and hydrothermal alteration
Silicification of limestone and dolomite
Accumulation of biogenic silica

The first hypothesis is alteration of volcanic ash associated with arc volcanism associated with extensive subduction and tectonic convergence as the Rheic Ocean began closing during Devonian-Mississippian time. If volcanism was occurring, the ash falls were deposited during a time when minimal detrital sediment was being delivered to the Ouachita Embayment. Organisms like siliceous sponges and radiolaria are thought to have thrived in the high silica environment, which explains the high fossil content of the Arkansas Novaculite (Goldstein and Hendricks, 1953; Goldstein, 1959; Lowe, 1975). The silica would then have been redeposited on the sea floor by organisms or by non-organic processes (Suneson, 1995). Evidence of volcanism during this time period is also supported by the presence of volcanic tuff found in southeastern Oklahoma, particularly in the Broken Bow Uplift (Nielsen, 1988). Although tuff has been found in some of the surrounding sandstone and shale, no tuff beds have been found within the Arkansas Novaculite (Suneson, 1995).

According to the second hypothesis, “the silica for the novaculite was deposited in the sea by chemical precipitation” (Miser and Purdue, 1923, p. 8). This hypothesis was popular during the early 20th century (Weed, 1902; Honess, 1923; Miser and Purdue, 1923, 1929; Henbest, 1936). Similar to the first theory, this theory also assumes that there was very little detrital material being deposited at the time. The lack of detrital material could have possibly been a result of high sea level, absence of actively eroding source terranes, or high rates of meteoric precipitation (Miser and Purdue, 1929). This hypothesis is not necessarily incompatible with volcanic or biogenic silica sources, and can be considered a simple Neptunian concept of precipitation of silica from seawater.

The third hypothesis describes the Arkansas Novaculite as being formed by metamorphic, hydrothermal, or diagenetic alteration of detrital quartz (Griswold, 1893; McBride and Thomson, 1970). Owen (1860) was one of the first scientists to propose a novaculite origin: sandstone that was altered or metamorphosed by the permeation of heated alkaline siliceous waters. Similarly,

Comstock (1888) believed the novaculite to be a product of the alteration of quartz in place, by the action of hot water. Branner (1888) did not think that novaculite originated from metamorphosed sandstone, but rather from the metamorphism of preexisting chert (Griswold, 1890). In 1892, Griswold proposed that the novaculite is simple, fine-grained siliceous sediment that was mechanically (detrital) deposited (Beecher et.al., 1895). This hypothesis was prevalent until 1918, when other ideas, primarily accumulation of biogenic silica, gained popularity. However, a reemergence of this hypothesis was precipitated by Cecil (2004), who recognized eolian quartz in the Huntersville Chert of the Appalachian Basin. Cecil further postulated that temporal and spatial variations in the particle size and composition of eolian dust can account for the variations between coeval shallow-water chert and the deep-water novaculite. The historical literature supporting metamorphism or alteration of terrigenous sediment goes into great detail about the mechanism that alters the rock, but makes little mention of the source of the detrital quartz. In addition, if a formation were altered from detrital quartz into chert, it would require either elevated temperatures or widespread pressure solution. Any alteration, as exhibited by the presence of polygonal, triple point textures, would be present throughout the entire formation if this mechanism were the origin of the novaculite. However, this submetamorphic texture is only found in four locations in the outer Ouachita thrust sheets and in the Arkoma and Anadarko Basins, not throughout the entire formation (Keller et. al., 1985).

The fourth hypothesis, silicification of limestone and dolomite, suggests that carbonate rocks have been replaced with silica during diagenesis. Supporters of this theory believed that the Arkansas Novaculite was limestone at the time of deposition, and silicification was largely epigenetic, a result of deep burial and intensification of hydrothermal action during the Ouachita orogeny (Goldstein and Hendricks, 1953). Rutley (1894) observed “irregular and rhomb-shaped cavities” in the novaculitic chert, which he concluded represented “crystals of a rhombohedral carbonate, probably dolomite”, and that the carbonate replacement was not entirely complete

(Rutley, 1894, p.19). Contrary to this, Griswold (1892) concluded that the presence of these cavities are not evidence for the whole formation being derived from siliceous replacement of limestone and dolomite. Still, some also thought that carbonate material was deposited synorogenically with the silica (Goldstein and Hendricks, 1953). In some locations, portions of limestone and dolomite are said to still be present after silicification has occurred, particularly in the Silurian and youngest Mississippian chert deposits in the Ouachita Orogen. Today, an outcrop at Beaver Bend State Park exhibits two distinctive thin carbonate units, which are apparent due to their weathered appearance compared to the novaculite, containing nodular chert within the upper division of the Arkansas Novaculite (Neilsen, 1988; Suneson, 1995). While these deposits may be present in the upper and possibly lower portion and, therefore, mapped with the novaculite in the Broken Bow Uplift, they are not equivalent to the main Upper Devonian-Lower Mississippian novaculitic chert succession.

Finally, the fifth hypothesis is that the novaculitic chert originated from the accumulation and diagenesis of biogenic silica. The presence of abundant radiolaria (Cambrian -Holocene), *Tasmanites*, and sponge spicules within the Arkansas Novaculite acts as supporting evidence for this hypothesis. Although this hypothesis did not gain popularity until the latter half of the twentieth century, scientists like Hinde (1894) and Van Hise (1904) recognized the role that biogenic silica could possibly play in the formation of the chert long before modern technological advances helped popularize the idea. The literature on siliceous deposits has increased dramatically since the 1970's. This is in part due to the development of an extraction technique to recover radiolaria from chert for biostratigraphic age dating (Pessagno and Newport, 1972; Hein and Parrish, 1987).

In addition to this, the exploration of today's oceans reveals potential modern analogs for siliceous sedimentation in shelfal and oceanic environments. These modern analogs, coupled with newer technology reveals evidence that supports this hypothesis (technology that was also not

present prior to the 1950's) are the reasons why the fifth hypothesis has gained wide support in the past half century. Modern oceanic circulation models for the novaculitic chert and Arkansas Novaculite indicate that sediments were deposited in epeiric seas in anoxic bottom-water conditions with strongly density-stratified water columns (Comer, 2008). Southeasterly trade winds and Ekman circulation forced surface waters west toward the open ocean (Ettensohn, 1981). This caused countercurrents containing upwelled, nutrient-rich oceanic water onto the craton (Comer, 2008). The upwelled oceanic nutrients, like phosphate and nitrogen, supported high biological activity, strong density-stratified water columns (which inhibit oxygen re-supply), and promoted organic matter preservation (Ettensohn, 1981, 1985; Heckel and Witzke, 1979). Depletion of oxygen below the thermocline not only occurs due to a lack of mixing, but also due to the decay of organic matter (Ettensohn, 1981). In this environment, high concentrations of organic matter coexist with abundant biogenic silica. This indicates that high biological productivity was supported by the aforementioned dynamic upwelling (Ettensohn, 1981; Comer, 2008). Processes associated with an ancient oxygen minimum zone (OMZ) can help explain many of the features within the novaculitic chert and Arkansas Novaculite, and Callner (2014) interpreted the upper portion of an ancient OMZ to have intersected a broad continental shelf along the southern portion of Laurussia. The intersection of an oceanic oxygen minimum zone and upwelling along the Ouachita margin appears to be a simple way to explain the abundant silica and phosphate deposition in the Woodford Shale and coeval novaculite units (Callner, 2014).

There are several hypothesis that attempt to explain the mechanisms that influenced the shale-chart rhythms present within the Woodford Shale. Hypothesis range from chemical and physical separation to time successive layers being distributed over the area. Taking a combination of these ideas into consideration, Hallam (1964) suggested that both processes help play a role in the formation of chert-shale rhythms. Conversely, Iijima (1985) hypothesized that

the alternating layers of novaculitic chert and shale, both present in the Ouachita and Arbuckle regions, are the result of rhythmic bedding sequences. The theory behind these types of sequences, according to Iijima (1985), is the deposition of chert beds in the form of accumulations biogenic silica, which are then overlain by shale partings caused by distal turbidity currents. The biogenic silica accumulations in Iijima's hypothesis are composed primarily of siliceous skeletons (radiolarian tests, sponge spicules, diatoms). Similar to Hallam, Hein and Parrish (1987) ascertained that both process types are responsible for the generation of chert sequences, but it is unknown which mechanism is prevalent. In 1992 Murray et. al. suggested that turbidity currents are not the cause chert-shale rhythms. They instead postulate that the beds were formed diagenetically from siliceous precursor oozes ($\text{SiO}_2 > 90\%$) by bedding-parallel chemical and physical segregation, of mud and shale (Murray et. al., 1992). Hori et. al. (2006) proposed that bedded radiolarian chert forms from rapid, cyclic accumulation of biogenic silica in areas with low rates of detrital input. Regardless of the specific mechanisms that influenced the stratigraphy of the Arkansas Novaculite and the novaculitic Woodford Shale, the two deposits are strikingly similar in appearance (Fig. 6) and conceivably have been mapped as the same formation.



Figure 6. (A) Woodford Shale in the Arbuckle Mountains and (B) Arkansas Novaculite in the Ouachita Mountains have strikingly similar in appearance.

CHAPTER III

METHODOLOGY

This study employed four major sets of techniques to characterize and interpret novaculitic chert from megascopic to nanoscopic scales. The basic methods include outcrop analysis, core analysis, thin section analysis, and SEM imaging. Outcrops and cores were chosen on the bases of location and sample freshness, as well as to span the range of depositional settings in Oklahoma (Fig. 1). The sample localities are presented in an order beginning on the Oklahoma Shelf and ending in the core of the Ouachita Orogen.

Three outcrops of the Arkansas Novaculite and the Woodford Shale were described and sampled using basic stratigraphic and sedimentologic procedures. The lithologic variables described include rock type, color, texture, bedding, physical sedimentary structures, biogenic sedimentary structures, and diagenetic features. Polished slabs of selected samples were made to examine bedding, natural fractures, and sedimentary structures.

From the outcrops on Interstate 35 (I-35), eight hand samples of novaculitic chert were taken from a variety of beds in the Devonian section. In the Atoka Chert Pit, seven Arkansas Novaculite samples were taken from chert beds spanning the Devonian-Mississippian section. In

the Broken Bow Uplift, nine Arkansas Novaculite hand samples were recovered from three locations in or near Beavers Bend State Park. Novaculitic chert was examined in two cores of the Woodford Shale: one from the southwest margin of the Anadarko Basin and the other from the western Arkoma Basin. The cores were described and sampled in a manner similar to the outcrops. Of particular importance were the identification and description of depositional and diagenetic features.

Thin sections from the outcrops and cores were made and studied. A total of 38 thin sections was examined, 28 of which were prepared by Wagoner Petrographic in Lindon, Utah. The remainder of the thin sections were prepared by Callner (2014) and are in the collection of the Boone Pickens School of Geology. The thin sections have standard dimensions (24x48mm), were impregnated with blue epoxy, and were stained with alizarin red-S and potassium ferricyanide to identify calcite, ferroan calcite, and plagioclase. Thin sections were cut to a thickness of 20 microns (half standard thickness), which facilitated the optical analysis of organic-rich chert, which has high opacity compared to most sedimentary rocks. The thin sections were examined visually under a petrographic microscope, which was used to characterize mineralogy, fabric, texture, crystal orientation, fossil content, and diagenetic features. The presence of minerals and microfossils (presence and current state) reveal critical information about depositional environment, silica sources, palaeoceanography, paleobiotic processes and diagenetic history.

Eight samples of novaculitic chert were analyzed using a FEI Quanta 600 field-emission gun Environmental Scanning Electron Microscope (SEM) with an Evex EDS X-ray microanalysis system. The SEM is housed in the Venture One microscopy laboratory at Oklahoma State University. The samples were chosen based on features identified by hand sample and thin section description cut to dimensions of 2 mm (L) x 10 mm (W) x 10 mm (H). The area of interest on the cut samples was argon-ion milled using JEOL IB-19500CP Cross-

Section Polisher, also located at the Venture One facility. This enabled the viewing of highly polished samples with minimal surficial artifacts. The milled area of each sample is about 1 mm². The milled samples were attached with silver paint to circular SEM sample stands. The samples were then coated with gold-palladium (Au-Pd) alloy, which helps concentrate the SEM electron beam and minimizes charging anomalies associated with irregularities of the milled surface. The samples were coated using a Balzers Union MED 010 coater.

Once the samples were milled and coated, they were then imaged at several scales of magnification and spot analyzed for elemental composition via electron dispersive spectroscopy (EDS). Analysis using this method allowed nanoscopic characterization of mineralogy, texture, fabric, physical sedimentary structures, biogenic structures, diagenetic features, and porosity. Features were imaged perpendicular to bedding. Characteristics revealed during this analysis enhanced knowledge of the distribution of silica, other minerals, organic matter, and porosity, and helped determine the significance of novaculitic chert as a potential petroleum source rock and reservoir rock.

CHAPTER IV

RESULTS

IV.1 Outcrop and Core Description: Overview

This section focuses on the description of the outcrops and cores analyzed during this study. The discussion begins with a prominent outcrop of the Woodford Shale on the southern flank of the Arbuckle Uplift (I-35), and continues with a core from the western Arkoma Basin (Poe#1-29) and another core from a fault block along the southwest margin of the Anadarko Basin (Hall 2B). From there, the focus shifts to the Ouachita Orogen. The first Ouachita outcrop features an exceptional outcrop (Atoka) in the cratonward part of the orogen, and the discussion concludes with outcrops in the Broken Bow Uplift, which forms the core of the exposed Ouachitas in Oklahoma.

IV.1.A I-35 Outcrop

The Woodford Shale is well exposed in the southwestern flank of the Arbuckle Anticline along the southbound lane of I-35 in southern Oklahoma (Krystyniak, 2005; Puckette et al., 2013) (Figs. 1, 7; Table 1). This location is approximately 14.2 miles north of Ardmore, OK, and 1.3 miles north of exit 42 on I-35 South and consists of two outcrops. Here the Woodford Shale

strikes N. 60° W. and dips about 38° SW (Fay, 1989; Krystyniak, 2004). The southern outcrop exposes the upper 125 feet of the formation (Fig. 8), and the northern outcrop exposes the basal 12 feet of the Woodford (Fig. 9). The thickness of covered section between the two outcrops is approximately 136 feet (Puckette et al., 2013), and so the total thickness of the Woodford at this location is estimated to be 373 feet.

The Hunton-Woodford contact is well exposed and relatively easy to access, whereas the Woodford-Sycamore contact is partially vegetated and largely covered by a thin veneer of float (Figs. 8, 9). The majority of samples were taken from the southern outcrop, and one sample was taken from the northern outcrop (Fig. 10). The Woodford Shale at this locality consists of alternating layers of organic-rich black shale and novaculitic chert (Fig. 11).

The shale is very dark gray to dark gray, and the novaculitic chert varies from very dark gray to light gray. Fresh surfaces of novaculitic chert feel gritty, but no grains are discernible. The shale layers tend to be planar to broadly lensoid and range in thickness from laminae to medium beds. The shale is highly fissile and internal laminae are on the order of 1 mm thick. The chert layers also range from laminae to medium beds, and tend to thicken upward in section (Fig. 11). However, chert content decreases abruptly in the upper 35 feet of the Woodford, and this decrease is thought to correspond with the Devonian-Mississippian boundary (Puckette et al., 2013). The chert beds have sharp to gradational contacts; bedding ranges from planar lensoid, and planar and undulatory bedding surfaces are common.

The shale and chert layers contain phosphate nodules and lenses that increase in abundance upward in section and range in shape from spherical to oblate or platy (Fig. 12). Most of the nodules are of pebble size, and some lenses are up to 3 cm thick and 30 cm long. The chert and shale also contain disseminated pyrite crystals and framboids, as well as granule- to pebble-size marcasite nodules. Some chert beds appear internally structureless, whereas others are

laminated. The laminae are planar to wavy, and wavy laminae tend to wrap around phosphate nodules and lenses. Biogenic structures are difficult to discern in the outcrop, although a fish scale was observed in the lower part of the section.



Figure 7. Woodford Shale outcrops along the southbound lane of I-35.



Figure 8. Woodford Shale outcrop along I-35. Pink arrow denotes the location of the Woodford/Sycamore Limestone contact. The white line denotes the Devonian/Carboniferous boundary according to Over (1990).



Figure 9. Location of sample 8 from outcrop on I-35. The thicker rock beds are the Woodford/Hunton Group contact.

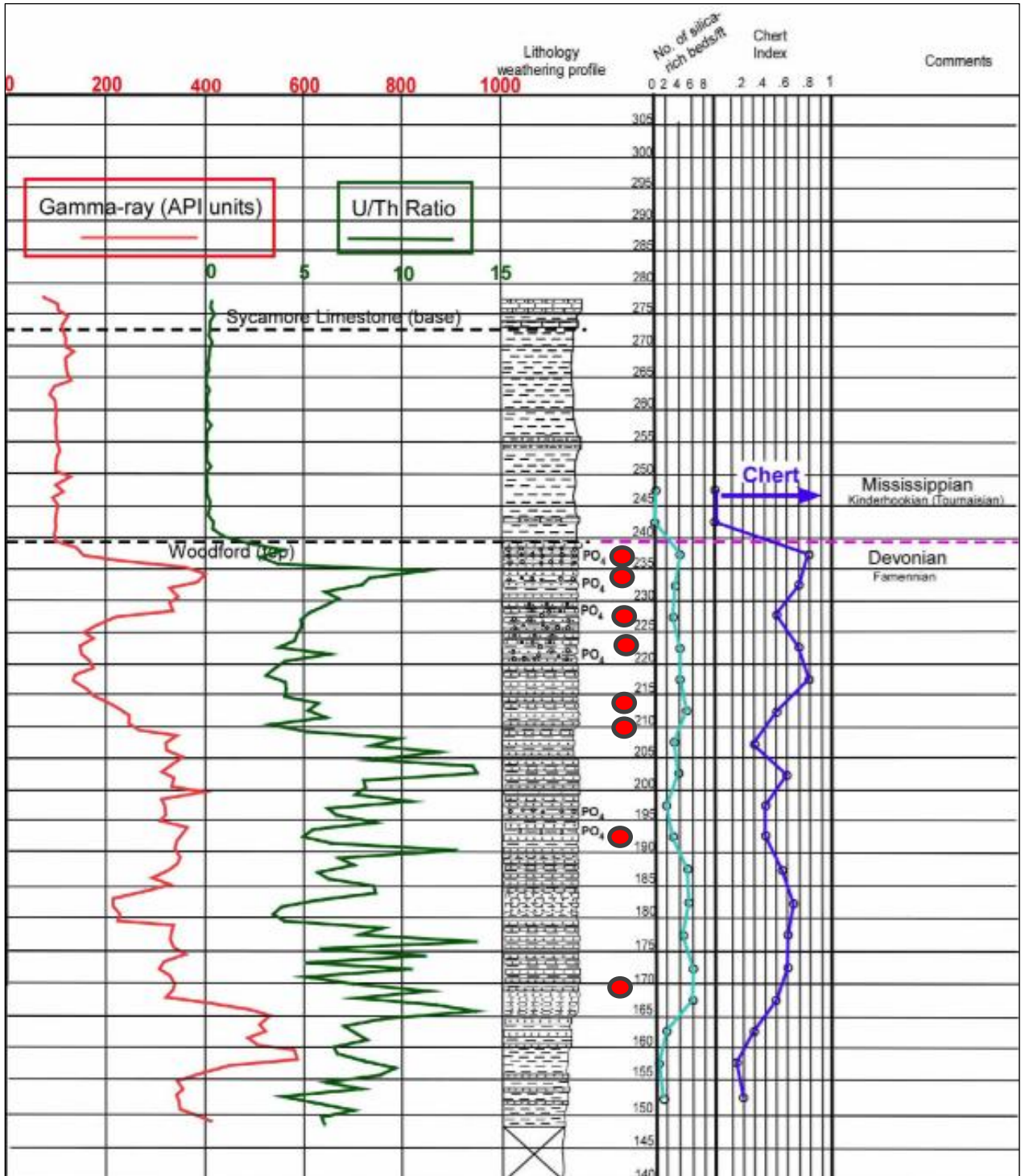


Figure 10. Measured section, total gamma-ray, U/Th ratio, and relative abundance of chert in the upper Woodford Shale section, I-35 outcrop. Locations of samples 1-8 are marked by red circles (after Puckette et. al., 2013).

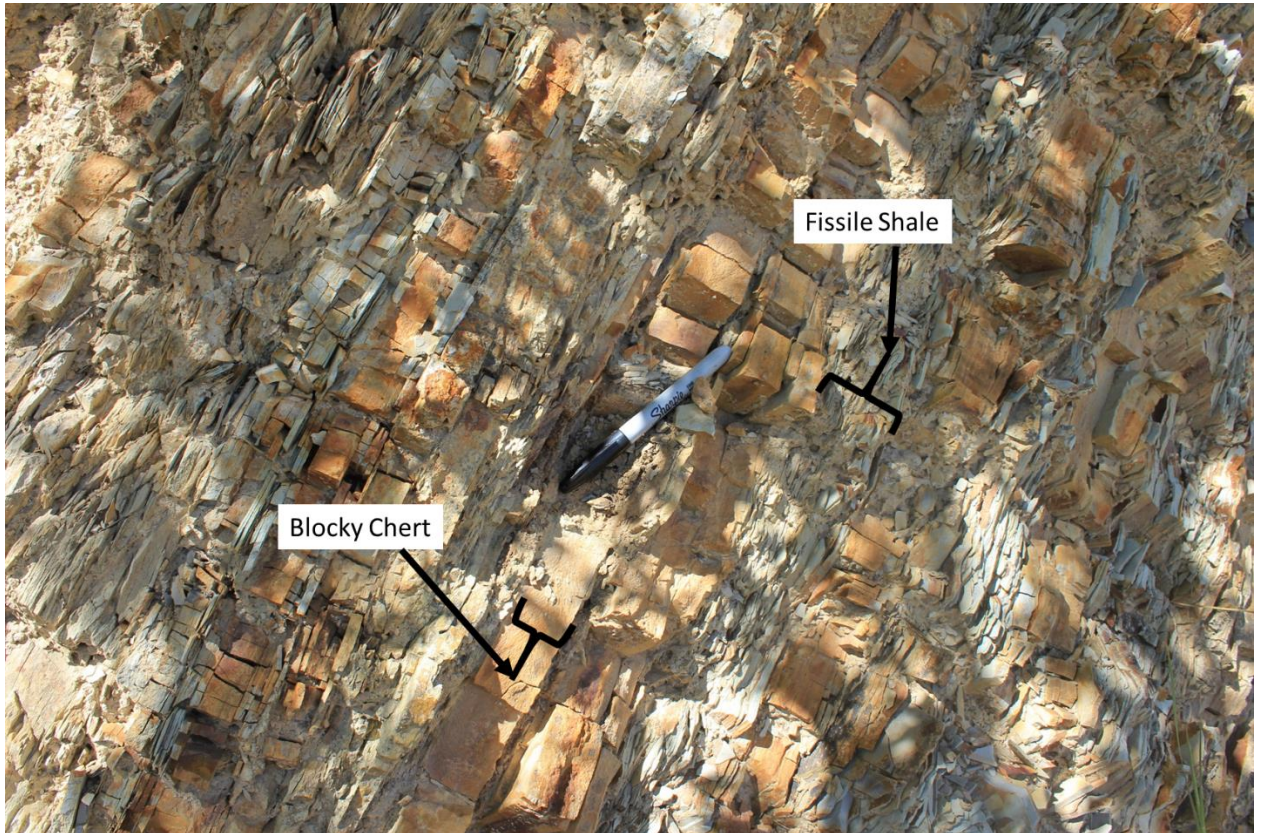


Figure 11. Alternating layers of fissile Woodford Shale and blocky novaculitic chert in the I-35 outcrop.

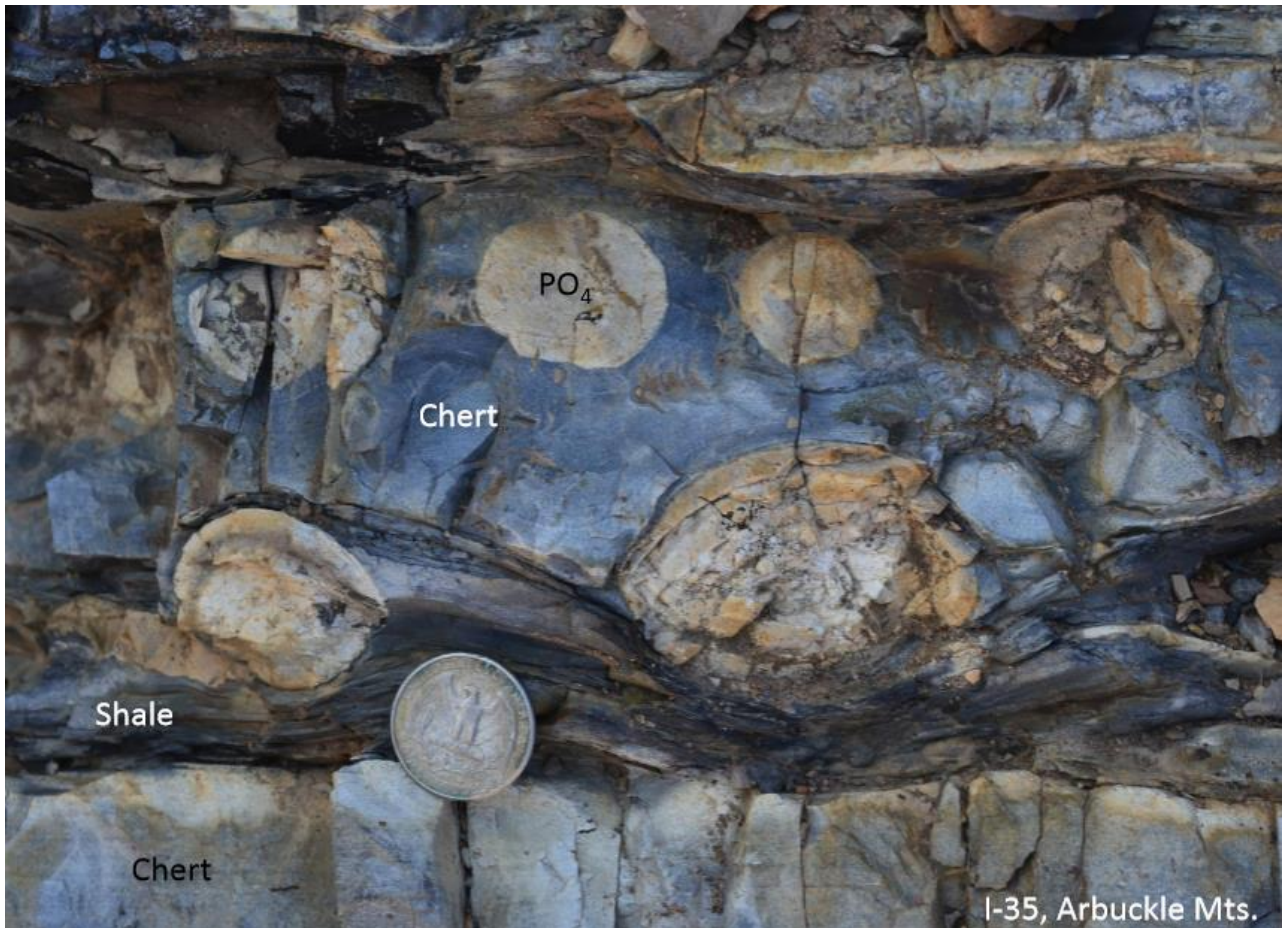


Figure 12. Abundant phosphate nodules in novaculitic chert within the Woodford Shale at the I-35 outcrop (Pashin and Callner, 2014).

IV.1.B Poe #1-29 Core

The Poe #1-29 core is from Hughes County in the western portion of the Arkoma Basin (Fig. 1, Table 1). The core is 120 feet in long (7,730-7,850 feet measured depth) (Fig. 13). The Woodford portion of the core extends from 7,738-7,875 feet according to geophysical logs. The lowest 25 feet of the core was not available for analysis. The core consists primarily of Devonian-age Woodford Shale (7,738 – 7,850 feet), and the upper portion of the core (7,730 – 7,737 feet) is from the Upper Mississippian Caney Shale. The Woodford Shale is composed of fissile shale and novaculitic chert, and is generally black shale with a few upper feet exhibiting medium-light gray color. Lower portion of the Woodford (7,831-7,850) feet consists of dark gray to black shale with

thin interbeds of novaculitic chert, while the upper portion of the Woodford, from 7,738-7,831 feet, is medium to dark gray and is composed primarily of chert. The core contains mainly thin to medium beds of argillaceous and siliceous mudrock that exhibit a variety of sedimentary and diagenetic features (Callner, 2014).

The Poe #1-29 core can be roughly divided into seven intervals based on sedimentology and diagenetic features (Callner, 2014). Overall, the core contains numerous silica and calcite filled fractures, pyrite nodules and laminae, and soft sediment deformation. The chert within the core contains various types of fractures and a broad range of soft sediment deformation features. The lowest interval (1) is predominantly black mudstone that lacks silty layers and exhibits soft-sediment deformation and a possible burrow fill (Fig. 14A). The second interval (2) contains small-scale normal faults, including growth faults (Fig. 14B). Centimeter-scale silica- and carbonate-filled veins are common in the core (Fig. 14B). Most of the veins are planar and perpendicular to bedding (Fig. 15A), whereas others are inclined (Fig. 14A) or ptygmatically folded (Fig. 15B). Marcasite and phosphate nodules are common in the core, as are laminae of pyrite and disseminated pyrite crystals and framboids. The uppermost Woodford section consists of alternating beds of clay- and silica-rich mudrock with abundant soft-sediment deformation structures, including isoclinal folds (Fig. 16). The contact between the Woodford and Caney is sharp and occurs at a measured depth of 7,737 feet.

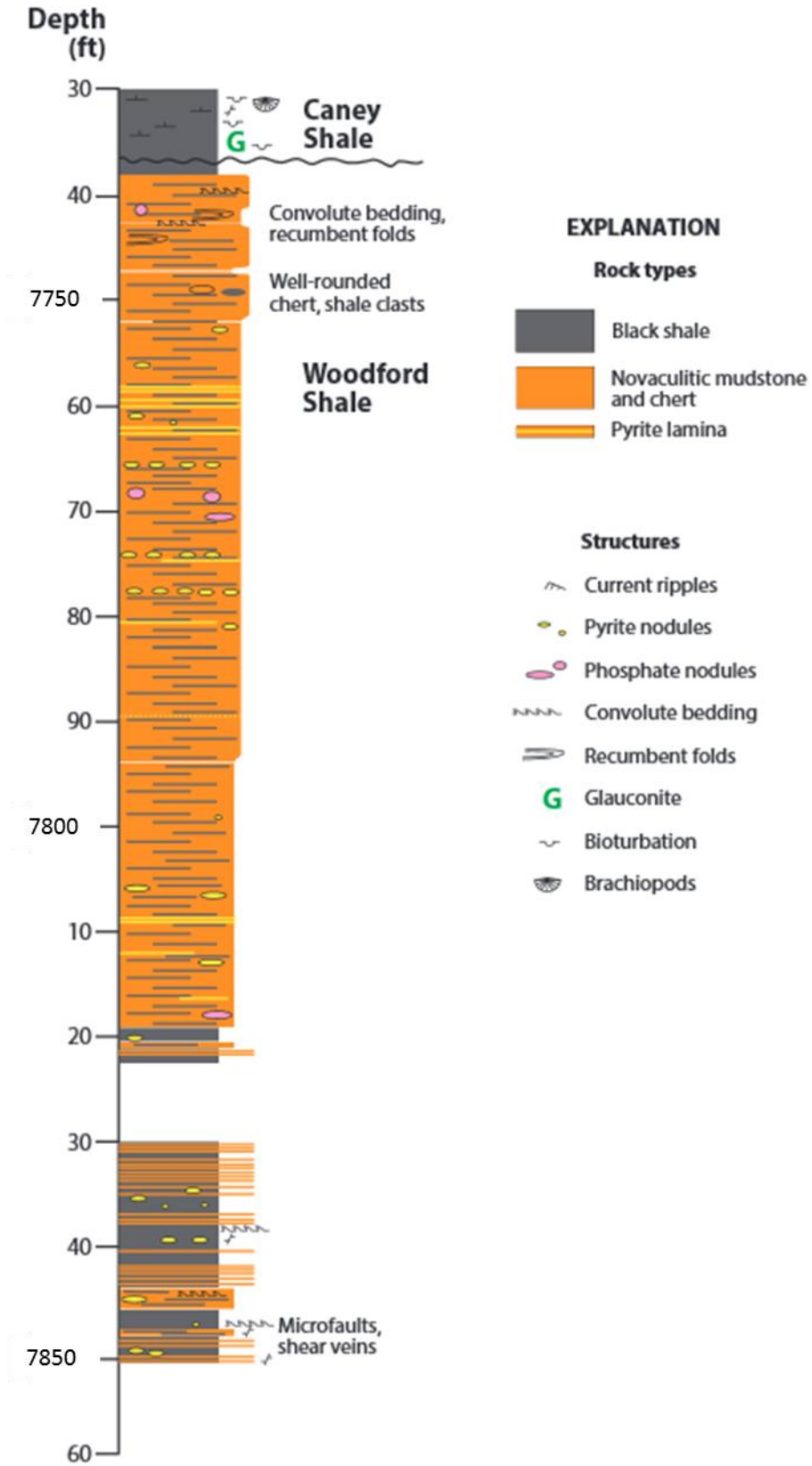


Figure 13. Measured section of the Poe #1-29 core (after Callner, 2014).

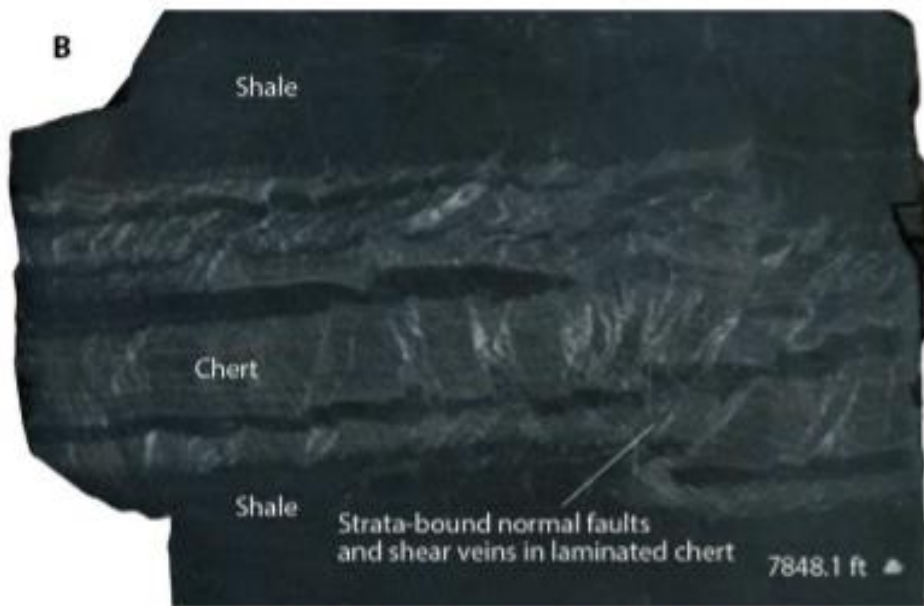
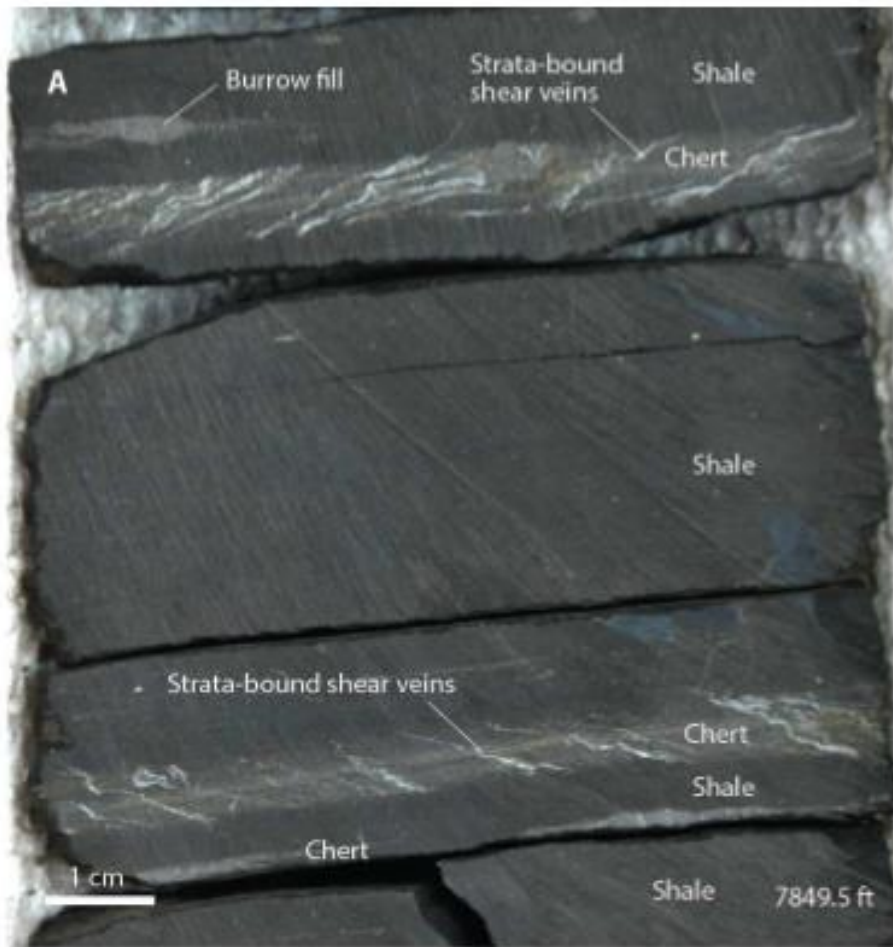


Figure 14. Chert layers containing strata-bound shear veins, Poe #1-29 core. (A) Weakly folded shear veins in chert act as supporting evidence that layer-parallel slip and smearing of chert beds occurred during compaction in Interval 1. (B) Normally faulted chert with associated shear veins in Interval 2. Such structures indicate extensional stress and dislocation of beds during sedimentation and early burial (after Callner, 2014).

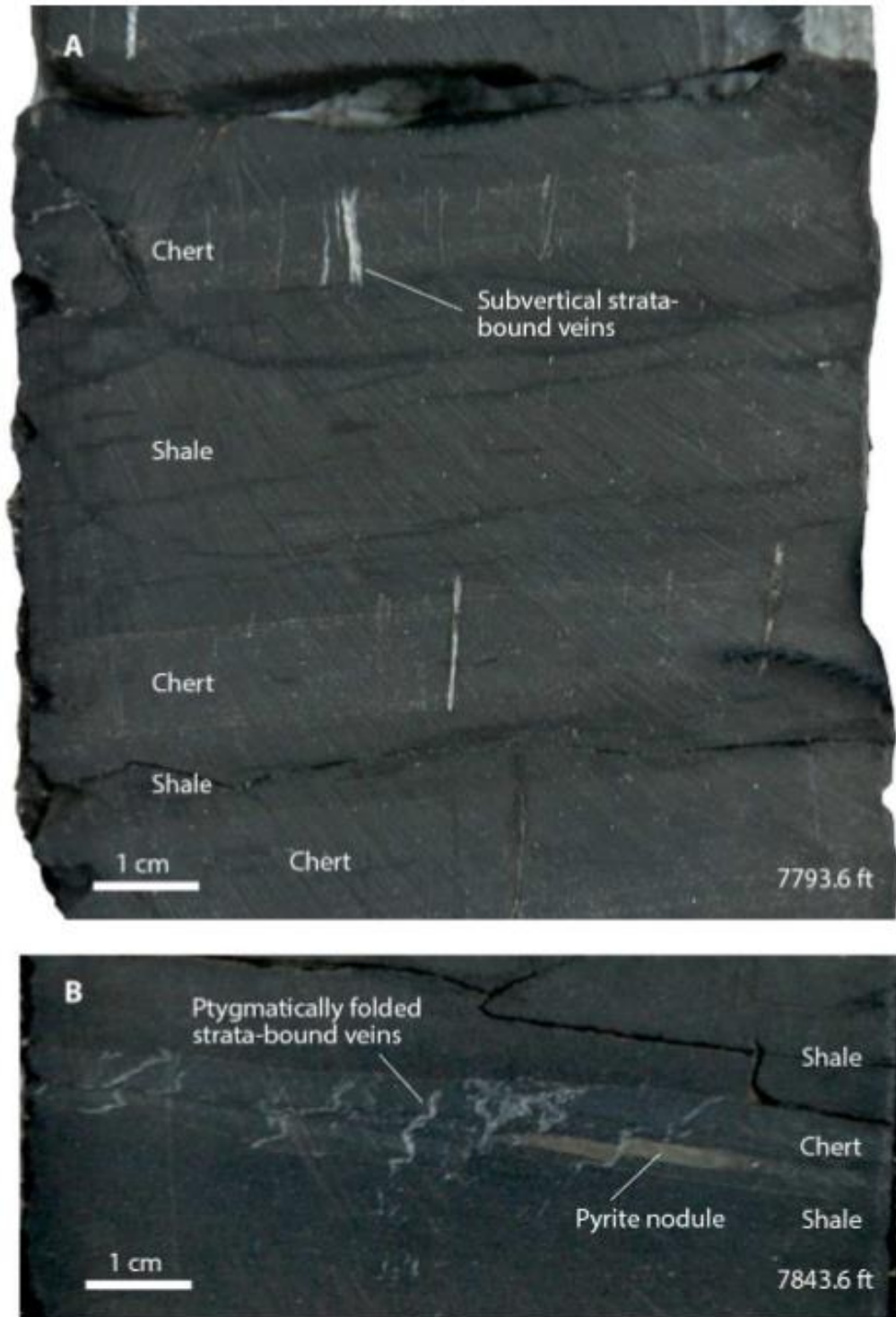


Figure 15. Strata-bound fractures in novaculitic chert, Poe #1-29 core. (A) Subvertical veins in chert in Interval 4. Note lack of veins in shale layers. (B) Ptygmatically folded veins, indicating chert beds were fractured prior to major compaction in Interval 2 (after Callner, 2014).

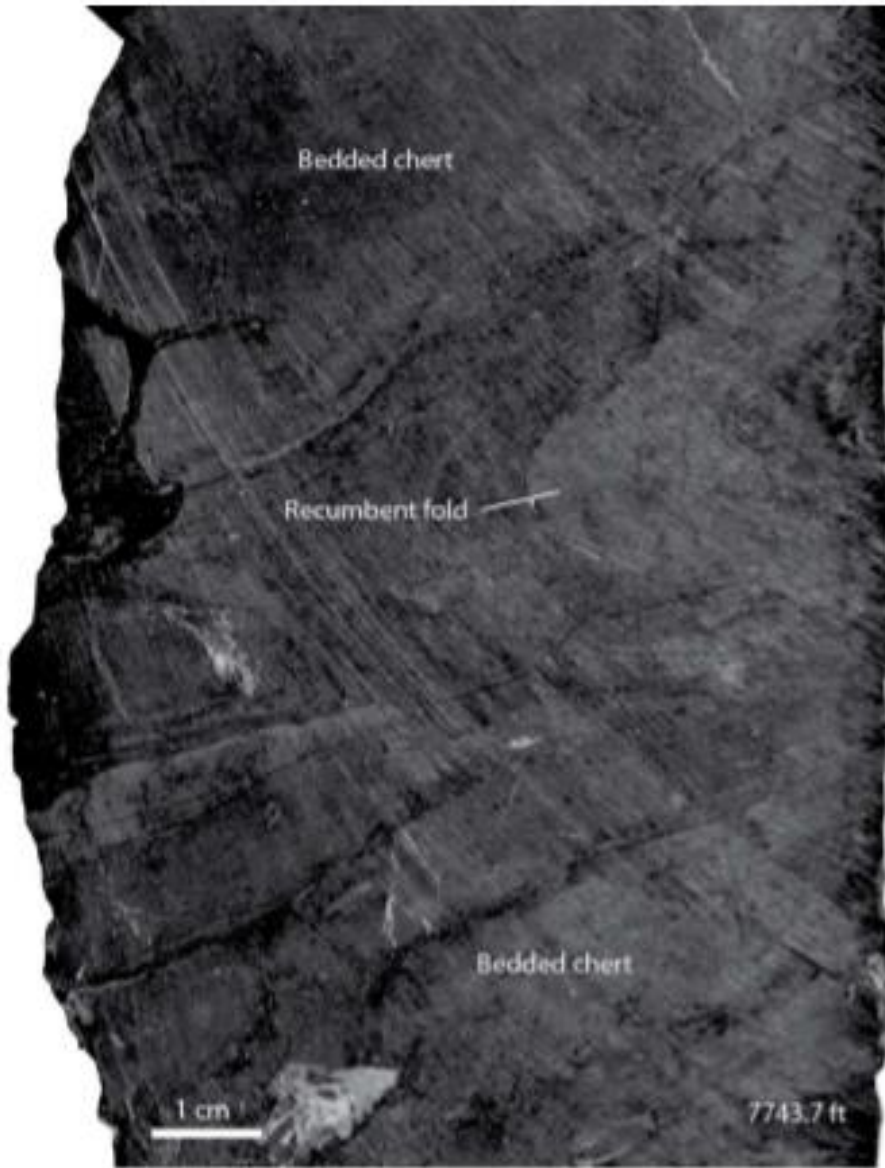


Figure 16. Recumbent fold in bedded chert near the top of the Woodford Shale, Poe #1-29 core, Interval 7 (after Callner, 2014).

IV.1.C Hall 2B Core

The Hall 2B core is from Caddo County along the southwest edge of the Anadarko Basin (Fig. 1, Table 1). This core comes from a fault slice along the frontal structures of the Wichita Mountains (Callner, 2014). The core is over 150 feet in length, and was retrieved from measured depths of 6,150-6,278 feet (Fig. 17). The bulk of the core studied (6,162-6,275 feet) comprises interbedded chert and shale of the Woodford Shale, and the upper portion of the core contains light gray shale and siltstone of the Sycamore Formation. The transition between the Woodford Shale and the Sycamore Formation is marked by a fault gouge zone (6,155-6,162 feet) containing intensely deformed Woodford and Sycamore strata. Bedding dips regionally at about 20° in most of the core, although numerous structural panels exist within the core with dip greater than 50°. Based on geophysical well logs, the contact between the middle and upper Woodford is at 6,238 feet, although the complete thickness of the Woodford was not drilled, and no major stratigraphic boundary within the Woodford is clear to the eye (Callner, 2014).

The Woodford Shale within the Hall 2B core consists primarily of laminae to thick beds of chert intercalated with laminae to thin beds of black, fissile shale and was divided into five intervals by Callner (2014) based on depositional features and geochemical characteristics. The overall core exhibits variable bedding dip and includes 12 steeply dipping panels, each bounded by a fault at the base and angular unconformities at the tops. Numerous fractures (silica and carbonate-filled), breccia layers, soft-sediment deformation, and some growth faults were identified by Callner (2014) (Figs. 18, 19). Fractures are most abundant and are typically strata-bound in the chert layers of the core than in the shale layers (Figs. 19, 20). As in the other Woodford sections, pyrite and marcasite are common, as are phosphate nodules (Fig. 21).

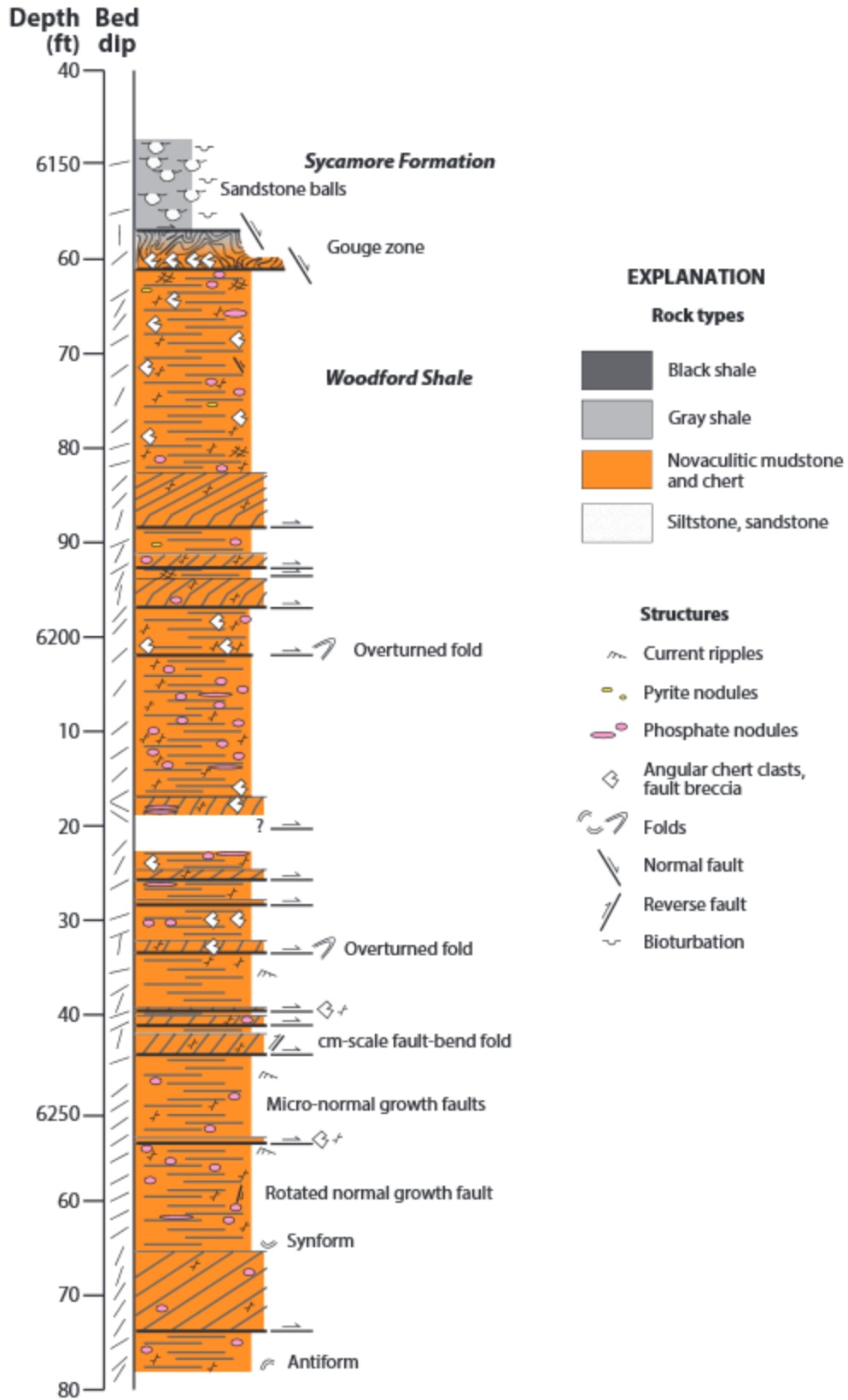


Figure 17. Measured section of the Hall-2B core (after Callner, 2014).

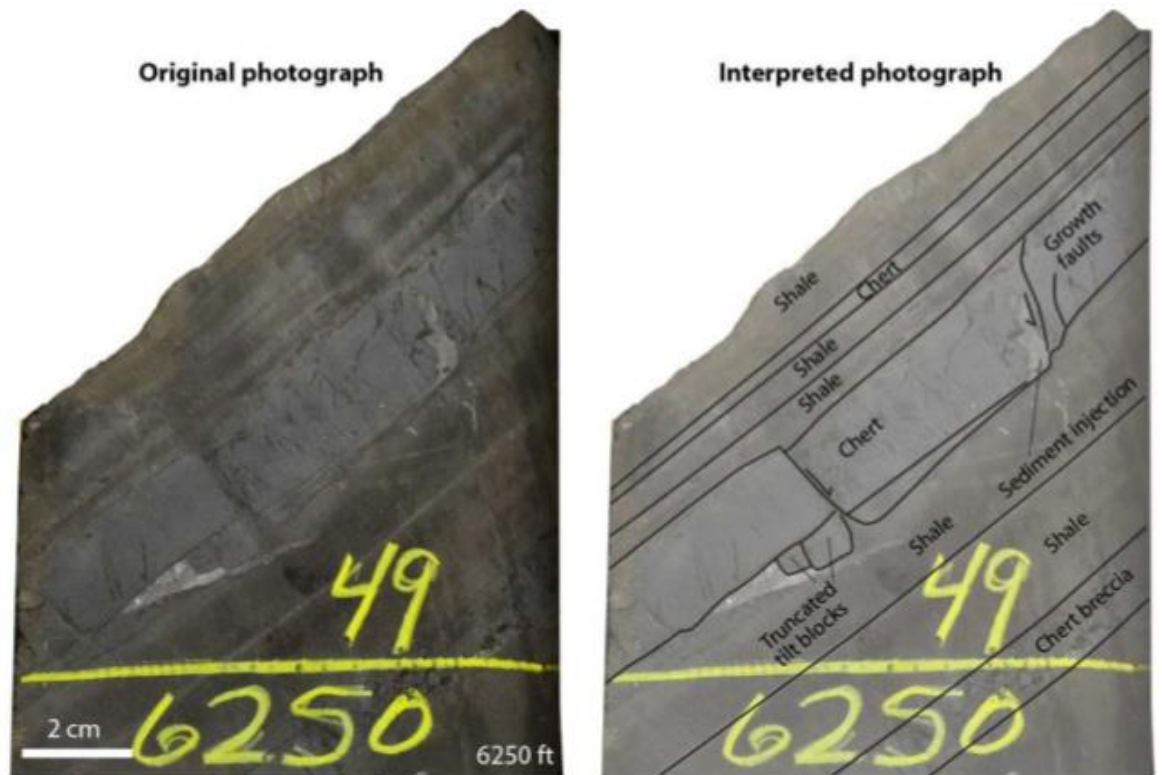


Figure 18. Normally faulted chert overlain by undeformed chert layers, Woodford Shale, Hall 2B core. Note truncated tilt blocks at base of chert bed providing clear evidence of penecontemporaneous erosion and deformation (after Callner, 2014).

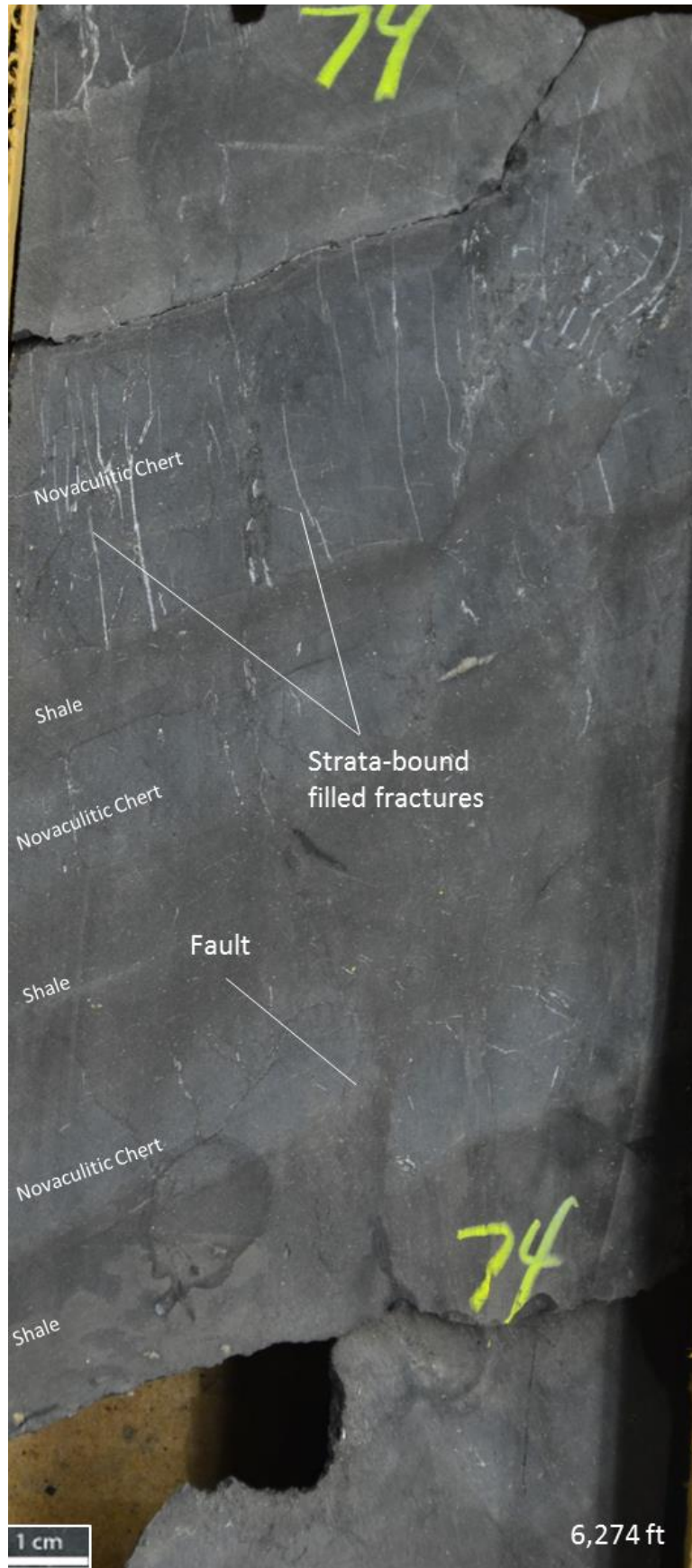


Figure 19. Reverse fault and strata-bound filled fractures within Woodford Shale, Hall 2B core. The blueish hue of the novaculitic chert is apparent. Note the grading in the layers at the bottom of the image.

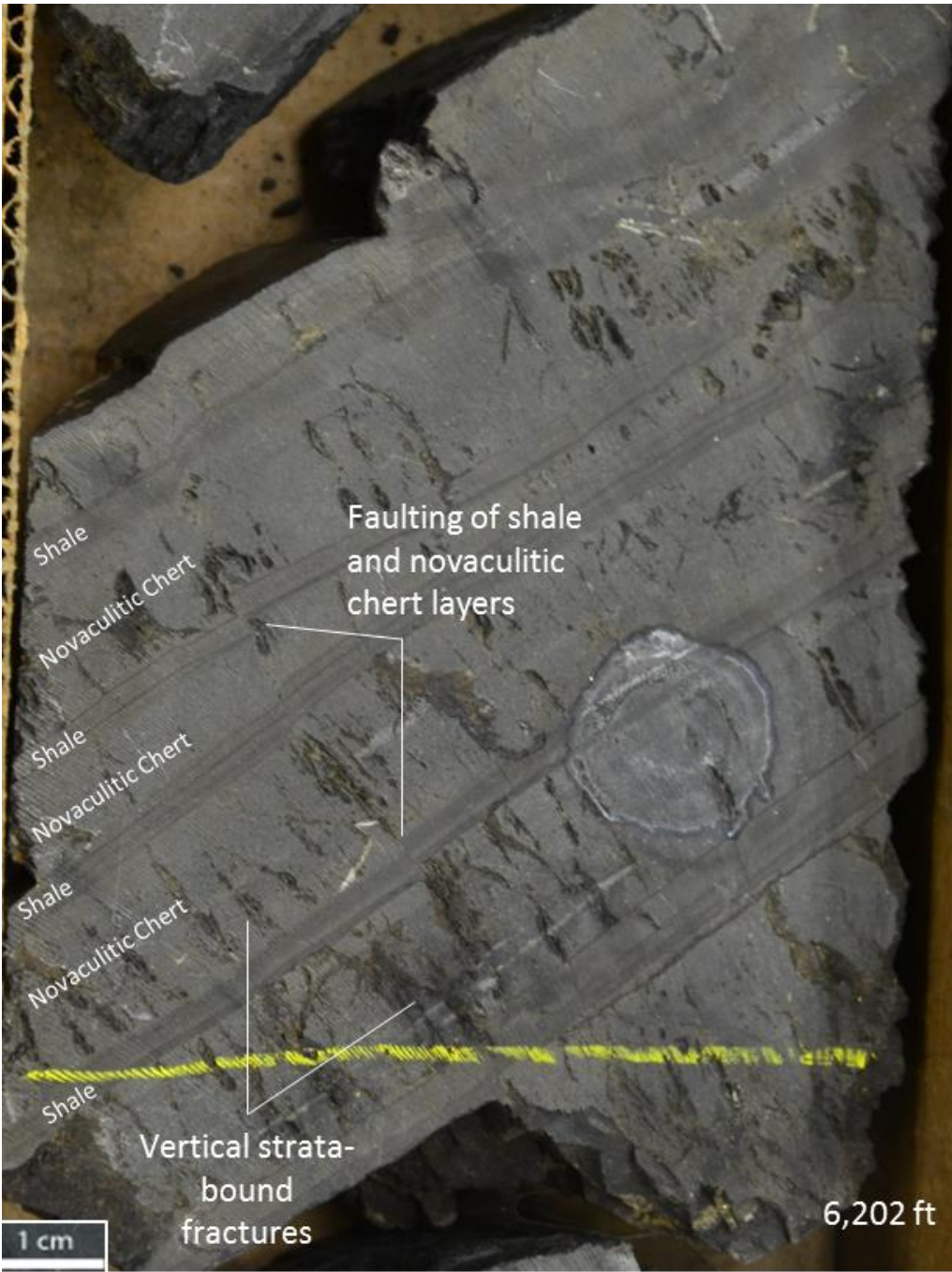


Figure 20. Shale laminae and thin chert beds in Woodford Shale, Hall 2B core. Note small-displacement fault that is subperpendicular to bedding. Vertical, strata-bound fractures are abundant in the chert layers.

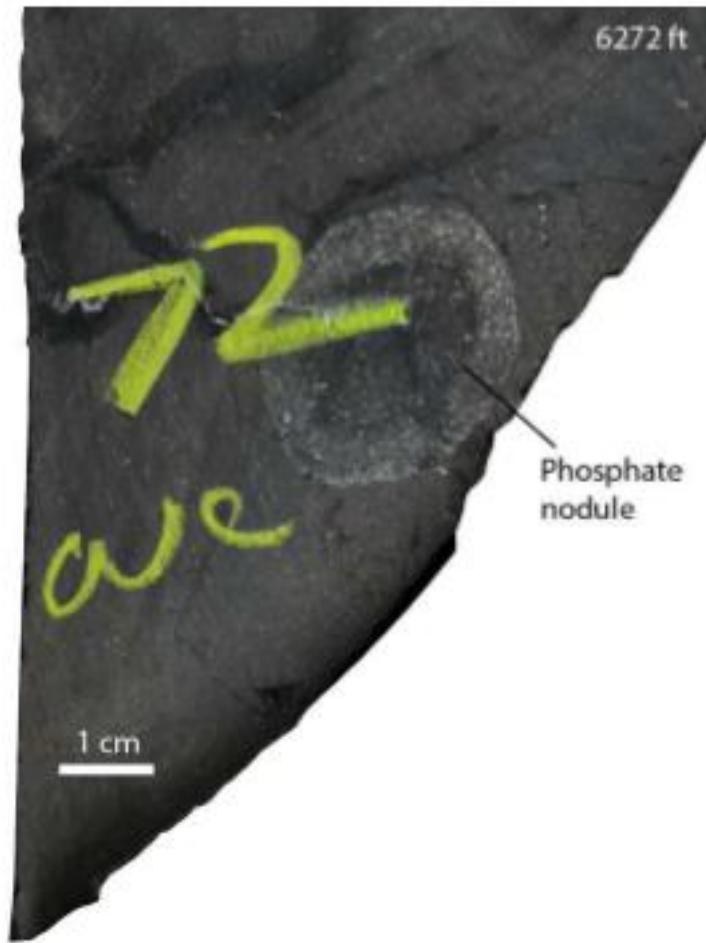


Figure 21. Subcircular phosphate nodule in bedded chert, Woodford Shale, Hall 2B core (after Callner, 2014).

IV.1.D Atoka Chert Pit Outcrop at Scratch Hill

An exceptional outcrop of Arkansas Novaculite is exposed in a chert pit that has been excavated into Scratch Hill near the town of Atoka, OK (Fig. 1, Table 1). This outcrop is in the Jackfork Belt of the Ouachita orogen and is part of an unusual outlier that exposes pre-orogenic strata in the cratonward part of the thrust belt. The site can be accessed from E. Court Street near the southeast edge of Atoka (Fig. 22). The total outcrop expanse in the Atoka Chert Pit is roughly

330 feet in length. Bedding strikes N. 25° E. and dips steeply at 76° SE. The outcrop contains some folds in the lower part of the section, and bedding is locally overturned (Fig. 23).

The outcrop consists of alternating layers of novaculite and fissile shale. The chert varies in color from dark gray to medium gray. Bedding ranges from planar to undulatory, with the chert occurring in laminae to medium beds and the shale occurring in laminae to thick beds. The shale, where fresh, is very dark gray and where weathered has distinct greenish and reddish hues, particularly in the upper section (Fig. 24). Interestingly, fresh black shale and dark chert in the deepest part of the excavation can be traced in the upper part of the hill into weathered greenish shale and tripolitic chert. Thickness of the chert layers ranges from laminae to thin beds, while the fissile shale thicknesses range from laminae to thick beds. The lower portion of the outcrop exhibits chert in medium beds with shale in the form of predominately laminae. Shale content increases abruptly in the upper part of the section, and as is the case along I-35, this increase appears to coincide with the Devonian-Mississippian boundary (Darwin Boardman, personal communication). Above this boundary, the outcrop is dominated by laminae to medium beds of chert, which is partially tripolitic, and laminae to thick beds of greenish and reddish shale.

The chert beds, especially in the lower part the outcrop exhibit a waxy texture, and individual crystals cannot be discerned with the naked eye (Fig. 25). Much of the chert is laminated internally, and some irregular, hummocky bedforms are exposed in the middle portion of the section at the top of a vertical chert bed (Fig. 26). The chert-rich layers contain phosphate nodules primarily in the lower portion the outcrop that range from platy to spherical in shape and range from pebble to cobble size (0.5-3.0 in) (Fig. 27). Some of the other features within the exposed outcrop include disseminated pyrite and nodular marcasite (Fig. 28).

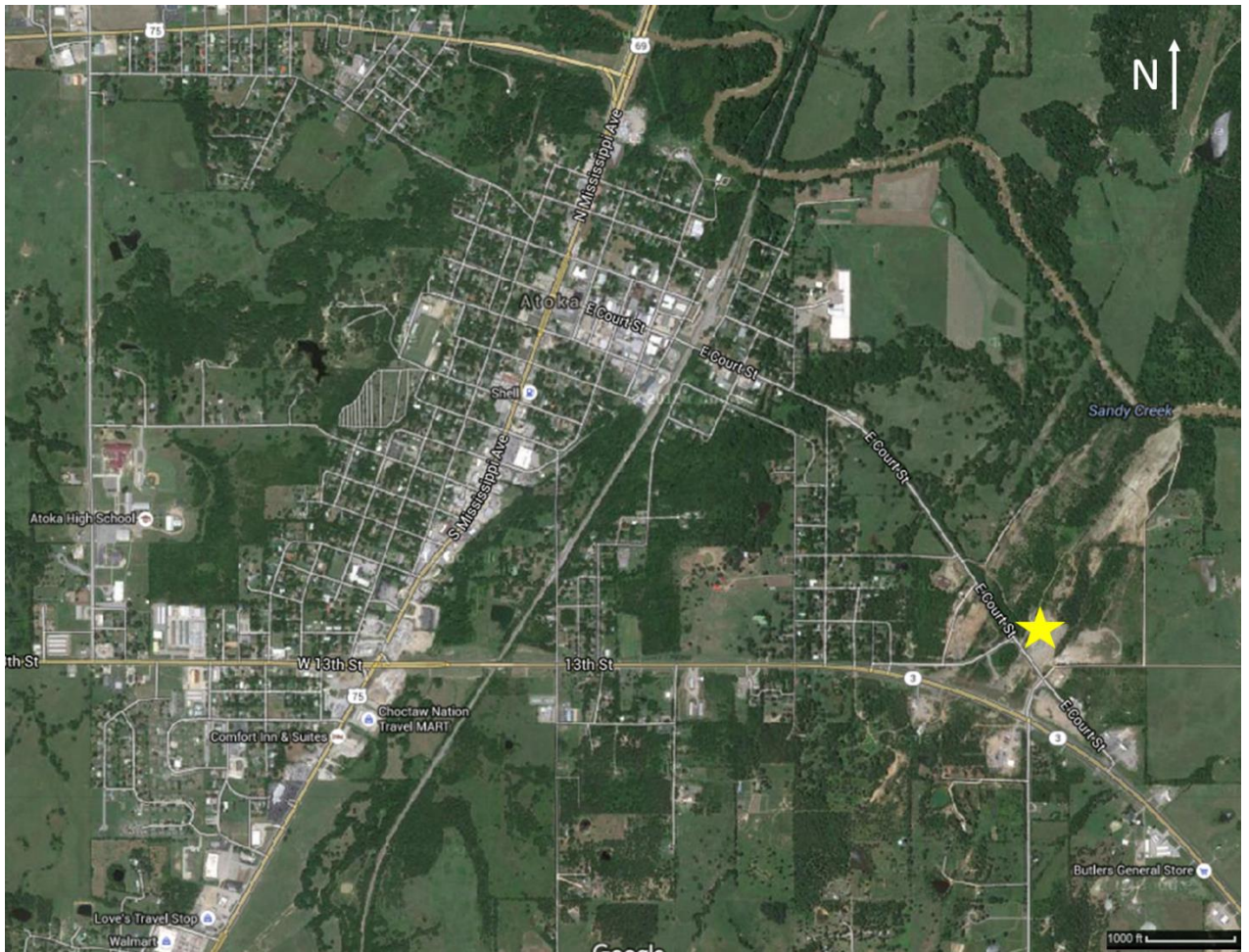


Figure 22. Map showing location of the Atoka Chert Pit at southeast corner of Atoka, Oklahoma. Yellow star marks outcrop location.



Figure 23. Steeply dipping and folded strata of the Arkansas Novaculite at the Atoka Chert Pit, which is in the Jackfork Belt of the Ouachita orogenic belt. Circles and numbers denote sample locations.



Figure 24. Reddish and greenish shale in the upper part of the Atoka Chert Pit outcrop. This part of the section is deeply weathered and contains partially tripolized chert.



Figure 25. Mottled texture on fresh broken surface sample #2 from the Atoka Chert Pit.



Figure 26. Hummocky bedding surface in steeply dipping novaculite layer in the Atoka Chert Pit.



Figure 27. Abundant phosphate nodules at and near the top of a chert bed near the base of the Arkansas Novaculite section in the Atoka Chert Pit.



Figure 28. Exposed marcasite nodule in chert at the Atoka Chert Pit.

IV.1.E Beavers Bend/Broken Bow Outcrop

A series of three outcrops in the Broken Bow Uplift was described and sampled in the area of Beavers Bend State Resort Park (Fig. 29). The park is approximately 10.9 miles north of the town of Broken Bow, Oklahoma (Fig. 1, Table 1). The uplift is commonly considered the core zone of the exposed Ouachita Orogen in Oklahoma (Suneson, 1995). The first three samples were taken from an outcrop along the east side of U.S. Highway 259A within Beavers Bend State Park. The samples include white Arkansas Novaculite and were taken from the basal portion of the formation just above the contact with the Silurian-age Blaylock Sandstone (Fig. 30). Here, the

basal strata of the Arkansas Novaculite are arguably of Silurian age (Nielsen, 1988; Suneson, 1995). The Blaylock Sandstone contains abundant vein quartz that in hand sample superficially resembles Arkansas Novaculite (Neilsen, 1988). The vein quartz is coarsely crystalline and paler than chert (Fig. 31). The basal Arkansas Novaculite, by contrast, is darker and much finer grained. The three hand samples collected from the Arkansas Novaculite are very light gray to light gray in color, and the chert has a waxy appearance that contrasts with the vein quartz, which is more translucent. The outcrop is weathered and partially vegetated, and so determining the precise thickness of the novaculite layers is difficult. However, it is apparent that the chert is thickly bedded and thus contrasts markedly with the thin- to medium-bedded chert that predominates elsewhere in the study area. Identifiable sedimentary structures are largely absent in the three hand samples.

Two samples were collected from a large outcrop at the Broken Bow hydroelectric plant that contains the Blaylock Sandstone, Missouri Mountain Shale, Arkansas Novaculite, and Stanley Shale (Figs. 32, 33) (Neilsen, 1988). Unfortunately, the outcrop was inaccessible for sampling because of security fencing at the hydroelectric plant. Hence, samples had to be collected from float at the end of the outcrop. The Arkansas Novaculite at this locality is very dark gray and has a conchoidal fracture. The dark Arkansas Novaculite samples are typically harder than those of the lighter colored novaculite samples. Crystals are not visible in these samples, and freshly broken surfaces appear dull to slightly waxy. Although bedding could not be measured directly, medium to thick beds appear to dominate in this section.

The final four samples are from an outcrop north of Beavers Bend State Park on the east side of U.S. Highway 259 (Fig. 34). This outcrop is mostly covered by vegetation and float, which makes it difficult to collect fresh samples (Suneson, 1995). Most samples collected from this site resemble the basal novaculite at Beavers Bend State Park—dull white in color and extremely fine grained. The final sample resembles the thicker novaculitic chert beds in the I-35

outcrop. This sample is different from the pale Arkansas Novaculite samples in that it has had a coarser texture and has a dark gray color on fresh surfaces (Fig. 35).

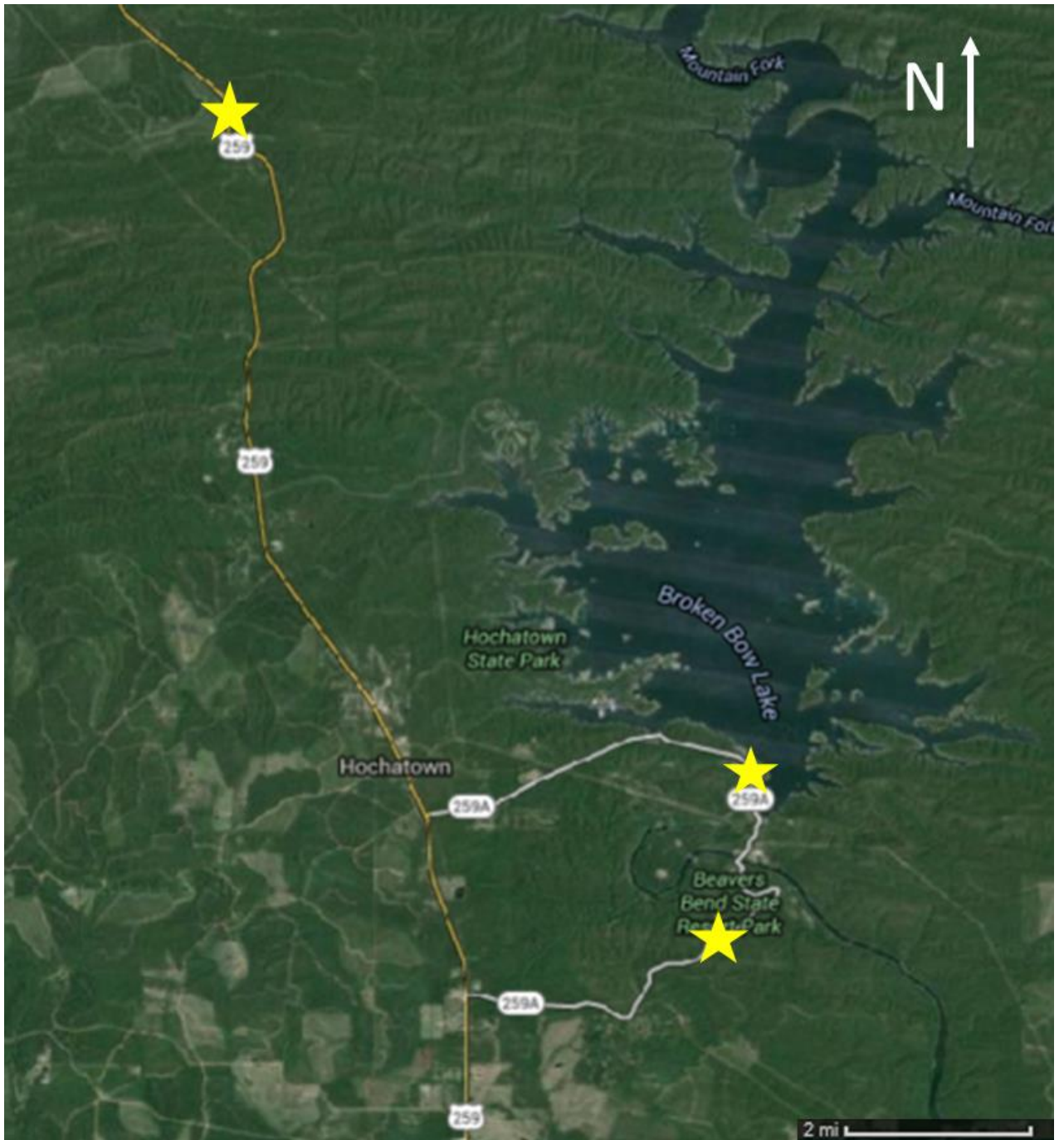


Figure 29. Map showing outcrop locations in the Broken Bow Uplift in and around Beavers Bend State Park. Yellow stars represent outcrop locations.



Figure 30. Outcrop containing contact between Blaylock Sandstone and Arkansas Novaculite at Beavers Bend State Park.



Figure 31. (A) Hand sample of Blaylock Sandstone containing quartz vein. (B) Hand sample of cryptocrystalline Arkansas Novaculite.

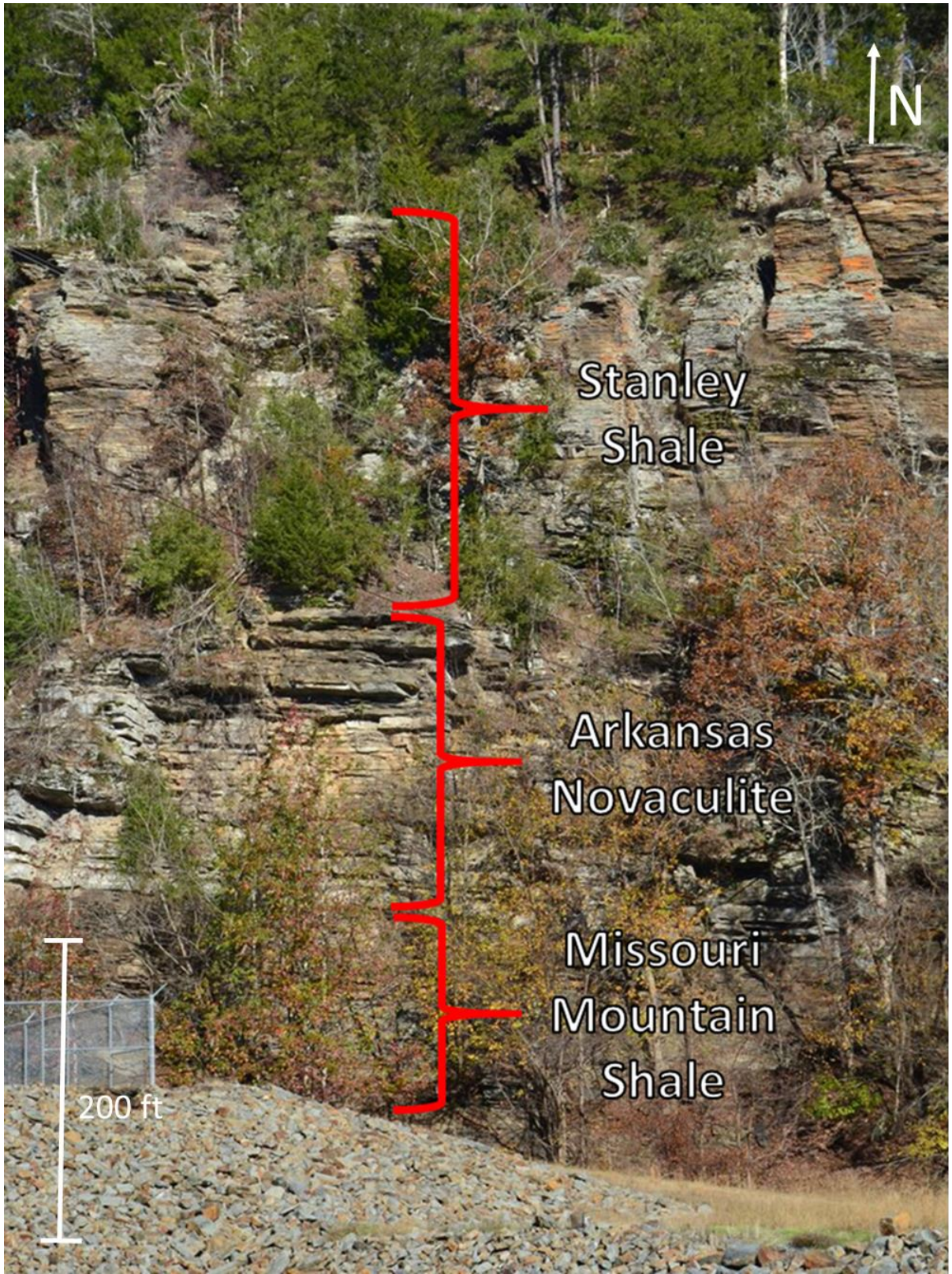


Figure 32. Beavers Bend/Broken Bow outcrop exposing the Missouri Mountain Shale, Arkansas Novaculite, and Stanley Shale next to the hydroelectric power station.



Figure 33. Beavers Bend/Broken Bow outcrop exposing the Arkansas Novaculite below the water tower.



Figure 34. Low outcrop north of Beavers Bend State Park exposing the Arkansas Novaculite.

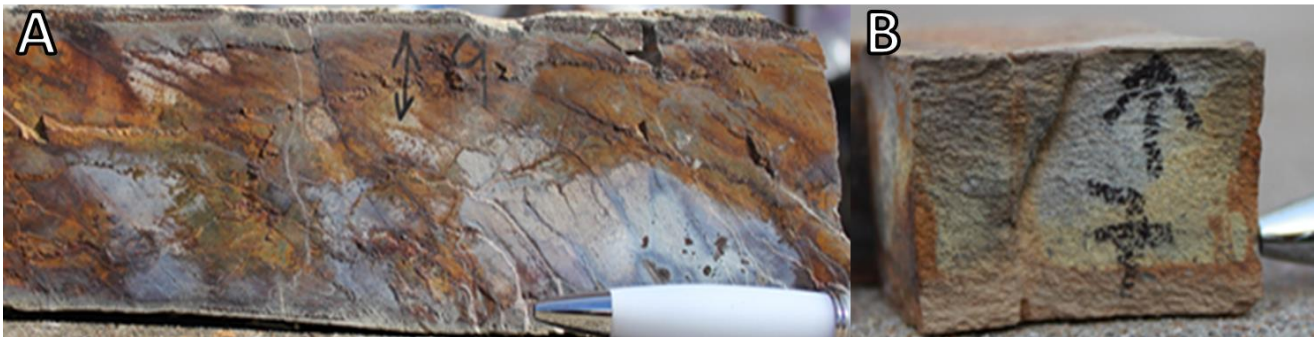


Figure 35. (A) Sample 9 from north of Beavers Bend State Park compared to (B) Sample 7 from I-35. The two samples are similar in appearance and features, yet were collected 175 miles apart. Moreover, the Broken Bow sample was translated a large distance cratonward during the Ouachita Orogeny.

IV.2 Thin Section Analysis: Overview

The 38 thin sections examined for this research were made from the I-35, Atoka Chert Pit, and Beavers Bend/Broken Bow outcrops, and from the Hall 2B and Poe 1-29 cores (Fig. 1, Table 1). The thin sections were taken from various locations in order to examine the range of settings in which novaculitic chert was deposited. The thin section descriptions are organized by the types of features observed within the chert. Features that are common to all locations, as well as features that are unique to each location, are identified. A register of the thin sections analyzed is given in Table 3.

Table 3. Chart showing thin section labeling system and location of each sample.

Thin Section #	Outcrop	Location In Outcrop	Sample #
A1	I-35	9' below top of Dev/Miss contact	1
A2	I-35	105' below the Dev/Miss contact	3
A3	I-35	105' below the Dvn/Miss contact	3
A4	I-35	13" below the 70' tape marker	4
A5	I-35	on 50' tape marker	6
A6	I-35	39' below the 50' tape marker	7
A7	I-35	105' below the Dev/Miss contact	3
B1	Atoka Chert Pit	Base of outcrop	N/A
B2	Atoka Chert Pit	Base of outcrop	N/A
B3	Atoka Chert Pit	6" above base of outcrop	2
B4	Atoka Chert Pit	directly above folds in outcrop	3
B5	Atoka Chert Pit	4" below Dev/Miss contact	7
B6	Atoka Chert Pit	Base of outcrop	N/A
C1	Broken Bow	Right below Blaylock/AN contact	1
C2	Broken Bow	~5ft below Blaylock/AN contact	2
C3	Broken Bow	~5ft below Blaylock/AN contact	3
C4	Broken Bow	Black AN float from powerplant	4
C5	Broken Bow	Black AN float from powerplant	5
C6	Broken Bow	Black AN float from powerplant	6
C7	Broken Bow	East side of Highway 259	7
C8	Broken Bow	East side of Highway 259	8
C9	Broken Bow	East side of Highway 259	9
C10	Broken Bow	East side of Highway 259 (~100 yards S of #6)	10
	Core:	Depth:	
D1	Hall 2B	Specifics unknown - btw 6,127-6,278 feet	1
D2	Hall 2B	Specifics unknown - btw 6,127-6,278 feet	2
D3	Hall 2B	Specifics unknown - btw 6,127-6,278 feet	3
D4	Hall 2B	Specifics unknown - btw 6,127-6,278 feet	4
D5	Hall 2B	Specifics unknown - btw 6,127-6,278 feet	5
E1	Poe #1-29	7741.8 feet	1
E2	Poe #1-29	7744.5 feet	2
E3	Poe #1-29	7746.7 feet	3
E4	Poe #1-29	7746.78 feet	4
E5	Poe #1-29	7755.6 feet	5
E6	Poe #1-29	7796.0 feet	6
E7	Poe #1-29	7840.0 feet	7
E8	Poe #1-29	7845.5 feet	8
E9	Poe #1-29	7848.0 feet	9
E10	Poe #1-29	7849.5 feet	10

IV.2.A Chert-Organic Matrix

Two major types of chert matrix were observed in thin section: (1) brownish to black cryptocrystalline to amorphous organic-rich matrix, and (2) white-gray cryptocrystalline matrix with a few microcrystalline textured areas (Figs. 36-43). The brownish matrix contains little porosity (exhibited by blue epoxy), except in some fractures and microfossils. Organic matter, observed as matrix bituminite (a.k.a. amorphenite), is dispersed throughout the brownish to black matrix. All of the novaculitic chert sample samples from the Woodford Shale (I-35, Poe #1-29, Hall 2B) and the Atoka Chert Pit contain brownish to black, organic-rich matrix. In addition, the weathered sample from the Broken Bow outcrop on U.S. Highway 259 also contains this type of matrix.

The Arkansas Novaculite samples vary in appearance however, and include the pale cryptocrystalline and microcrystalline textures described above (Fig. 39). The Poe core is unique in that it exhibits a texture resembling grainstone- and packstone, as well as light beige colored amorphous textures within the same thin section (Figs. 40-42). The only samples to contain cryptocrystalline-microcrystalline textures were the white novaculite overlying the Blaylock Sandstone and the black novaculite float samples from the power plant site, both of which were from Broken Bow/Beavers Bend, and a thin section (7,746.78 feet) from the Poe #1-29 core (Fig. 39,43). Cryptocrystalline and amorphous chert textures were identified in all thin sections and therefore all locations. However, the only samples dominated by vein fill and microcrystalline silica were the Broken Bow Uplift samples.

The brown chert matrix exhibits porosity primarily in veins and occasionally in the ghosts of where silica spherules used to exist through the chert matrix. The dark brown chert matrix in these samples may be influenced by the thickness of the thin sections (40 μm) versus the lighter, white chert matrix (20 μm). The white chert matrix displays randomly dispersed porosity that it often filled with organic matter and exhibits porosity where carbonate rhombs used to exist. The black-type chert matrix contains very little obvious porosity.

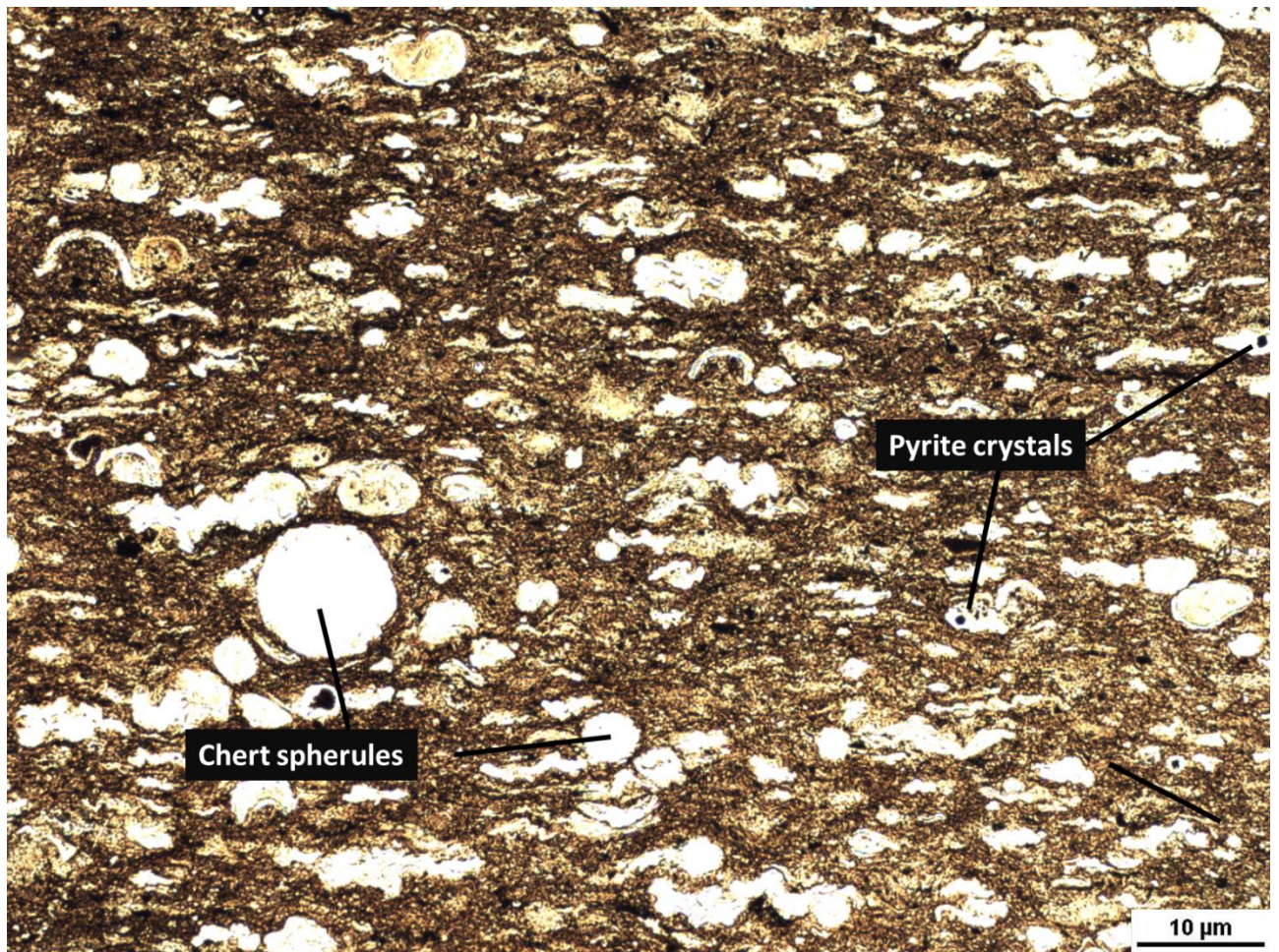


Figure 36. Thin section photomicrograph of radiolarian-rich novaculitic chert from the I-35 outcrop (sample A5). The brownish chert-organic matrix, abundant chert spherules, spicules and scattered pyrite crystals in thin section are representative of chert from this locality. Many of the spherules include walls of perforated radiolarian tests.

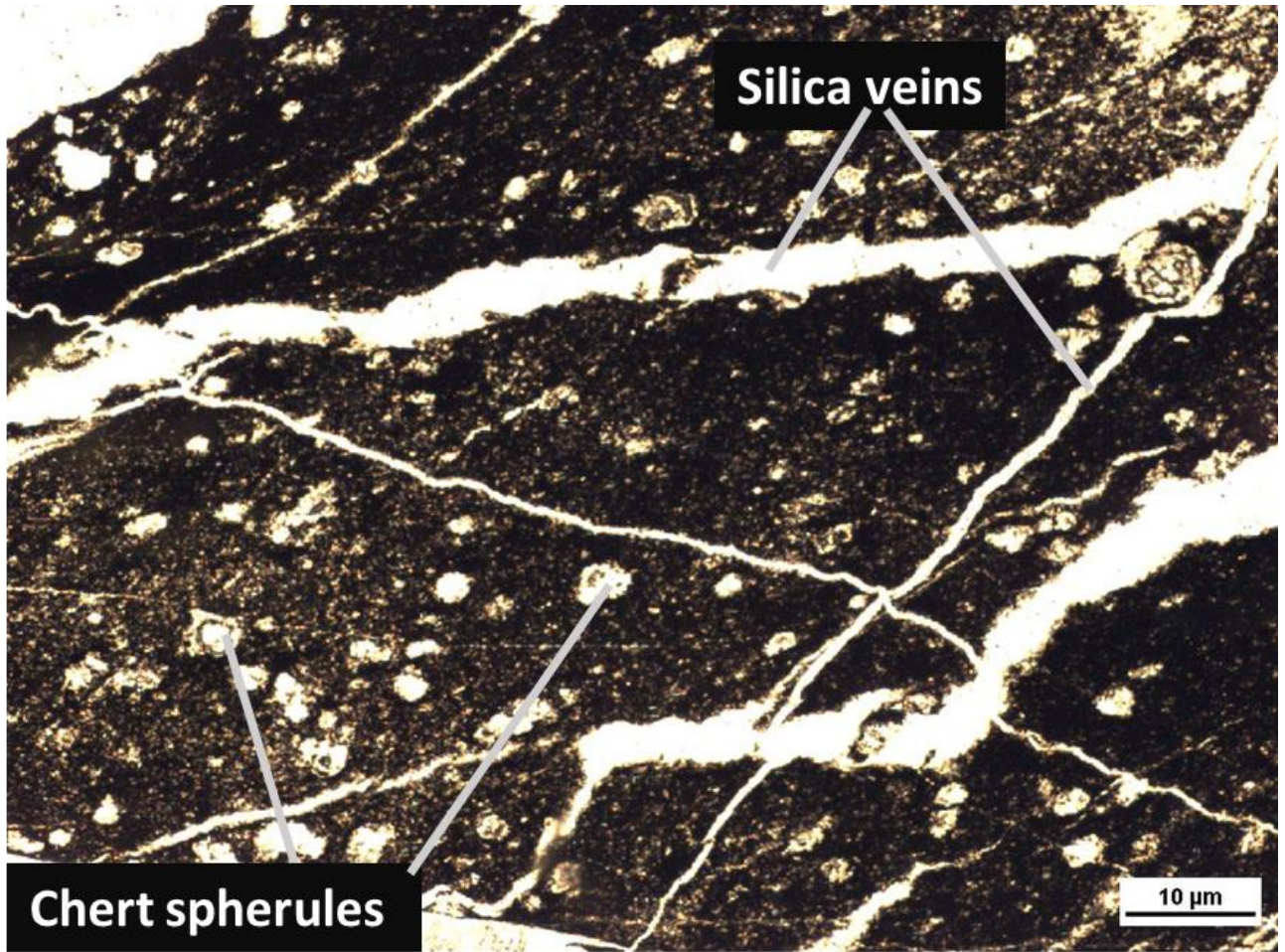


Figure 37. Dark novaculite specimen from the power plant at the Broken Bow/Beavers Bend outcrop (sample C4). The black Arkansas Novaculite contains abundant silica spherules and white silica veins. This type of novaculite looks similar to the Devonian chert in the Woodford Shale.

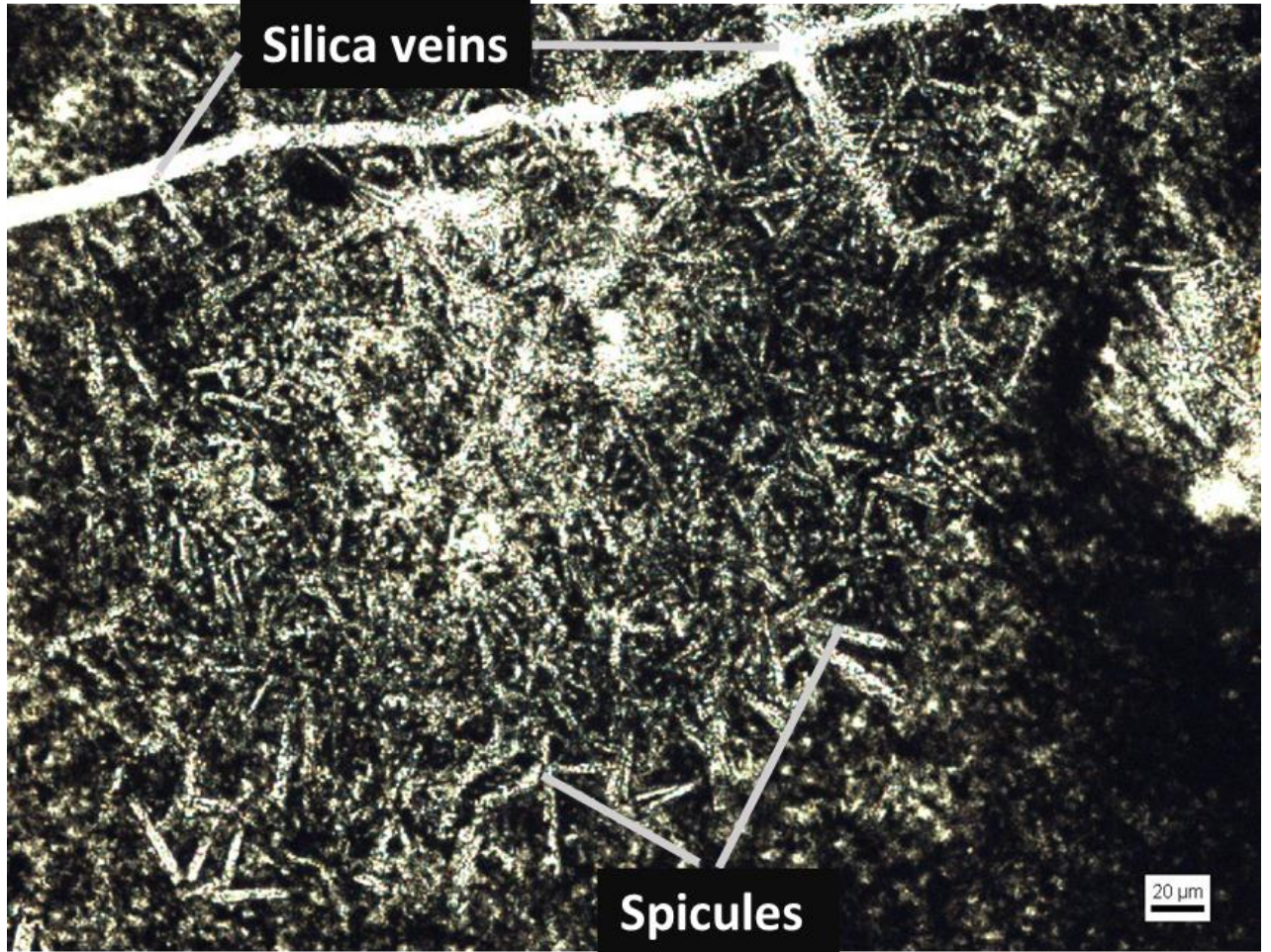


Figure 38. Dark spicular chert with silica veins from the power plant at the Broken Bow/Beavers Bend outcrop (sample C4). Spicular Arkansas Novaculite was first identified by Goldstein (1959) and was only found in the dark power plant samples from the Broken Bow outcrop during this research.

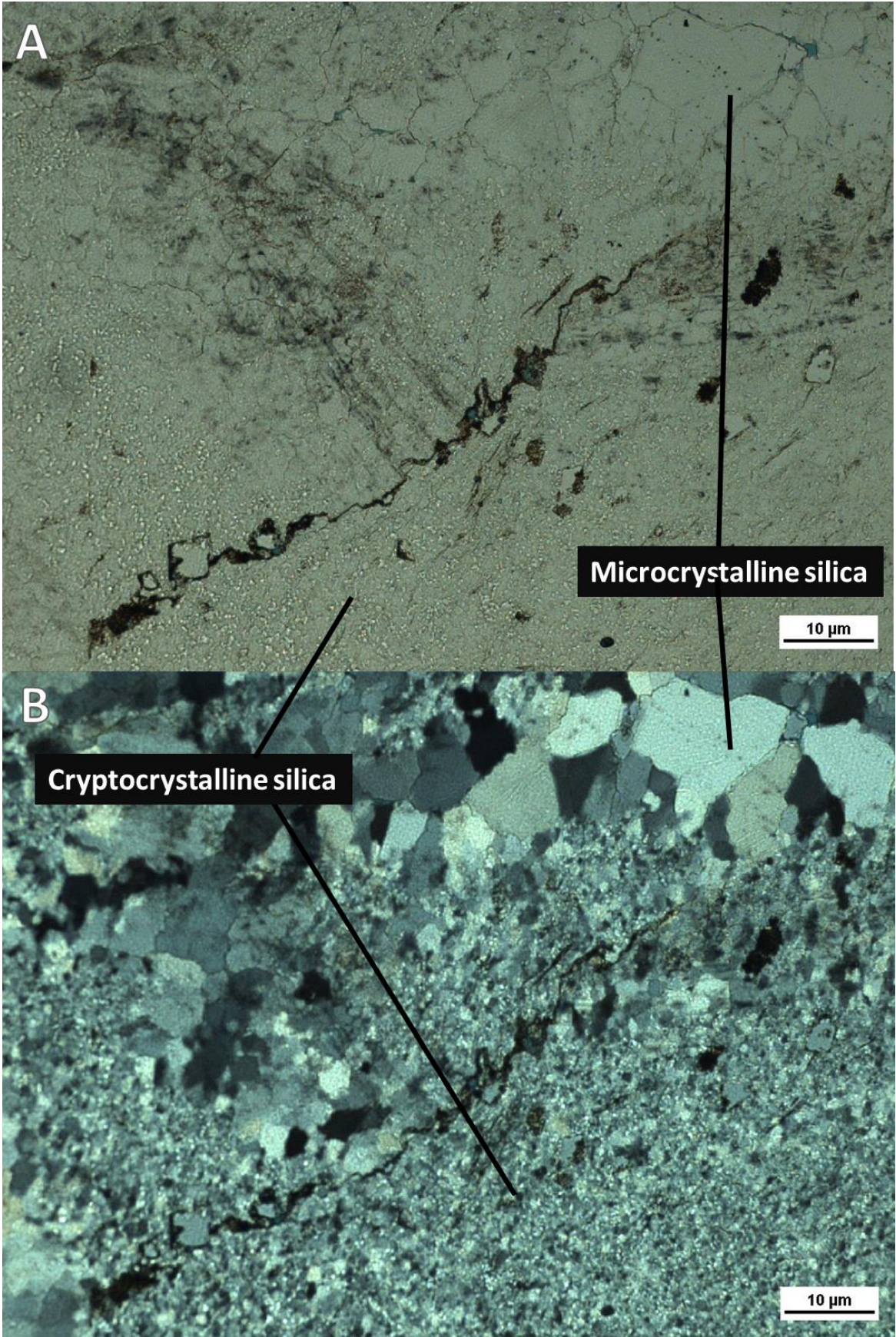


Figure 39. Photomicrograph of chert and vein quartz from the Arkansas Novaculite near the Blaylock Sandstone contact, Broken Bow/Beavers Bend outcrop (sample C3). A) Plane-polarized-light photomicrograph showing transparent chert and vein fill. Note prominent stylolite and faint crystal fabric. B) Sample viewed in cross-polarized light showing cryptocrystalline chert in lower part of photomicrograph, microcrystalline vein quartz in upper part, and stylolite dissecting cryptocrystalline chert.

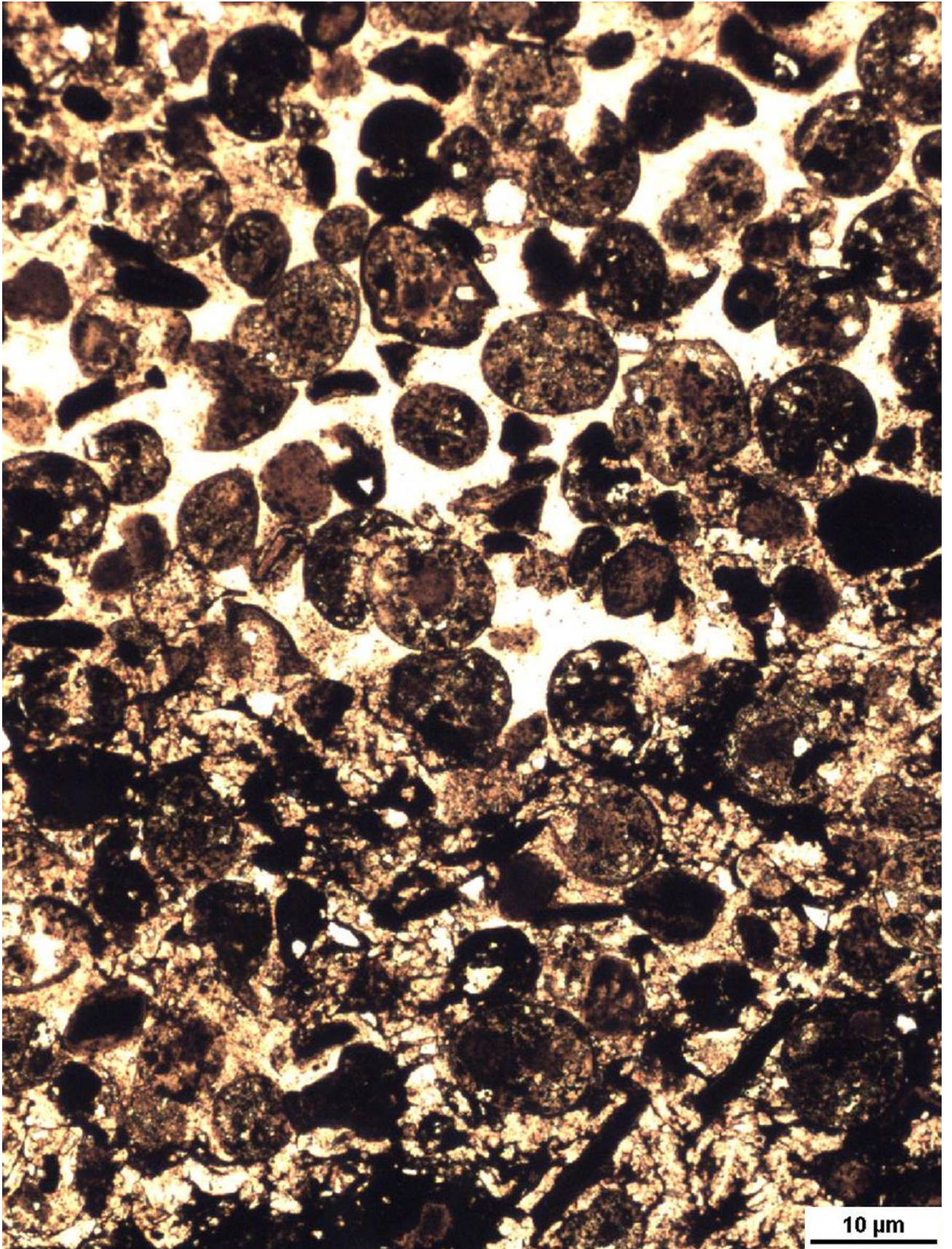


Figure 40. Novaculitic chert from the Poe #1-29 core (sample E2). The novaculitic chert exhibits texture resembling grainstone and packstone in this specimen. Spheroidal bodies include Spumellarian radiolaria. Note that chert on bottom of the image appears phosphatic and spicular.

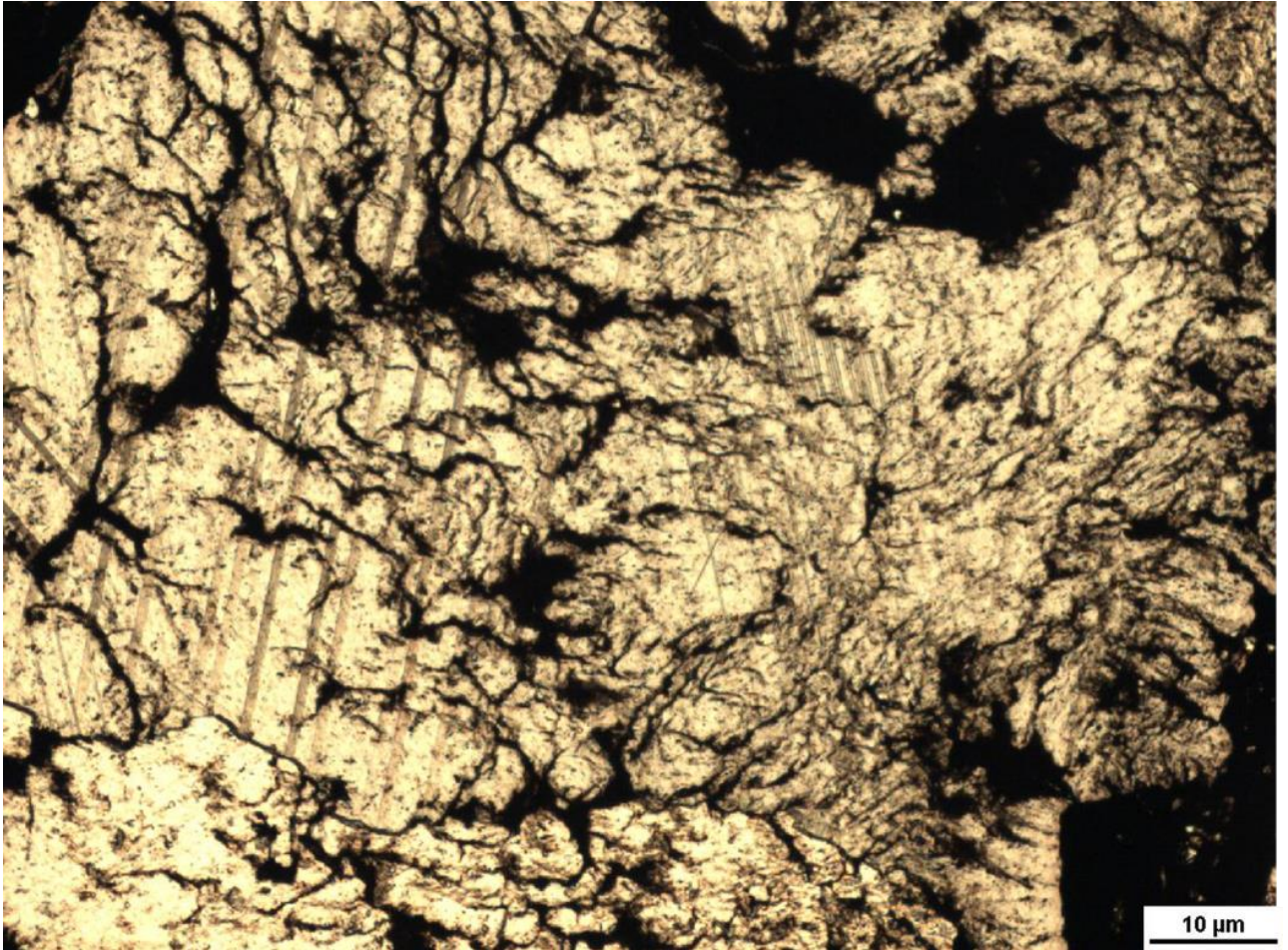


Figure 41. Novaculitic chert from the Poe #1-29 core (sample E2). The chert exhibits possible twinning within the lighter amorphous areas.

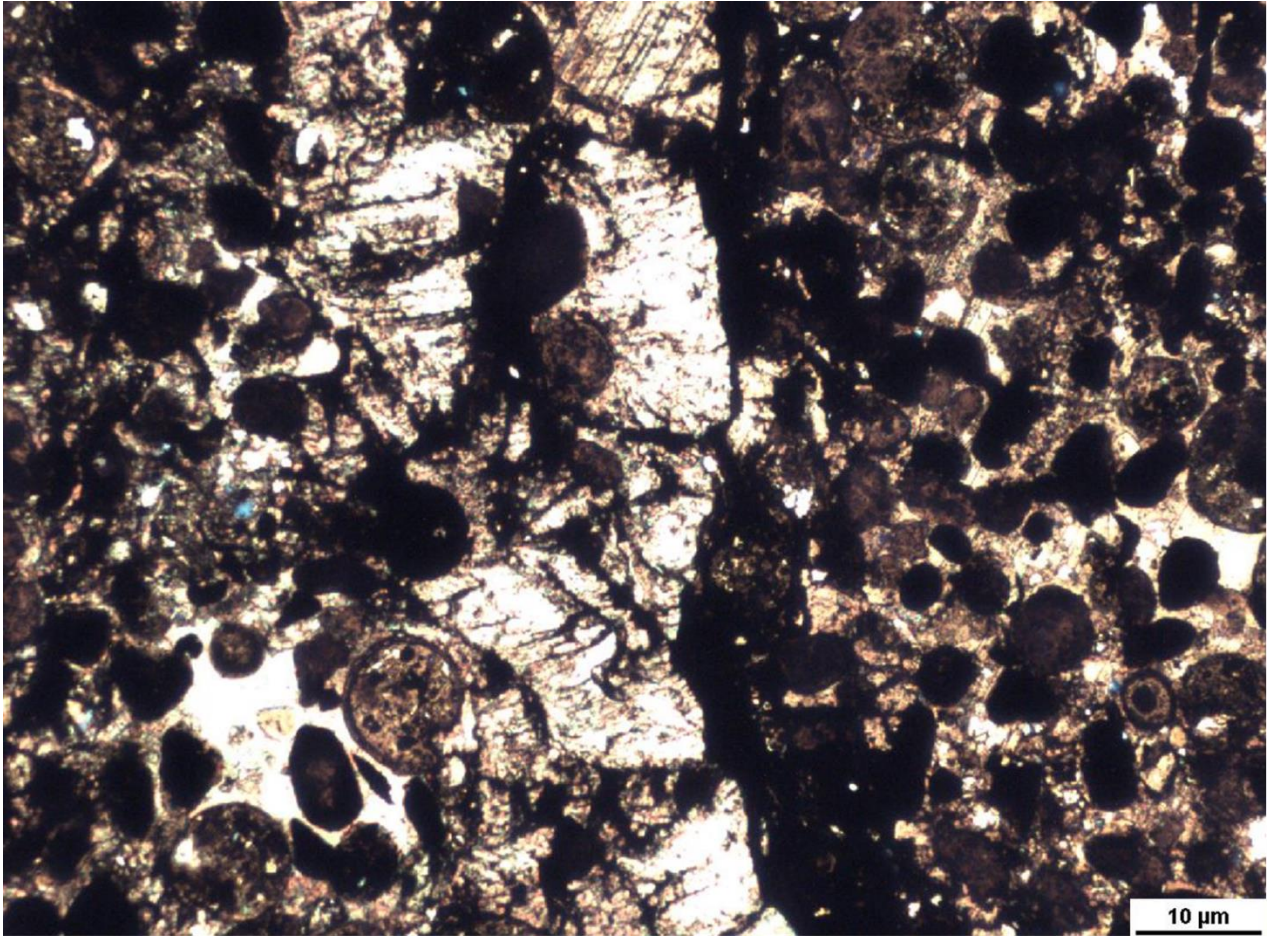


Figure 42. Novaculitic chert from the Poe #1-29 core (sample E2). The cross-polarized image exhibits a packstone-like texture along with possible twinning within the lighter-colored portions.

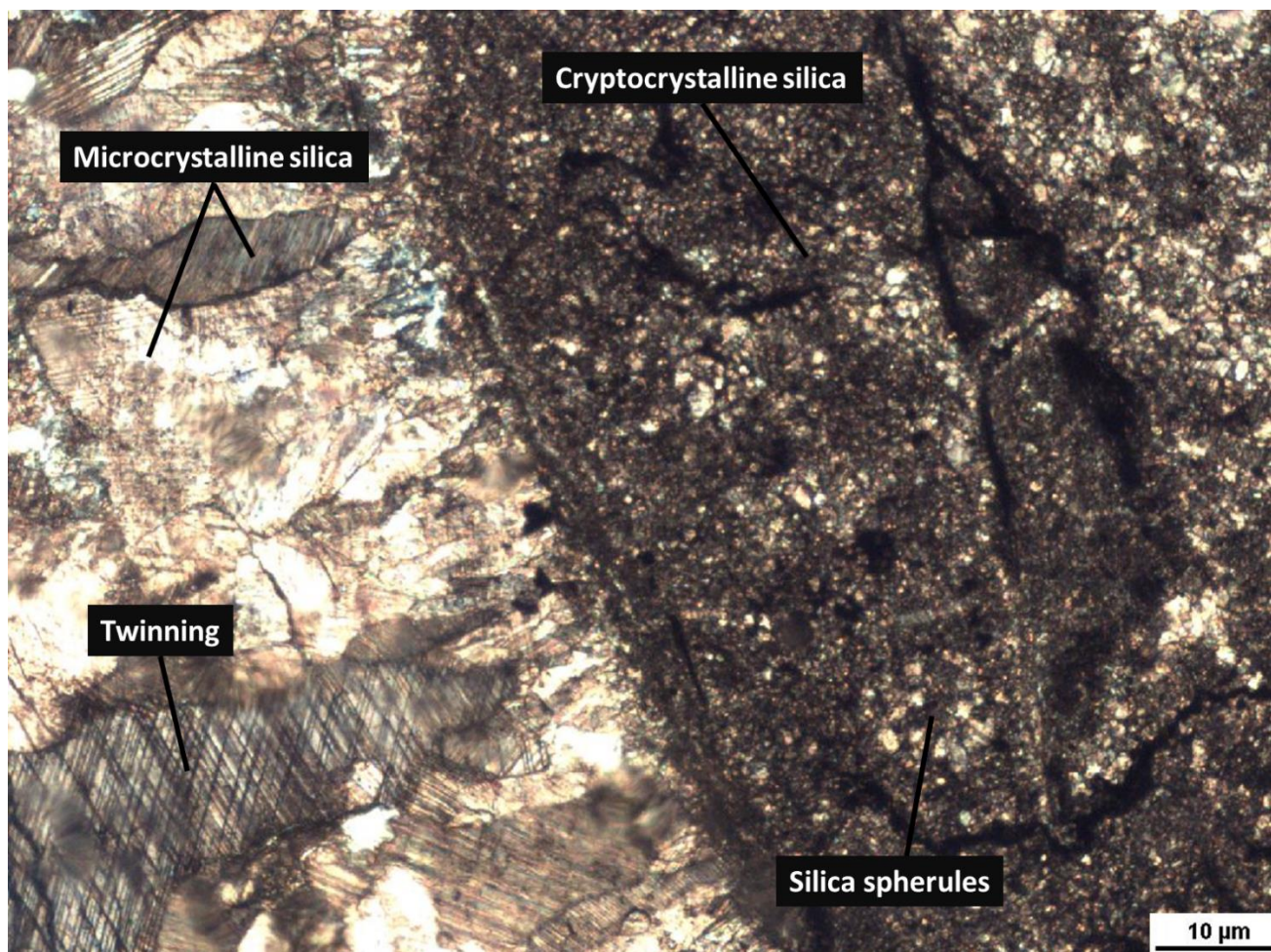


Figure 43. Novaculitic chert from the Poe #1-29 core (sample E4). Cross-polarized image displaying various silica crystal sizes (cryptocrystalline-microcrystalline) within the novaculitic chert. The microcrystalline texture is likely vein fill.

IV.2.B Biogenic Structures

The organic-rich chert with cryptocrystalline to amorphous silica matrix contains abundant botryoidal chalcedony spherules (Figs. 44-47). The spherules appear to most commonly fill the tests of radiolaria (Fig. 46, 47). However, the spherules also fill a variety of spherical, organic-walled microfossils, including acritarchs (Fig. 48) and *Tasmanites* algal cysts (Figs. 49, 50). However, many of the spherules are coated with organic films that superficially resemble

Tasmanites but are clearly different. For example, some of the organic-coated spherules contain faint ghosts of spumellarian radiolaria tests (Fig. 47).

Sponge spicules constitute a large part of the identifiable fossil material in the chert. As mentioned previously, spicular chert is common in the core zone of the Ouachita orogen (Goldstein, 1959) (Fig. 38). The spicules in this type of chert are densely packed, which makes it difficult to determine if they are monaxon spicules from demosponges or other forms, such as triaxon spicules from hexactinellid sponges. Indeed, numerous triaxon spicules were observed in phosphatic chert and phosphate nodules, indicating that hexactinellids were an important component of the novaculite fauna (Fig. 51, 52). The pale cryptocrystalline matrix contains some sponge spicules, but generally lacks other identifiable biogenic structures. A phosphate nodule in the Hall 2B core contains exceptionally well preserved siliceous microfossils, including a variety of Radiolaria (Spumellaria and Nassellaria) and triaxon sponge spicules (Figs. 53, 54).

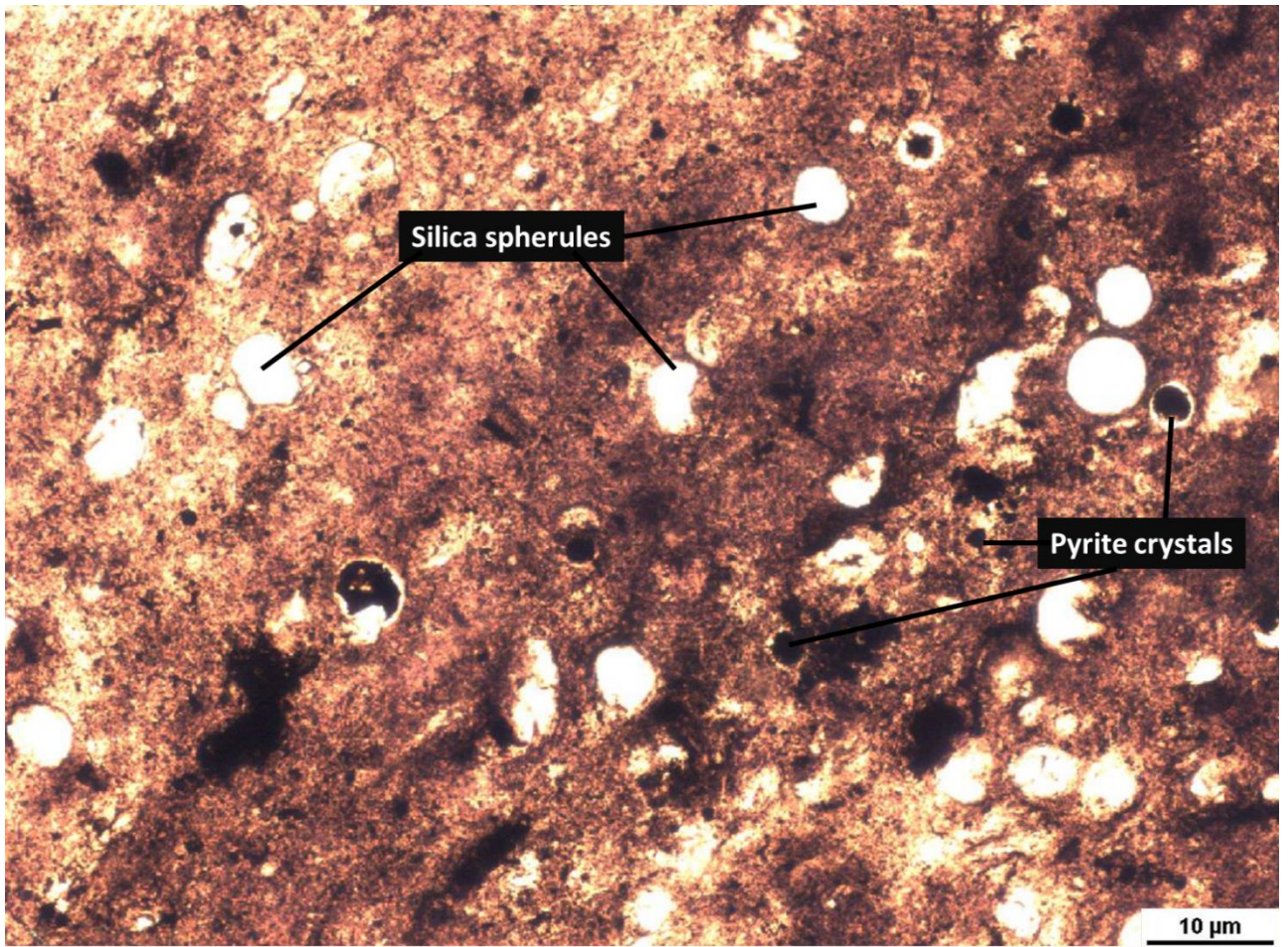


Figure 44. Novaculitic chert thin section with abundant silica spherules in organic-rich amorphous to cryptocrystalline silica matrix Hall 2B core (sample D5).

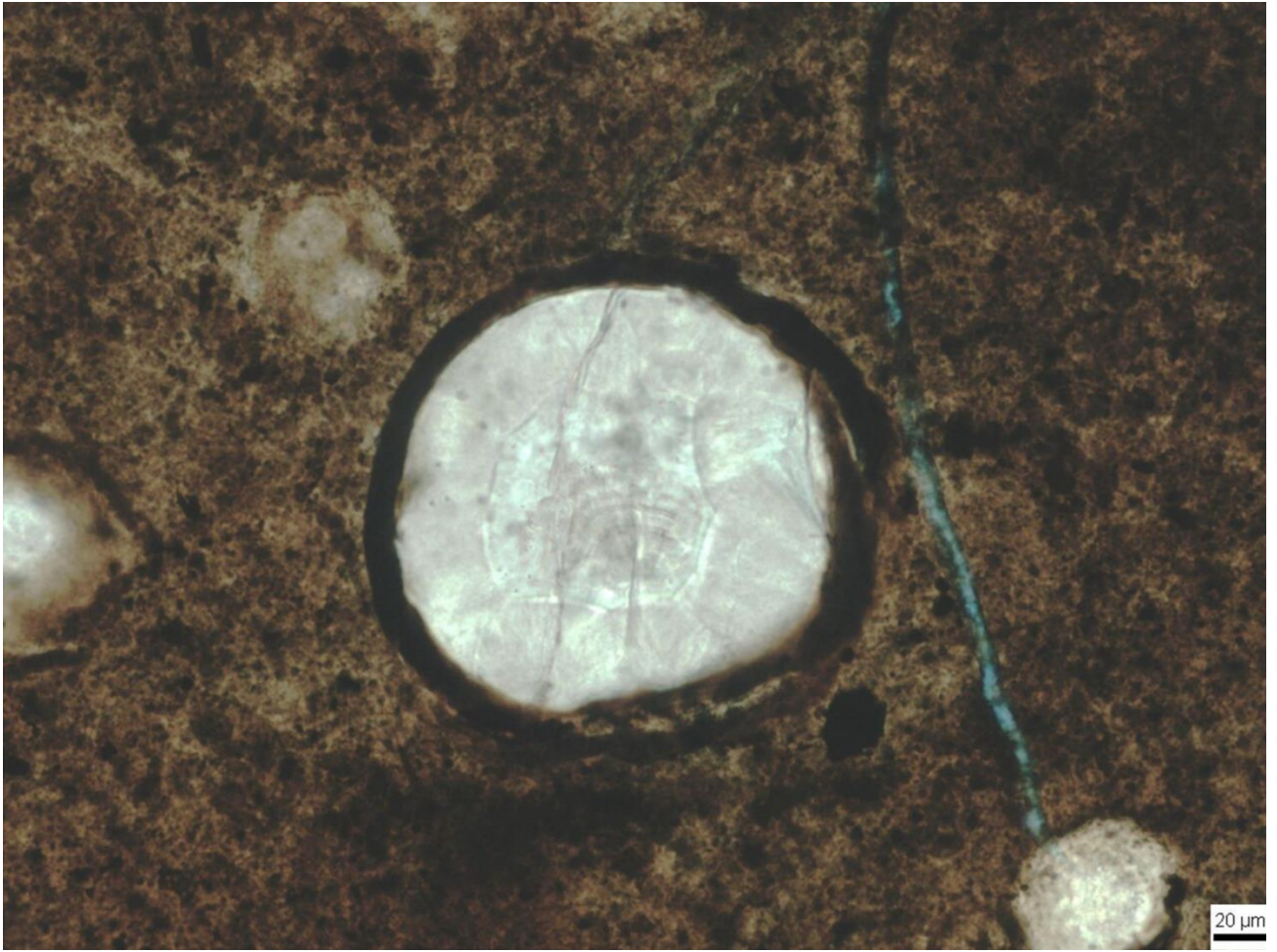


Figure 45. Thin section photomicrograph of organic film coating a botryoidal silica spherule from the Hall 2B core (sample D5).

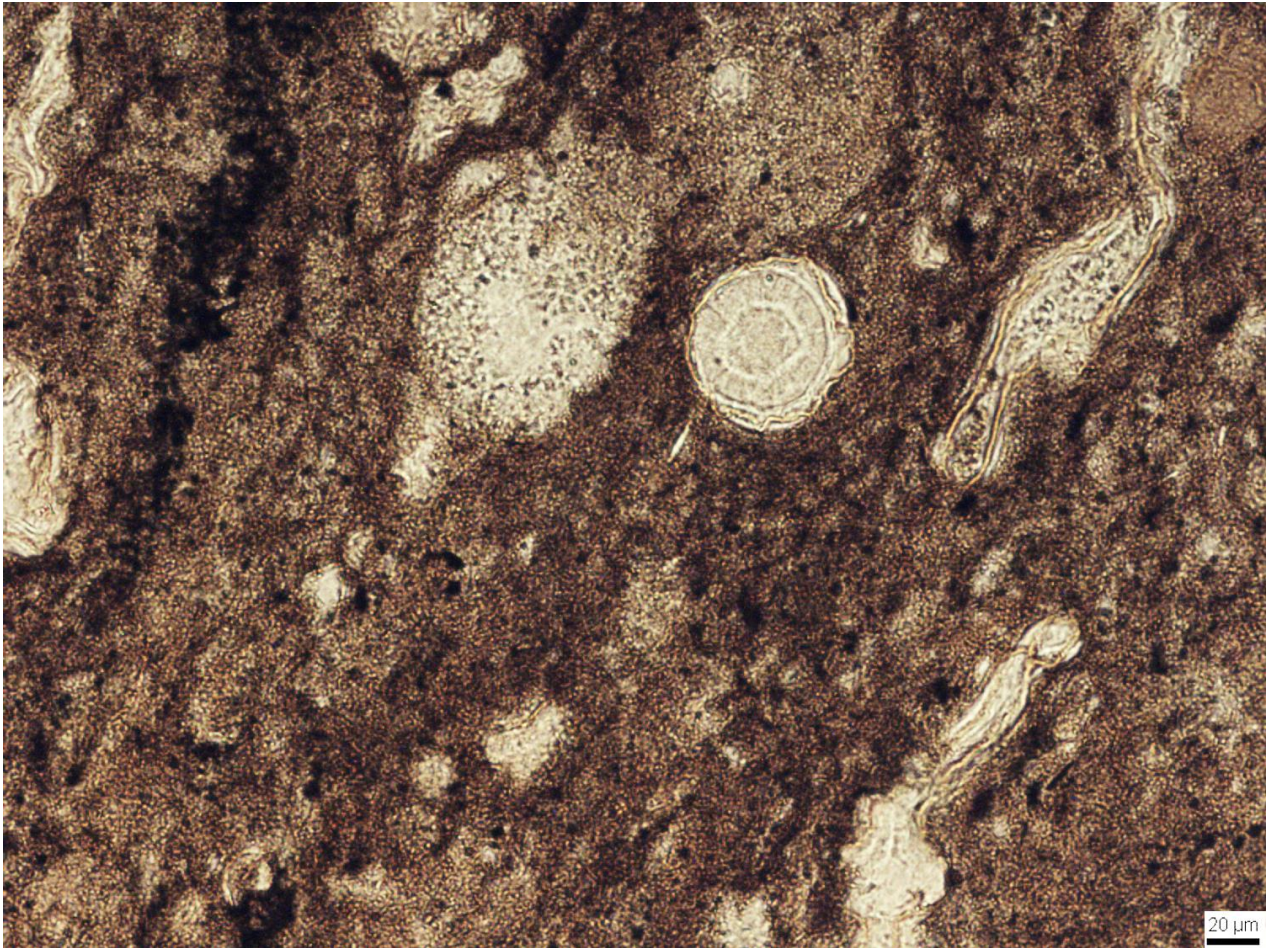


Figure 46. Thin section photomicrograph of novaculitic chert from the I-35 outcrop (sample A3).
The image shows spherules containing faint ghosts of radiolaria tests.

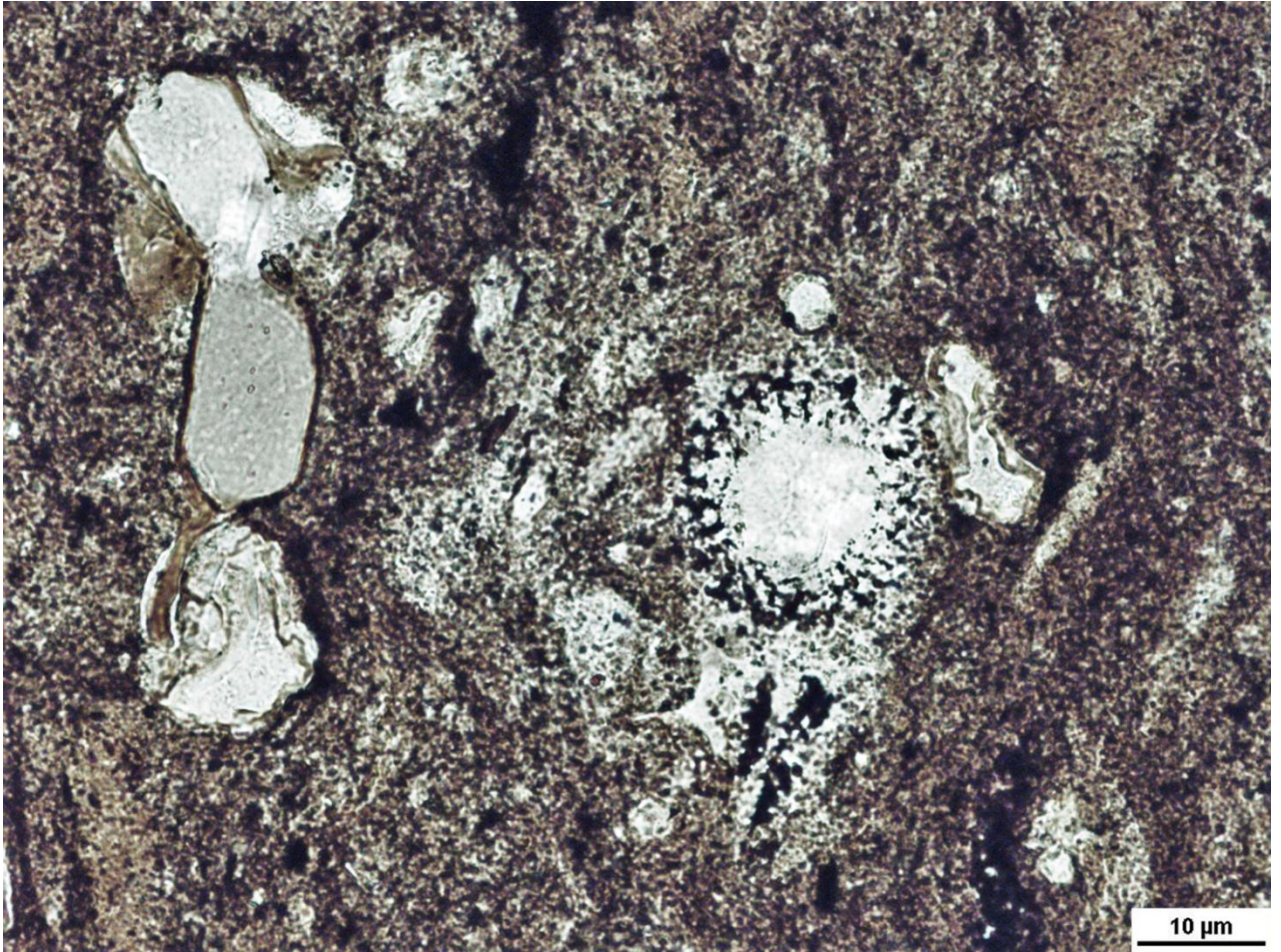


Figure 47. Novaculitic chert thin section from I-35 (sample A3). A botryoidal silica spherule inside of possible *Spumellaria* radiolarian test with one possible spine. Note the organic film of unidentifiable origin on the left side of the image.

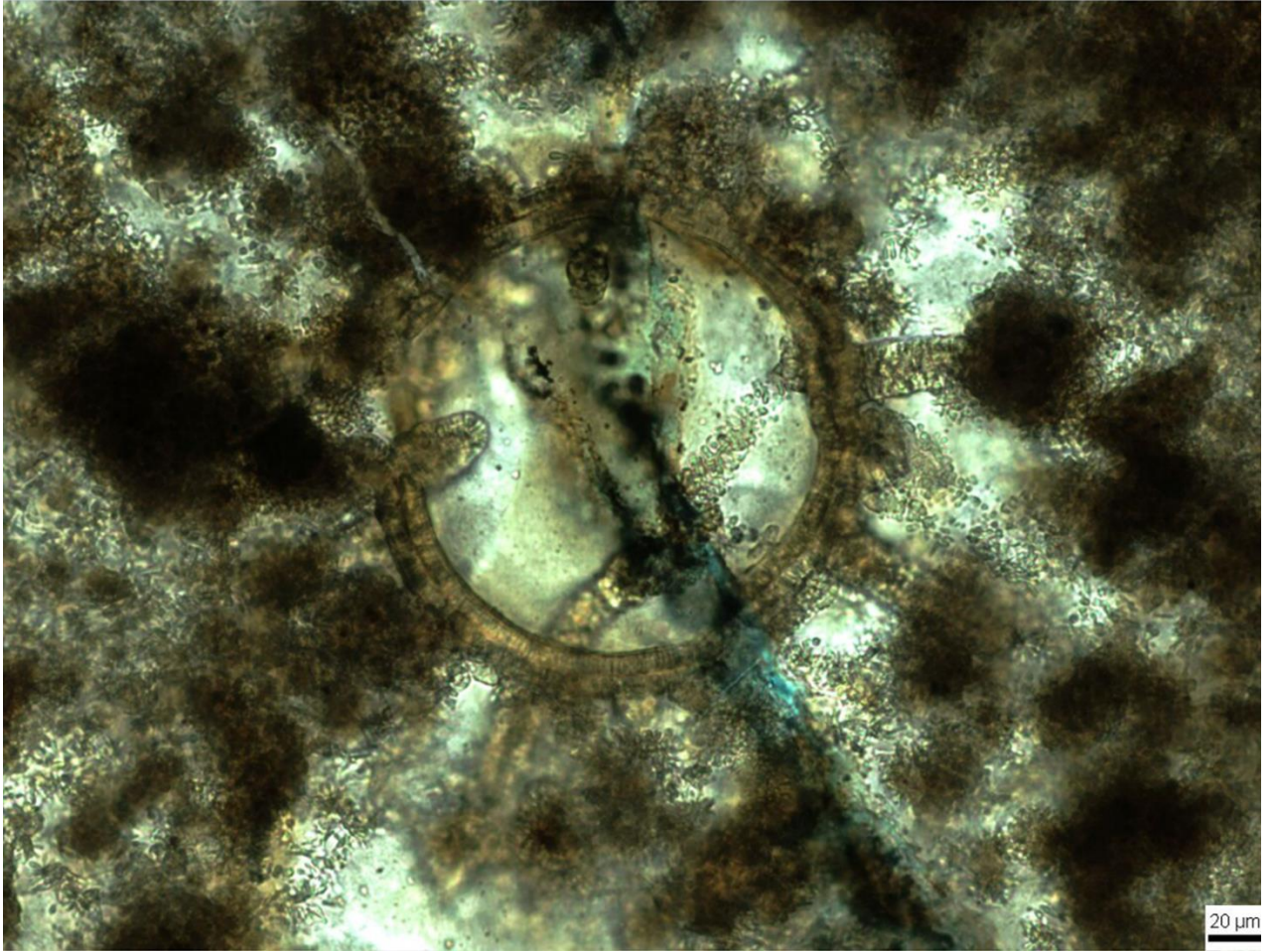


Figure 48. Novaculitic chert thin section from the Hall 2B core (sample D5). In the center of the image a silica spherule fills an acritarch.

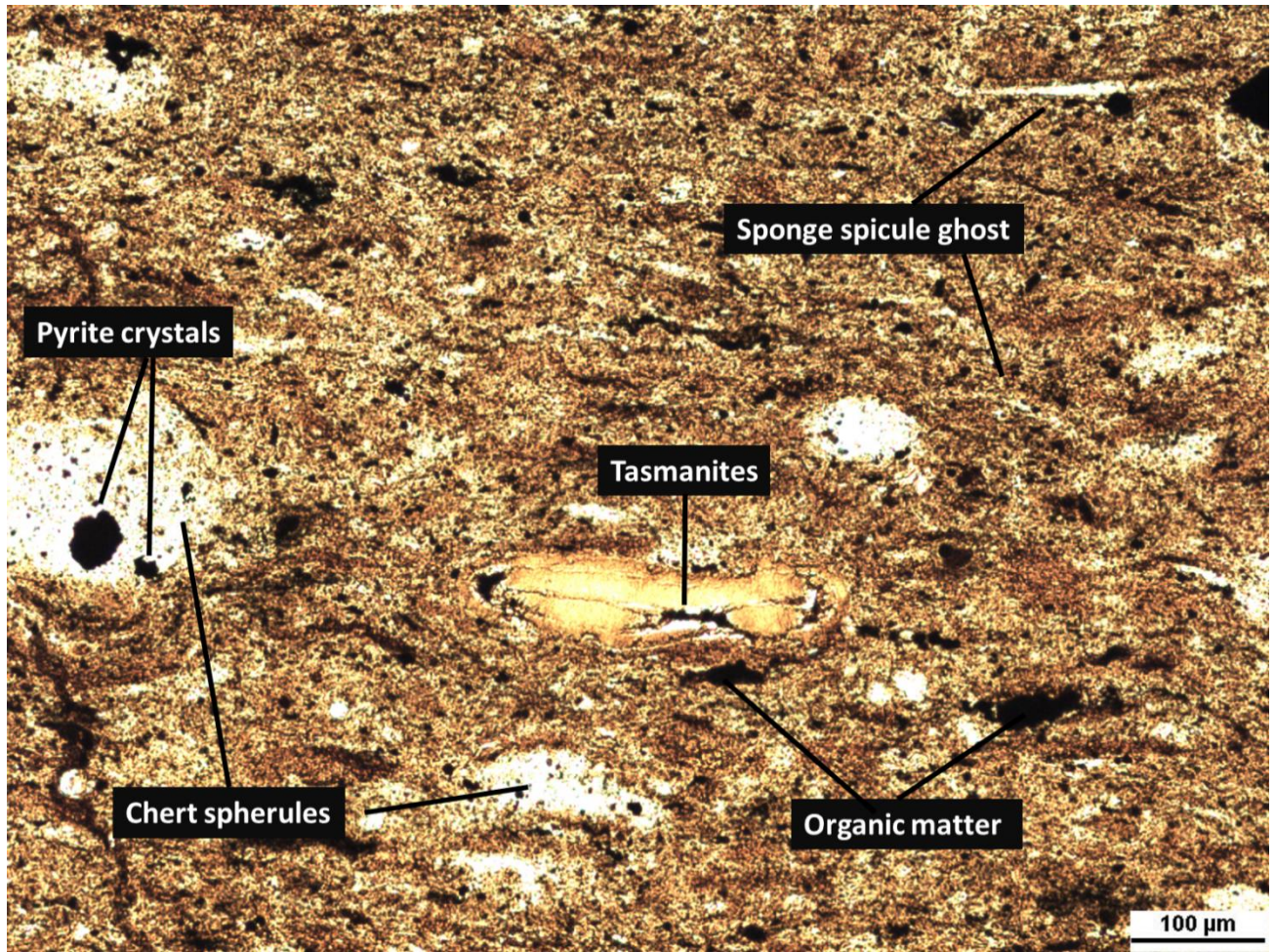


Figure 49. Thin section photomicrograph of novaculitic chert from the I-35 outcrop (sample A1). Note organic-walled *Tasmanites* specimen with thick organic body preserved within cyst lining. Recrystallized spicules also are common in this sample, and pyrite euhedra are preserved in some chert spherules.

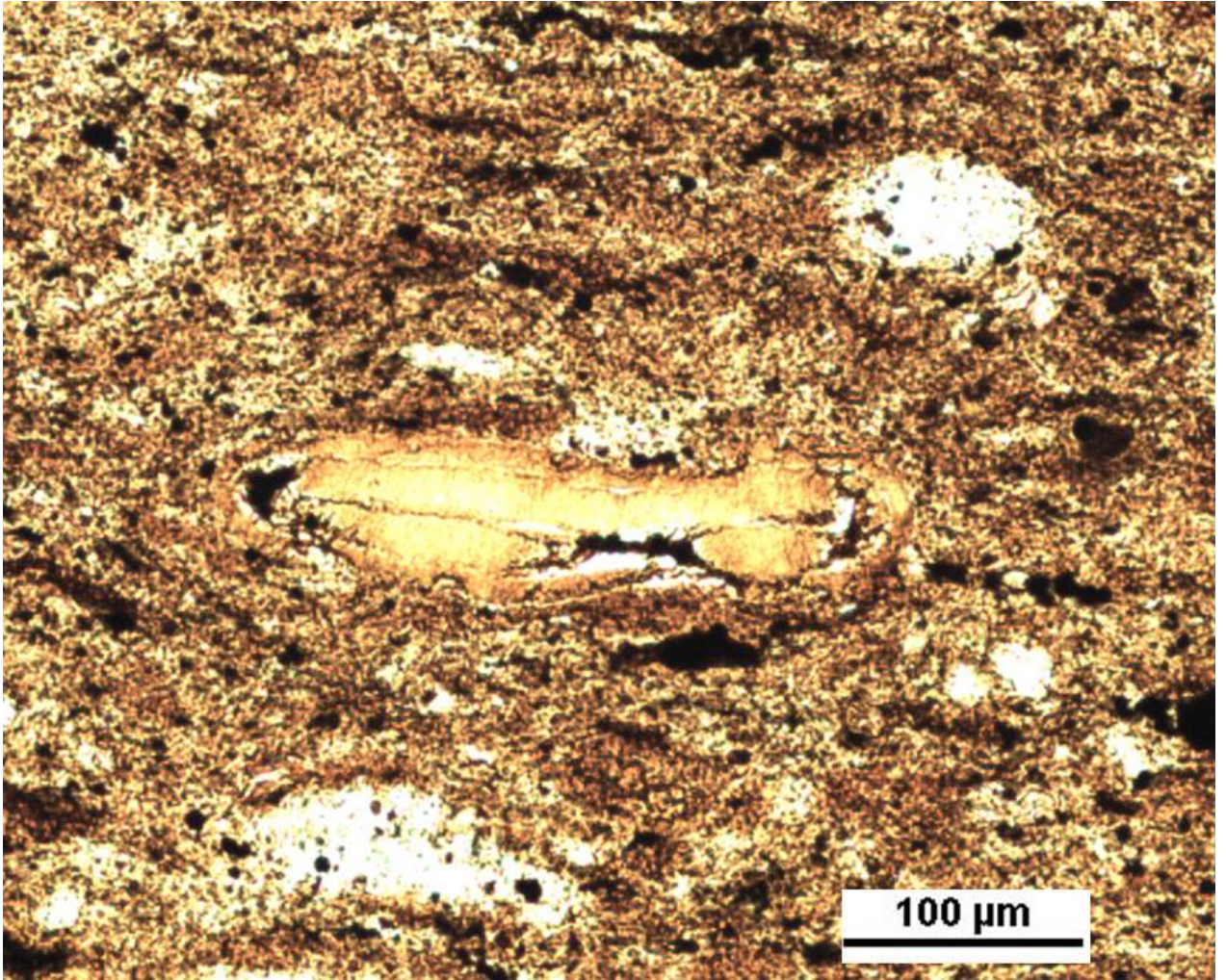


Figure 50. Thin section photomicrograph of novaculitic chert from the I-35 outcrop (sample A1). Close up of organic-walled *Tasmanites* specimen with thick organic body preserved within cyst lining.

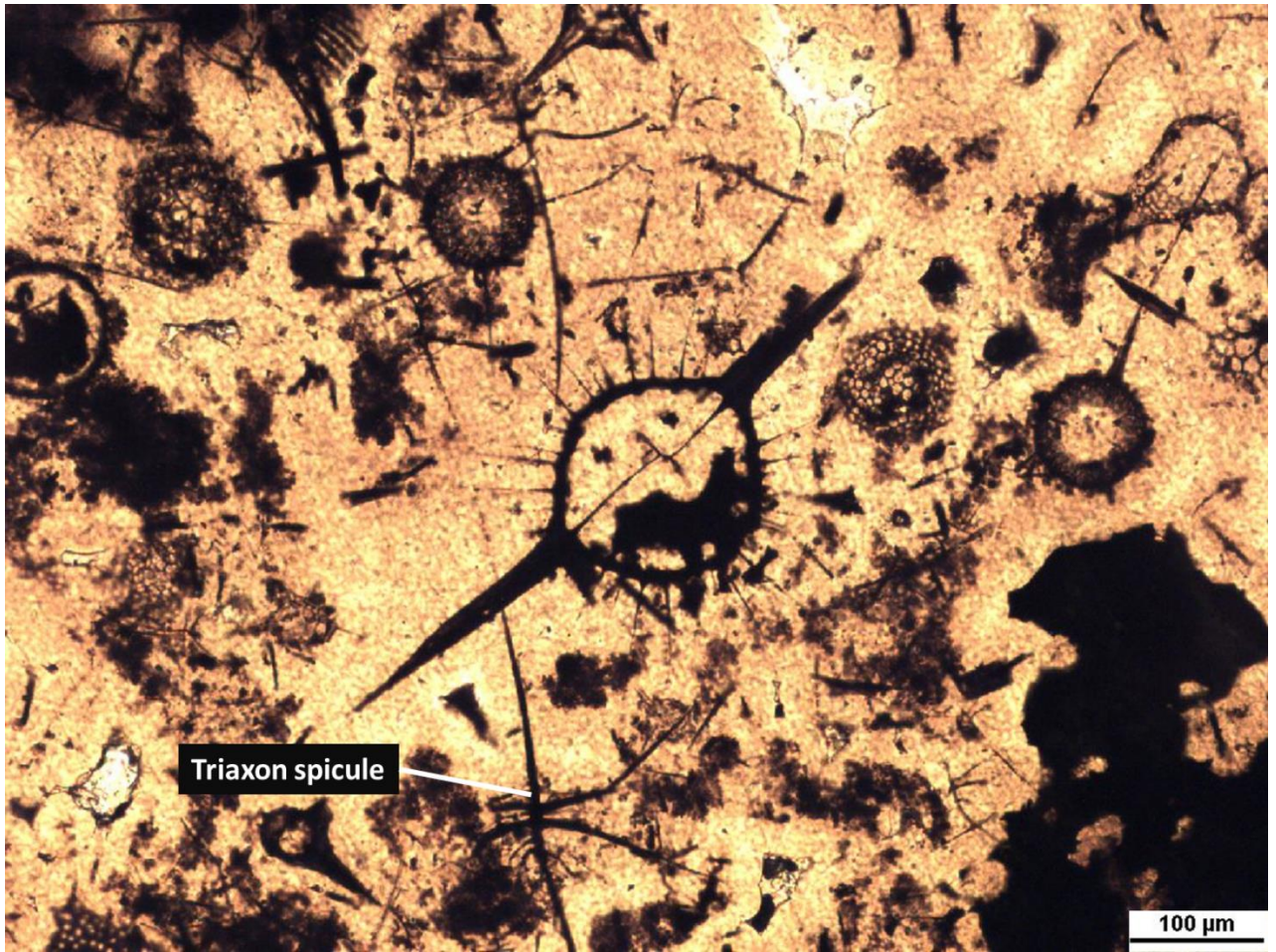


Figure 51. Thin section photomicrograph of a phosphate nodule showing diversity of Spumellaria in the Woodford Shale, Hall 2B core (sample D3). Note triaxon spicule in lower part of photomicrograph.

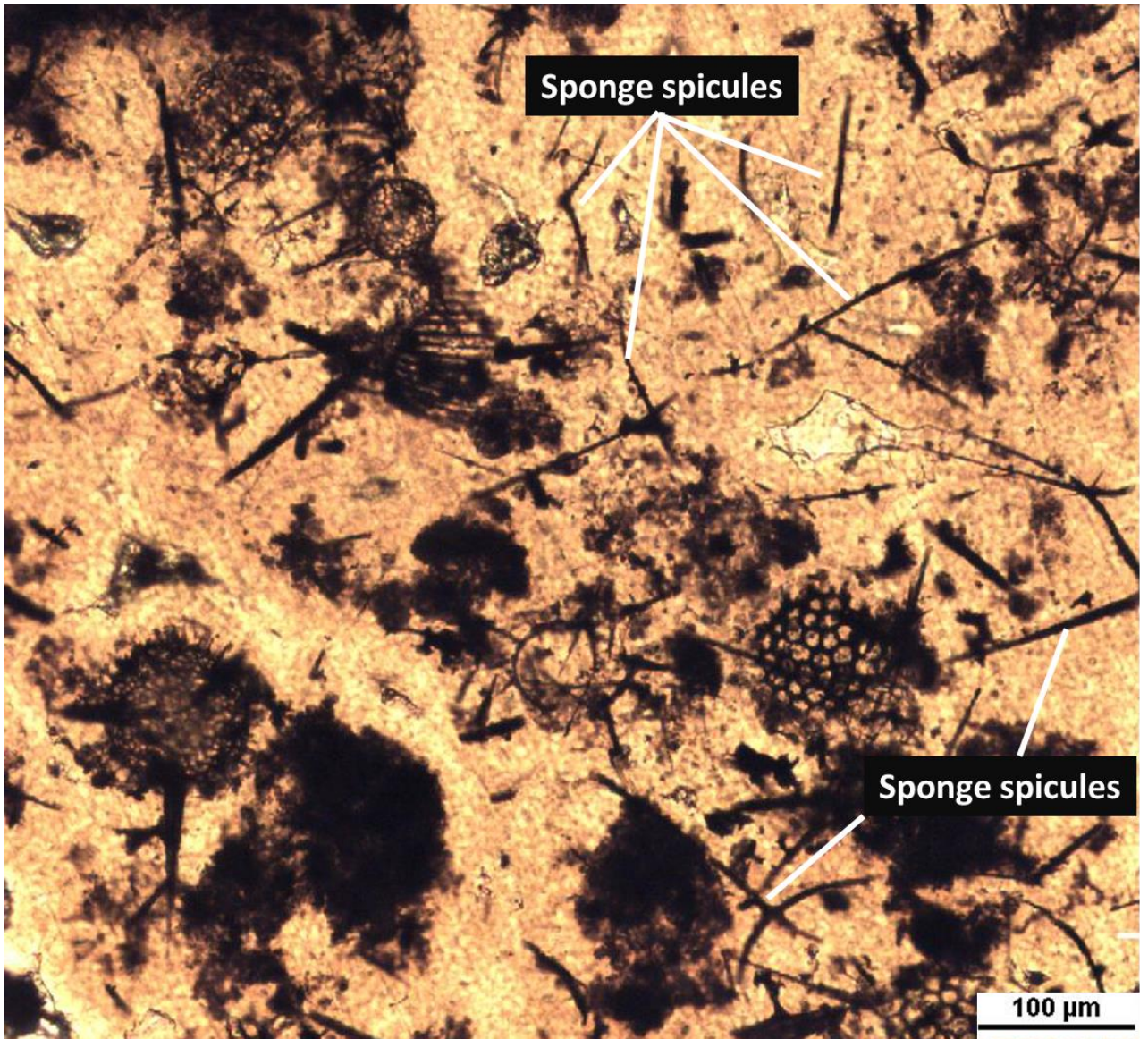


Figure 52. Thin section photomicrograph showing abundant sponge spicules and Radiolaria, Hall 2B core (sample D3). The branching triaxon spicules are indicative of glass sponges (Order Hexactinellida), which are benthic organisms.

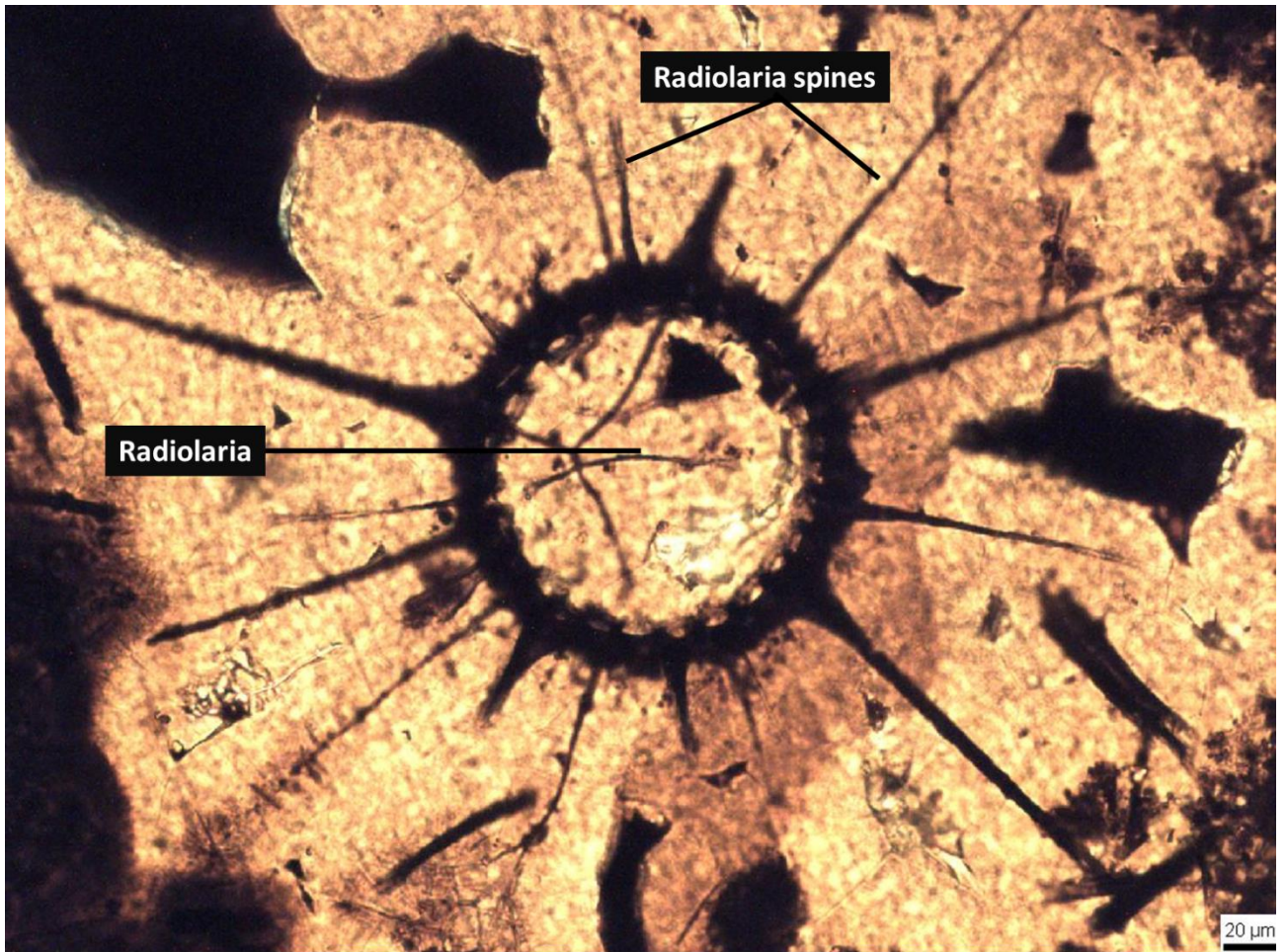


Figure 53. Spumellarian radiolarian with preserved spines, Hall 2B core (sample D3). This phosphate nodule contains extremely well preserved Radiolaria and sponge spicules.

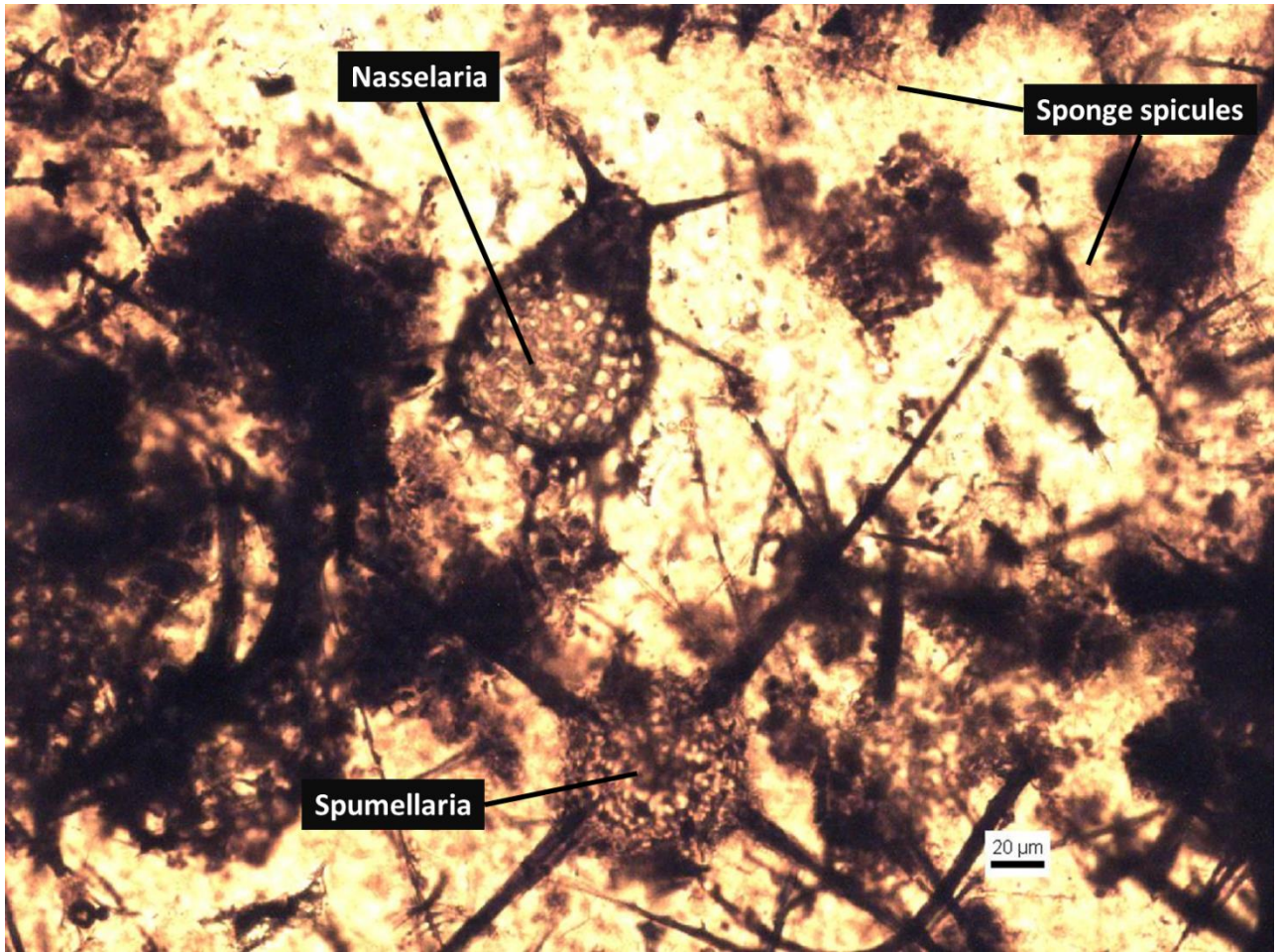


Figure 54. Thin section photomicrograph showing well-preserved Spumellaria and Nassellaria, Hall 2B core (sample D3).

IV.2.C Diagenetic Features

Pyrite was observed in all samples and locations. Pyrite forms range from very small ($1\mu\text{m}+$) and scattered euhedra, large subhedral-euhedral crystals, pyrite veins and pyrite crystals contained within biogenic structure and pyritization of some of the walls of the microfossils (Fig. 55). Although the samples contained abundant pyrite, no pyrite framboids were readily visible. The most predominant diagenetic features in the massive white Arkansas Novaculite are euhedral

pyrite cubes (Fig. 56). Some veins within the black float samples from the Broken Bow/Beavers Bend power plant contain acicular crystals that commonly form spherulites (Figs. 57, 58). The Hall 2B core contains late-stage breccia with possibly dolomite mineralization within the voids (Fig. 59). The dark Arkansas Novaculite samples from the power plant in Broken Bow/Beavers Bend also contain large (up to 10 μm) zoned ferroan dolomite crystals (Fig. 60). Individual ferroan dolomite rhombs are preserved as rhombic crystals in some of the samples, particularly the massive white Arkansas Novaculite samples from near the Blaylock Sandstone contact in Beavers Bend (Fig. 61, 62). The black float samples from the Broken Bow power plant contain ferroan dolomite crystals that are present throughout the chert matrix in veins (Fig. 63).

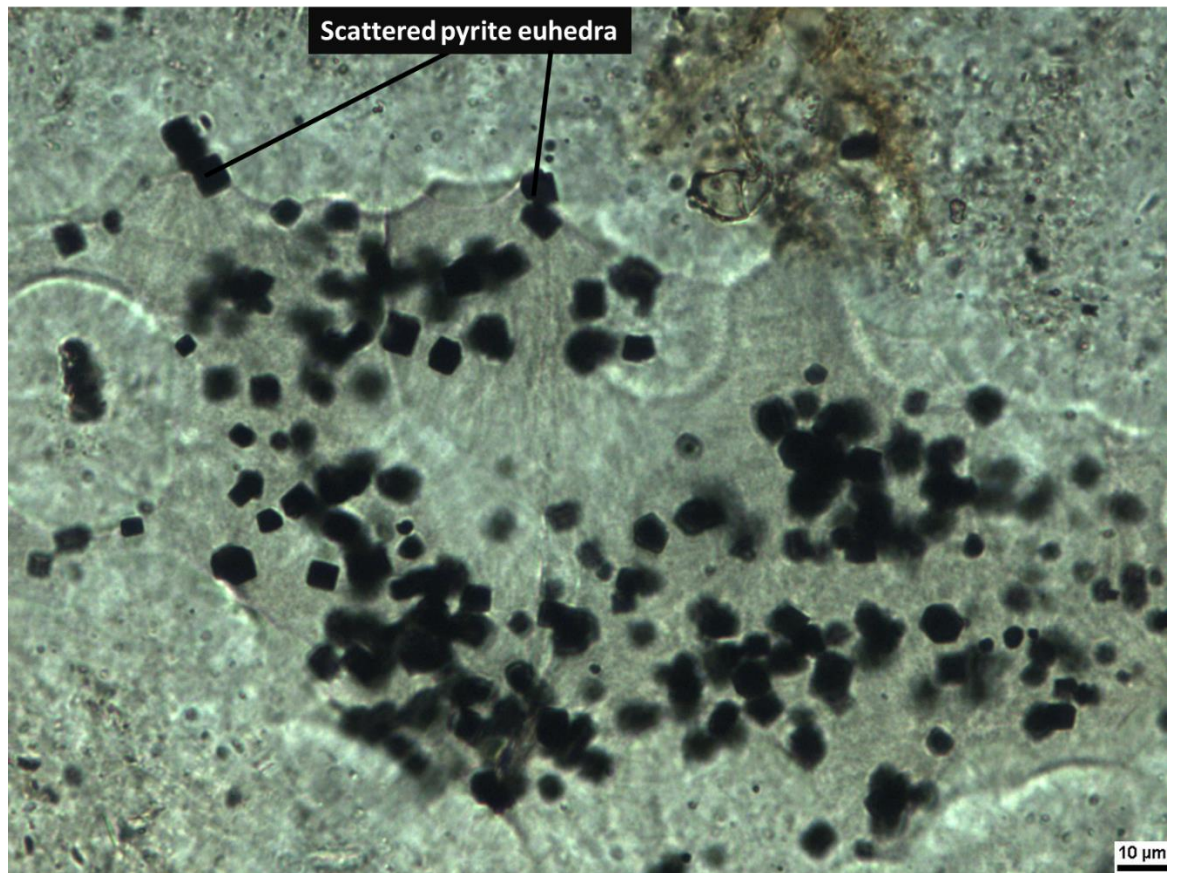


Figure 55. Photomicrograph a phosphate nodule from the Atoka outcrop (sample B1). The nodule exhibits a botryoidal texture around the scattered pyrite euhedra.

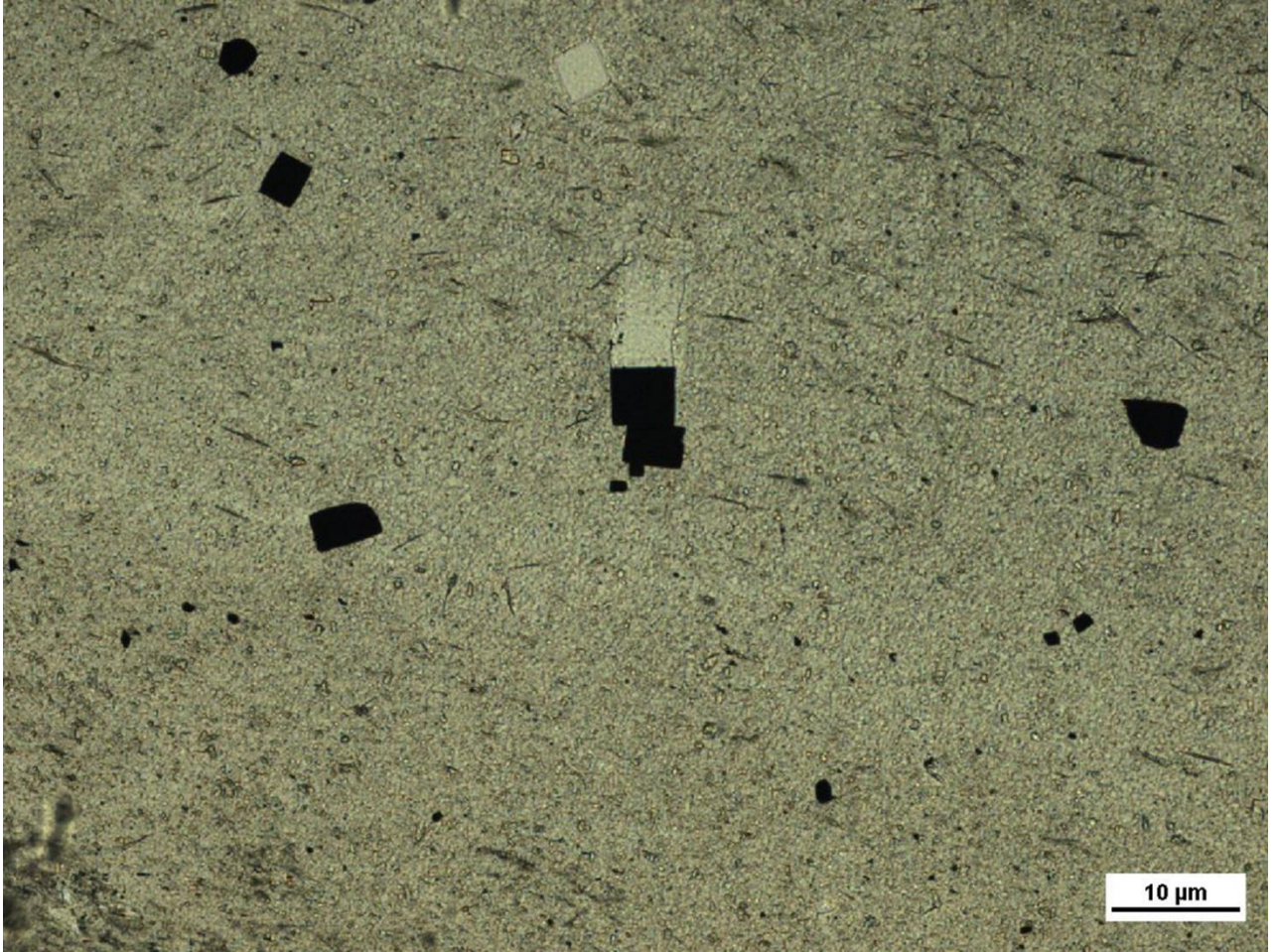


Figure 56. Photomicrograph of dark Arkansas Novaculite from the power plant at Broken Bow/Beavers Bend (sample C6). The novaculite contains cubic pyrite euhedra.

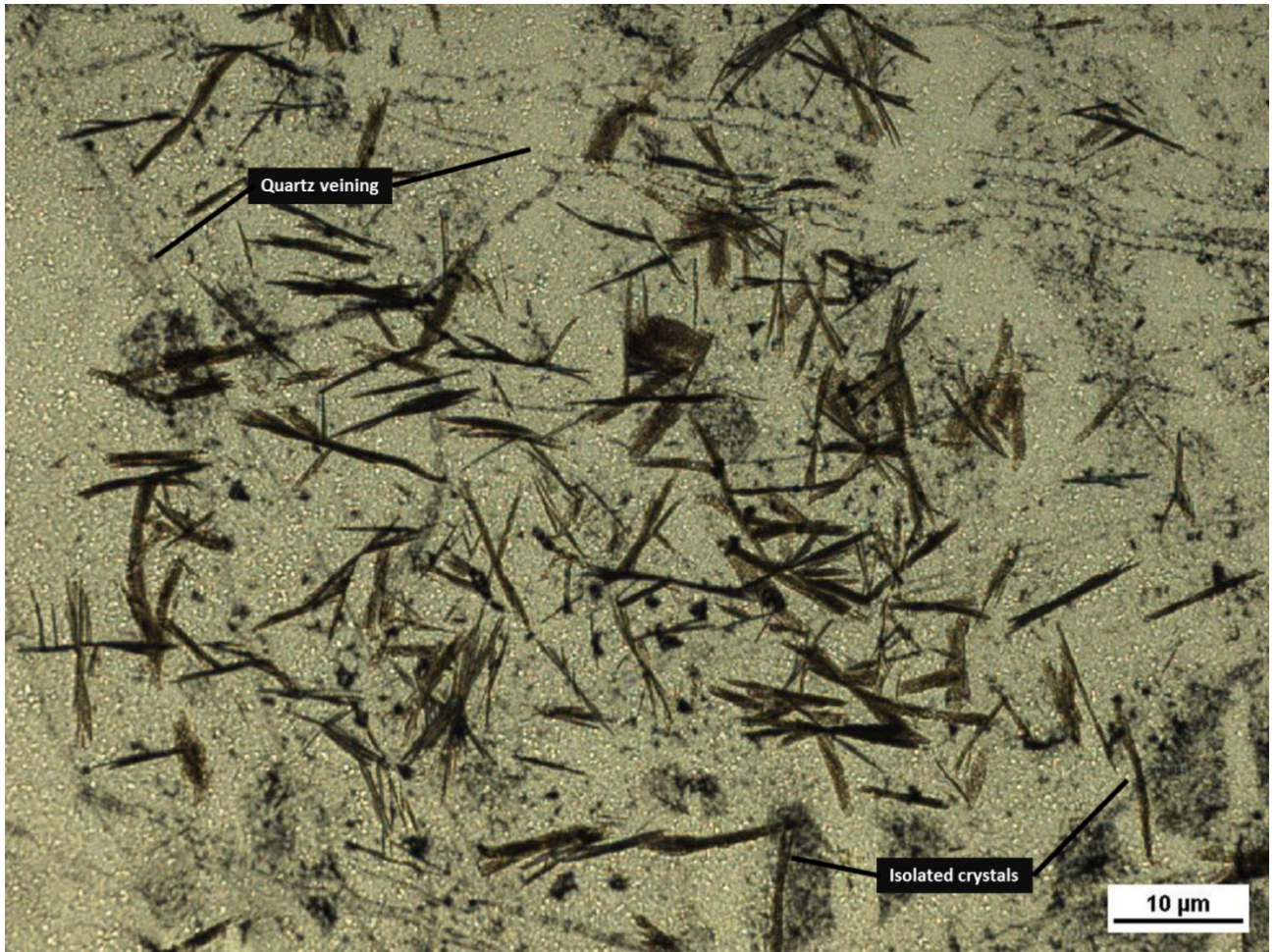


Figure 57. Arkansas Novaculite sample from the power plant at Broken Bow/Beavers Bend (sample C5). The sample contains isolated crystals, a few rectilinear arrays, and some partial spherulites. Note quartz veins that cross-cut the silica containing the acicular crystals.

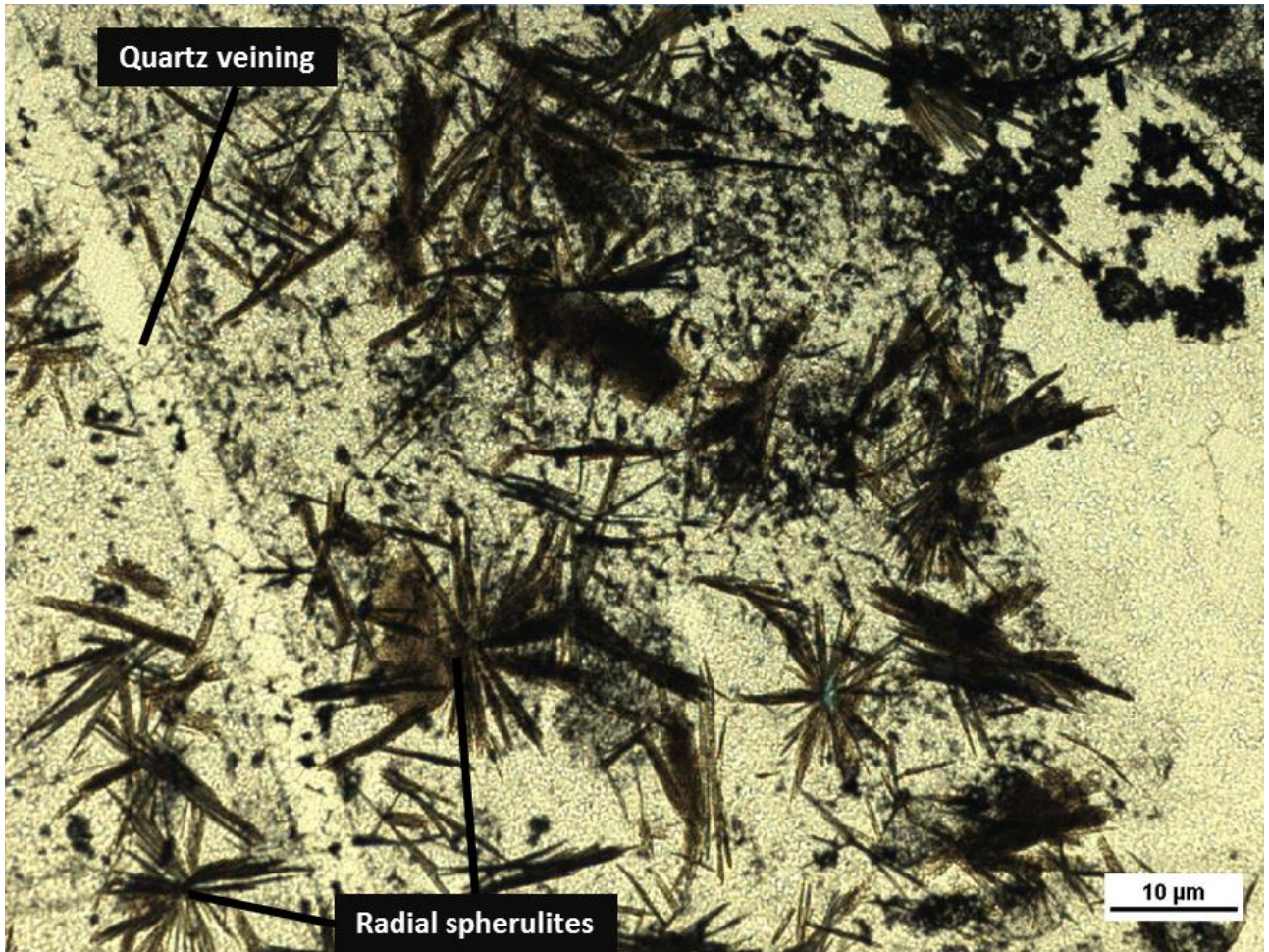


Figure 58. Photomicrograph of dark Arkansas Novaculite from the power plant at Broken Bow/Beavers Bend (sample C5). Note dark, acicular crystals within transparent chert. These crystals are in places isolated and in places form distinctive radial spherulites. The prominent quartz vein running through the image indicates a cross-cutting relationship where the veining post-dates spherulite formation.

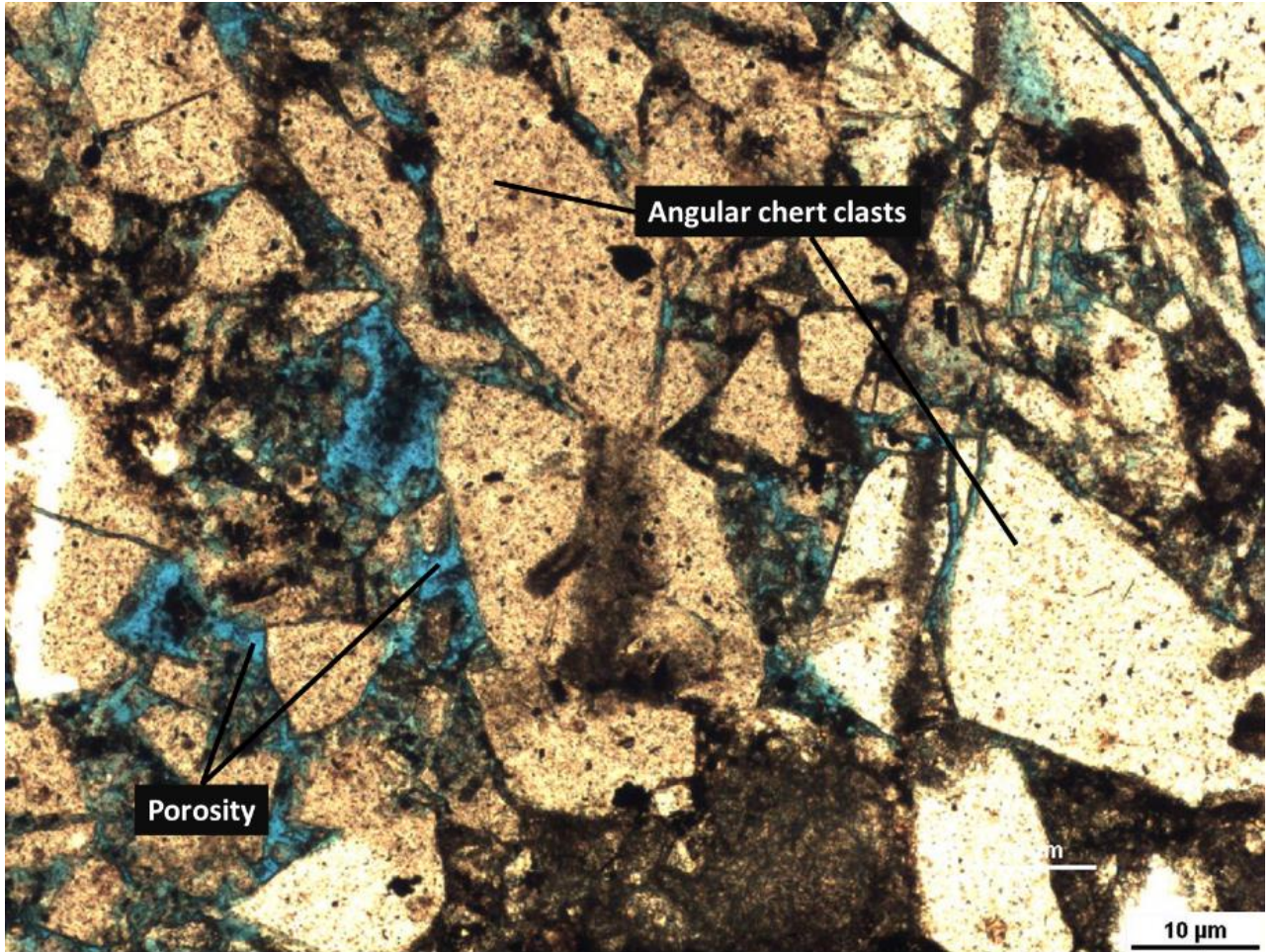


Figure 59. Novaculitic chert thin section from the Hall 2B core (sample D4). The medium-brown chert matrix is veined and brecciated in the Hall 2B core. According to Power (2015), the brecciation post-dates quartz veining along the southwest margin of the Anadarko Basin.

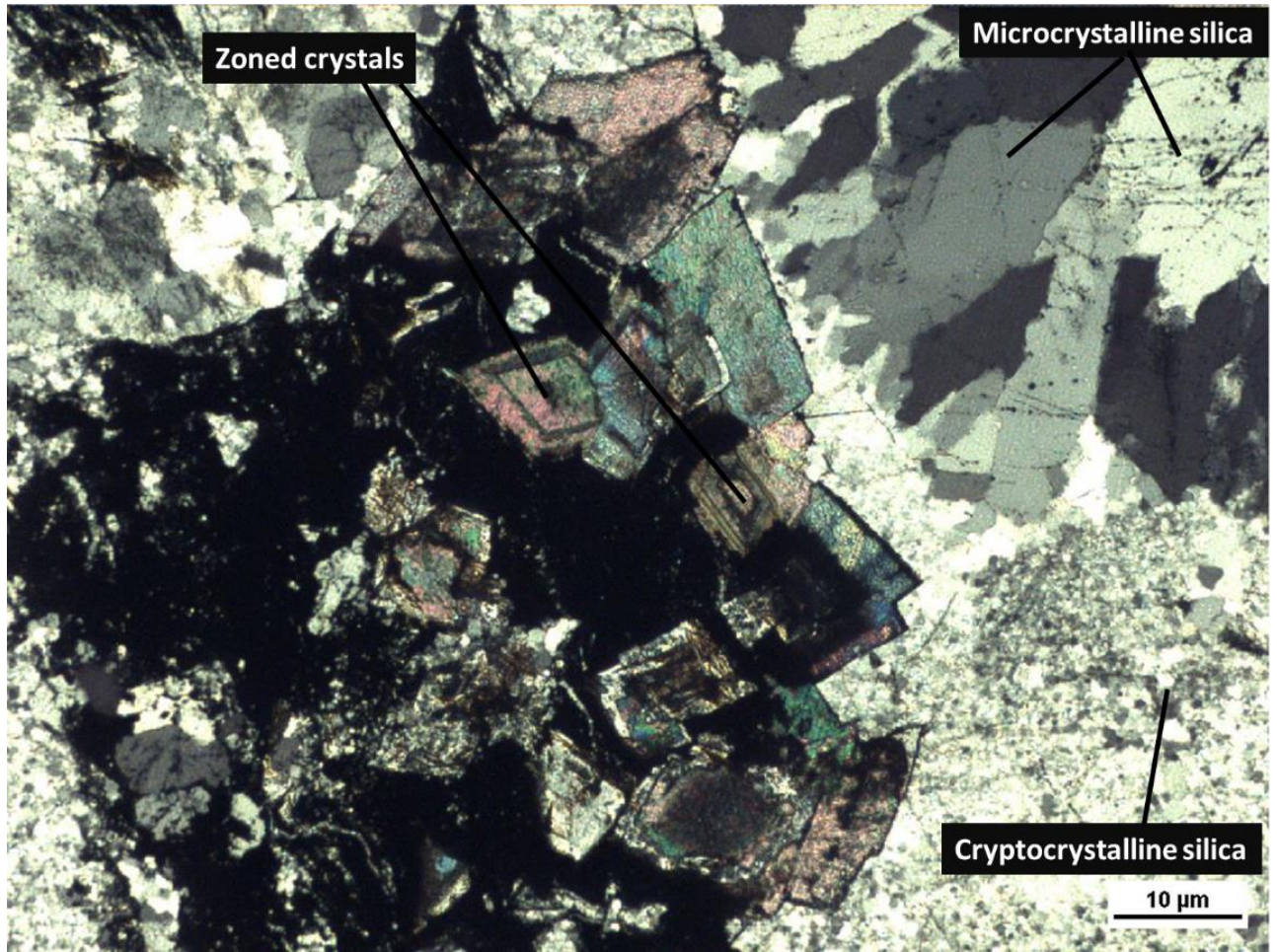


Figure 60. Sample showing the complexity of veining in a sample from the power plant at Broken Bow/Beavers Bend (sample C5). The vein contains silica and zoned ferroan dolomite crystals. Optical zoning of crystals reflects changes in fluid chemistry while the crystal is growing.

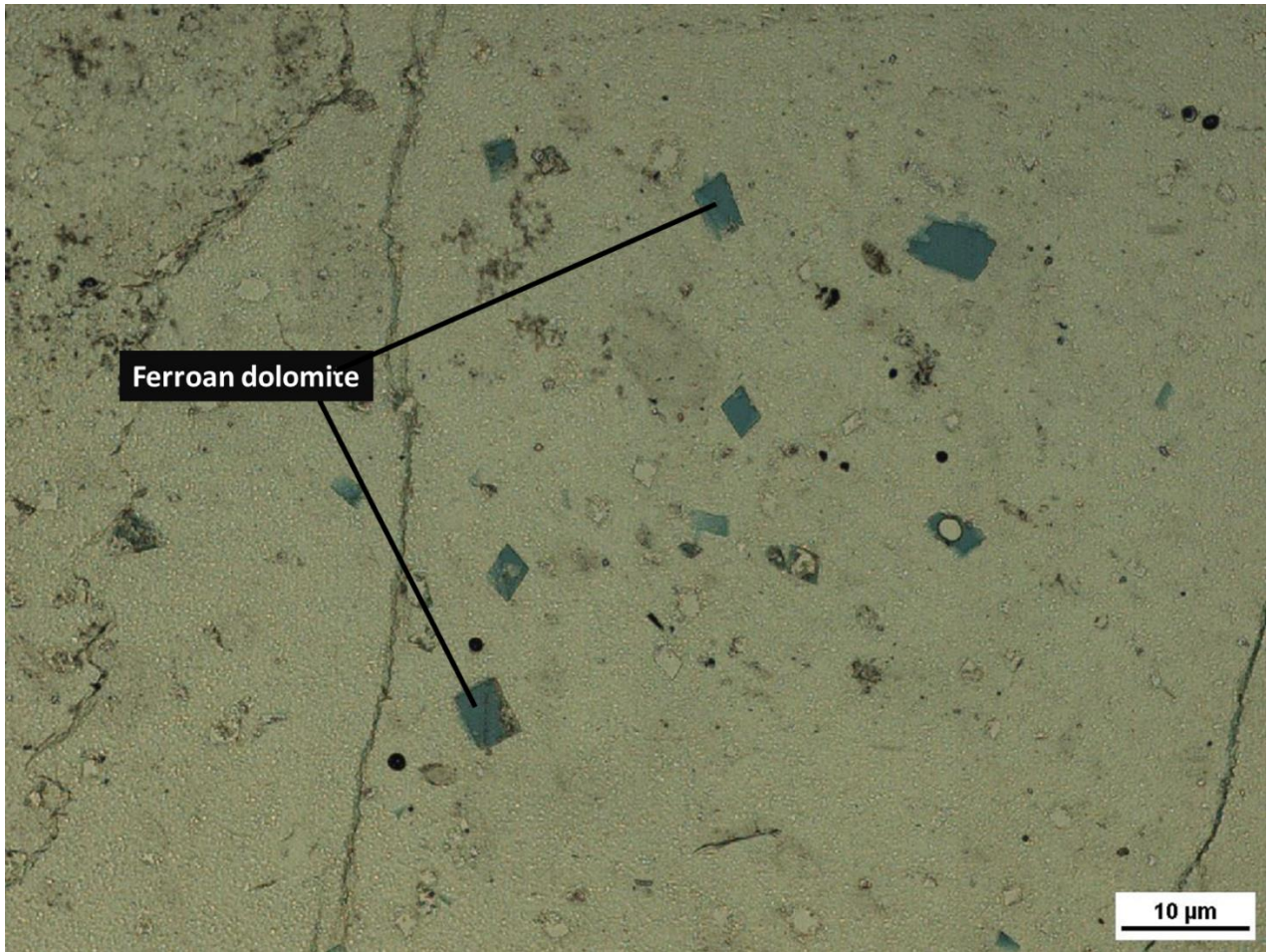


Figure 61. Arkansas Novaculite sample from Highway 259 from Broken Bow/Beavers Bend (sample C8). The Arkansas Novaculite samples contain isolated rhombohedra of ferroan dolomite.

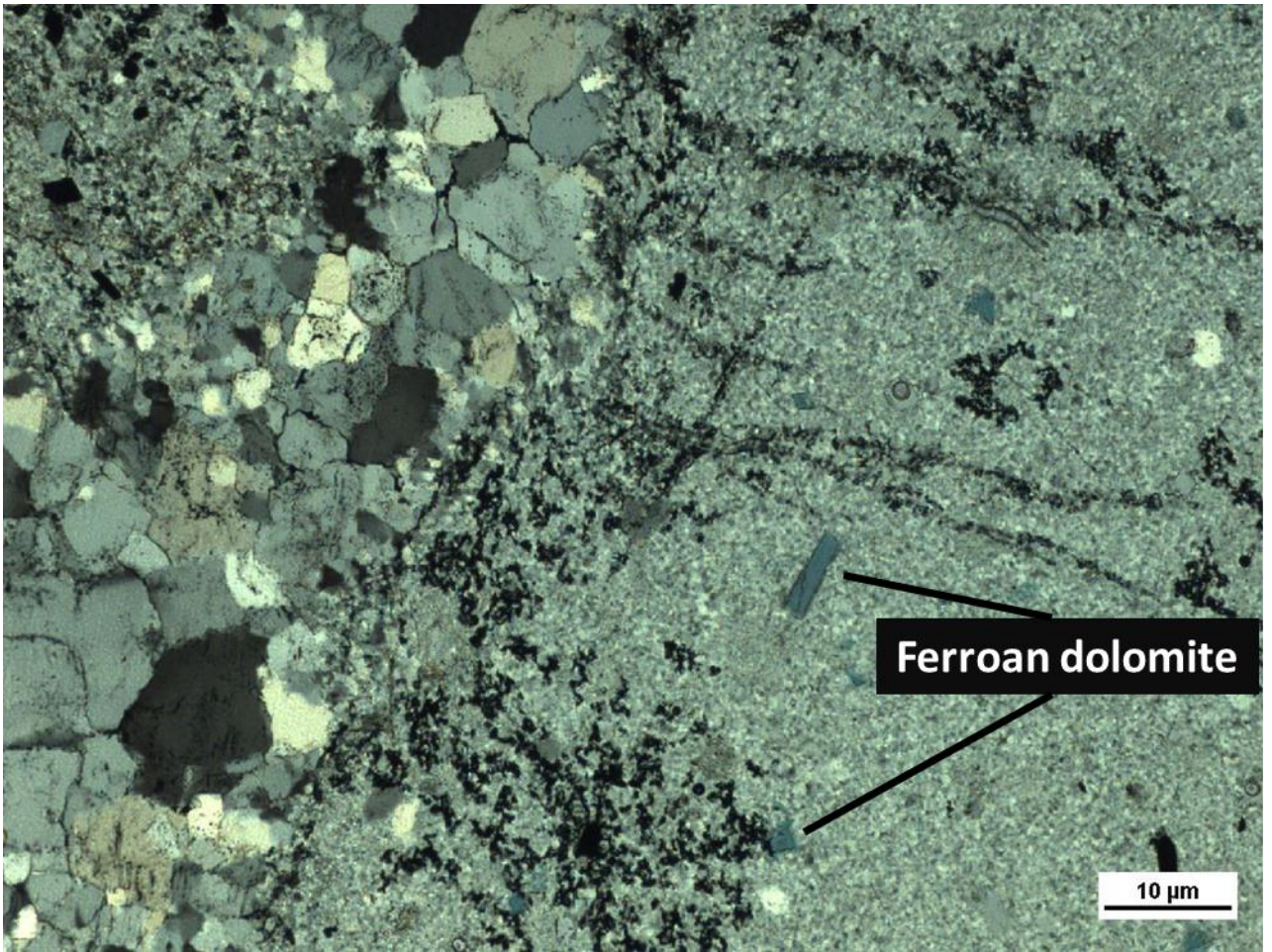


Figure 62. Arkansas Novaculite sample from Highway 259 in Broken Bow/Beavers Bend (sample C8). The cross-polarized Arkansas Novaculite image shows microcrystalline vein fill as well as cryptocrystalline matrix. It also contains isolated rhombohedra of ferroan dolomite.

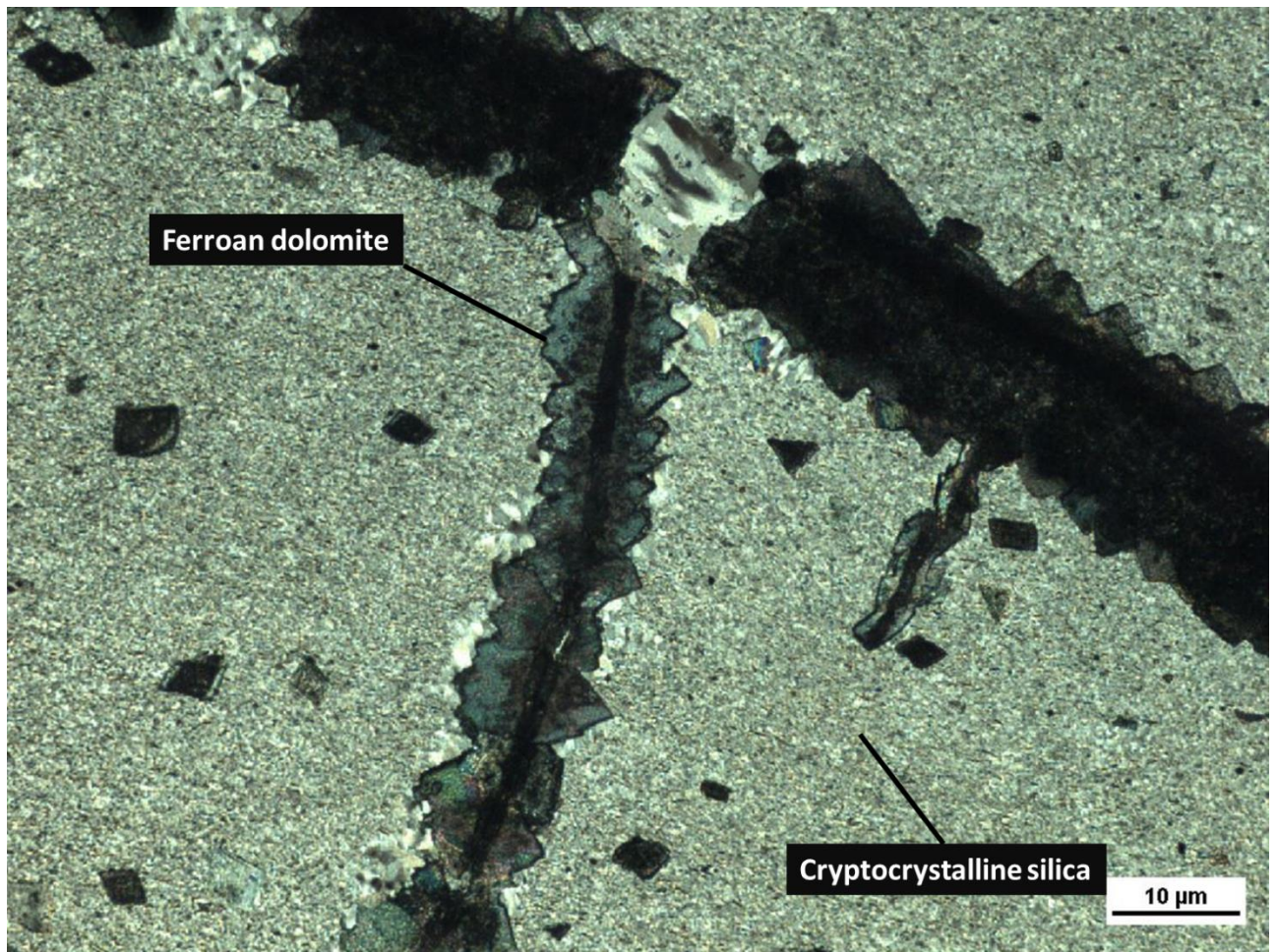


Figure 63. Cross-polarized photomicrograph of dark Arkansas Novaculite from the power plant at Broken Bow/Beavers Bend (sample C6). The photomicrograph displays veins lined and bridged by microcrystalline silica and filled with ferroan dolomite.

IV.2.D Phosphate Nodules

Phosphate nodules were observed in all cores and outcrops except for those in the Broken Bow uplift. Similarly, Nielsen (1988) and Suneson (1995) also did not report phosphate nodules in the Broken Bow outcrops. The phosphate is cryptocrystalline to microcrystalline and commonly exhibits a peloidal to botryoidal texture (Figs. 64-68). All of the phosphate nodules

studied are cemented with white chalcedony. The white silica cement exhibits a botryoidal and chalcedonic texture in most thin sections, especially the Atoka Chert Pit thin sections (Figs. 64-65). In an I-35 phosphate nodule, orthogonal fractures are developed locally in the botryoidal cement (Fig. 66). The I-35 phosphate nodules also contain prismatic apatite crystals that in places define remnant radiolarian tests (Fig. 67) and locally form linear arrays of radial spherulites (Fig. 68). Different crystal morphology was observed in many of the nodules. I-35 phosphate nodules contain prismatic apatite (Figs. 67, 68), whereas the Hall 2B core contains botryoidal apatite and short prismatic crystalites with blunt edges (Fig. 69).

Porosity is developed in the phosphate nodules sporadically, and the pores commonly have a thin lining of dolomite (Fig. 70). In the I-35 and Atoka phosphate nodules, porosity is more common than in the host chert beds. Bitumen is also present inside several of the pore spaces within the phosphate nodules (Figs. 70, 71).

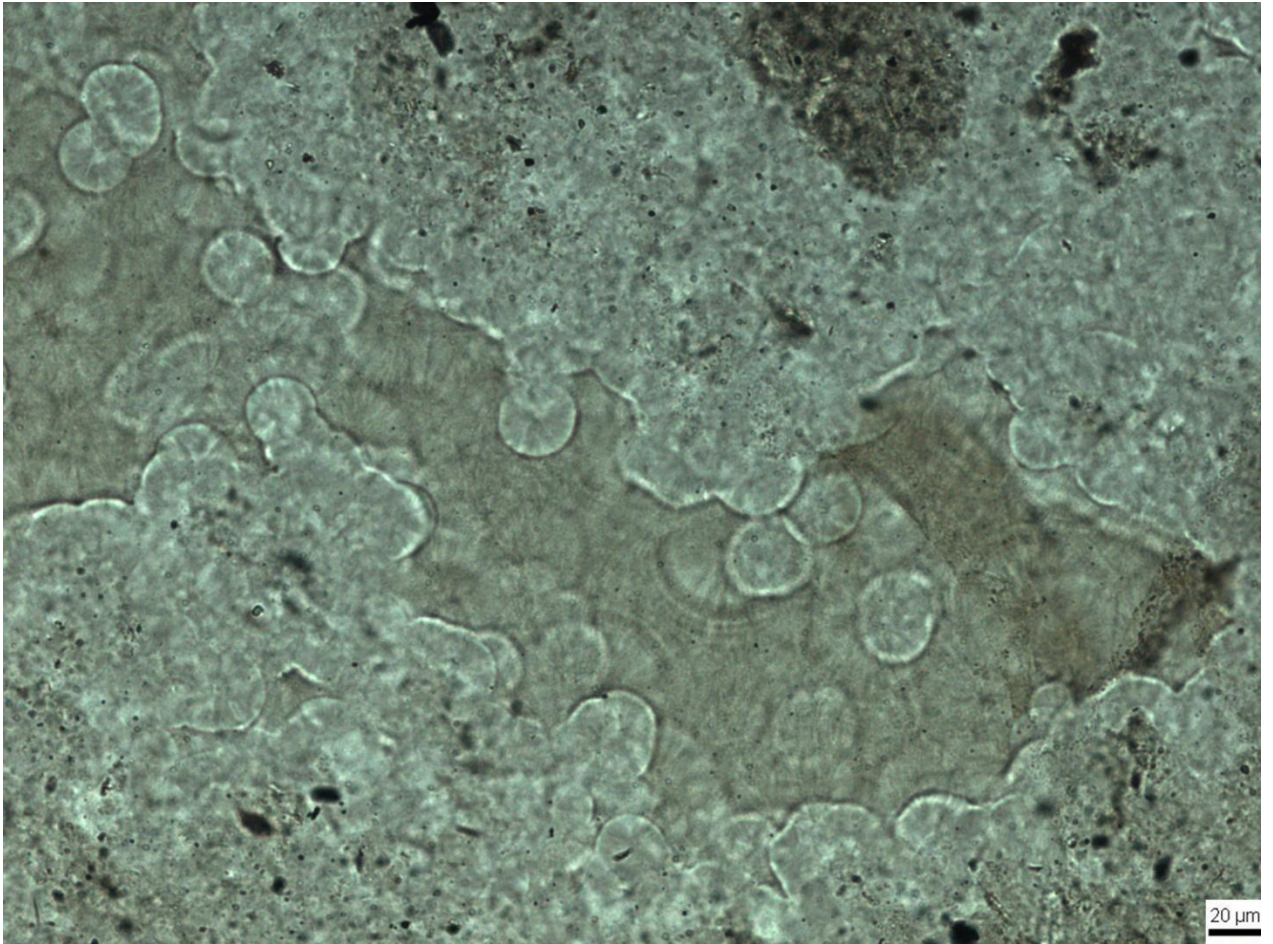


Figure 64. Phosphate nodule from the Atoka Chert Pit (sample B1). Both phosphate nodules from the Atoka Chert Pit contain botryoidal phosphate with chalcedony filling the voids.

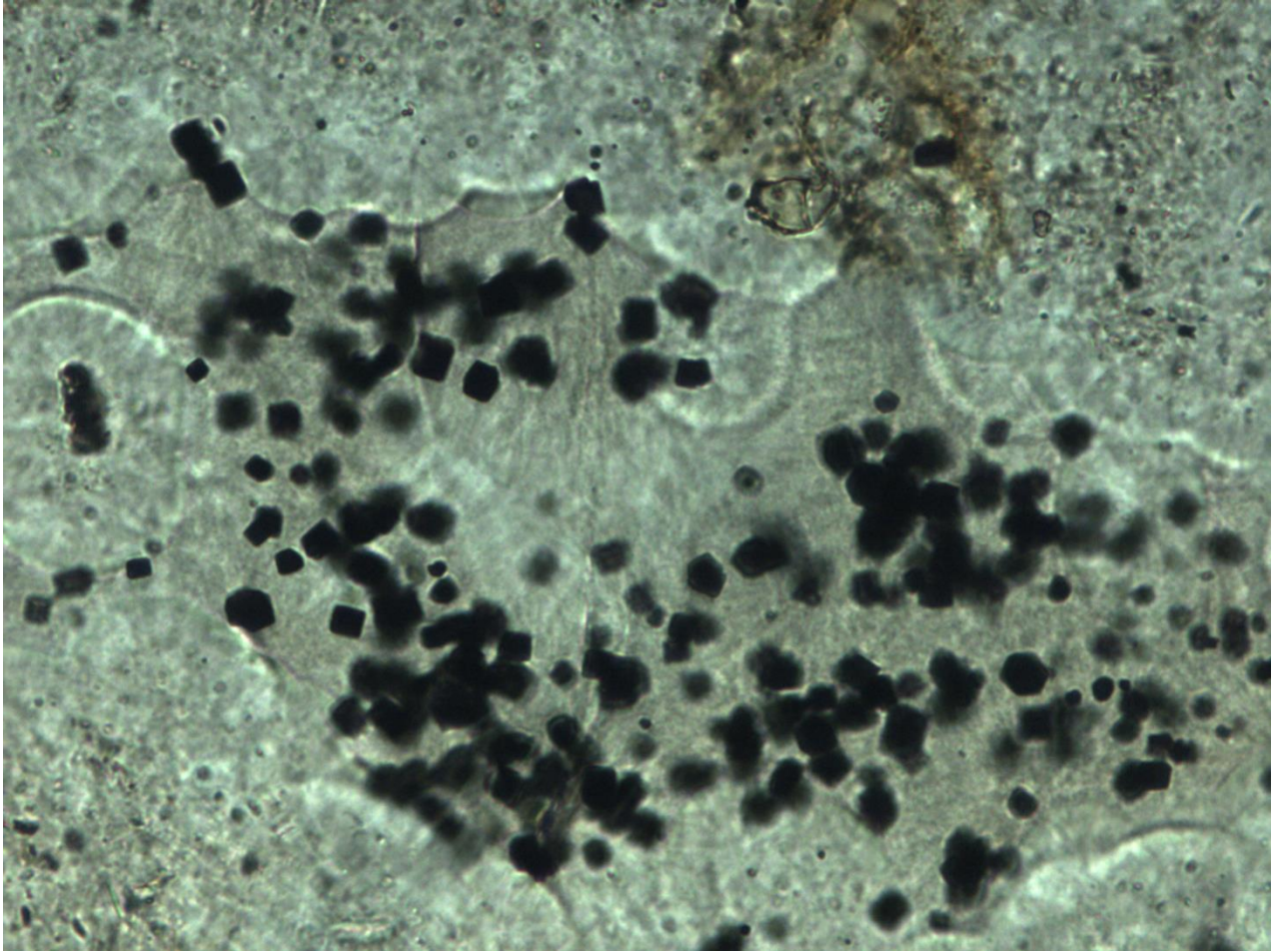


Figure 65. Photomicrograph of a phosphate nodule from the Atoka Chert Pit (sample B1). Note phosphate spherules with botryoidal textures at the rim. These features commonly contain dispersed pyrite euhedra and chalcedonic-like textures.

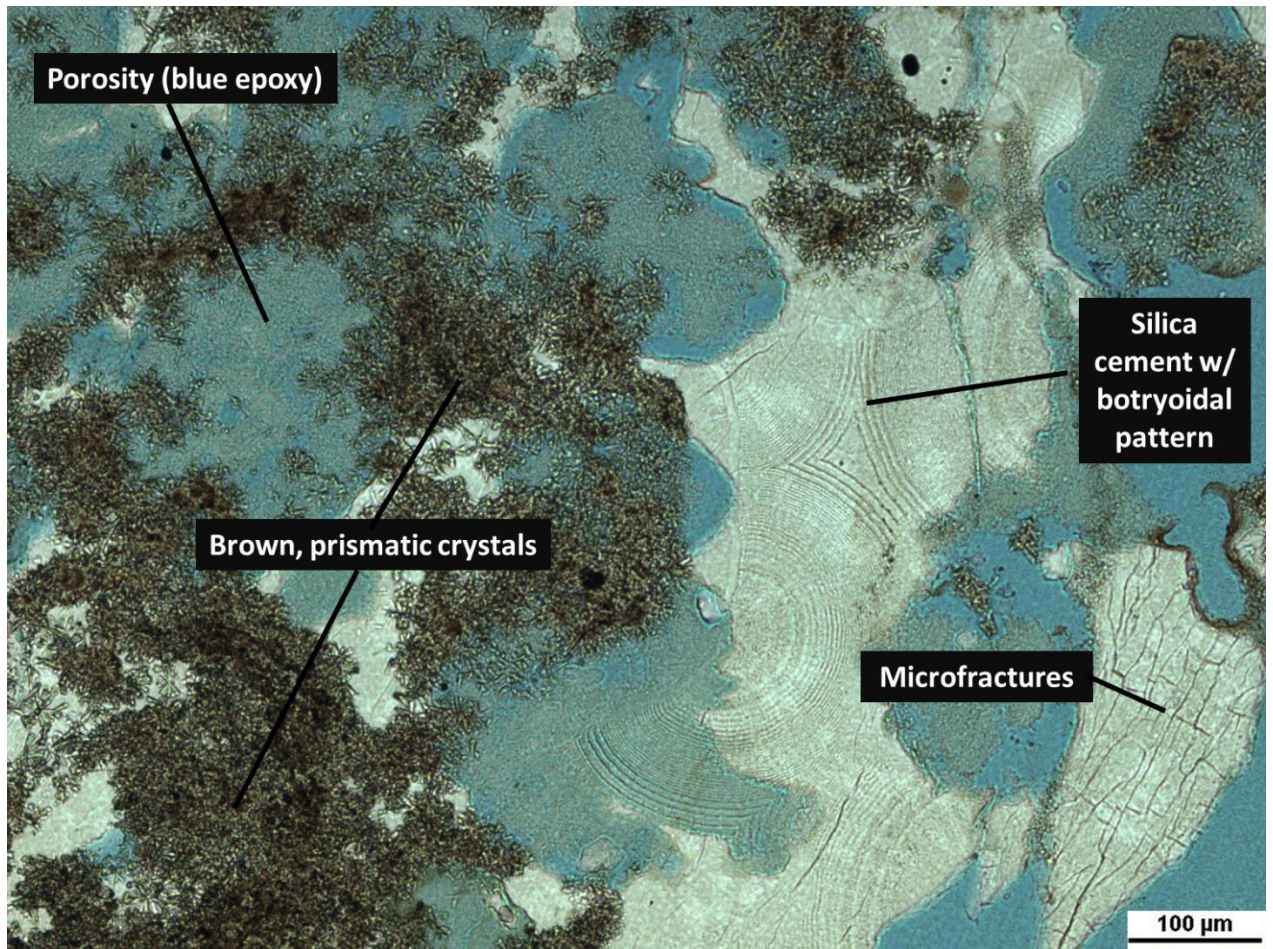


Figure 66. Thin section photomicrograph of phosphate nodule from I-35 (sample A2). The phosphate in this sample is largely microcrystalline and has a clotted, peloidal texture. Brown, prismatic crystals are abundant within the phosphate nodule. The silica cement is botryoidal and locally contains orthogonal microfractures.

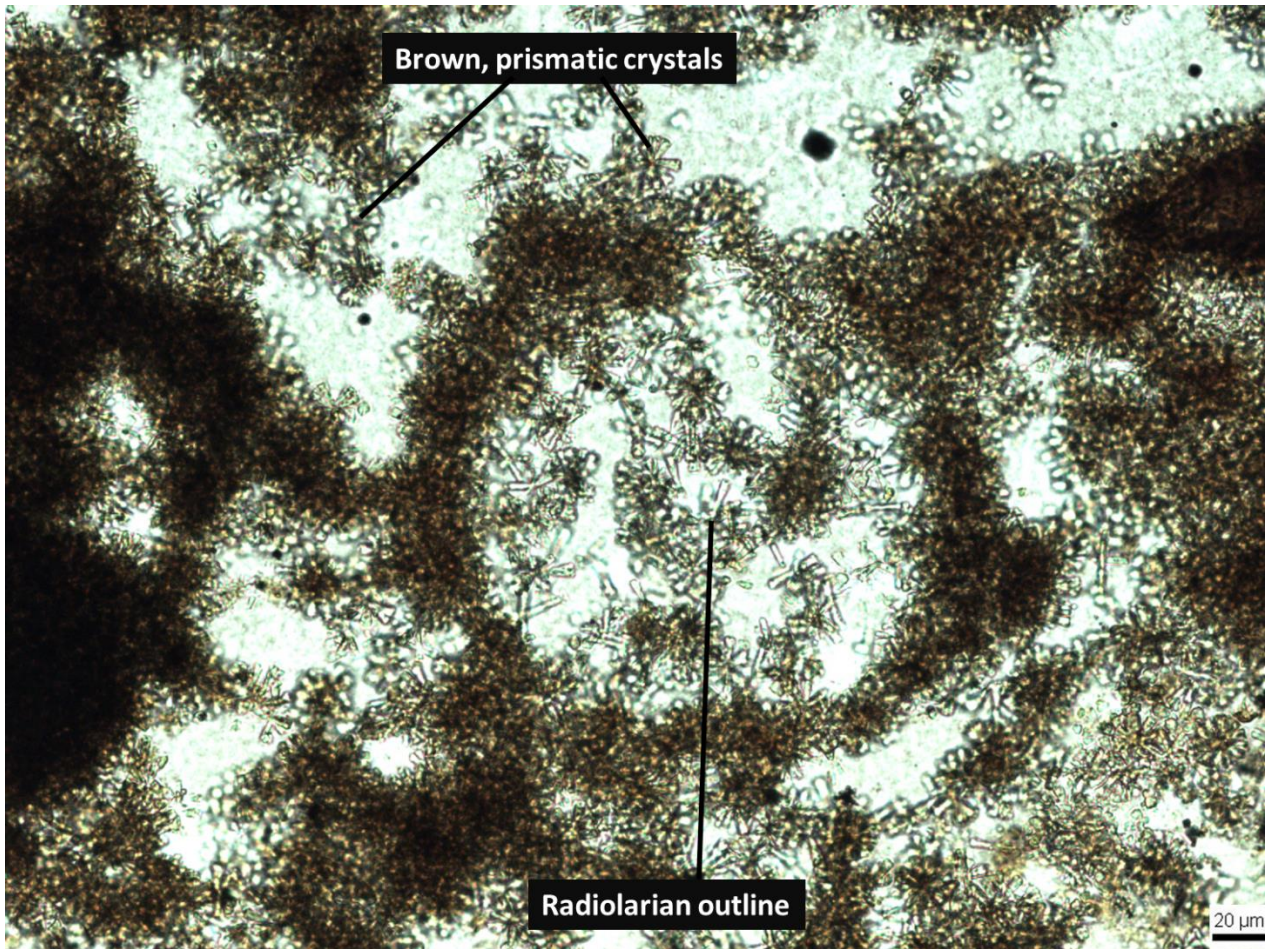


Figure 67. Thin section photomicrograph of phosphate nodule containing spherulites of prismatic apatite crystals within a groundmass of chalcedony from the I-35 outcrop (sample A2). The concentric circular pattern in the center of the photomicrograph suggests that the apatite precipitated in the pattern of a Spumellarian radiolarian test.

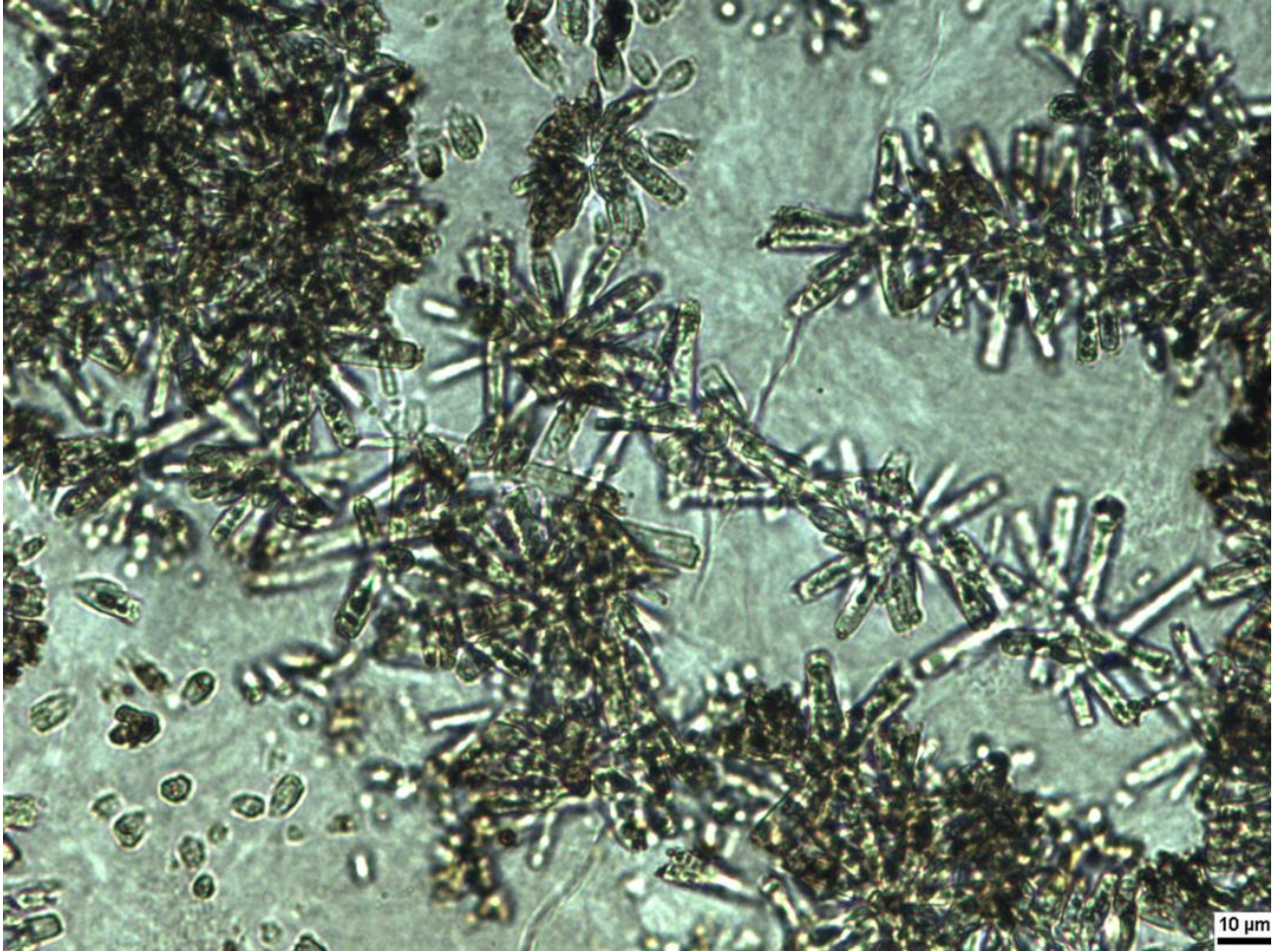


Figure 68. Thin section of photomicrograph phosphate nodule showing spherulites of prismatic apatite in a chalcedony groundmass from the I-35 outcrop (sample A7). Note linear arrays of spherulites.

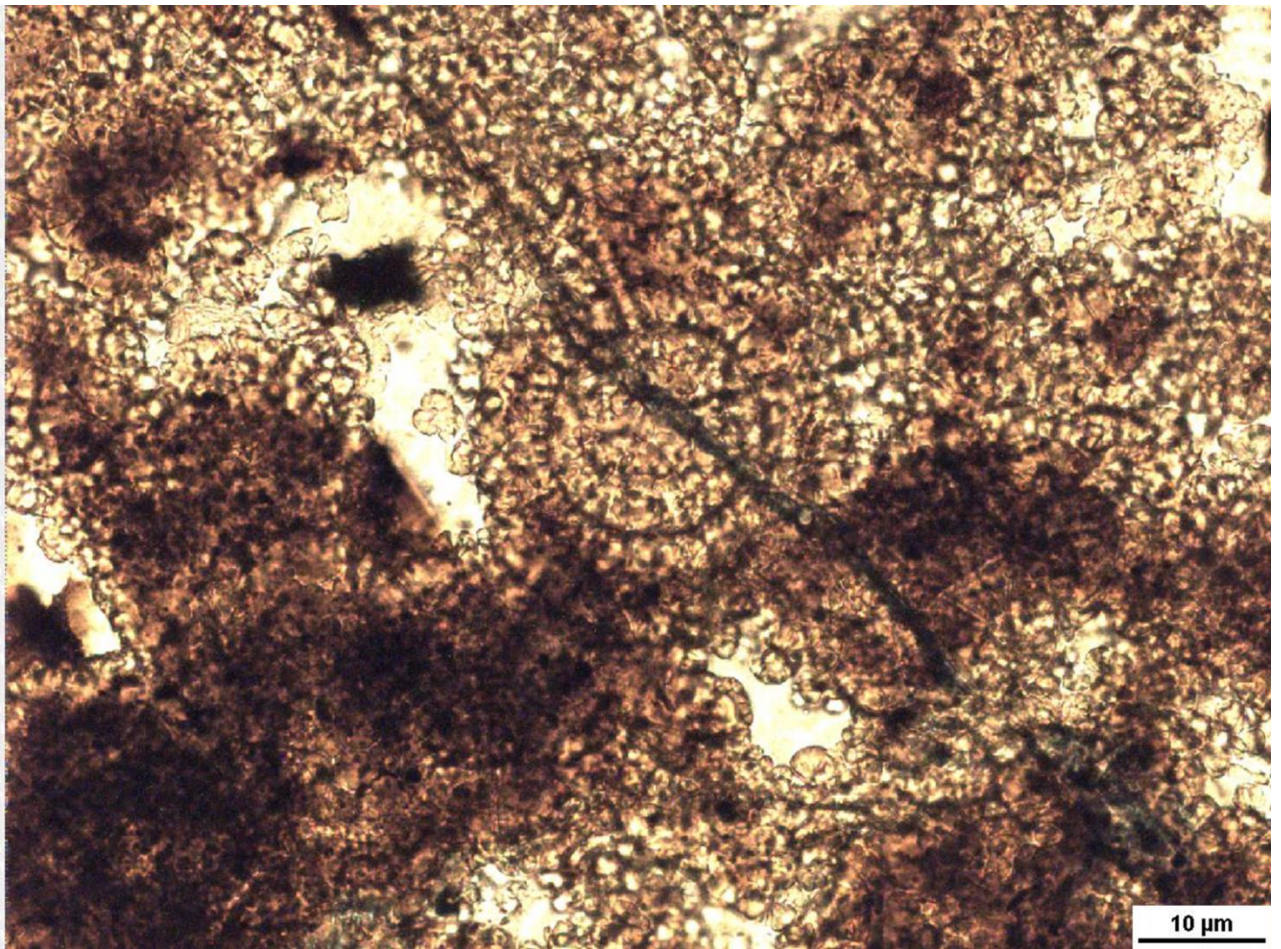


Figure 69. Thin section of photomicrograph phosphate nodule with botryoidal apatite crystals from the Hall 2B core (sample D2). The apatite crystals outline the shape of Radiolaria in many of the phosphate nodule samples.

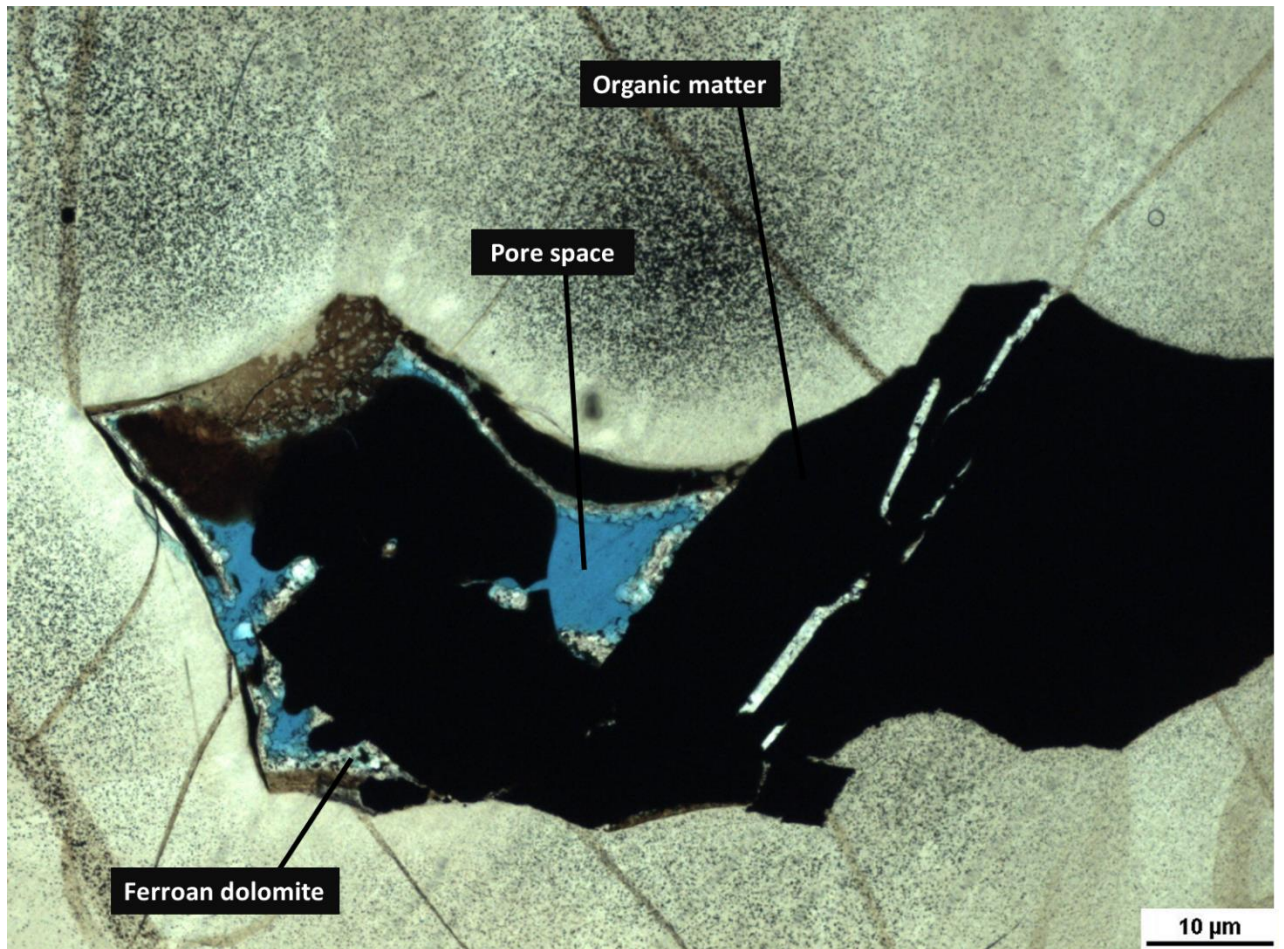


Figure 70. Photomicrograph of phosphate nodule from the Atoka Chert Pit (sample B1). The image shows pore filled mostly with bitumen. Note that veins cross-cut bitumen and that dolomite partially coats open pores.

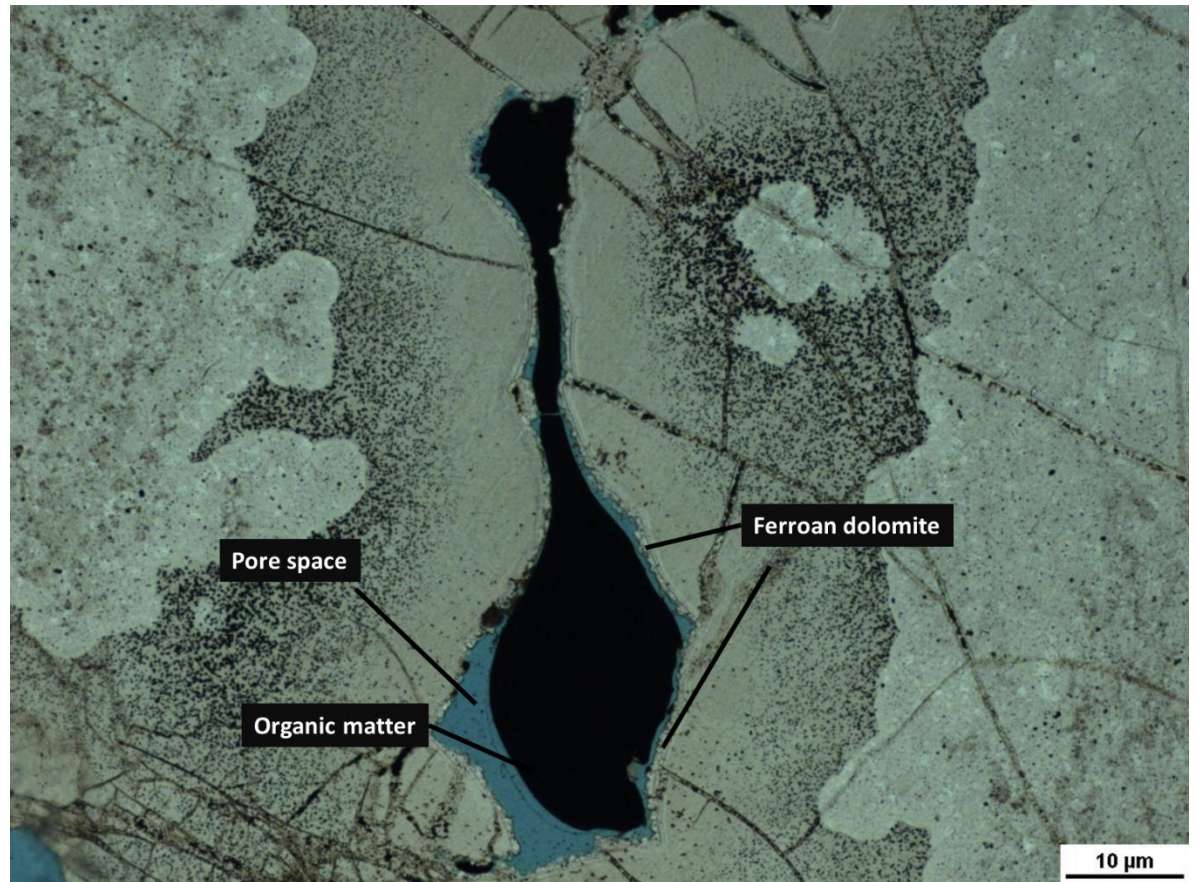


Figure 71. Photomicrograph of phosphate nodule from the Atoka Chert Pit outcrop (sample B6). The image shows two generations of phosphate and a large pore lined with dolomite and filled with bitumen. Note open porosity between dolomite pore lining and bitumen.

IV.2.E Veining

All of the novaculitic chert samples studied in this investigation are veined. The vein fills include quartz, pyrite, dolomite, and bitumen (Fig. 72-75). The Broken Bow black float samples from the power plant within Broken Bow/Beavers Bend contain the most obvious veining due to the black chert matrix (Fig. 72). In those samples, veins are composed of microcrystalline, and to a lesser extent, cryptocrystalline quartz. The Atoka outcrop thin sections exhibit veins that are often filled with white silica and occasionally pyrite (Fig. 73). In all of the novaculitic chert

samples within the Woodford Shale, veins filled with pyrite and bitumen are more common (Fig. 74). The same samples, particularly the Broken Bow/Beavers Bend samples taken from float at the power plant, contain some open fractures that are lined with ferroan dolomite crystals (Fig. 63). Pyrite veins and microcrystalline quartz veins are both present in the white Arkansas Novaculite samples from the Blaylock contact within the Broken Bow/Beavers Bend area (Fig. 75).

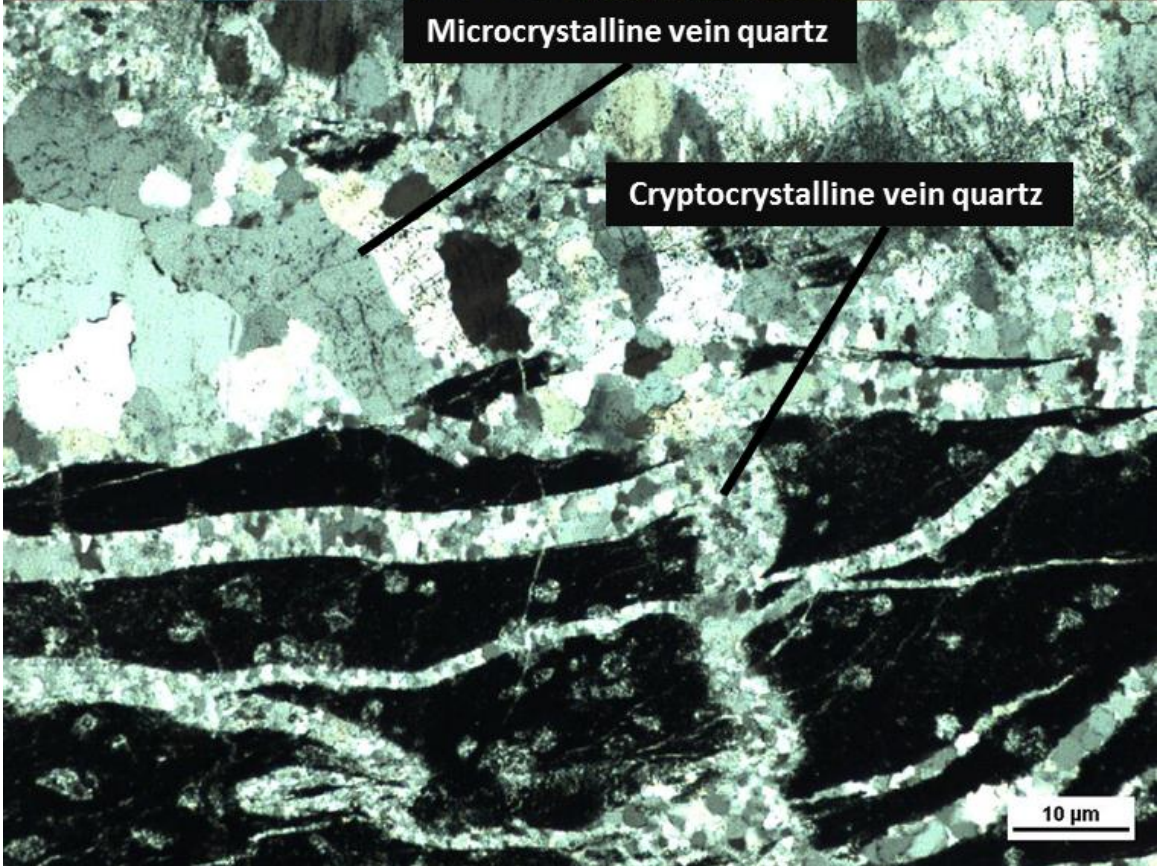
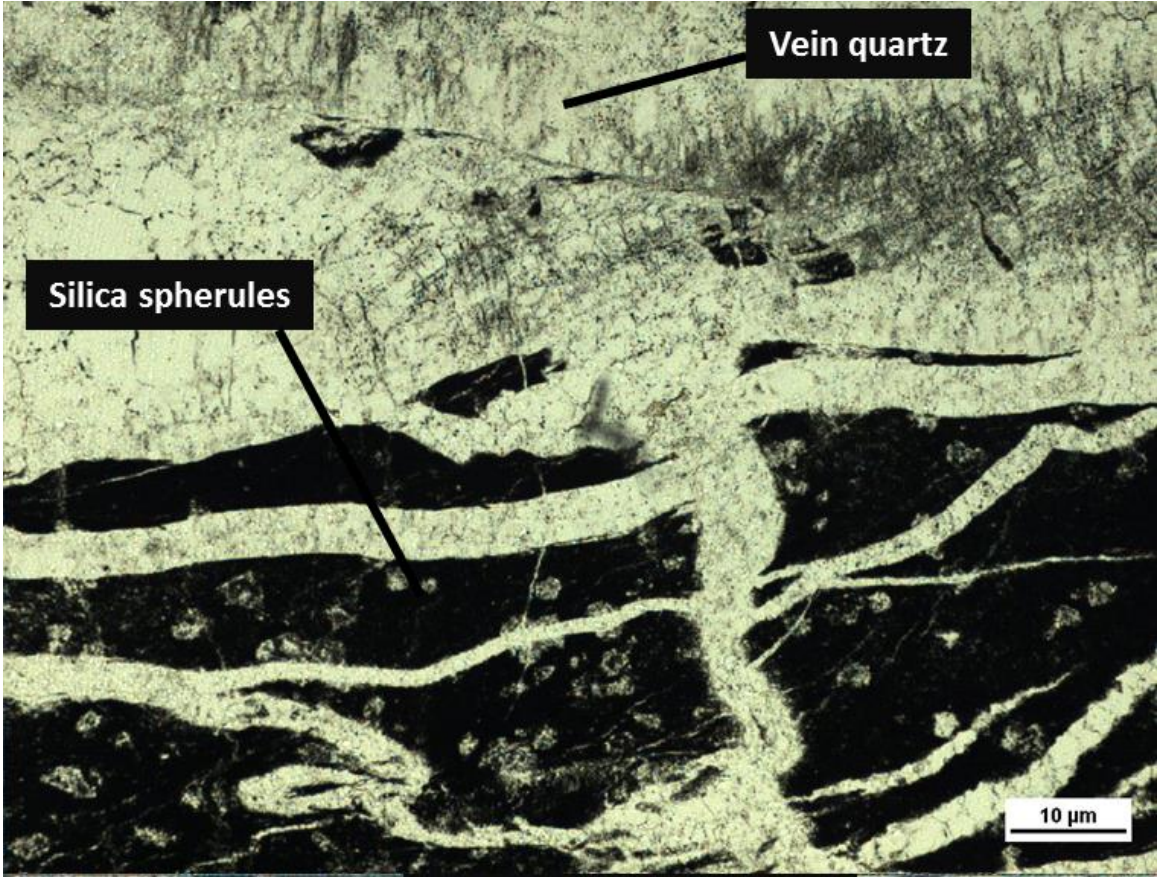


Figure 72. Quartz veining in black Arkansas Novaculite from the power plant Broken Bow/Beavers Bend (sample C4). A) The host rock for the veins is classic novaculitic chert with matrix composed of amorphous silica and organic matter and containing chalcedony spherules. B) A cross-polarized photomicrograph demonstrating variable quartz crystal sizes.

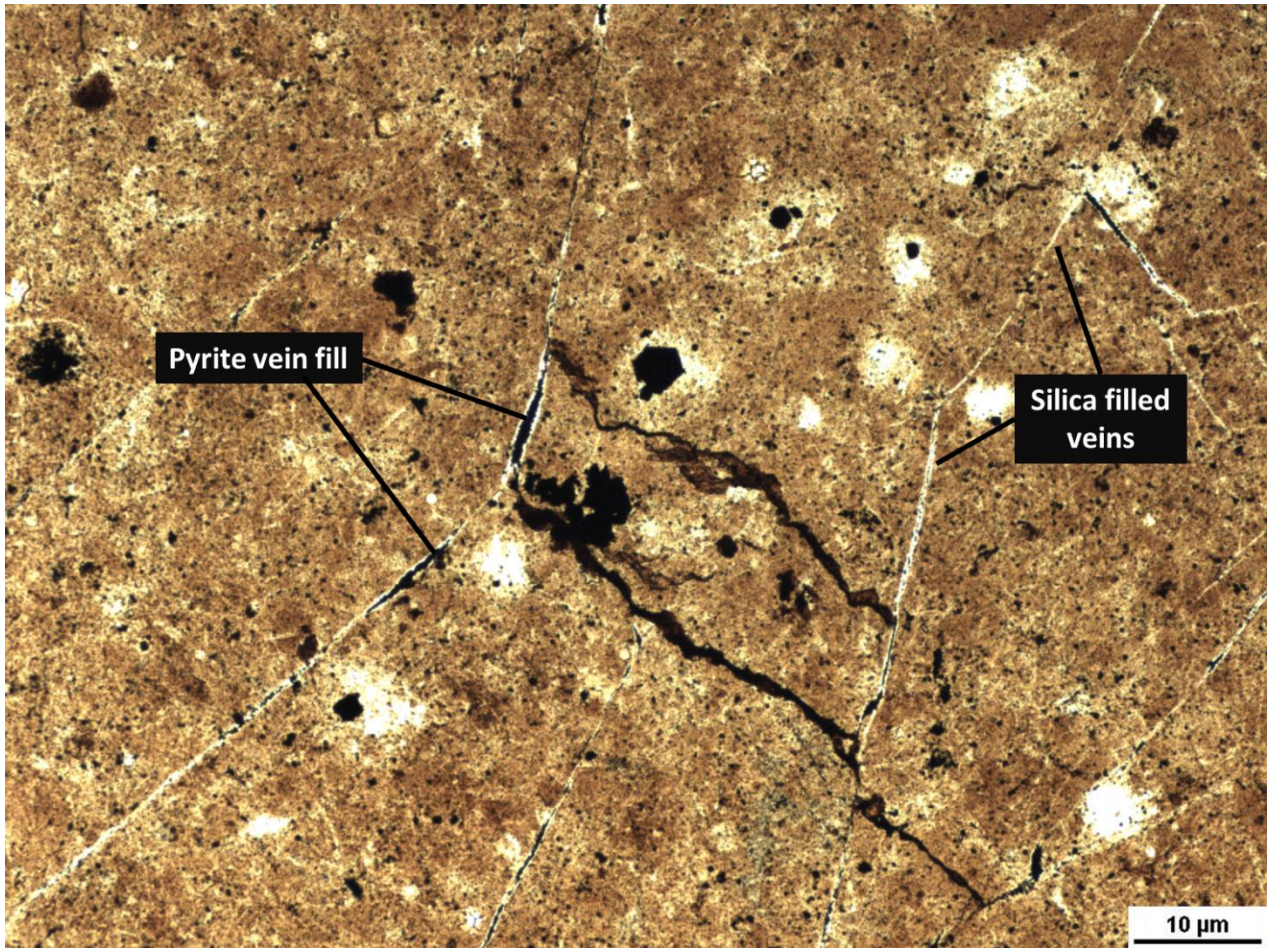


Figure 73. Thin section photomicrograph of Arkansas Novaculite from the Atoka Chert Pit (sample B4). Note planar veins with silica lining and pyrite fill. Late-stage veins that abut the planar fractures are filled only with pyrite.



Figure 74. Thin section photomicrograph of the I-35 outcrop (sample A1). The vein running through the image is filled with pyrite and the three subcircular feature in the middle are likely filled with bitumen.

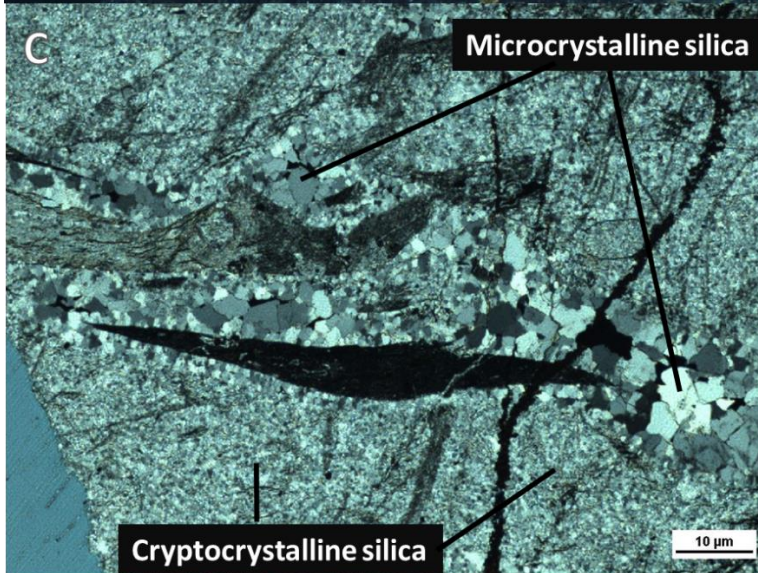
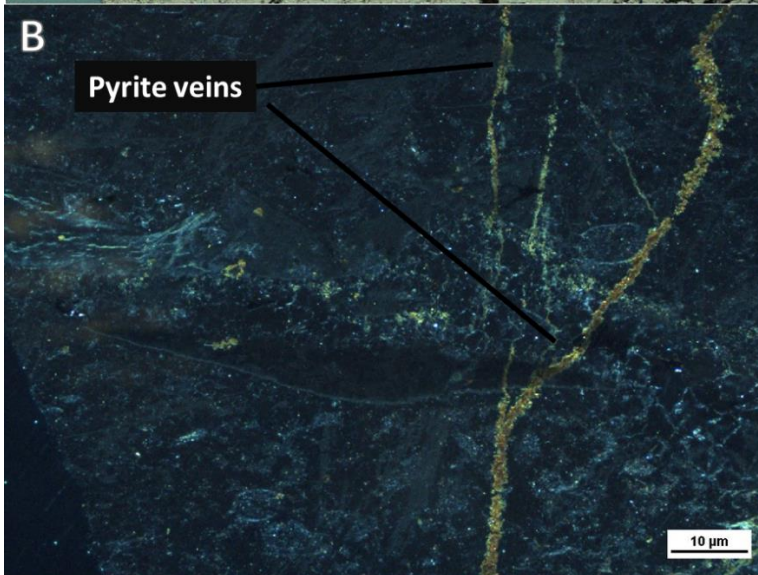
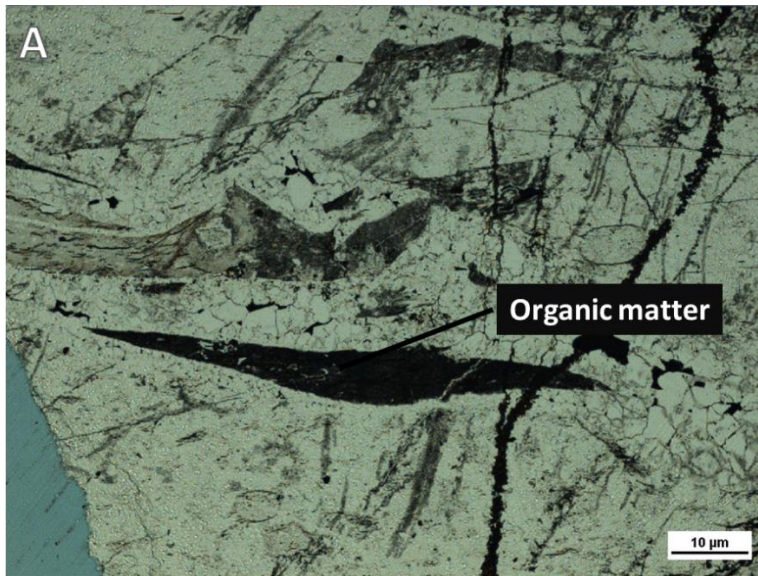


Figure 75. Arkansas Novaculite sample from near the Arkansas Novaculite and Blaylock Sandstone contact in Broken Bow/Beavers Bend (sample B2). A) Plane polarized light image highlighting elongate bitumen mass along keel of quartz vein. B) Reflected light image reveals pyrite veins, which cross-cut all structures within the photomicrograph. C) Cross-polarized light image showing contrast among microcrystalline silica vein fill, cryptocrystalline chert, and angular clasts containing amorphous silica. The microcrystalline quartz is a vein running through the sample.

IV.3 SEM-Image Analysis: Overview

Eight samples of novaculitic chert were imaged via Scanning Electron Microscopy (Table 4). Samples were chosen based on thin section characteristics, particularly samples that contain materials with significant density contrast, such as organic matter, silica, and pyrite, that are likely to image in SEM. The goal of SEM-imaging was to characterize microfabric and porosity. EDS analysis indicates that the samples are composed almost exclusively of silica with minor amounts of iron and sulfur; detrital clay and other silicate minerals are extremely rare. The discussion begins by characterizing chert-organic matrix and biogenic structures and concludes by characterizing diagenetic features and porosity.

Table 4. Register of samples analyzed by SEM and EDS.

SEM Sample #	Outcrop	Location in Outcrop	Outcrop Sample #
1	I-35	Middle part of outcrop	6
2	Atoka Chert Pit	Lower part of outcrop, near large folds	3
3	Atoka Chert Pit	Upper (Miss) tripolitic area	7
4	Broken Bow	Right below Blaylock/AN contact	1
	Core:	Depth:	
5	Hall 2B	5899.0 feet	N/A
6	Hall 2B	6178.5 feet	N/A
7	Poe #1-29	7832.0 feet	N/A
8	Poe #1-29	7849.6 feet	N/A

IV.3.A Chert-Organic Matrix

The chert matrix in all samples was similar: amorphous to cryptocrystalline silica with amorphous organic matter and a variety of discrete organic constituents. Most of the chert has a peloidal texture, and the amorphous organic matter has a lacelike pattern, filling the interstices between the peloids, particularly in the I-35 outcrop and Poe and Hall 2B core samples (Fig. 76). The Atoka and Broken Bow outcrop contains less of the amorphous organic matter, but exhibits more well defined, curled organic linings (Fig. 77). In the Hall 2B core, angular to subround chert clasts are interspersed with the organic-rich silica matrix (Fig. 78). Larger particles of organic matter range in form from round to blocky, but identifying precise kerogen types beyond possible *Tasmanites* is difficult.

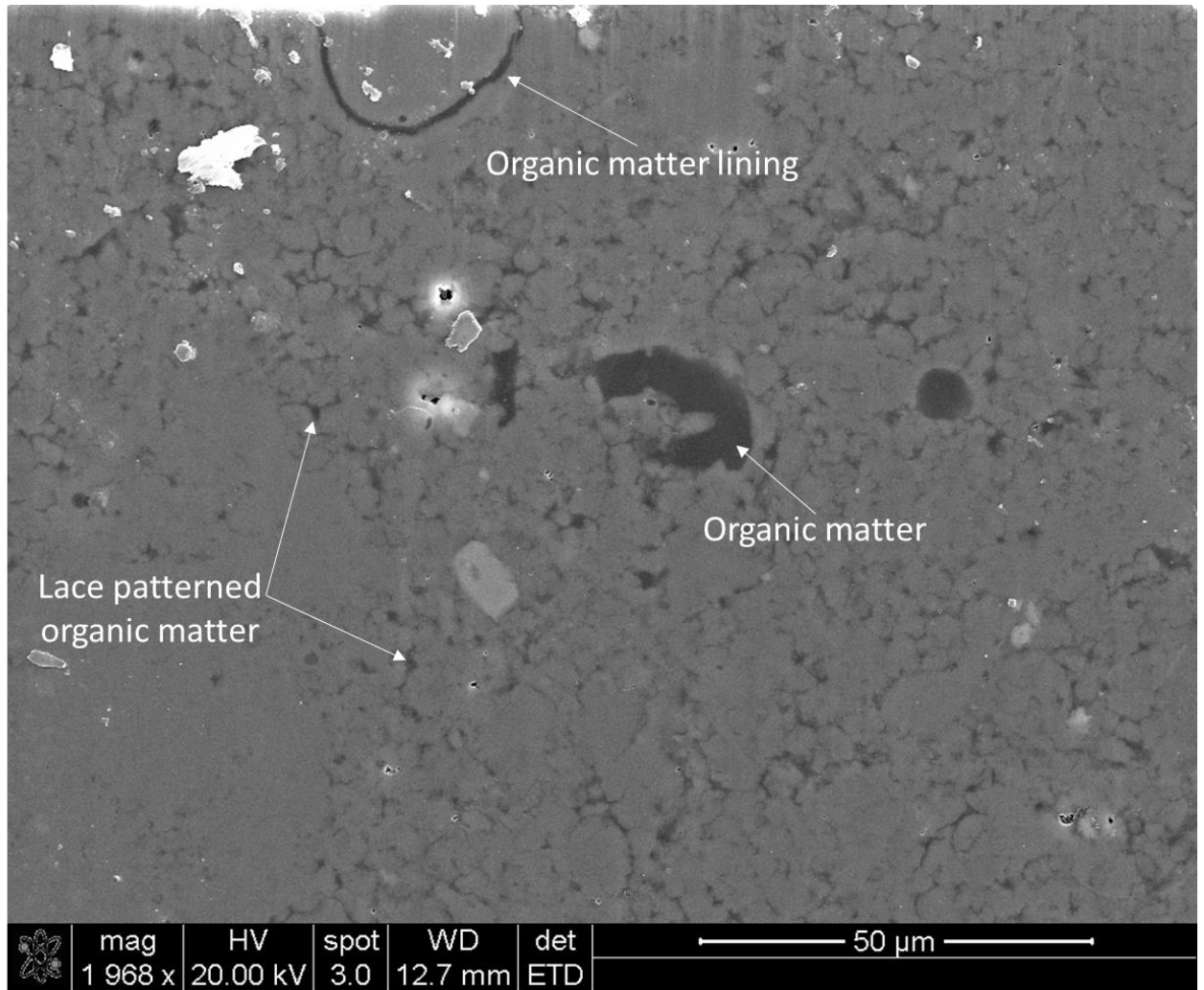


Figure 76. Backscattered electron micrograph showing peloidal chert matrix with interstitial amorphous organic matter from the I-35 outcrop (sample 1). Note discrete organic particles that may be fragments of *Tasmanites*, as well as an organic film coating a silica spherule at the top of the image.

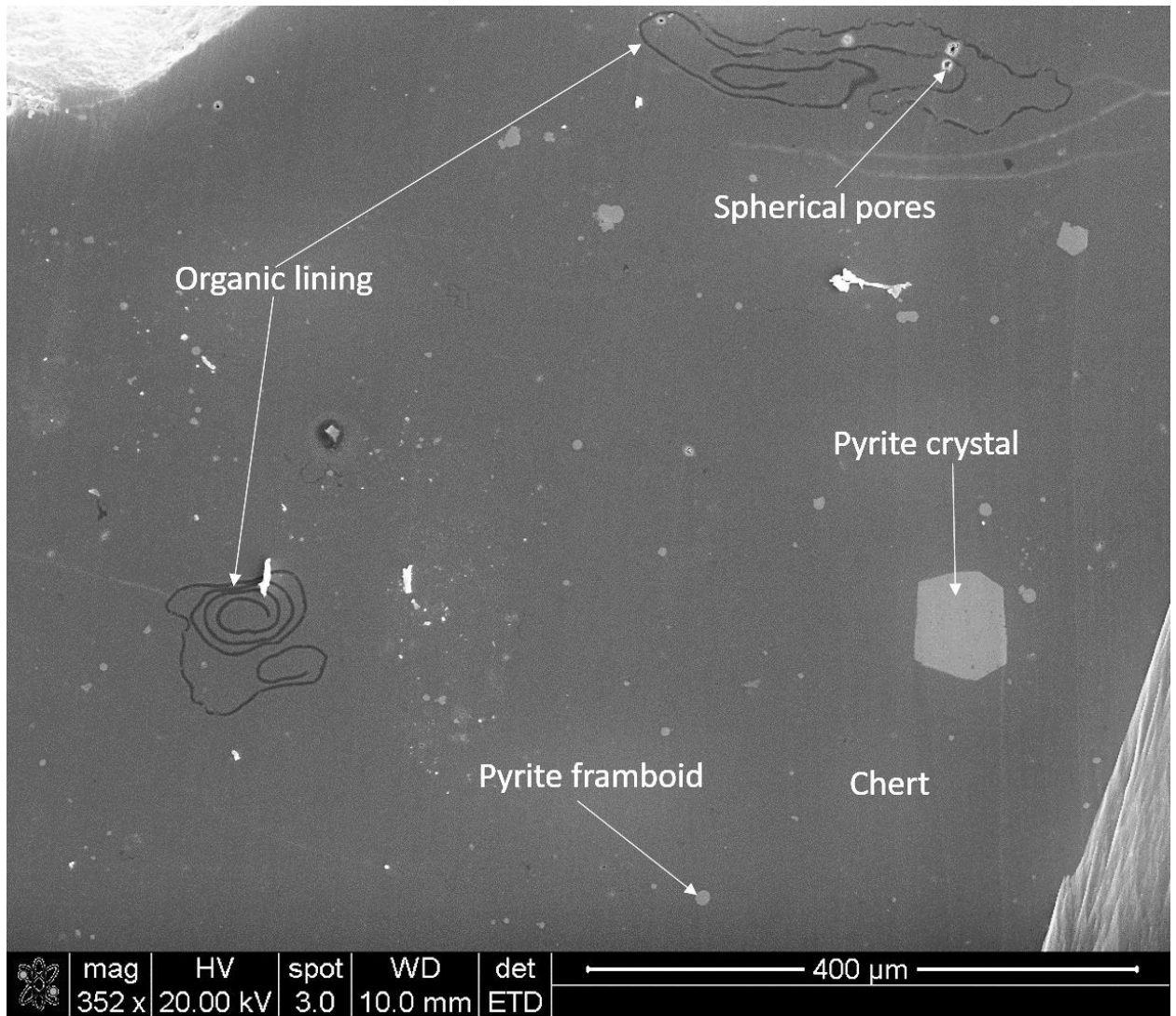


Figure 77. SEM image showing homogeneous chert matrix with curled organic films in Arkansas Novaculite from the Atoka Chert Pit (sample 3). Note cubic pyrite crystals, and pyrite framboids.

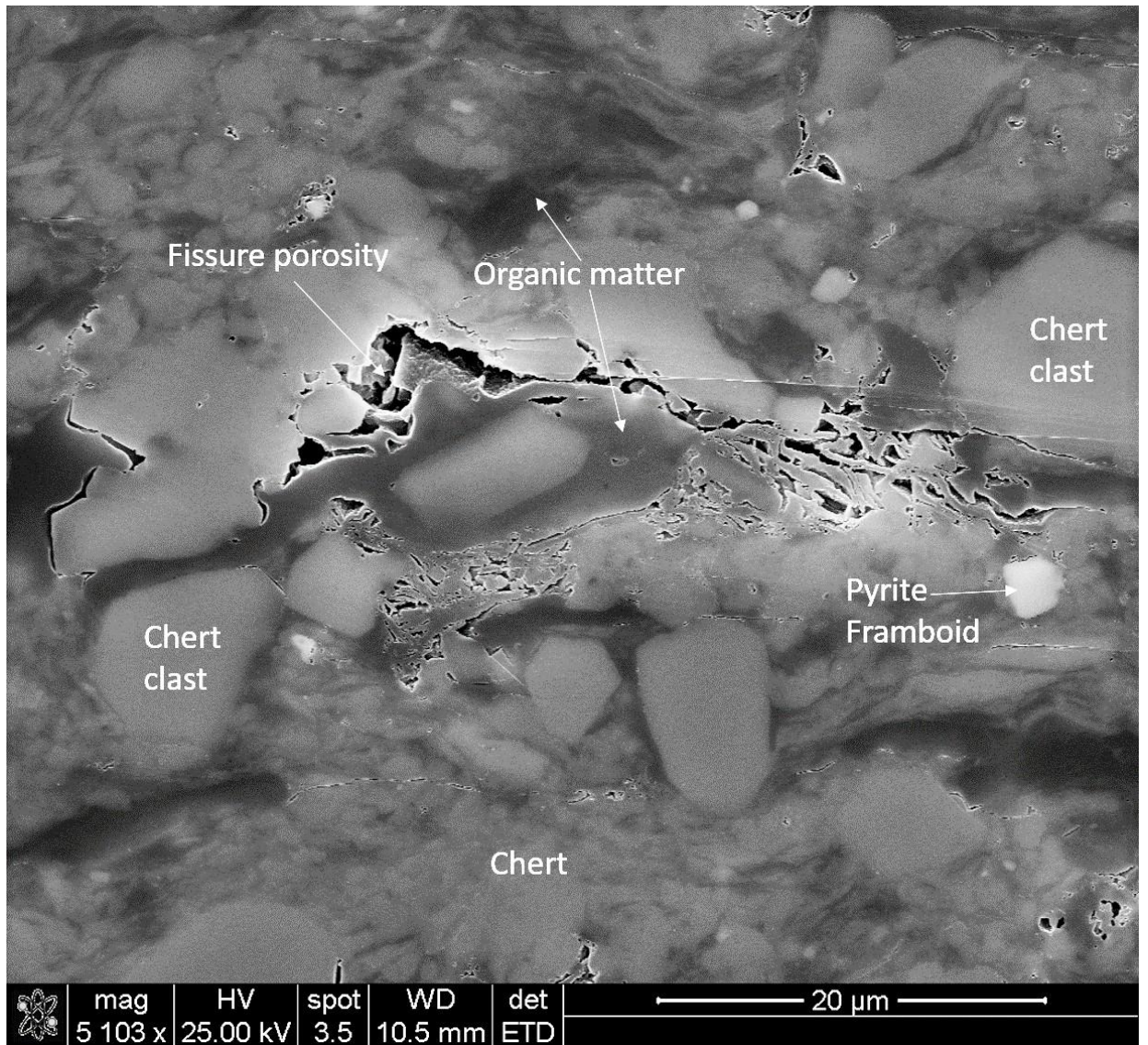


Figure 78. SEM image showing abundant organic matter, peloidal chert matrix, and angular to subround chert clasts in the Woodford Shale from the Hall 2B core (sample 6). Note fissure porosity in central part of image.

IV.3.B Biogenic Structures

Most biogenic structures are difficult to discern in chert because of insufficient density contrast between siliceous fossils and rock matrix. However, the SEM revealed a range of organic structures that are not visible in thin section. For example, organic linings were observed not only

on the exteriors of the siliceous spherules, but on the interiors as well (Figs. 79). Some of the films within the interior of the spherules appear to be developed as linings on the interior tests of Spumellaria. Of special interest are organic films that do not appear to be associated with silica spherules. These films vary greatly in terms of size and shape (Figs. 80-82). Some of the films have asymmetrical spiral forms suggestive of films curled at both ends (Figs. 80, 81), whereas others are highly irregular (Fig. 82). The Hall 2B core and Broken Bow/Beavers Bend outcrop samples do not exhibit any of these particular types of biogenic structures.

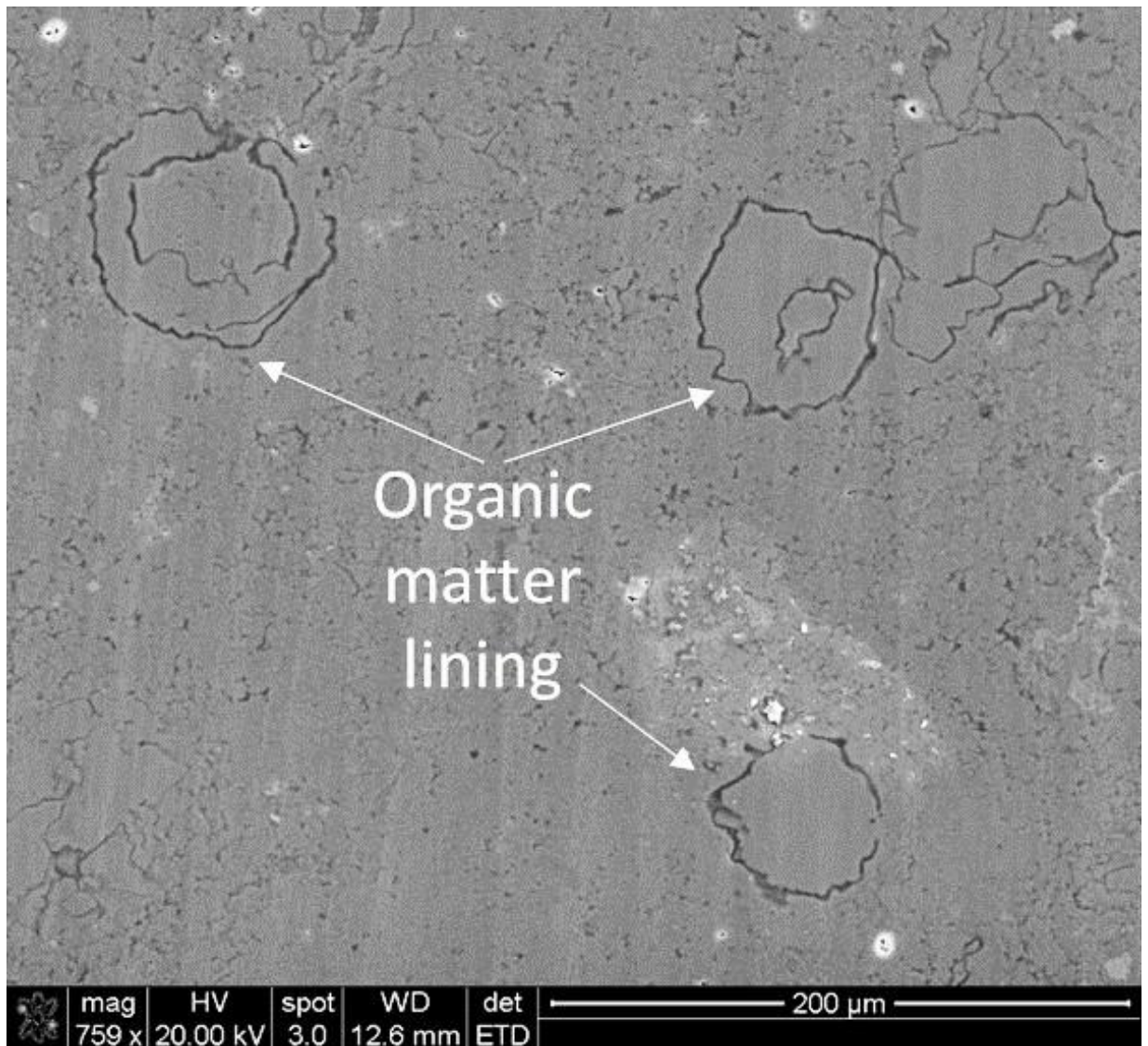


Figure 79. SEM image showing organic films coating and within silica spherules, I-35 (sample 1).

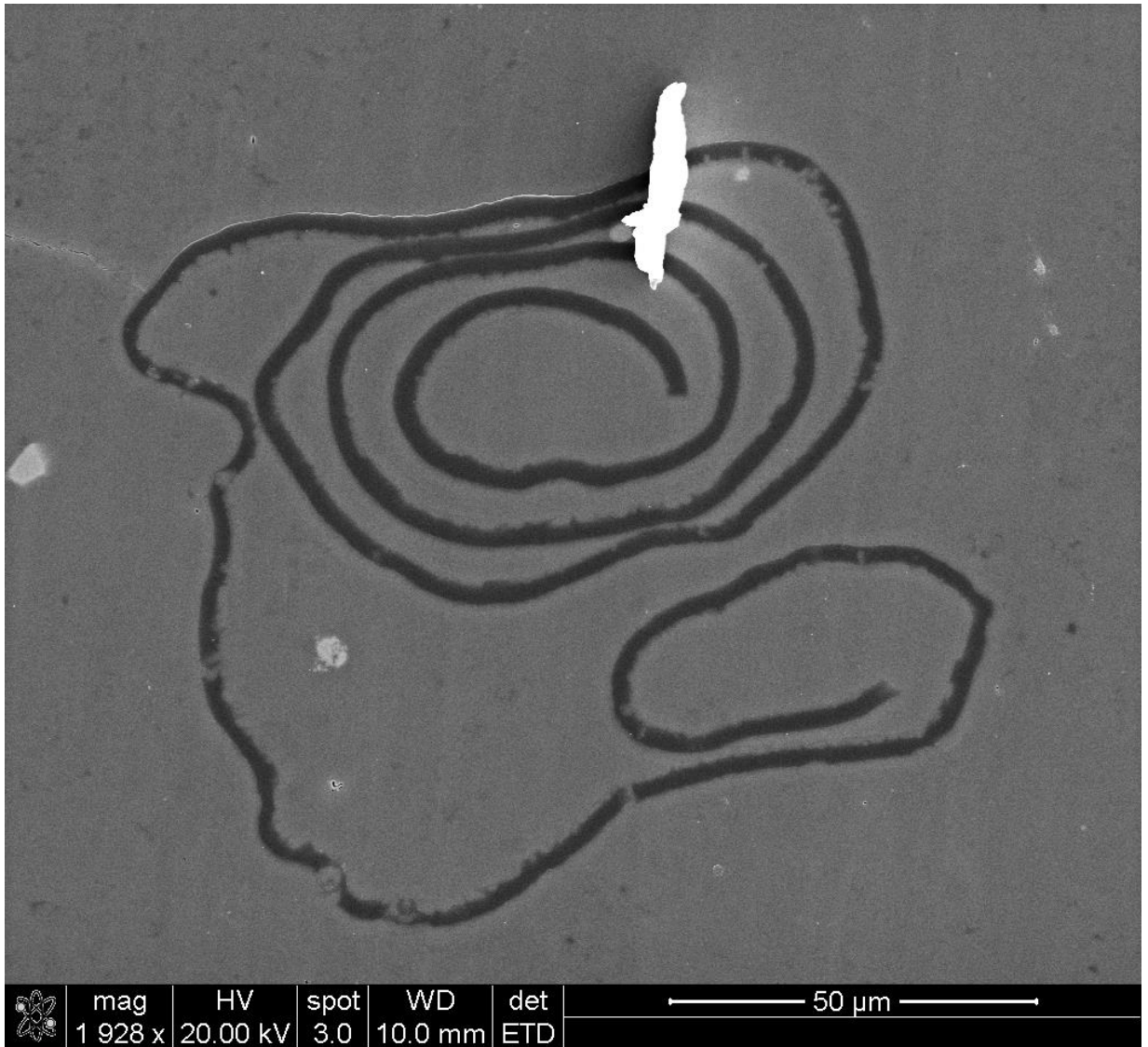


Figure 80. SEM image showing complex spiral forms in organic film, Atoka Chert Pit (sample 3). Note that spiral resembles a scroll with multiple whorls at one end and a single whorl at the other.

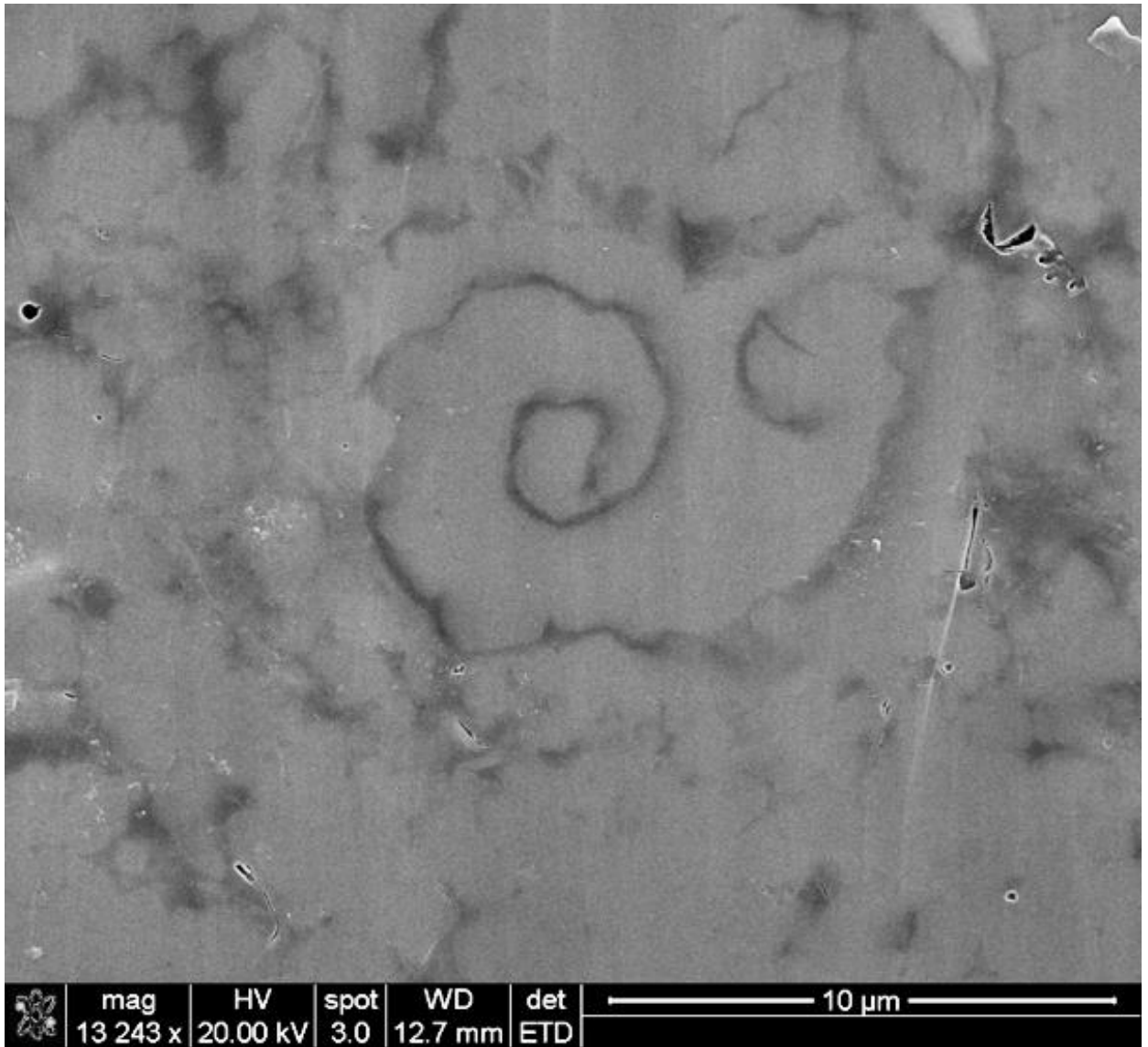


Figure 81. SEM image showing irregular spiral film in novaculitic chert that is curled at both ends from novaculitic chert at the I-35 outcrop (sample 1). Similarity to the film from the Atoka Chert Pit (Fig. 77) suggests that such films are common in novaculitic chert.

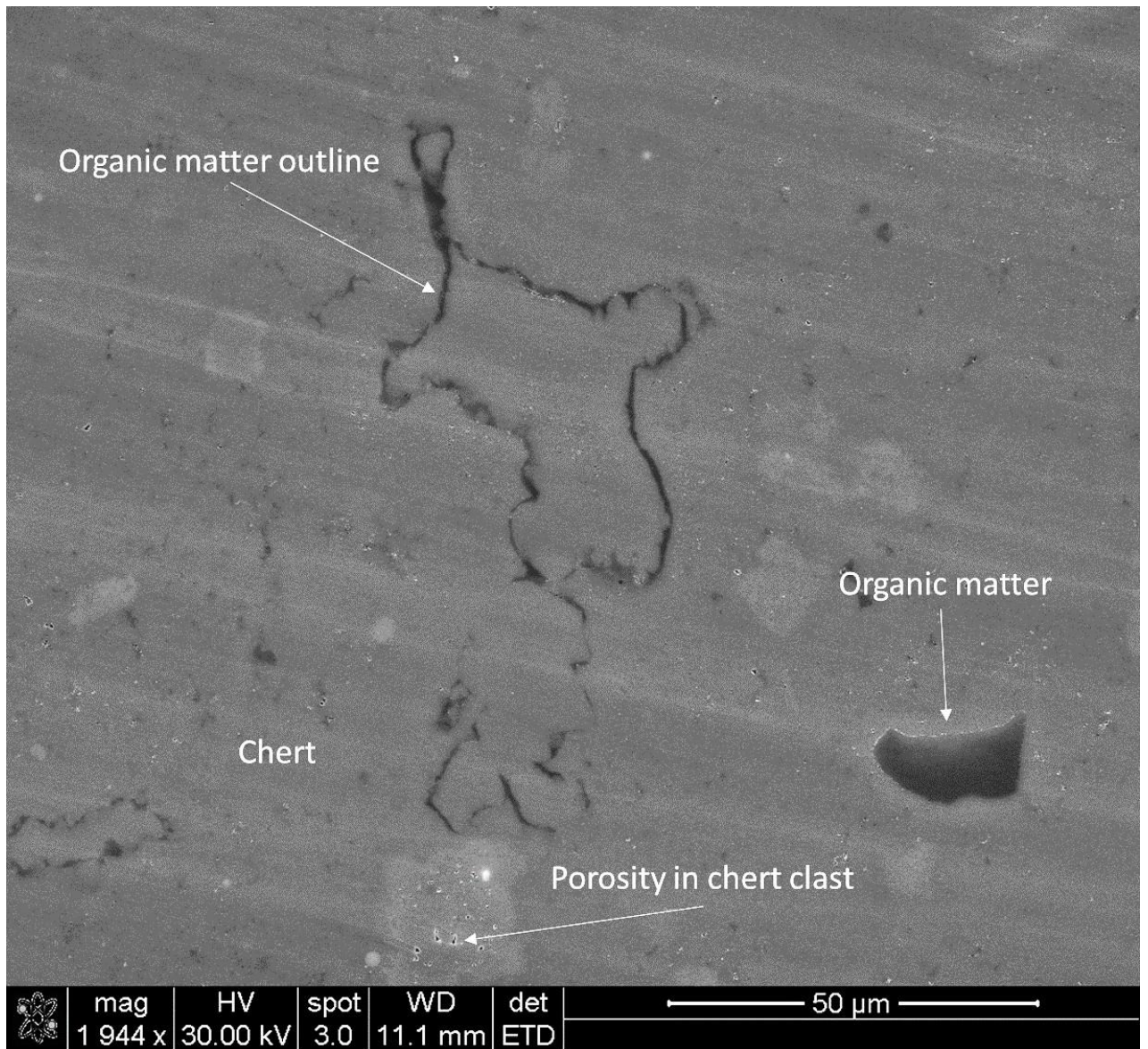


Figure 82. SEM image showing irregular organic film in novaculitic chert, Woodford Shale from the Poe #1-29 core (sample 8).

IV.3.C Diagenetic Features

Diagenetic features found in the SEM images include cubic pyrite crystals, which are denser and thus appear lighter in color than the surrounding chert matrix, very small hexagonal quartz crystals, hexagonal-shaped pores, large subhedral to euhedral pyrite crystals, and pyrite framboids. The I-35 sample contains both pyrite crystals and framboids. The Atoka Chert Pit samples contain abundant pyrite framboids (Figs. 83, 84). The Poe #1-29 core contains euhedral pyrite crystals, some with two generations of pyrite growth (Fig. 85). The hexagonal shapes (pyrite euhedra) within the Atoka outcrop samples and the Hall 2B and Poe #1-29 cores are micrometer scale crystals. The tripolitic Atoka sample is the only sample that contains abundant iron cross pyrite twins (Fig. 86).

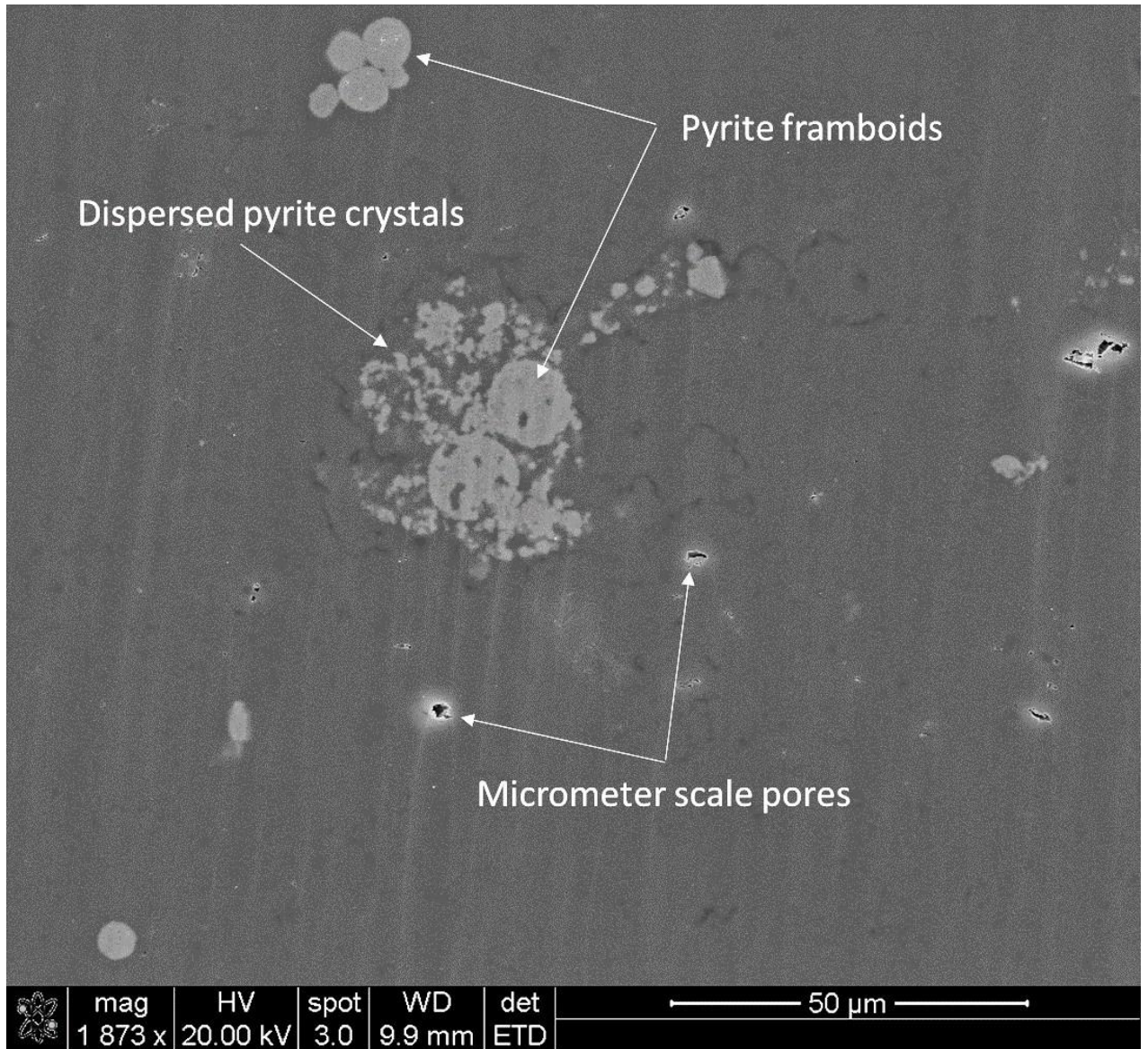


Figure 83. SEM image showing framboidal and dispersed euhedral pyrite within Arkansas Novaculite, Atoka Chert Pit (sample 3). Note the silica-filled filled voids within some pyrite framboids.

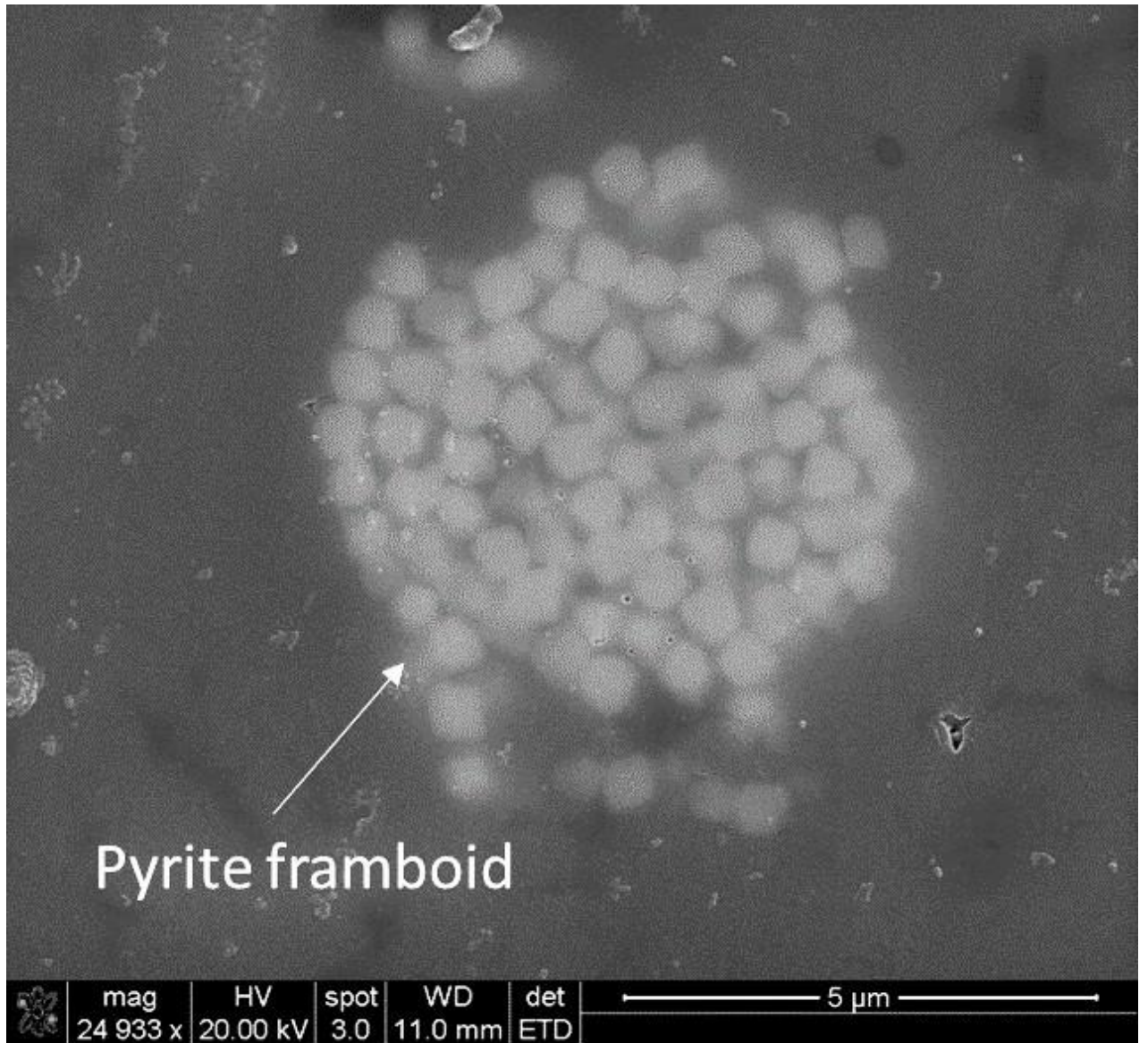


Figure 84. SEM image showing pyrite framboid, Arkansas Novaculite, Atoka Chert Pit (sample 2). Pyrite framboids are present in all SEM samples.

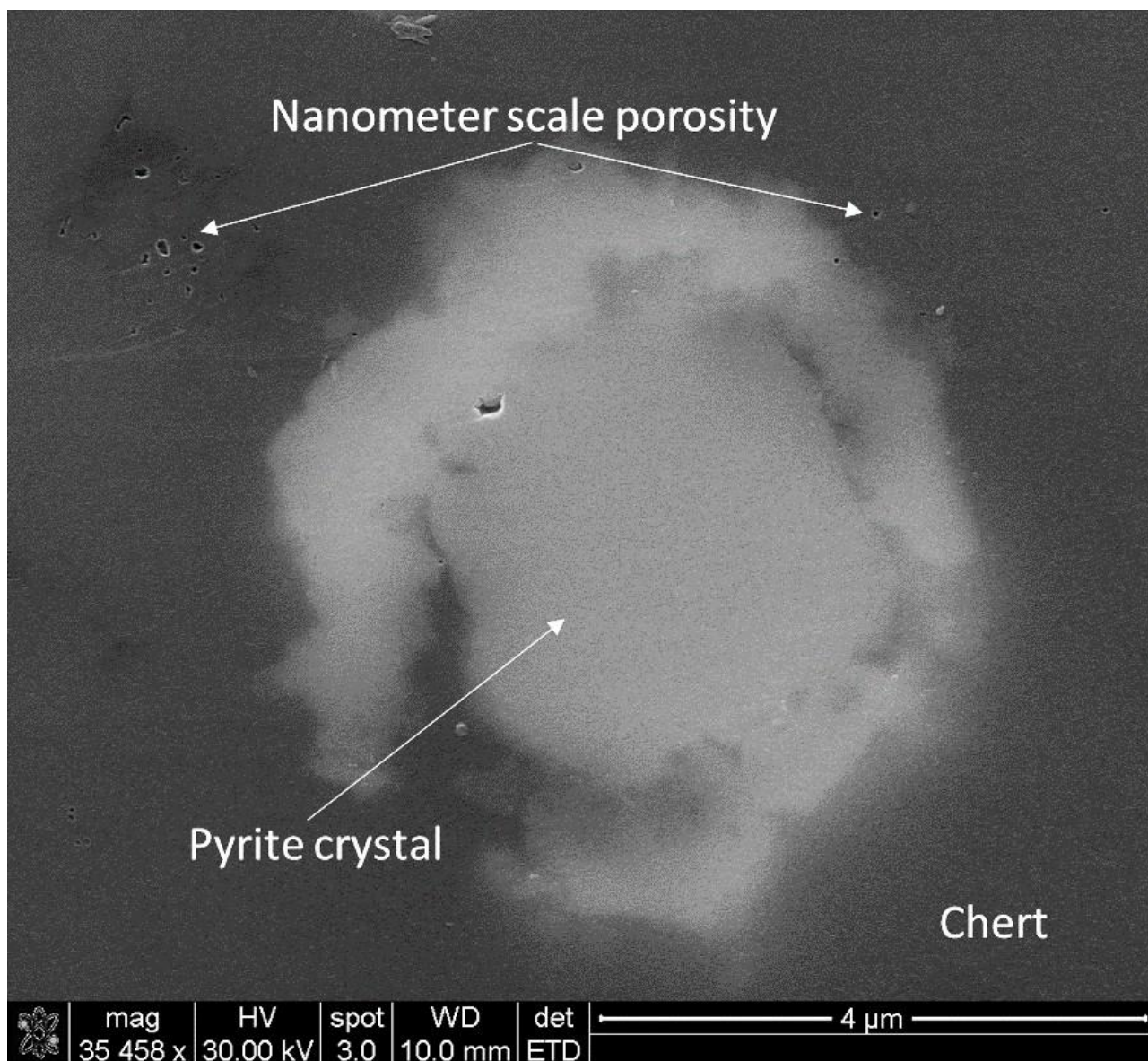


Figure 85. SEM image showing cubic crystal and nanometer-scale porosity within an argon ion milled sample of novaculitic chert from the Woodford Shale, Poe #1-29 core (sample 7). Note the two generations of pyrite growth.

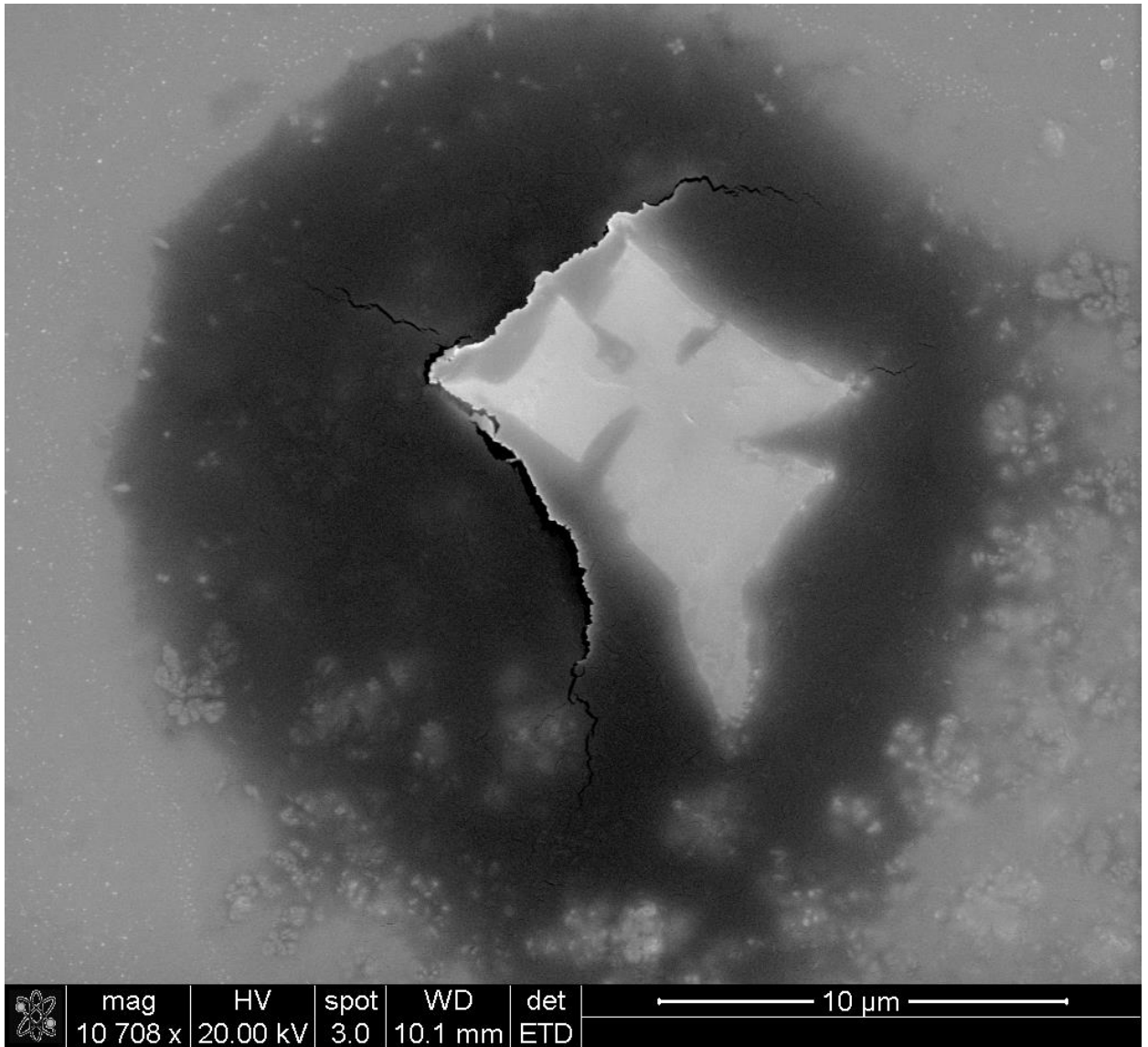


Figure 86. SEM image showing iron cross pyrite twin in circular mass of organic matter within Arkansas Novaculite, Atoka Chert Pit (sample 3).

IV.3.D Porosity

Porosity was observed in all samples analyzed. The most form of porosity is isolated pores of micrometer to nanometer scale, and ranging in shape from irregular to polygonal or spherical (Fig. 87, 88). Porosity is also present in the form of micrometer to nanometer-scale fissures along the edges of silica crystals and organic matter bodies, pyrite crystals, and within

pyrite framboids and crystals. The largest pores are fissure pores ranging in length from 1->50 microns and aperture on the order of 0.1-1.0 microns and are present in the Poe core (Fig. 89, 90). In the Hall 2B core, the samples exhibit micrometer-scale fracture slits that follow the edges of chert clasts (Fig. 78). Similar fractures were imaged by micro CT from this core by Powers (2015). Individual nano-scale pores occur randomly throughout the sample, including in chert clasts. Within the Broken Bow Uplift porosity is present as nanometer-scale elongated to irregularly shaped pores (Fig. 91). It also exists as fissure porosity usually near organic material or outlining mineral grain boundaries. The Atoka Chert Pit samples contain nanometer-scale fissures, and irregularly-shaped pores are abundant in each of the samples. Many of the isolated pores take the form of intraparticle and intercrystalline porosity within pyrite, quartz crystals and organic matter (Fig. 92). Several of the isolated pores have edges that resemble sides of hexagonal quartz crystals (Fig. 93). Finally, the porosity in the form I-35 is micrometer- and nanometer-scale isolated pores and as nanometer-scale fissure pores along interfaces between minerals and organic matter (Fig. 94).

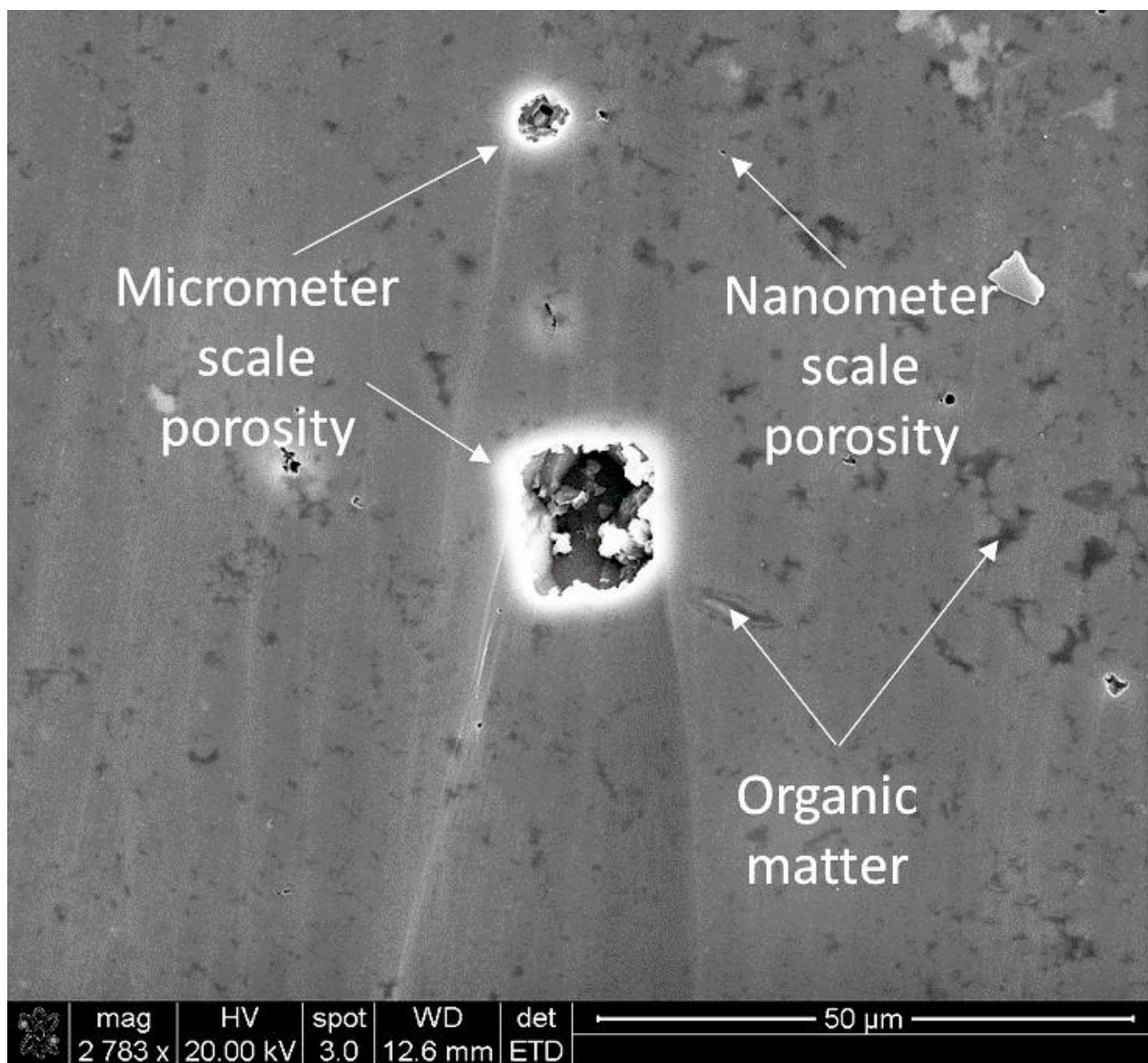


Figure 87. Backscattered SEM image showing isolated pores in novaculitic chert, I-35 (sample 1). Pore sizes range from 1-15 microns. Individual pores often contain euhedral crystals, possibly dolomite.

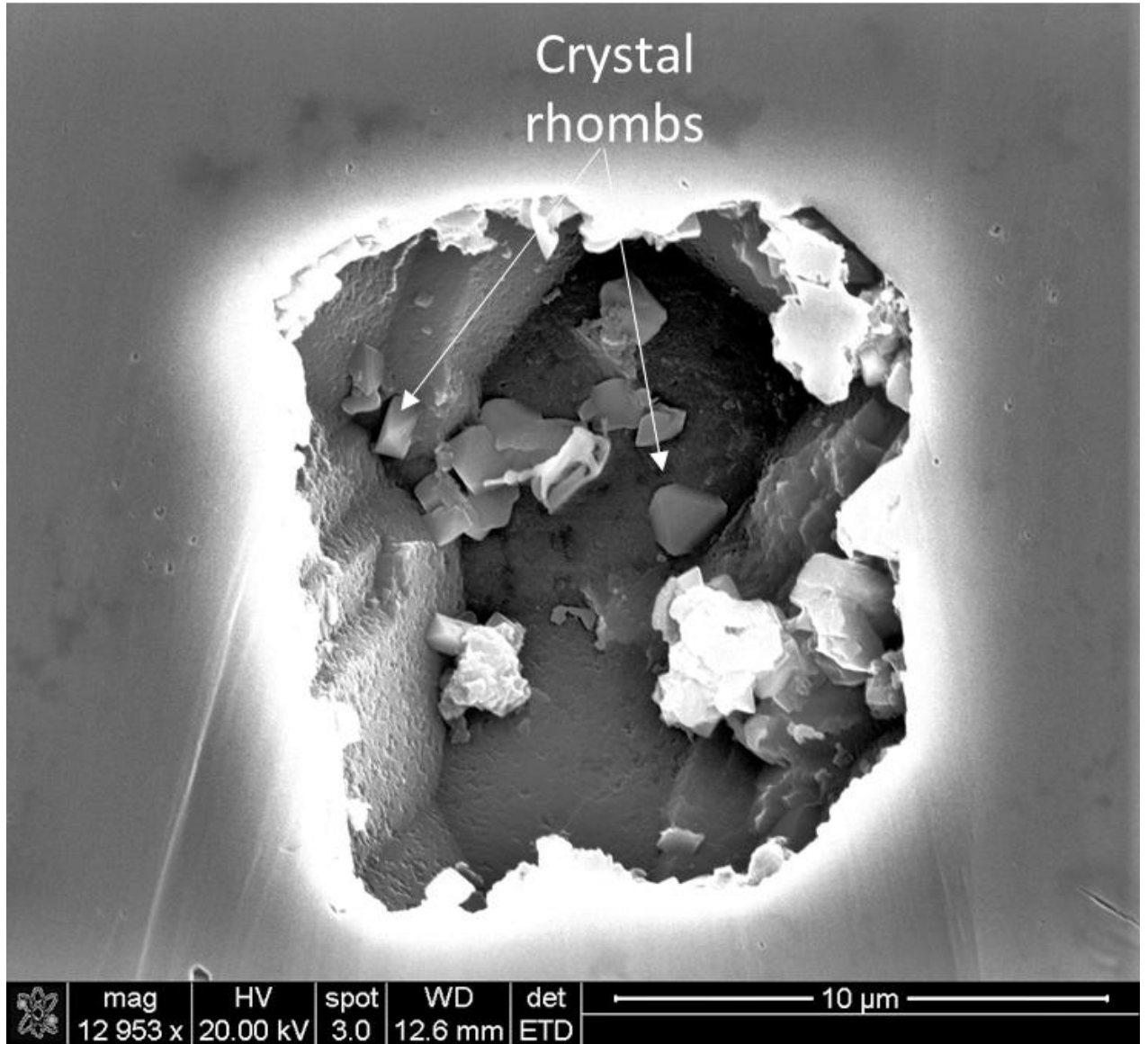


Figure 88. Close up SEM image showing pore surface in novaculitic chert, I-35 (sample 1). This large pore contains euhedral crystals, possibly dolomite, within the pore space.

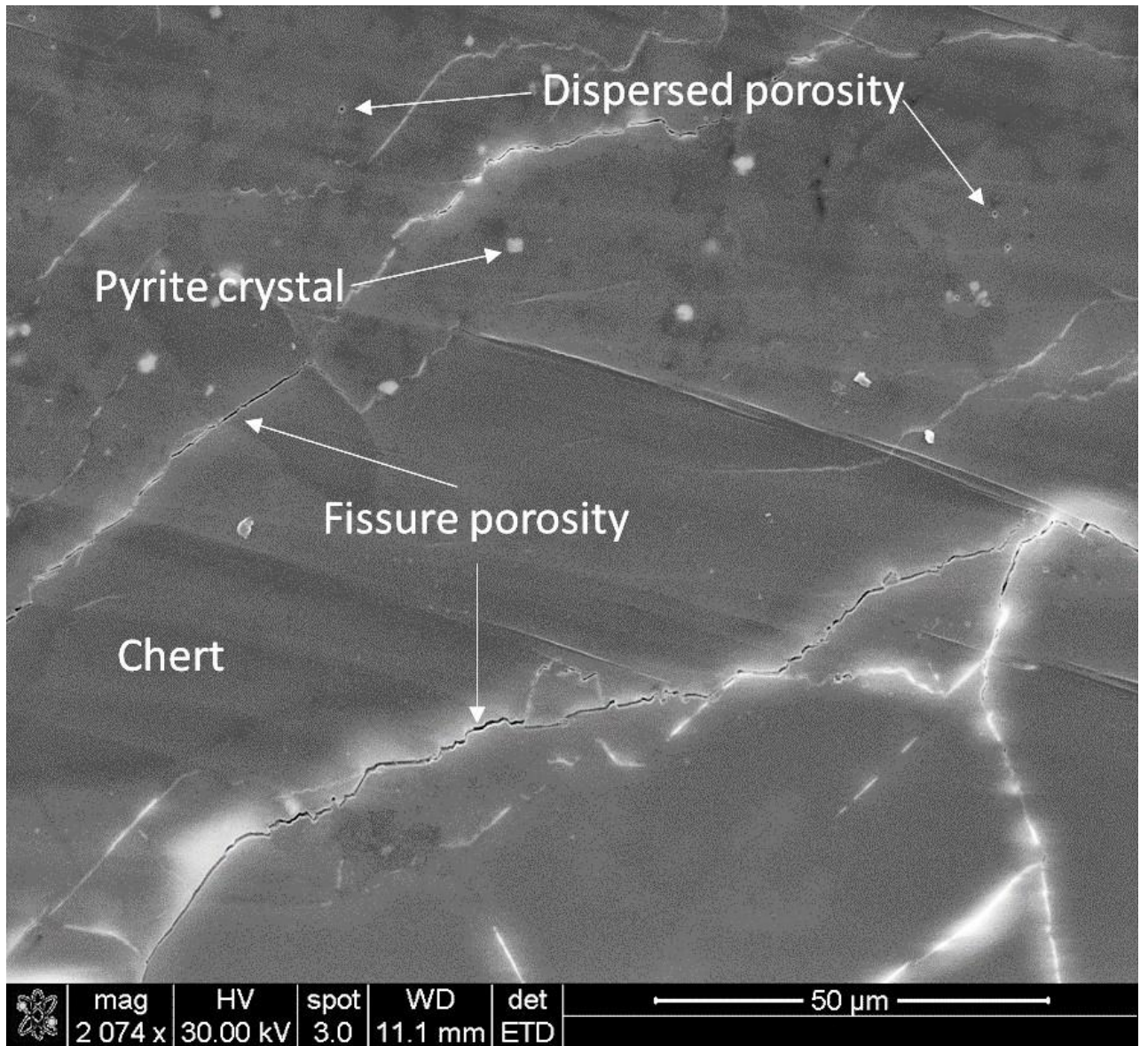


Figure 89. SEM image showing fissure porosity associated with natural fractures in Woodford chert, Poe #1-29 core (sample 8).

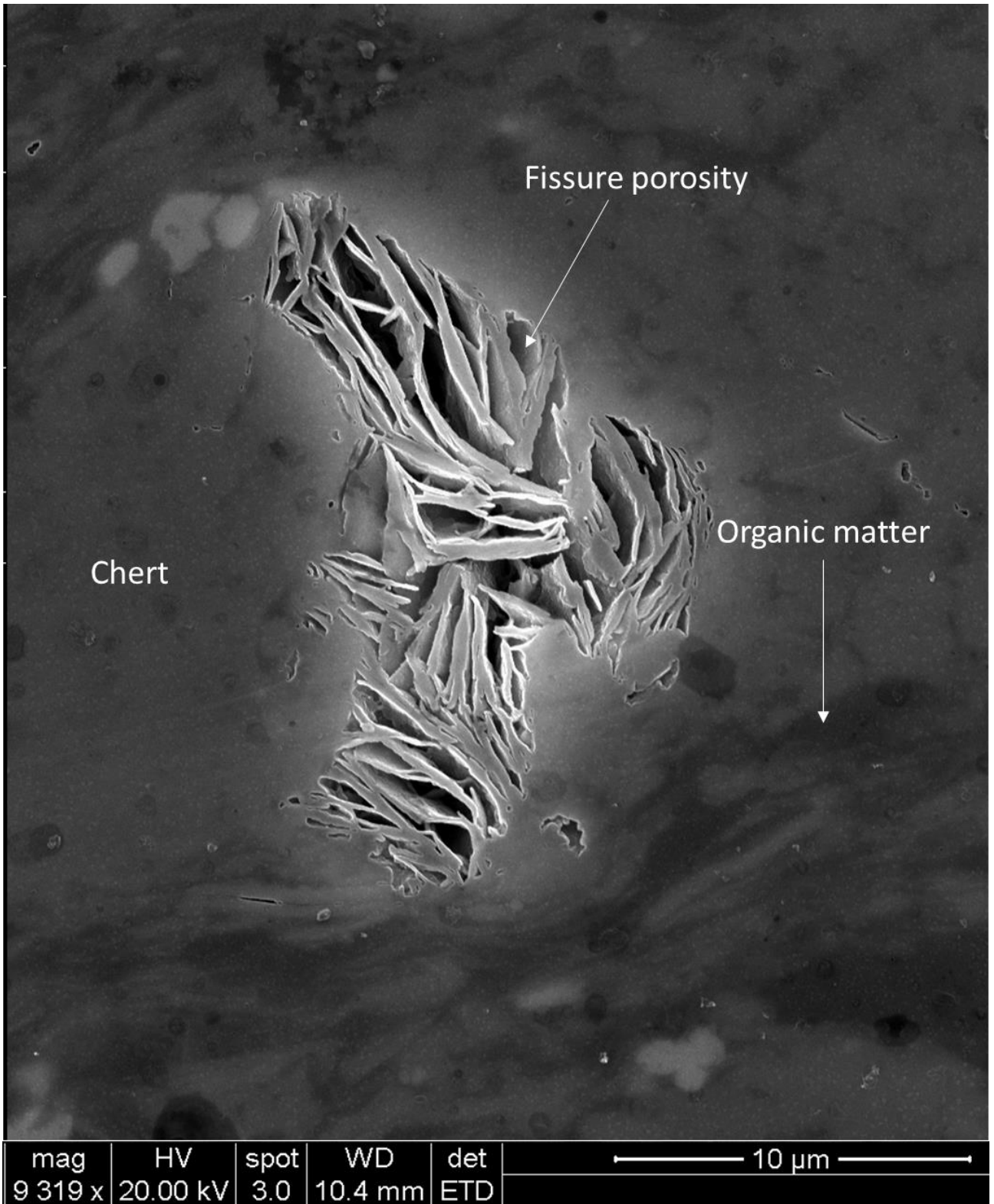


Figure 90. SEM image showing abundant fissure porosity in a platy clay particle, Woodford Shale, Poe #1-29 core (sample 8). Clay minerals are extremely rare in chert of the Woodford Shale and the Arkansas Novaculite.

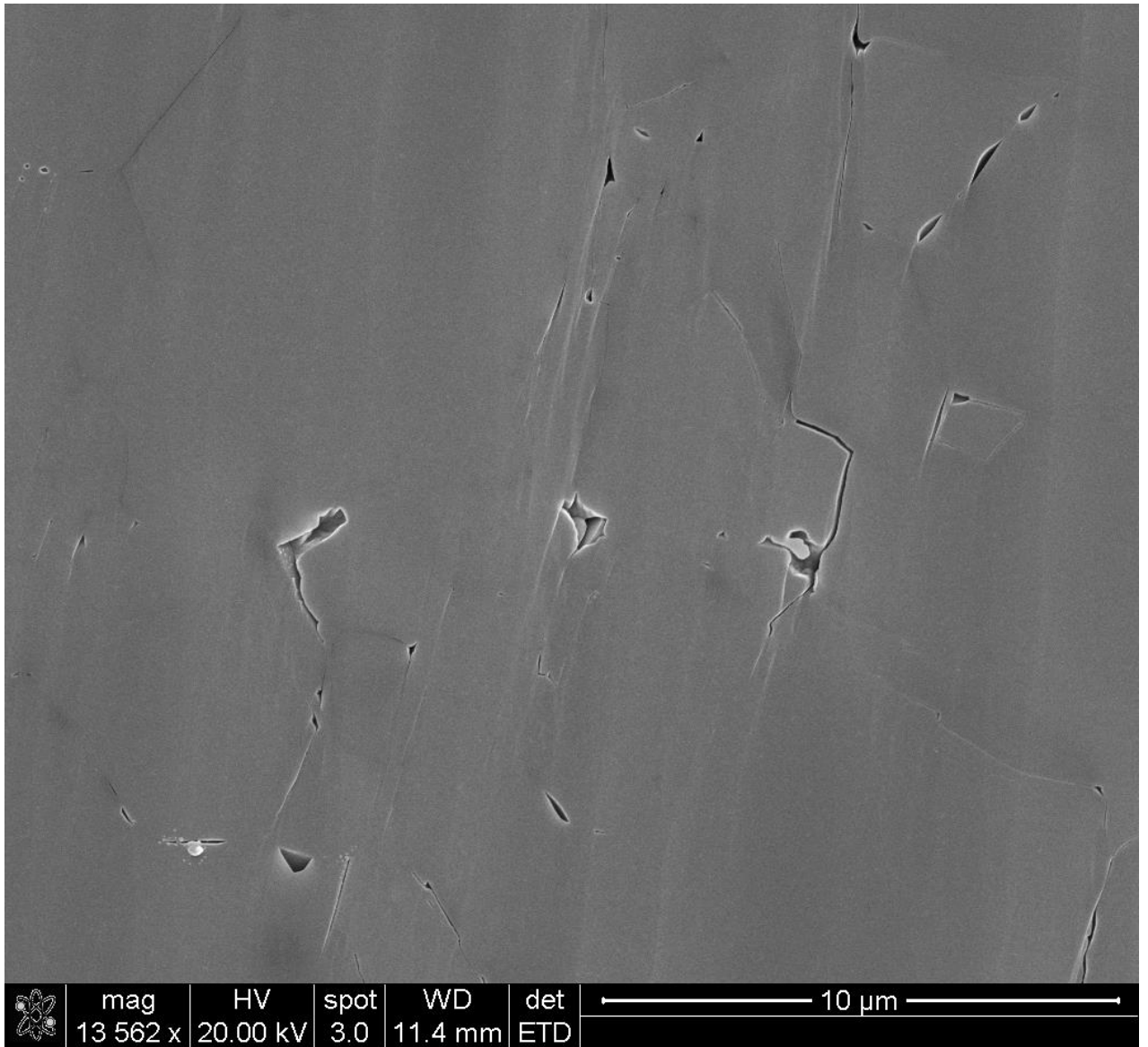


Figure 91. SEM image showing fissure porosity and irregularly shaped pores in the Broken Bow/Beavers Bend outcrop (sample 4).

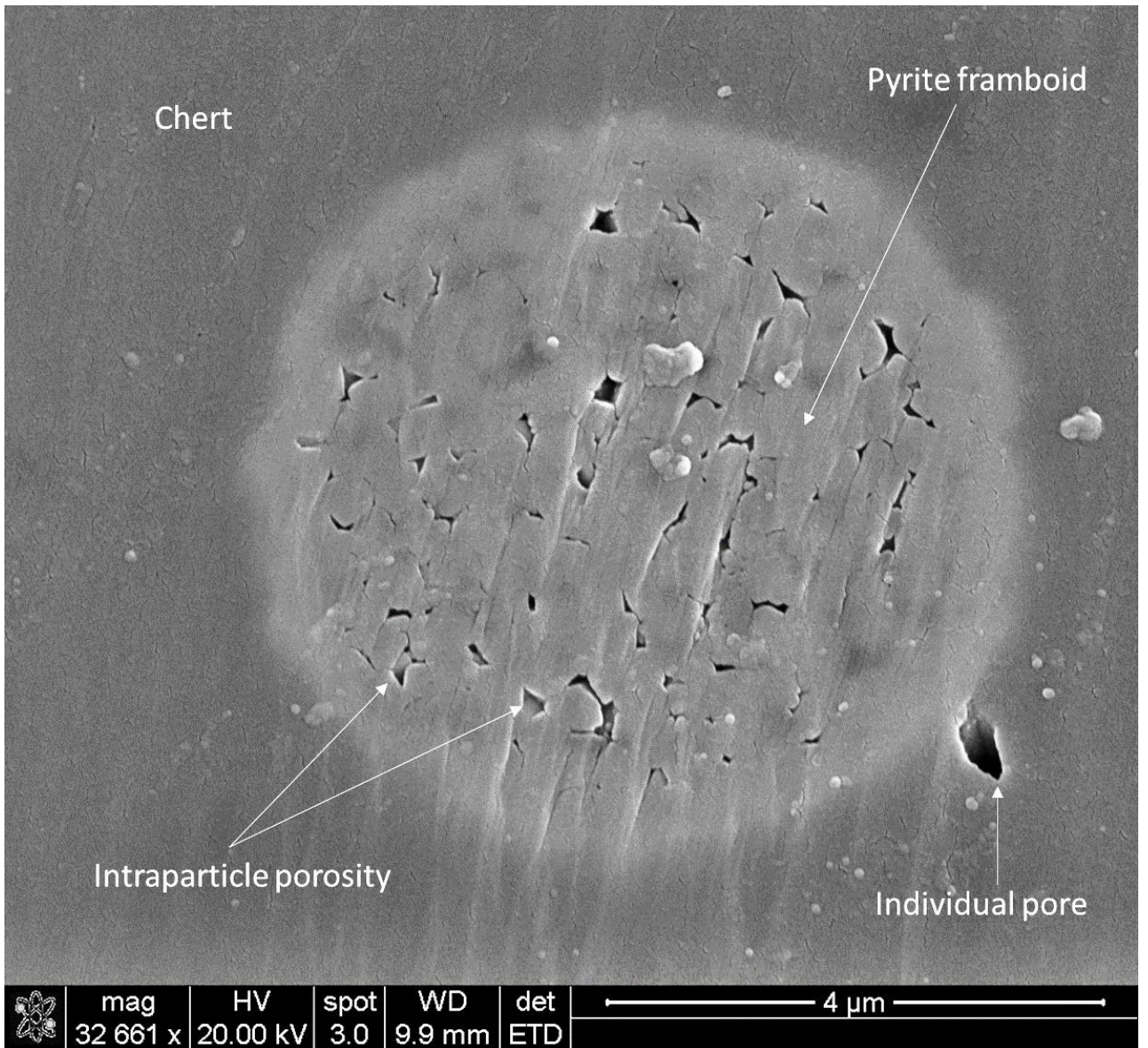


Figure 92. SEM image showing intercrystalline porosity within a pyrite framboid, Atoka Chert Pit (sample 3).

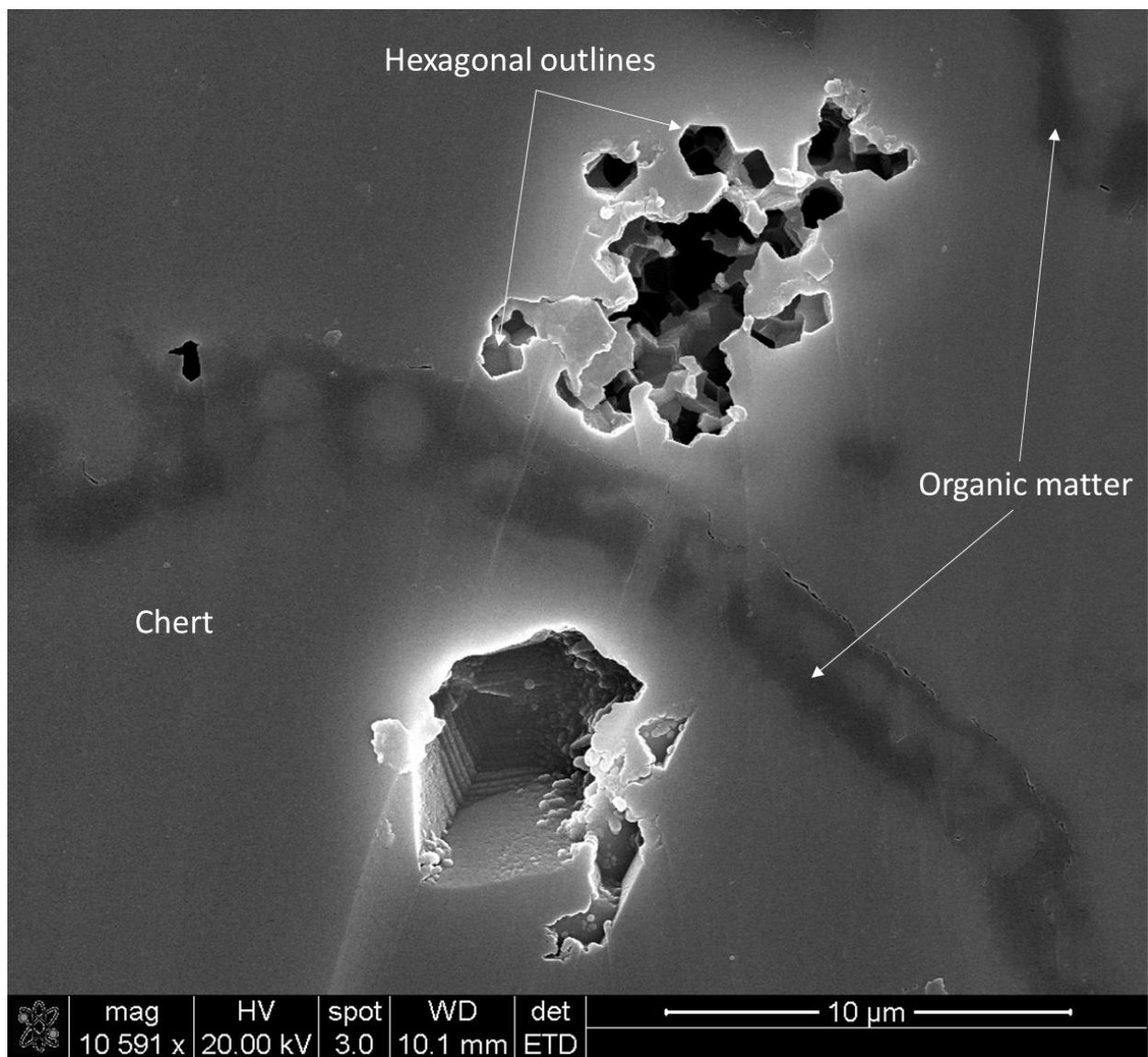


Figure 93. SEM image showing porosity within an argon ion milled sample of Arkansas Novaculite Atoka Chert Pit (sample 3). Hexagonal voids within silica matrix suggest dissolution of a prismatic mineral, such as apatite.

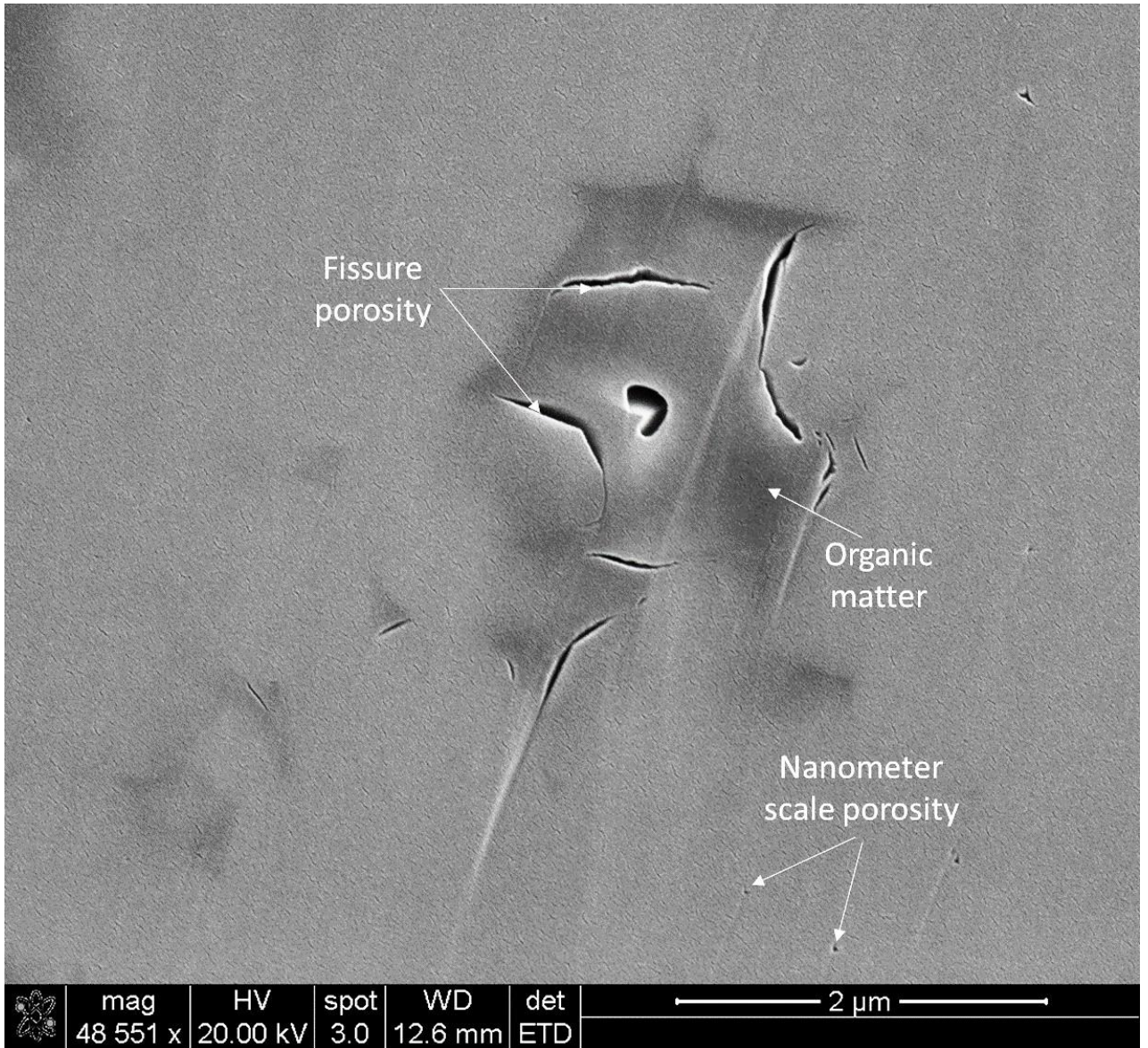


Figure 94. SEM image showing nanometer-scale fissure porosity within organic matter, I-35 (sample 1). Fissure pores occur within or along the margins of organic matter.

CHAPTER V

DISCUSSION

The origin of the Arkansas Novaculite and the novaculitic chert within the Woodford Shale remains fertile ground for research, and many questions remain. The chert formations were studied primarily from the late 19th Century through the 1970s and since that time concepts of Devonian marine sedimentation have progressed greatly (Ettensohn, 1981). Modern characterization of the novaculitic chert in the Woodford Shale and Arkansas Novaculite can lead to a better understanding of what implications those characteristics may have for the origin of the chert. The progression of unconventional hydrocarbon plays into strata containing novaculitic chert makes the understanding of these formations even more imperative.

The source of the silica in the Arkansas Novaculite has been debated for as long as the formation has been studied (Jones and Knauth, 1979; Hesse, 1988; Viele, 1989; Suneson, 1995). Early investigators interpreted its origin in terms of the five major processes discussed in the introduction of this thesis (Table 2). Based on the results of this study, it is questionable that volcanism and/or chemical precipitation are the primary source of the silica due to the presence of abundant radiolaria and sponge spicules within the rock, as well as the peloidal silica-organic

matrix, which is arguably of microbial origin. If the silica source were strictly the result of chemical precipitation or volcanogenesis, there would be a lack of microfossils and organic matter. Chemical precipitation of silica from a volcanic or abiogenic source from sea water is technically a possibility, but is unlikely because the siliceous organic remains seen in the chert were originally amorphous, biogenic silica (Park and Croneis, 1969). Indeed, results of this study indicate that a significant fraction of amorphous silica remains in the formation, although much has been recrystallized to cryptocrystalline forms. Other than the possibility of volcanogenic silica, there is a distinct lack of other volcanogenic minerals in the chert such as zircon, chlorite, sericite, tourmaline, and feldspars like sanidine. Moreover, clay minerals, which may be derived from degradation of labile volcanogenic minerals, appear to be no more than an occasional rarity in the chert (Fig. 90). Additionally, XRF analysis of Woodford chert by Callner (2014) also indicated a paucity of clay.

However, volcanism as the ultimate source of the biogenic silica cannot be wholly ruled out, yet accumulation biogenic silica alone could have provided all of the necessary silica for the Arkansas Novaculite (Sholes and McBride, 1975). The presence of tuff in shale and sandstone of the Ouachita Embayment outside the Arkansas Novaculite does support the possibility of volcanism in the region (Suneson, 1995). Furthermore, it is possible that inception of subduction and convergence as the Rheic Ocean and Ouachita Embayment began to close could have provided a rich silica source of volcanogenic silica that helped supply blooms of siliceous microplankton, as well as a bottom fauna including glass sponges. Although arc volcanism associated with the initial stages of Ouachita orogenesis may have contributed silica to the water column and to the skeletal material in the plankton and benthos that is preserved in novaculitic chert, there is no inherent necessity for a nearby volcanic source to explain any of the features observed in this study.

Alteration of detrital quartz by diagenesis or metamorphism is improbable due to the presence of abundant biogenic material and an apparent lack of detrital quartz beyond brecciated and reworked chert derived directly from novaculite. Detrital quartz is present in the shale intervals separating the chert beds, but none was identified within the chert. Detrital quartz in the Woodford is thought to originate from many sources, including estuarine flushing of terrigenous sediment onto the shelf and eolian sources (Comer, 2008; Callner, 2014; Kvale and Bynum, 2014). Cecil (2004) documented eolian silt expressed as angular, shard-like silt grains in the Huntersville Chert in the Appalachians. The lack of similar grains in the novaculitic chert of the midcontinent suggests that eolian input was limited and was diluted by biogenic production of opaline silica. Moreover, according Honjo (1996), tests made of opal, calcite, or aragonite are major ballasting constituents of sinking biogenic particles, and that smaller-size terrigenous grains would not sink fast enough to reach the sea floor in order for detrital quartz to be the major source of the formation. Indeed, based on the work of Cecil (2004), if detrital silica were a significant component of the novaculite, it would be reasonable to expect some grains to have been preserved. Although sand-size silica crystals exist in some of the Broken Bow/Beavers Bend Arkansas Novaculite samples, they are clearly vein quartz of chemical or even hydrothermal origin (Fig. 72). Heat and pressure associated with low-grade metamorphism and hydrothermal activity could have contributed to recrystallization of some novaculite and development of the cryptocrystalline fabrics observed locally in the Broken Bow Uplift (Fig. 75).

Silicification of limestone and dolomite is improbable as the source of the Arkansas Novaculite for several reasons. Silicification of an original carbonate rock would typically not exhibit the well-developed bedding and sedimentologic features observed in the novaculite. Indeed, Knauth (1979, p. 277) pointed out that “Chert that has replaced limestone occurs as nodules, thin beds, and irregular accumulations,” which is contrary to the most basic field observations of novaculitic chert throughout the study area. Silicified limestone is widespread and

is readily recognized, such as the Oklahoma Chat, as cryptocrystalline silica nodules or irregularly bedded chert (Huneke and Mulder, 2011). Such chert is more coarsely crystalline than novaculite and lacks the peloidal texture with interstitial organic matter that is so characteristic of the novaculite. Additionally, there is an abundance of siliceous microfossils present in the novaculite that were originally composed of opaline silica. Degradation and diagenesis of opaline silica provides an adequate explanation for preservation of well-bedded siliceous ooze as novaculitic chert, and further hypotheses incorporating detrital material, in part or as a whole, are unnecessary to explain the origin.

The results of this study indicate that the dominant processes associated with novaculitic sedimentation are associated with the accumulation of opaline biogenic silica. During the past 50 years there has been a growing understanding of basic oceanic processes, which has given insight into and helped support this idea. Emerging technology, such as SEM analysis of ion milled samples, has allowed a new, more detailed look at the mechanisms that play a role in the formation of the chert, versus previous decades when detailed technology was lacking. An abundance of opaline tests of radiolaria on the sea floor commonly correlates with patterns of surface water productivity (Huneke and Mulder, 2011). Siliceous ooze deposits forming today and in the Neogene occur in regions where siliceous plankton blooms and phosphate deposition are driven by oceanic upwelling and are characterized by extensive oxygen minimum zones (California, Namibia, Peru, and Chile), and these regions provide modern analogs that can provide insight into the formation of the novaculite in the southern midcontinent (Lochte et al., 2003; Huneke and Mulder, 2011). Anoxic layers or zones may also develop in deep water where turbidites cover the sea floor and prevent oxygen exchange with the water column (Lochte et. al., 2003). Hence, a basic application of the theory of uniformitarianism utilizing modern oceanographic processes acts as support for the idea that the Arkansas Novaculite and novaculitic chert could have formed in a similar fashion.

Phosphate nodules within the Woodford Shale and novaculitic chert are composed of microfossils, peloids, phosphate, silica and calcite cement, and well developed apatite crystals. Spesshardt (1985) observed similar characteristics in a study of Woodford phosphate nodules in the Arbuckle Mountains. Based on these features they determined the following sequence of events occurred during the formation of the nodules: 1) precipitation of carbonate fluorapatite cement on grains in nodules and around intergranular and intragranular voids, 2) silica cementation (microchalcedony), 3) calcite cementation in some voids and replacement of silica along rims of some nodules, and 4) pyrite mineralization. However, there is no calcite found within the samples of this research. The nodules studied in this thesis have similar characteristics, but dolomite was observed as a late-stage cement that in places post-dated bitumen formation (Fig. 70).

During the Devonian, oceanic upwelling is thought to have played an important role in phosphate and Woodford chert deposition (Kvale and Bynum, 2014). Upwelling provides large amounts of nutrients, like phosphate and nitrogen, for Protozoa, which supports extensive plankton blooms. Comer proposed that high evaporation rates and aridity were the primary driver for upwelling at the time, but this interpretation is not compatible with either the overall paleogeographic setting in the temperate-tradewind transition or the great extent of the novaculitic chert and phosphate deposits on the Oklahoma Shelf and in the Ouachita Embayment. Kvale and Bynum (2014) instead suggested that upwelling result of tradewinds that blew parallel to a west facing North American craton. Taking their interpretation a step further, the location of the Ouachita Embayment in the temperate-tradewind transition may have had a significant impact on the upwelling system. Whereas tradewinds driven by the descending Hadley Cell may have driven major upwelling and biotic productivity, episodes where the opposite winds driven by the temperate Ferrel Cell impinged on the Ouachita Embayment may have suppressed upwelling. Such changes may have operated at seasonal to much longer time frames and may have been

influenced by incipient monsoonal conditions as Pangea began coming together (e.g., Parrish, 1987). This may help explain the complex lamination and bedding patterns within the novaculite, as well as the alternation between novaculite and sapropelic shale.

It is interpreted that the upper portion of an ancient oxygen minimum zone (OMZ) was to have intersected a broad continental shelf along the southern portion of Laurussia (Fig. 95). Like modern OMZs, the Devonian OMZ apparently was the product of exceptional biotic productivity and organic matter production driven by upwelling (Callner, 2014). Today, a major OMZ is developed in the eastern Indian Ocean at the edge of the northern tradewind belt and is strongly influenced by the Himalayan-Tibetan monsoon, which causes the intertropical convergence zone to shift by 30° seasonally. This is an extreme case, and shifting of climatic belts at this stage of supercontinent assembly was probably less pronounced.

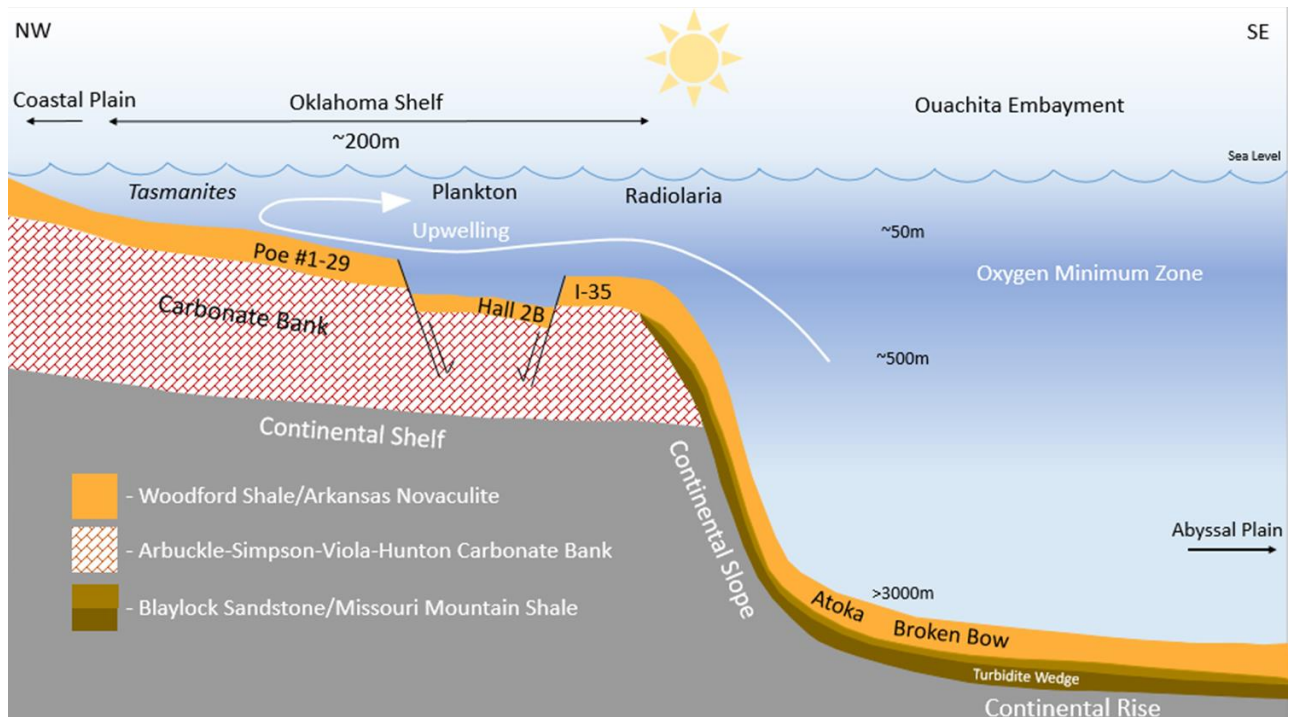


Figure 95. Depositional model of the Woodford Shale and Arkansas Novaculite based on features analyzed in outcrops, core, thin sections and SEM images.

In modern systems, biogenic silica provided by upwelling is deposited on the sea floor as diatoms, radiolaria, and siliceous sponges - the remains of which, save for diatoms, occur in novaculite. Biogenic opal-A forms at or just below the seafloor by the dissolution of the siliceous skeletal material (Lee, 2005). Opal-A forms biogenically and is the most common form of highly disordered opaline silica (Knauth, 1994), and so perhaps the peloidal nature of the silica-organic matrix (Fig. 64) is the product of microbial processes. During diagenesis, the siliceous deposits underwent mineralogical changes from amorphous opal-A to cryptocrystalline opal-CT/C (Fig. 96). Some places, like the Broken Bow outcrop, exhibit cryptocrystalline and microcrystalline quartz, which could have occurred during veining and low-grade metamorphism (Keller et. al., 1985; Hein and Parrish, 1987). In modern continental shelves, the opal-A to opal-CT phase transition occurs at a burial depth of about 3,280 feet, and the opal-CT to quartz transition occurs at about 4,500 feet (Peters et. al., 2011). The opal-A to opal-CT and opal-CT to quartz phase transition is partly controlled by temperature, clay content and water chemistry (Hein and Parrish, 1987; Peters et. al., 2011). While porosity decreases during this transition, permeability increases, which can be an important consideration during hydrocarbon properties evaluation (Reid and McIntyre, 2001). Water and methane are expelled from siliceous ooze during the opal A-CT transition, and this process has been used to explain gas hydrate mounds at the sea floor in modern systems (Peters et al., 2011). In the case of novaculitic chert, this process may help explain the strata-bound veins in the Poe #1-29 core (Figs. 14, 15), and ptygmatic folding of the veins and shear structures may reflect volume loss associated with water expulsion, gas expulsion, and mineral transformation.

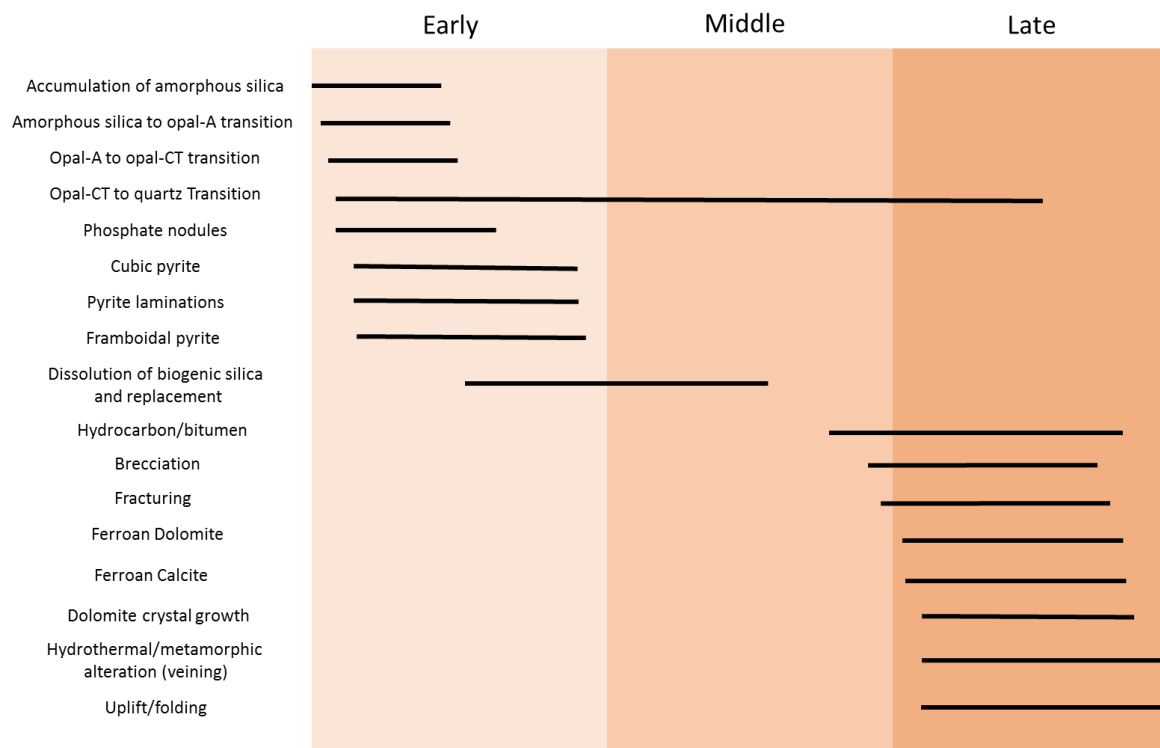


Figure 96. Paragenetic sequence for the Arkansas Novaculite and novaculitic chert in Oklahoma.

Novaculite formations were originally suggested to be deposited in deep water conditions off the southern margin of North America (Sholes and McBride, 1975). While this might be plausible for some of the more massive bedded Arkansas Novaculite formations mentioned above, it is an unlikely depositional environment for other western portions of the Arkansas Novaculite and novaculitic chert, which are clearly on the continental shelf. The I-35 novaculitic chert is a type novaculite locality that displays the basic properties of the rock type without too many complicated features. Evidence gathered during this research suggests that chert interbedded with fissile, black shale found at the I-35 outcrop was deposited on the Oklahoma Shelf (Fig. 95). This is also supported by the presence of the underlying Arbuckle-Simpson-Viola-Hunton carbonate bank beneath the Woodford Shale. Nearby, the Atoka Chert Pit almost certainly links the Arkansas Novaculite to the Woodford Shale based on features observed

throughout this study (Fig. 6). The presence of an imbricate zone near the Atoka outcrop, may suggest that the strata of the Woodford Shale was thrust over the edge of the carbonate platform and/or major basement faults (Fig. 97).

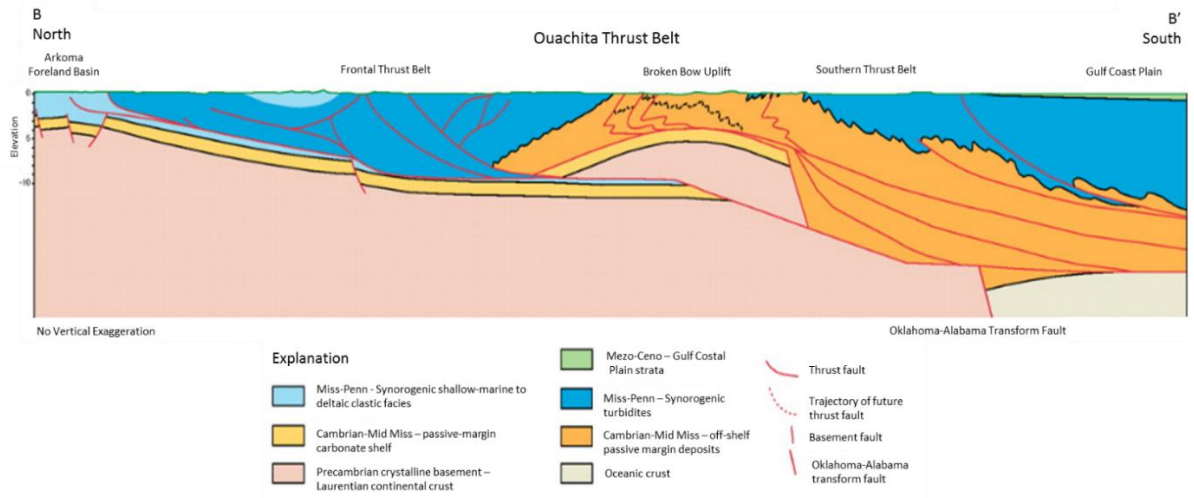


Figure 97. Present day cross-section through the Ouachita Mountains fold and thrust belt in Oklahoma (Thomas, 2011).

The Poe #1-29 core, taken north of the Southern Oklahoma Aulacogen in Hughes county, displays similar type section novaculite features like the I-35 and Atoka outcrops. However, it also contains prevalent synsedimentary deformation, which could indicate unstable grounding and gravity effects at the time of deposition, particularly instability on the Oklahoma Shelf (Callner, 2014). The core also exhibits abundant strata-bound fractures in the chert layers, which were likely highly influenced by the deformation that occurred to the rocks (Fig. 14, 15). Both the Poe#1-29 and Hall 2B cores were likely deposited along the Oklahoma Shelf setting similarly to the I-35 Woodford Shale. Additionally, the two cores also both overlay the Arbuckle-Simpson-Viola-Hunton carbonate bank. The Hall 2B core provides evidence for multiple catastrophic events and slope instability associated with a normal fault scarp at the southwestern edge of the

Southern Oklahoma Aulacogen. Abundant synsedimentary deformation was observed in the Hall 2B core. However, both cores exhibit vertical veining and synsedimentary faulting which indicates that parts of the substrate were undergoing tension and extension (Callner, 2014). The deformation is likely associated with penecontemporaneous normal faulting and subsurface sediment creep during burial, including twelve slump deposits overlain by angular unconformities. Much of the chert is brecciated and reworked, and there are numerous erosional surfaces that suggest significant bottom currents were active during chert sedimentation (Fig. 59). Additionally, water expulsion during diagenesis and hydrocarbon expulsion may have further fractured the chert during burial.

The Woodford Shale overlies shelf carbonate formations, whereas the Arkansas Novaculite of the Atoka and Broken Bow outcrops overlies an off-shelf turbidite formation of the Ouachita Orogen. The difference in underlying formations, as well as the presence of an imbricate zone near the Atoka outcrop, may suggest that the more eastern/northeastern strata of the Woodford Shale was thrust over the edge of a carbonate platform and/or major basement faults. Therefore, it is likely that the Atoka and Broken Bow outcrops were deposited further basin-ward on transition crust along the continental rise, with the Atoka outcrops being more likely deposited slightly higher along the rise than the massive Arkansas Novaculite seen in southeast Oklahoma and Arkansas outcrops.

The Broken Bow/Beavers Bend outcrops are vastly different in appearance from one another, at not only the outcrop scale but also at the thin section and SEM-imaging scale. This is likely due to the prominent quartz and pyrite veining in the area. However, some of the rock fabric is obscured by veining in the Broken Bow thin sections, and further analysis would need to be completed to determine this conclusively. The white Arkansas Novaculite of the Broken Bow region exhibits thick sequences of massive, pure cryptocrystalline chert (Fig. 56). Such massive bedding is likely a result of having been deposited in a deeper, distal environment largely beyond

the reach of terrigenous material (Fig. 95). It is likely that these strata travelled a large distance cratonward during regional thrusting.

The Arkansas Novaculite from the Atoka outcrop and equivalent novaculitic chert within the Woodford Shale from the I-35 outcrop are strikingly similar in appearance. Based on the numerous similarities and proximity of the two different formations, it is likely that they formed from similar depositional processes. Both outcrops exhibit rhythmic alternation of fissile, organic-rich shale and bedded chert, contain phosphatic portions and abundant pyrite. Dispersed pyrite euhedra may have precipitated directly from an euxinic water column, which may have existed at times in the OMZ, whereas the pyrite framboids probably formed by microbial sulfate reduction below the sediment-water interface. However, the occurrence of sponges indicates that the bottoms were episodically if not permanently suboxic or even oxic (Fig. 95). Moreover, the angular unconformities and syndimentary breccias in the Hall 2B core indicate that bottom currents were active at least locally and that gravitational collapse and slumping were important processes in fault zones. The presence of pyrite framboids indicate reducing conditions below the sediment-water interface, which would help hinder the decay of organic matter and help preserve some of the organic-walled microfossils (Figs. 79). The curled organic films may be the remnants of microbial mats that formed on the bottoms, and the abundant amorphous kerogen observed in the SEM images also may be microbial in origin (Figs. 80-82). Both outcrops contain phosphate-rich zones, which, along with the plankton blooms, is indicative of upwelling conditions during formation. The chert layers in both formations were likely deposited during periods of high productivity due to upwelling mentioned previously. Interbedded black shale layers were likely deposited during episodes of weak upwelling, or perhaps even episodic downwelling that could have been driven by shifting wind gyres. Within the Woodford, total organic carbon amounts range from 6-14% within the shales, and from 0.6-6% within the chert (Krystyniak, 2003). Lower

organic carbon content of the chert could be due to sedimentary dilution during periods when biogenic silica production was high.

The origin of the rhythms are likely not diagenetic as Murray et. al. (1992) suggested, due to the presence of detrital silt and clay within the shale but not in the chert. The presence of erosional surfaces at the bases of chert beds supports this idea (Figs. 20). The rhythm's origin perhaps more closely aligns with Iijima's (1985) hypothesis, which suggests that the chert beds are deposited as accumulations biogenic silica, which are then overlain by shale partings. The biogenic silica accumulations in Iijima's hypothesis are composed primarily of siliceous skeletons (radiolarian tests, silica spherules, sponge spicules, diatoms). Thin section images of novaculitic chert support this theory (Fig. 51). According to Roberts and Mitterer (1988) a 20,000 ky year rhythm for the chert and shale is possible. This rhythm roughly aligned with that of orbital precession and is also similar to Cretaceous chalk-marl rhythms (Bottjer et. al., 1986). Although, the Woodford Shale is a much less organized system than what would be expected from a truly periodic astronomical cycle. Conditions were likely erratic at the boundary between the Hadley and Ferrel cells, although astronomical processes likely play a background role.

It is widely known that the Woodford Shale is a world-class unconventional petroleum source and reservoir. Although novaculitic chert is interbedded between the Woodford Shale layers, research into its hydrocarbon properties have largely been absent. It has long been understood that the chert contributed brittleness to the reservoir, which helped facilitate fracturing during hydraulic fracturing of the Woodford Shale (Morrison, 1984; Foltz et. al., 2016). Research on the novaculitic chert indicates that the chert not only acts as a fractured brittle layer that helps transmit hydraulic fractures, but may also contribute to the hydrocarbon sourcing and reservoir quality of the play (Kvale and Bynum, 2014). One example of a siliceous deposit exhibiting prolific source rock and fractured properties is the Monterey Formation in California. The formation is one of California's principal sources and reservoirs of hydrocarbons, and underlies

the economic significance of organic matter-rich biogenic siliceous sediment accumulations (Issacs, 1984; Hesse, 1988).

Characteristics revealed during thin section and SEM-image analysis support both the novaculitic chert and the Arkansas Novaculite as significant possible hydrocarbon reservoir and source. Other than fractures, which are commonly cemented, observed open pores are largely isolated and are poorly interconnected. Porosity for both formations is present on a micrometer scale and more abundantly on a nanometer scale. Obvious permeability is not readily apparent, but permeability in the form of newly formed fractures and lace-patterned organic material is possible (Fig.76). The organic matter matrix is pervasive and may help transmit hydrocarbons via diffusion through nanopores. Organic matter is abundant in the samples, taking the form of filled veins, random masses, filled radiolaria and acritarchs, and as lining for Tasmanites. TOC values taken by Krystyniak (2003) and Fishman (2010) reveal that the fissile shale contains between 6-14% TOC and the associated chert contains 0.6-6% TOC. According to Fishman et al., (2010), the novaculitic chert and shale contain type I and II oil-prone kerogen. Additionally, because of the chert's resistance to mechanical compaction, it is possible that hydrocarbon storage capacity is preserved in this type of rock. However, the minute pore storage within the novaculitic chert are likely an important source of adsorbed gas rather than free gas. While the reservoir properties of the chert may not be of the same quality as the Woodford Shale, they are still characteristics to consider as unconventional play exploitation grows and becomes more sophisticated.

CHAPTER VI

CONCLUSION

Based on the identification and analysis features contained within chert outcrops, core, thin sections and SEM images, there are several conclusions that are proposed for the Arkansas Novaculite and equivalent Woodford Shale novaculitic chert that was examined in this study. Based on the high abundance of biologic organisms and the highly phosphatic nature of the chert, it is proposed that it formed from a biogenic silica source in a region influenced by marine upwelling. Coastal upwelling during the Devonian time frame, in what is now Oklahoma and Arkansas, was a result of the formation of a southeasterly tradewind that blew parallel to a west facing North American craton and a function of Hadley circulation. It is highly likely that presence of an oxygen minimum zone contributed to the organic productivity and preservation of organic matter. It is interpreted that the upper portion of an ancient OMZ to have intersected a broad continental shelf along the southern portion of Laurussia. The intersection of an oceanic oxygen minimum zone and upwelling along the Ouachita margin result in abundant silica and phosphate deposition in the Woodford and related units. In addition to this, there is an overall lack of evidence to provide solid support for the other four theories put forth to explain the origin

of formation. There is high similarity between the structures, sedimentation, and appearances on all scales of the novaculitic chert and Woodford Shale at the I-35 outcrop within the Arbuckle Mountains and the Arkansas Novaculite at the Atoka Chert Pit outcrop within the Ouachita Mountains. Based on this, it is reasonable to believe that the two formations were formed by similar depositional processes and in depositional environments that were near one another.

The Arkansas Novaculite and novaculitic chert have a depositional setting ranging from shelf, slope and basinal environments. Based on the cyclical nature of the novaculitic chert and shale rhythms, it is likely that chert of this type was deposited closer to the shore in an anoxic environment along the Oklahoma Shelf. More massive bedding, lack of terrigenous sediment, and abundant biologic features suggests that white and black Arkansas Novaculite near Atoka, Broken Bow and further east was deposited in a more basin-ward, quiet setting like the continental rise where pelagic ooze can be deposited massively in thick sections.

Novaculitic chert within the Woodford Shale is an important component of unconventional reservoirs in the southern Midcontinent, from not only the standpoint of brittleness, but also in terms of organic content and hydrocarbon storage potential. Evidence from both thin section and SEM images support the theory that the chert contains 0.6-6% organic content but also has abundant porosity, on both a micrometer and nanometer scale, and potential permeability in various forms that are adequate in terms of unconventional reservoirs. Although it has been much less examined, the Arkansas Novaculite has similar hydrocarbon properties to the novaculitic chert and has the potential to yield parallel results if thoroughly geologically mapped and explored.

REFERENCES

- Allaby, M., 2013, A dictionary of geology and earth sciences: Oxford University Press:
<http://www.oxfordreference.com/view/10.1093/acref/9780199653065.001.0001/acref-9780199653065-e-3770?rskey=9vExA3&result=4045> (3 Sept 2015).
- Andrews, R. D., 2011, Outcrop characteristics for the Woodford Shale: AAPG Search and Discovery Article 80200, p. 1-3.
- Arbenz, J. K., 2008, Structural framework of the Ouachita Mountains, *in* Suneson, N. H., ed., Stratigraphic and structural evolution of the Ouachita Mountains and Arkoma Basin, southeastern Oklahoma and west-central Arkansas: applications to petroleum exploration - the Arbenz – Misch/Oles volume: 2004 field symposium: Oklahoma Geological Survey Circular 112A, p. 1– 40.
- Arbenz, J. K., 1989, The Ouachita System, *in* Bally, A., ed, and Palmer, A., ed, The Geology of North America – An Overview, v. A: The Geological Society of America, Boulder, Colorado, The Geology of North America, p. 371-396.
- Beecher, C. E., Calvin, S., Clarke, J. M., Claypole, E. W., Frzer, P., Gragin, F. W., Ulrich, E. O., Eterman, J., Upham, W., Wadsworth, M. E., Write I. C., Winchell, N. H., 1895, The origin of the Arkansas Novaculites: America Geologists, v. 16, p. 1-?.
- Byers, C. W., 1973, Biogenic structures of black shale paleoenvironments, Ph. D. dissertation, Yale University, New Haven, Connecticut, p. 1-134.
- Callner, S. A., 2014, An integrated approach to understanding sedimentary structures and depositional processes in Devonian-Mississippian black shale: the Woodford Shale

- and associated strata in the southern midcontinent [M.S. Thesis]: Stillwater, Oklahoma State University, p. 1-103.
- Cardott, B. J., 2005, Overview of unconventional energy resources of Oklahoma, *in* B. J. Cardott, ed., Unconventional energy resources in the southern midcontinent, 2004 symposium: Oklahoma Geological Survey Circular, v. 110, p. 1-133
- Cardott, B. J., 2012, Thermal maturity of Woodford Shale gas and oil plays, Oklahoma, USA: International Journal of Coal and Geology, v. 103, p. 109-119.
- Cardott, B. J., 2013, Woodford Shale: from hydrocarbon source rock to reservoir: AAPG Search and Discovery Article 350817, p. 1-85.
- Comer, J. B., 1992, organic geochemistry and paleogeography of Upper Devonian formations in Oklahoma and western Arkansas, *in* K. S. Johnson and B. J. Cardott, eds., Source rocks in the southern midcontinent, 1990 symposium: OGS Circular, n. 93, p., 70-93.
- Comer, J. B., 2008, Woodford Shale in the southern Midcontinent, USA – transgressive system tract marine source rocks on an arid passive continental margin with persistent oceanic upwelling: AAPG Annual Meeting, AAPG Search and Discovery Article 90078.
- Cecil, C. B., 2004, Eolian dust and the origin of sedimentary chert: U. S. Geological Survey Open-File Report 2004-1098, p. 1-9.
- Ettensohn, F. R. and Barron, L. S., 1981, Depositional model for the Devonian-Mississippian black-shale sequence of North America: a tectono-climatic approach: United States Department of Energy, p. 1-85.
- Ettensohn, F.R., 1985, Controls on the development of Catskill Delta complex basin-facies: Geologic Society of America Special Paper 201, p. 65-77.
- Fay, R. O., 1989, Geology of the Arbuckle Mountains along interstate 35, Carter and Murray Counties, Oklahoma: Oklahoma Geological Survey: Guidebook 26, p. 1-59.
- Fishman, N., Ellis, G. E., Paxton, S. T., Abbott, M. M., and Boehlke, A. R., 2010, From Radiolarian ooze to reservoir rocks: microporosity in chert beds in the Upper Devonian-Lower Mississippian Woodford Shale, Oklahoma: Search and Discovery Article 10268, p. 1-19.
- Folk, R. L., 1973, Evidence for peritidal deposition of Devonian Caballos Novaculite, Marathon Basin, Texas: The American Association of Petroleum Geologists Bulletin, v. 57, n. 4, p. 702-725.
- Folk, R. L. and McBride, E. F., 1976, The Caballos Novaculite revisited part I: origin of novaculite members: Journal of Sedimentary Petrology, vol. 46, no. 3, P. 659-669.

- Folk, R. L. and McBride, E. F., 1977, The Caballos Novaculite revisited part II: chert and shale members and synthesis: *Journal of Sedimentary Petrology*, vol. 47, no. 3, p. 1261-1286.
- Foltz, K., Snider, A., and Puckette, J., 2016, Composition and mechanical properties of the Woodford Shale, Northern Oklahoma: AAPG Search and Discovery Article 51220, p. 1-33.
- Folk, R. L. and Weaver, C. E., 1952, A study of the texture and composition of chert: *American Journal of Science*, vol. 250, p. 498-510.
- Goldstein, A. and Hendricks, T. A., 1953, Siliceous sediments of the Ouachita facies in Oklahoma: *Geological Society of America Bulletin*, v. 64, p. 421-442.
- Goldstein, A., 1959, Cherts and novaculites of the Ouachita facies, in Ireland, H. A., Ed, *Silica in sediment: Society of Economic Paleontologists and Mineralogists Special Publication 7*, p. 135-149.
- Godo, T. J., Li, P., and Ratchford, M. E., 2011, Exploration for the Arkansas Novaculite reservoir, in the southern Ouachita Mountains, Arkansas: *American Association of Petroleum Geologist Search and Discovery Article #10337*, p. 1-25.
- Griswold, L. S., 1890, Whetstones and the novaculites of Arkansas: *Annual Report of the Geological Survey of Arkansas for 1890*, v. 3, p.169-180.
- Griswold, L. S., 1893, The origin of the Arkansas Novaculites: *Annual Report of the Geological Survey of Arkansas*, v. 3, p. 239-242.
- Hallam, A., 1964, Origin of the limestone-shale rhythm in the Blue Lias of England: a composite theory: *The Journal of Geology*, v. 72, p. 157-169.
- Harlton, B. H., 1953, Ouachita chert facies, southeastern Oklahoma: *American Association of Petroleum Geologists Bulletin*, v. 37, p. 778-796.
- Hein, J. R. and Parrish, J. T., 1987, Distribution of siliceous sediments in space and time: *ResearchGate Publication 244478385*, p. 2-25.
- Hesse, R., 1988, Origin of chert: diagenesis of biogenic siliceous sediments: *Geoscience Canada*, v. 15, p. 171-192.
- Honjo, S., 1996, Fluxes of particles to the interior of the open oceans: *Particle Flux in the Ocean*, p. 91-154.
- Hori, R. S., Cho, C. F., and Umeda, H., 2006, Origin of cyclicity in Triassic-Jurassic radiolarian bedded cherts of the Mino accretionary complex from Japan: *Island Arc*, v. 2, p. 170-180.
- Huneke, H., and Mulder, T., 2011, Deep-sea sediments: *Developments in Sedimentology*, v. 63, p. 1-848.

- Iijima, A., Matsumoto, R. and Tada, R., 1985, Mechanism of sedimentation of rhythmically bedded chert: *Sedimentary Geology*, v. 41, p. 221-233.
- Issacs, C. M., 1984, The Monterrey – key to offshore California boom: *Oil and Gas Journal*, v. 82, p.75-81.
- Jones, D. L. and Knauth, L. P., 1979, Oxygen isotopic and petrographic evidence relevant to the origin of the Arkansas Novaculite: *Journal of Sedimentary Petrology*, v. 49, p. 581-598.
- Keller, G. and Cebull, S., 1973, Plate tectonics and the Ouachita system in Texas, Oklahoma and Arkansas: *Geological Society of America Bulletin*, v. 83, p. 1659-1666.
- Keller, W. D., Stone, C. G., Hoersch, A. L., 1985, Textures of Paleozoic chert and novaculite in the Ouachita Mountains of Arkansas and Oklahoma and their geological significance: *Geological Society of America Bulletin*, v. 96, p. 1353-1363.
- Kuenen, P. H., 1959, Sand, its origin, transportation, abrasion and accumulation: *Geological Society of South Africa Transcript*, v. 62, p. 1-33.
- Knauth, L. P., 1979, A model for the origin of chert in limestone: *Geology*, v. 7, p. 274-277.
- Knauth, L. P., 1994, Petrogenesis of chert, *In*: Heany, P. J., Prewitt, C. T., and Gibbs, G. V., eds. *Silica. Physical Behavior, Geochemistry and Materials Applications*, p. 233-258. *Reviews in Mineralogy*, 29.
- Krystyniak, A. M., 2003, Outcrop-based gamma-ray characterization of the Woodford Shale of south-central Oklahoma [M.S. Thesis]: Stillwater, Oklahoma State University, p. 1-160.
- Kvale, E. P. and Bynum, J., 2014, Regional upwelling during Late Devonian Woodford deposition in Oklahoma and its influence on hydrocarbon production and well completion: *American Association of Petroleum Geologist Search and Discovery Article # 80410*, p. 1-34.
- Lee, D. R., 2005, Characterization and the diagenetic transformation of non- and micro-crystalline silica minerals: Department of Earth and Ocean Sciences, University of Liverpool, UK, p. 1-20.
- Lochte, K. R., Anderson, F., Francois R., Jahnke, R. A., Shimmield, G., and Vetrov, A., (2003), Benthic process and the burial of carbon, in *Ocean Biogeochemistry: The Role of the Ocean Carbon Cycle in Global Change*, edited by M. J. R. Fasham, p. 196-216.
- Lowe, D. R., 1975, Regional controls on silica sedimentation in the Ouachita system: *Geological Society of America Bulletin*, v. 86, p. 1123-1127.

- Lowe, D. R., 1985, Ouachita trough: part of a Cambrian failed rift system: *Geology*, v. 13, p. 790-793.
- Lowe, D. R., 1989, Stratigraphy, sedimentology, and depositional setting of pre-orogenic rocks of the Ouachita Mountains, Arkansas and Oklahoma, *in* Hatcher, R. D., Jr., Thomas, W. A., and Veile, G. W., eds., *The Geology of North America*, v. F-2, *The Appalachian-Ouachita Orogen in the United States*: Geological Society of America, p. 575-590.
- McBride, E. F. and Thomson, A., 1970, The Caballos Novaculite, Marathon region, Texas: Geological Society of America, Special Paper #122, p. 76-77.
- Misch, P. and Oles, K. F., 1956, Stratigraphic and structural studies in the Ouachita Mountains, Oklahoma and Arkansas (1956), *in* Suneson, N., Ed, *Stratigraphic and Structural Evolution of the Ouachita Mountains and Arkoma Basin, Southeastern Oklahoma and West-Central Arkansas: applications to petroleum exploration: The Arbenz-Misch/Oles Volume: 2004 field symposium: Oklahoma Geological Survey and ConocoPhillips School of Geology and Geophysics*, p. 43-86.
- Miser, H. D., 1929, Structure of the Ouachita Mountains of Oklahoma and Arkansas: Oklahoma Geological Survey Bulletin 50, p. 3-30.
- Miser, H. D. and Purdue, A. H., 1929, Geology of the De Queen and Caddo Gap quadrangles, Arkansas: U.S. Geological Survey Bulletin #808, p. 131-132.
- Miser, H. D., 1954, Geologic map of the state of Oklahoma: Oklahoma Geological Society: <http://ogs.ou.edu/docs/geologicmaps/GeologicMapofOklahoma.pdf> (31 Mar 2016).
- Morris, R. C., 1974, Sedimentary and tectonic history of the Ouachita Mountains: Society of Economic Paleontologists and Mineralogists Special Publication 22, p. 120-142.
- Morrison, L. S., 1984, Ouachita facies – an overview: AAPG Mid-Continent Regional Meeting, p. 83-88.
- Murray, R. W, Jones, D. L., Brink, M. R. B., 1992, Diagenetic formation of bedded chert: evidence from chemistry of the chert-shale couplet: *Geology*, v. 20, p. 271-274.
- Nielsen, K. C., 1988, Beavers Bend State Park, Broken Bow Uplift, Oklahoma: Geological Society of America Centennial Field Guide – South-Central Section, no. 496, p. 195-202.
- Oklahoma Geological Survey, 2014, Major geological provinces of Oklahoma: <http://www.ogs.ou.edu/MapsBasic/Provinces.jpg> (6 Jan 2016).
- Over, J. D., 1990, Conodonts and the Devonian-Carboniferous boundary in the upper Woodford Shale, Arbuckle Mountains, south-central Oklahoma: *Journal of Paleontology*, v.66, p. 293-311.

- Owen, D. D., 1860, Second report of geological reconnaissance of the middle and southern counties of Arkansas made during the years of 1859-1860: Philadelphia, PA., C. Sherman & Sons, p. 433.
- Park, D. E. and Croneis, C., 1969, Origin of the Caballos and Arkansas Novaculite Formations: American Association of Petroleum Geologists Bulletin, v. 53, p. 94-111.
- Pashin, J. C., and Callner, S. A., 2014, Paleooceanographic and estuarine influences on sedimentation in an unconventional source rock-reservoir system: Devonian shale in the southern midcontinent, USA: 2014 Eastern Unconventional Oil and Gas Symposium, Lexington, Kentucky.
- Pashin, J. C., and Ettensohn, F. R., 1992, Palaeoecology and sedimentology of the dysaerobic Bedford fauna (late Devonian), Ohio and Kentucky (USA): Palaeogeography, Palaeoclimatology, Palaeoecology, v. 91, p. 21-34.
- Pashin, J. C., and Ettensohn, F. R., 1995, Reevaluation of the Bedford-Berea sequence in Ohio and adjacent states: forced regression in a foreland basin: Geological Society of America, v. 298, p. 1-68.
- Pashin, J. C., Kopaska-Merkel, D. C., Arnold, A. C., McIntyre, M. R., 2011, Geological foundation for the production of natural gas from diverse shale formations: Research Partnership to Secure Energy for America (RPSEA) Final Report 0712217.01, p. 1-156.
- Pessagno, E. A. and Newport, R. L., 1972, A technique for extracting Radiolaria from radiolarian cherts: Micropaleontology, v. 18, p. 231-234.
- Piper, D., and Calvert, S., 2009, A marine biogeochemical perspective on black shale deposition: Earth-Science Reviews, v. 95, p. 63-96.
- Pomar, L., Morsilli, M., Hallock, P., and Badenas, B., 2012, Internal waves, an under-explored source of turbulence events in the sedimentary record: Earth-Science Reviews, v. 116, p. 195-205.
- Powell, L., 2002, Tectonic origins of the ancestral Rocky Mountains: left-lateral movement along the Wichita megashear:
<http://www.colorado.edu/geosci/Resources/WUSTectonics/AncestralRockies/megashear.html> (4 Sept 2015).
- Puckette, J. O., Boardman, D. R., and Watney, W. L., 2013, Woodford Shale: correlating rock properties in outcrop and core with wireline log characteristics: AAPG Search and Discovery Article #50885.
- Purdue, A. H. and Miser, H. D., 1923, Description of the Hot Springs District: U.S. Geological Survey Atlas, Folio 215., p. 1-12.

- Rich, J. L., 1951, Three critical environments of the deposition and criteria for recognition of rocks deposited in each of them: *Geological Society of America Bulletin*, v. 62, p.1-19.
- Reid, S., and McIntyre, J., 2001, Monterey Formation porcelanite reservoirs of the Elk Hills field, Kern County, California, *AAPG Bulletin*, v. 85, p.169-189.
- Roberts, C. T and Mitterer, R. M., 1988, Laminated black shale-chert cyclicity in Woodford formation (Upper Devonian of southern Midcontinent): *AAPG Search and Discovery Article #91030*.
- Rutley, F., 1891, On the origin of certain novaculites and quartzites: *American Geologist*, v. 14, p. 253.
- Schieber, J., 1994, Evidence for high-energy events and shallow-water deposition in the Chattanooga Shale, Devonian, central Tennessee, USA: *Sedimentary Geology*, v. 93, p. 193-208.
- Schieber, J., and Zimmerle, W., 1998, Petrography of shales: a survey of techniques. In: Schieber, J., Zimmerle, W., Sethi, P., (Eds.), *Shales and Mudstones, Petrography, Petrophysics, Geochemistry, and Economic Geology*, v.2, p.3-12.
- Schieber, J., and Riciputi, L., 2004, Pyrite ooids in Devonian black shales record intermittent sea-level drop and shallow-water conditions: *Geology*, v. 32, p. 305-308.
- Schmoker, J. W. and Hester, T. C., 1990, Formation resistivity as an indicator of oil generation – Bakken Formation of North Dakota and Woodford Shale of Oklahoma: *Society of Petrophysicists and Well Log Analysts*, v. 31, p. 1-9.
- Sholes, M., and McBride, E. F., 1975, A guidebook to the sedimentology of Paleozoic flysch and associated deposits, Ouachita Mountains – Arkoma Basin, Oklahoma: *Arkansas Novaculite: Dallas Geological Society*, p. 69-87.
- Slatt, R. M., Buckner, N., Abousleiman, Y., Sierra, R., Phil, P. R., Miceli, A. M., Portas, R., O'Brien, N., Tran, M., Davis, R., Warzyniec, T., 2012, Outcrop behind outcrop (quarry): Multiscale characterization of the Woodford Gas Shale, Oklahoma, in J. A. Breyer, ed., *Shale reservoirs Giant resources for the 21st century: AAPG Memoir 97*, p. 382–402.
- Spesshardt, S. A., and Barrick, J. E., 1985, Late Devonian-Early Mississippian phosphorite-bearing shales, Arbuckle Mountain region, south-central Oklahoma: *Unpublished MS thesis, Texas Tech University*, p. 1-101.
- Sullivan, K. L., 1985, Organic facies variation of the Woodford Shale in western Oklahoma: *The Shale Shaker Digest XI*, v. XXXIII-XXXV, p. 185-198.
- Suneson, N. H., 1995, *The geology of the Broken Bow Uplift: an introduction and field-trip guide: Oklahoma Geological Survey*, p. 1-31.

- Suneson, N. H., 2008, Introduction to the Arbenz-Misch/Oles volume: The Arbenz-Misch/Oles Volume: 2004 field symposium: Oklahoma Geological Survey and ConocoPhillips School of Geology and Geophysics, p. V-VI.
- Taff, J. A., 1902, Description of the Atoka quadrangle [Indian Territory]: U.S. Geological Survey Atlas Folio, v. 79, p. 1-8.
- Thomas, W. A., 2006, Tectonic inheritance at a continental margin, 2005 GSA Presidential Address: GSA Today, v. 16, n. 2, p. 4-11.
- Viele, G. W., 1979, Geologic map and cross section, eastern Ouachita Mountains, Arkansas: map summary: Geological Society of America Bulletin, Part I, v. 90, p. 1096-1099.
- Viele, G. W., 1989, The Ouachita orogenic belt, *in* Hatcher, R., Thomas, W., and Viele, G., eds, The Appalachian-Ouachita Orogen in the United States: The Geology of North America Volume F-2, Geological Society of America, p. 555-561.
- Vigran, J. O., Mørk, A., Forsberg, A. W., Weiss, H. M., and Weitschat, W., 2008, Tasmanites algae – contributors to the Middle Triassic hydrocarbon source rocks of Svalbard and the Barents Shelf: Polar Research, v. 27, p. 360-371.
- Wickham, J., Roeder, D., Briggs, G., 1976, Plate tectonic models for the Ouachita foldbelt: Geology, v. 4, no. 3, p. 173-176.
- Witzke, B. J., 1987, Models for circulation patterns in epicontinental seas applied to Paleozoic facies of North American craton: Paleooceanography, v. 2, p. 229-248.

VITA

Kyrsti A. Cecil

Candidate for the Degree of

Master of Science

Thesis: CHARACTERISTICS AND ORIGIN OF SILURIAN-MISSISSIPPIAN
NOVACULITIC CHERT IN THE SOUTHERN MIDCONTINENT

Major Field: Geology

Biographical: Kyrsti A. Cecil was born in McAlester, OK, and moved to Norman, OK in

4th grade where she remained until she attended college at Oklahoma State University in Stillwater, OK.

Education: Completed the requirements for the Master of Science in Geology at Oklahoma State University, Stillwater, OK, May 2016.

Completed requirements for the Bachelor of Science in Geology at Oklahoma State University in Stillwater, OK, December 2011.

Experience: Held petroleum geology Internships at Laredo Petroleum in Tulsa, OK, and at Devon Energy in Oklahoma City, OK; Teaching Assistant and Tutor for Oklahoma State University during both Undergraduate and Graduate semesters; United State Air Force Intelligence Analyst Officer specializing in weaponeering and targeteering for F-16/F-35 platform.

Professional Memberships: AAPG, OCGS, TGS, GSA